Hydrogeological system analysis of the Abaya Chamo Lakes basin, with special emphasis on using chemical and isotopic signatures in the characterization of the system

Abrham Asha

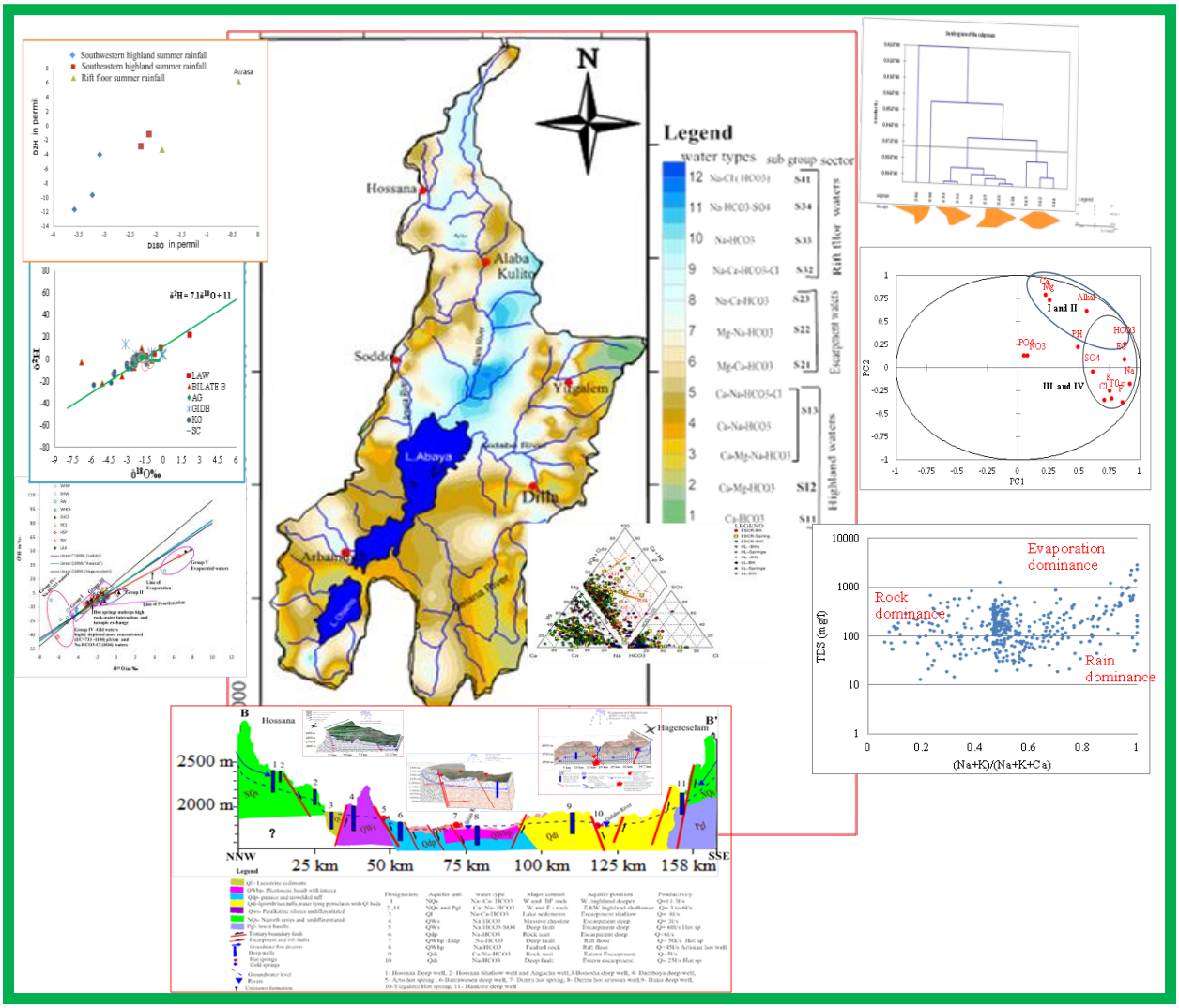

A dissertation for the degree of Doctor of Philosophy (PhD) in Hydrogeology

Addis Ababa University, Ethiopia

June 2018

ADDIS ABABA UNIVERSITY

COLLEGE OF NATURAL AND COMPUTATIONAL SCIENCE, SCHOOL OF EARTH SCIENCE

Hydrogeological system analysis of the Abaya Chamo Lakes basin, with special emphasis on using chemical and isotopic signatures in the characterization of the system

A Dissertation submitted to the School of Graduate Studies of Addis Ababa University in partial fulfillment of the requirements for the Degree of Doctor of Philosophy (Ph.D.) in Hydrogeology

By Abrham Asha

Advisor Prof. Tenalem Ayenew

05,June 2018

ADDIS ABABA UNIVERSITY

SCHOOL OF GRADUATE STUDIES

This is to certify that the dissertation prepared by Abrham Asha, entitled: Hydrogeological system analysis of the Abaya Chamo Lakes basin, with special emphasis on using chemical and isotopic signatures in the characterization of the system, submitted in partial fulfillment of the requirements for the Degree of Doctor of Philosophy (Ph.D.) of science in Hydrogeology complies with the regulations of the university and meets the accepted standards with respect to originality and quality

By : Abrham Asha

Approved by the examining board

		signature	Date
Chairman, Examining Board	----------	----------	----------
External examiner	----------	----------	----------
Internal examiner	----------	----------	----------
Advisor	Prof. Tenalem Ayenew	----------	----------

Chair of school of Earth science or Graduate program coordinator

---------- Signature ---------- Date ----------

Title :- Hydrogeological system analysis of the Abaya Chamo Lakes basin, with special emphasis on using chemical and isotopic signatures in the characterization of the system

Abstract

Hydrochemistry and stable isotopes have been used as powerful tool in the analysis of the hydrogeological system analysis of the Abaya Chamo Lakes basin. This large basin (18,100km^2) is situated in the complex volcano-tectonic terrain of the southern main Ethiopian rift with three distinct physiographic sectors where major surface drainage converges towards the Lakes. The source and mechanisms of the recharge, the configuration and relations of tectonic structures controlling the occurrence, composition, and flow of the groundwater systems have been investigated and conceptualized in the study area.

The stronger summer rainfall contributing half of annual amount is depleted (ŏ^{18}O‰=-4.2 to -0.39) having altitude effect Ő^{18}O =-0.2‰ per 100m (depletion) and pseudo altitude effects of $\delta^{18}O$ = 0.12‰ per 100m (enrichment). Whereas, slightly enriched (ŏ^{18}O‰=-2.6 to -0.01) Spring rainfall contributes about 35% of the annual showed an altitude effect about 0.1‰ per 100m (enrichment) and pseudo-altitude enrichment rate of 0.15‰ per 100m. Direct recharge form infiltration of rainfall is the dominant source for groundwaters in all River basins.

Combined with the sets of tectonic systems, the hydrostratigraphic units determined the mechanism of the recharge, groundwater occurrence, distribution, flow dynamics, mixing of the groundwaters, the composition and hydrogeochemical processes. The groundwater head is deeper in the highlands and escarpments, shallower in the rift floor, and complex where inter-basin transfer and faults control the flow. The hydraulic properties of volcanic rocks increase from the highlands towards the rift floor (T=50 to more than 800m^2/d and K=1 to 15m/day) in the well depth range of 60 to 400mbgl. The discharge of the spring flow increases from the highlands towards the rift floor (0.036 to 260lit/Sec).

Water type maps, piper plot and dendrogram clustering diagram revealed the occurrence of four main groups and eleven subgroups of groundwaters. The highlands Group I (G1) $Ca^{2+}$and HCO_3^- rich and the escarpment Group II (G2) $Mg^{2+}$and HCO_3^- rich waters are dilute with average EC= 324 µS/cm and 237 µS/cm respectively. These hydrogeological systems are unconfined to semi-

confined/ and confined having depleted (ȯ^{18}O‰= -4.2 to -1.4, and d-excess ‰ = 10.6 to 25.1), groundwaters , but in places, where there is evaporation, there occur relative enrichment. The rift floor Group III (G3) Na^+ and HCO_3^- rich hot springs and wells are located along active rift faults and are relatively more mineralized (average EC=467 µS/cm) compared to Group I and II. The fourth highly evolved outlier Group IV (G4) water Na-Cl/HCO_3^- type volcanic water is represented by one thermal spring with EC (5450µS/cm) and at a temperature of 96^0c. The groundwaters evolution showed that G1→G2→G3→ G4 along the groundwater flow direction as indicated in PC1 and the reverse in PC2. But, in places, the existence of deep escarpment faults blocked the consistent groundwater evolution. This has clearly revealed the NNE-SSW inland alignment of $NaHCO_3$ rich and less d-excess groundwater across the Gidabo basin towards Dilla. Rift floor hot springs in recent volcanics, Pleistocene basalt, and rift sediments are interconnected and meteoric in origin. But, deeper depleted (ȯ^{18}O‰= -6.82 to -5.07) rift hydrogeological systems in sand and gravel aquifers (below150mbgl) of old waters sources and highly enriched (ȯ^{18}O ‰ = 5.04 to 6.54) waters from evaporated sources (Lakes) showed no hydraulic connection with other aquifers. These groups of waters are formed mainly due to silicate weathering, ion exchange and evaporation hydrogeochemical processes occurred in the hydrogeological systems.

Based on the findings, the hydrogeological systems are conceptualized including into: highlands (dilute, Ca–HCO3 type, EC=324 µS/cm, ŏ^{18}O‰ ≥ -4.2), escarpment (dilute, Mg–HCO3 type, EC=237 µS/cm, mixed waters), upper rift floor (Na-HCO3 and Na-Cl type, EC= up to 5450µS/cm, meteoric origin), and deeper rift floor (Na-HCO3 type, EC= 341 to 1179µS/cm,ŏ^{18}O‰= -6.82 to -5.07 , non-recent meteoric origin). The study addressed major objectives and ends with recommendation of some instrumental issues to upgrade the research in future.

Keywords: Abaya Chamo Lakes basin, Aquifers, Groundwater recharge, Hydrogeological Systems, Hydrochemistry, Hydrogeochemical processes, Stable isotopes, volcanic rocks

Acknowledgments

First of all, I thank God almighty, who provided me unlimited mercy and strength to go this long journey of the academic career.

I would like to express my genuine thankfulness to my advisor Prof. Tenalem Ayenew for his acceptance to supervise my Ph.D. work through investing his time, sharing his enriched practical and research knowledge, given critical scientific comments, and showing future upgrading areas. A special thank is forwarded to Dr. Seifu Kebede who has been fully committed to transfer the knowledge of isotope hydrology and hydrogeochemistry to me both during MSc and Ph.D. works. I could not have been able to write this paper unless he had contributed it to my career. I am very appreciative of Dr. Mulugeta Alene for his sustainable supervision and amicable solutions as school graduate coordinator of earth science. My deepest appreciation goes to Dr. Dessie Nadew as batch coordinator and instructor whose kind communication of creation of conducive learning environments for me regardless of challenges. I am grateful to my colleagues Dr. Fikadu W/Mariam, Dagnachew Daniel, Dr. Bisrat Elias, Dr. Mersha Alemu and Dr. Daniel for their great contribution of experiences and materials necessary during the start of this study. The assistance of work from department office is very critical for me and is highly acknowledged. Great thankfulness is deserved to southern region's water resources development bureau for allowing me to use the regional water chemistry laboratory for chemical analysis of water samples and existing data for my study. Department of environmental science and Geology of wolaita soddo university is acknowledged for creating me nice learning environments.

I can’t express in words my appreciation which I have for my wife Rahel Samuel for her enduring patience of carrying all double burdens in places of me. God bless Rahel and my kids (Yeab and Ruhama) for their time they share with me. I am indebted to my late brother Dr. Amenu Asha who had always been encouraging me for further study, my father and mother for their special care and love. God save my brother’s soul in heaven. Spiritual support through comforting prayers of Christian sisters and brothers of my local church had been strengthening me during the challenges that I met and I thank you very much, God, bless you.

Table of Contents

List of figures

List of tables

List of Acronyms

Amsl: Above mean sea level

BoWI : Bureau of Water and Irrigation

DEM : Digital Elevation Model

EWTEC : Ethiopian Water Technology

GMWL : Global Meteoric water Line

GNIP : Global Network of Isotopes in Precipitation

GSE : Geological Survey of Ethiopia

IAEA : International Atomic Energy Agency

ITCZ: Inter-Tropical Convergence Zone

JJAS: June July August September

LMWL: Local Meteoric Water Line

MAMy: March April May

NMA: National Meteorological Agency

OND: October November December

SRTM: Shuttle Radar Topography Mission

SWWCE: South Water Works Construction Enterprise

UNDP: United Nations Development Program

USGS: United States Geological Surveys

1. INTRODUCTION

1.1. Background

Groundwater accounts about 30% of global freshwater and is essential to focus on its sustainability (Allay et al., 1993). In Ethiopia groundwater has been the base of civilization, including old urban settlements around mountain springs and the modern groundwater development started in the late 1860's by British military through the drilling of wells (Abyssinian wells). But the groundwater resource assessment started in 1960 and continued to the recent paradigm of steady state (Seifu k., 2013). By now groundwater is becoming a strategic resource of the country shifting from the pattern of the simple hydrogeological mapping towards economic resources, reducing poverty and functioning the environment regardless of scant detailed hydrogeological knowledge, uneven groundwater resource distribution, lack of scientific and technical capacity and little experience in water-related developments (Ayenew et al., 2013).

Two third of Ethiopian landmass is covered by volcanic rocks where the usable proportion of the groundwater occurs in fractures and joints formed during or after the formation of the rocks. Different scholars conducted scientific investigations in volcanic terrain of Ethiopia and remark that the aquifers are very complex, heterogeneous and anisotropic. The formation of boundary isolated volcanic uplifts, escarpment faults, rift floor volcanic cones and tectonic structures, control the occurrence, distribution, and quality of groundwaters in central and southern Ethiopia. In most cases, volcanic rocks are confined and inter-bedded with paleosoils and volcanic ashes but shallow fractured aquifers are unconfined to semi-confined and confined (Ayenew, 1998; Seifu, 2013).

The hydrostratigraphic set up of Abaya Chamo Lakes basin is due to the early Tertiary volcanic rocks dominantly localized in highlands, late Tertiary volcanic rocks mostly confined within the rift floor, fissural volcanism forming rhyolitic ignimbrites with voluminous flood basalts and recent rocks consisting alluvial, lacustrine and volcano-sedimentary formations covered around Lakes, along plains and River deltas in the rift (Woldegebriel et al., 1990). Temporal processes of occurrence of rock units and spatial variability in deposition are the reason for a different

degree of weathering and fracturing. Due to different eruptions and time gap in between them, the rocks formed prior have been weathered and /or eroded with a subsequent deposition of alluvial material giving rise to layers of paleosoils. The frequency and extent of weathering, jointing, fractures and flow contacts are the most hydrogeological factors imparting porosity and permeability of volcanic aquifers. Based on this, extrusive volcanic rocks of highlands are generally massive /weathered to the top and have low primary porosity whereas the volcanic pyroclastics in the rift floor have high primary porosity. Escarpment formations are cut by regional faults and are areas where many cold springs of bigger discharge occur in the basin.

Previous studies in the Abaya Chamo Lakes basin focused on regional scale hydrologic, geologic, hydrogeological, hydrochemistry and isotopes of the River basins (Matkin et al., 1975 ; Gibb, 1980 ; Zenettine et al., 1978 ; M.Raunet, 1978 ; UNDP,1973 ; Tesfaye T., 2010 ; Sintayehu L., 2009 ; McKenzie *et al.*,2001 and Abraham et al., 2016). The studies are either regional and scant in detail information or limited to sub-basins or catchments in Abaya Chamo Lakes basin. Organized and conceptualized knowledge is not available to understand the basin scale groundwater recharge source and mechanism, localities of ground-surface water interaction, groundwater flow, the control of tectonics in groundwater (occurrence, flow, and evolution), hydrogeological systems frameworks in all the sectors of the basin and deeper aquifer frame systems.

This Ph.D. study focuses on the hydrochemistry and isotopic signatures to analyze the hydrogeological systems based on the variations of geology, geological structures, and geomorphology. It provided better knowledge of the Abaya- Chamo Lakes basin by accounting three important physiographic regions i.e. the highlands, escarpments and the rift floor.

1.2. Previous studies

Some of the previous studies related to hydrological, geological and hydrogeological aspects have been conducted in the Abaya Chamo Lakes basin and its environs. The development prospects of the Southern Ethiopian Rift aimed at the water resources based classification of regional and local development areas were studied by (Matkin et al., 1975). (Gibb, 1980) studied Gelana Basin with respect to the irrigation potential and irrigable areas. Previous works of the

isotope data collection and analysis of water (Lake, Rain, and Groundwater) samples in the Ethiopian Main Rift valley include: (UNDP, 1973), (MOWE, 2012), (GSE, 2000), (GSE, 2007), (IAEA-TC-ETH006 project, 2002), (Kebede *et al.*, 2002b), (McKenzie *et al.*, 2001) and (Abraham et al., 2016).

The above previous studies mainly focused on the limited and fragmented regional scale geological, hydrogeological, hydrochemistry and stable isotope investigation of the River basins and thus no knowledge is available in the analysis of the Lakes basin-scale integrated hydrogeological system. This Ph.D. thesis, therefore, focuses on the analysis of the systems by the conceptualization of the results of hydrochemistry and isotopic signatures of the water samples (Rain, River, Lakes, and groundwater) based on variations in the geology and tectonic structures of the basin. This assisted in adding more knowledge of the basin's source and the mechanism of the recharge, controls of the geology and tectonics, groundwater flow, the interaction of surface and groundwaters, the evolution of the groundwater, fractionation of the isotopic contents and the occurrence of different hydrogeological systems.

1.3. Objectives

The general objective of the research is to analyze the hydrogeological systems of the Abaya Chamo Lakes basin through converging the evidence of the results by focusing on hydrochemical and environmental isotope signatures.

Specific objectives of the study include:-

- To characterize the stable isotopic composition of rain/meteoric waters and their spatial variability so as to understand the spatial variability and sources of groundwater recharge
- To describe the hydrostratigraphic and tectonic structure in relation to the hydrogeologic system and their control on groundwater occurrence, composition and flow using water chemistry and environmental isotopes
- To understand the groundwater recharge (source and mechanisms) and its evolution along different physiographic regions (plateau, escarpments and rift floor) of the basin
- To conceptualize the different hydrogeological systems framework and groundwater dynamics in the basin

1.4. Approach and Methodology

In the complex rift zones like Abaya Chamo Lakes basin where recent tectonic structures affected the geologic setups and in turn the hydrogeological environments, the application of various hydrogeological methods has to be used to understand and conceptualize the systems. Therefore, synchronization of results from different data sets of multiple disciplines of Hydrogeology is applied. To do this, the following methodologies and materials are used to undertake the research.

Review of all the previous works both from Published or unpublished sources related to the aspects of hydrology, geology, Hydrogeology, hydrogeophysics, hydrochemical and isotopes was done. The important database was organized and the strategic base maps were prepared to identify the data gaps and to undertake the field survey along the selected routes of the highlands, escarpments, and rift floor. Geologic units of the exposed area (quarry sites, fault scarps, river cuts, erosion gullies), lithologic contacts, fracture lines, faults and water points were mapped using materials such as Garmin GPS 72 and 1:50,000 scale topographic map. The photos of lithological units were taken from the route for the correlation of the units. The inventory of water points (cold springs, shallow drilled wells, deep wells, hot springs) was made in the basin for generation of the data sets including location of water points, water level, well and spring discharges and physical characteristics of water samples. Water well-pumping test data and well lithologic logs were used in the mapping of hydraulic properties of the different volcanic aquifers. This resulted in the spatial distribution of groundwater level, its flow direction, hydraulic property, hydrogeological and structural elements used to prepare the first hand geological, hydrogeological maps and cross sections to synergize with chemical and isotope data.

Water sample collection was done with the development of a preliminary conceptual hydrogeological view of the basin. The existing data on the major water chemistry and stable isotope (ȯ2H and ȯ18H) from all available sources were organized and the gaps were filled by the newly generated hydrochemical data (109 new water samples) that were analyzed in south water and irrigation bureau regional water chemistry laboratory (fig. 49). The selections of water sampling sites were based on the hydrogeological reasoning to observe the variations in the

occurrence, distribution and movement of groundwater. Water samples consisting of 5 Rain, 159 deep drilled Boreholes, 228 shallow drilled wells, 166 cold and hot springs, 3 Lakes and 15 Rivers were clustered in highland, escarpments and rift floor (Table 5). Monthly average isotopic data (ȯ18O and ȯ2H) of summer rainfall of one to two years were used for GNIP (Global Network of Isotopes in Precipitation stations of the basin (IAEA/WMO, 2004). In addition to GNIP precipitation stations (Awasa, wolayta sodo and Hagereselam), single record of the precipitation isotope analysis result of four sites (Arbaminch, Gerese, Chencha and Humbo) are used as proxies. Existing groundwater environmental isotope data used in the study (Fig.75) was collected from different sources as discussed in previous works part.

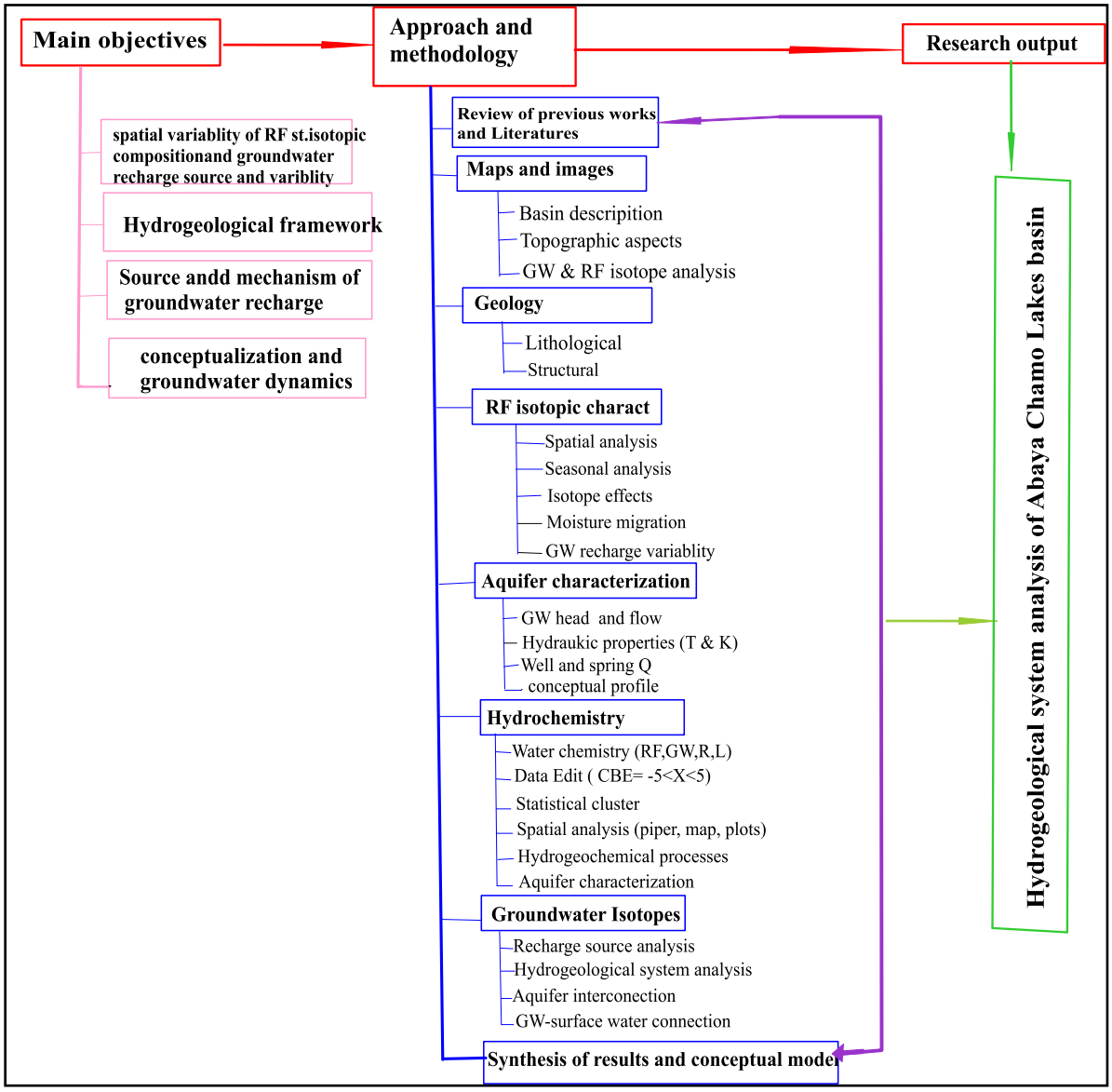

Fig 1. Flow chart of approach and methodology

The hydrochemical variables such as electrical conductivity (EC), TDS, PH, Temperature, Na^{+}, Ca^{2+}, Mg^{2+}, K^{+}, $Fe^{2+,}$ Mn^{2+}, Cl^{-}, SO_4^{2-}, HCO_3^{-}, F^{2+} and the stable isotopic composition of $\dot{o}^{18}O$ and $\dot{o}^{2}H$ were used in the evaluation of the aquifer systems in the basin. The hydrochemical database was edited for the units of measurement (mg/lit and meq/lit). Censored values which have detection values less/greater than are rejected. The data gap was filled by calculating the amount using linear regression of ions and geochemical relations. The edited chemical analyses in the database used to estimate the charge balance error (Freeze and Cherry, 1979). As the samples were analyzed in the different laboratories and collected from various sources, the analytical errors are variable. For the majority of the samples, the analytical error is less than ±4.5% (Fig. 1, Fig. 41). For the great majority of the data, the error is less than ±2% which is an acceptable error limit (C. Güler et al, 2002). From the point of view of showing the spatial variations at the mapping scale (1:50,000) the quality of the data was believed to be satisfactory. The isotopic ratios $^{18}O/^{16}O$ and $^{2}H/^{1}H$ were analyzed at the Isotope Hydrology Laboratory, IAEA, in Vienna and reported in per mil (‰) deviation with respect to the Vienna Standard Mean Oceanic Water (V-SMOW). The analysis has uncertainty levels of ±0. 1 and ±1. 0‰ for ^{18}O and ^{2}H respectively (IAEA, 1981).

Grouping and descriptive analysis of the aquifer systems was done using the Aquachem 4.0 (Waterloo, 2003) and the statistical software (XL-stat, 2017). The major statistical data of the hydrochemical variables of the water samples were represented to show how the different physiography (highland, escarpment and lowland) vary. Relating the different ions (ion ratios and their relations) using the plots and maps were helped in the description of the hydrogeochemical processes. This defined the evolution and flow direction of the groundwater, the analysis of aquifer systems and the distinction of the waters and their origins. The Isotope data analysis in relation with hydrochemistry identified the groundwater origin (using LMWL) and its composition. Spatial mapping is done in groups of the waters using application software, including Arc GIS, Surfer 12 and Global mapper 12. This was used to understand the hydrochemical facies based on factors such as geomorphology, tectonics, and geology of the different hydrogeological systems in the basin. Synergizing all the data gave rise to a conceptual model of the hydrogeological systems with distinct recharge sources and mechanism, processes in aquifers, the composition of water types and flow within systems.

1.5. Structure of the thesis

This thesis is organized into 10 chapters. Chapter one, two and three provide mainly the introductory background of the research, including objectives, methodology, and description of the area, whereas the remaining chapters, four to ten showed the results of observations and the implications of the hydrogeological systems of the Abaya Chamo Lakes basin. Chapter one presents previous studies, objectives, and methodology to undertake the research. Chapter two describes the physical characteristics of the basin related to location, physiography, drainage and general climatic conditions of the study area. Chapter three discusses the geologic units in their age sequence, geological structures and their controls in the hydrogeological system.

Chapter four characterizes the stable isotopic composition of the rainfall and its spatial variability to understand the source of moisture, the effect of seasonal microclimates on the basin physiography and the difference of rainfall amount and its fractionation. The local meteoric water lines (LMWL) of some stations and their isotopic effects finally conceptualize how the moisture sources migrate along the mountains and escarpments while coming from the source to the basin. The effect of isotopic modification /fractionation is also used in the tracing of direct recharges to the basin watersheds. Chapter five deals with the aquifer configuration and hydraulic properties of the volcanic aquifers of Abaya Chamo Lakes basin. In this section, the major hydro strata, the groundwater head, and flow, the yield of wells and springs, the role of geological structures, the hydraulic properties of volcanic rocks and conceptualization of the aquifer frames of the basin is discussed.

Chapter six presents the hydrochemistry as an important tool in the analysis of the hydrogeological system. In this chapter the chemistry of Rain, Lake and groundwaters are discussed in detail. The groundwater chemistry is analyzed based on the chemical composition of the groundwaters and its spatial variability, the statistical associations among the hydrochemical variables, the groundwater evolution, and its chemical stratification. Chapter seven deals with the ionic ratio relations in the understanding the hydrogeochemical processes of the aquifer systems and the sources of ions using plots and spatial maps. Silicate weathering, ion exchange, and evaporation become a dominant hydrogeochemical process. Chapter eight comparatively describes the isotopic composition of groundwater and rainfall to identify the sources and

mechanisms of recharges, the groundwater-surface water interaction, the basic variation among the hydrogeological systems and the interconnections of aquifers. Chapter nine converges the evidence of the major results of the research to conceptualize the hydrogeological systems of highlands, escarpments and rift floor. The thesis ends with chapter ten containing the conclusion and recommendations, giving more emphasis to the basic issues to be improved for further work by scientific research and intervention of decision makers.

2. PHYSICAL CHARACTERISTICS OF ABAYA-CHAMO LAKES BASIN

2.1. Location

Abaya Chamo Lakes Drainage basin is located in the southern part of the Main Ethiopian Rift with extreme west-east stretch (longitude) of $37^0$16.3'E at $5^0$51.5'N to $38^0$39.3'E at $6^0$45.5'N and extreme North-South (Latitude) stretch ranging between $5^0$19'N at $37^0$45'E to 8^0.8' to $38^0$12'E. It has a total area of about 18100km^2. The basin of the Lake Awasa and the central Lakes basin to the northeast and north, Omo-Gibe basin to the Northwest and West, Chew Bahir basin to the south, and Genale-Dawa basin to the east and southeast direction border Abaya Chamo Lakes basin. The location and drainage map of the basin is shown (Fig.2). The area is set at the lower elevation profile compared to another central Ethiopian rift Lakes basin (Fig.3).

2.2. Physiography

As Part of the East African rift system the Ethiopian Rift Valley is a fault-bounded depression about 600km long and 50 to 90km wide trending generally in NE-SW and NNE-SSW direction. In the north, it opens fanlike into the Afar Depression. Further north, the structural trend of the Ethiopian Rift Valley continues to the triple junction near Lake Abbe where the Ethiopian Red Sea and Gulf of Aden rifts meet.

The Main Ethiopian Rift is bounded by discontinuous boundary faults that give rise to major fault escarpments separating the rift depression from the Ethiopian and Somalian plateaus. These faults are normally longer widely spaced and characterized by large vertical offsets up to 1 km (Boccaletti et al., 1998). The main Ethiopian rift valley is a low-lying region between the western plateaus and southeast plateaus. Large topographic scarps up to 1500m as in garage scarp (DI Paola, 1979) and even extending 3000m as in northern Shoa (Zenettin *et al.*, 1974) mark the margins of these upland regions. The Main Ethiopian Rift (MER) covers an area of about 52,000 km² extends from southern Afar to Konso highlands in southern Ethiopia. Based on structural features, the MER is divided into northern MER (Fentale- Nazareth), Central MER (Nazareth - Awassa) and southern MER (Awassa- Chew Bahir) (G. woldeGabriel *et al*., 1999).

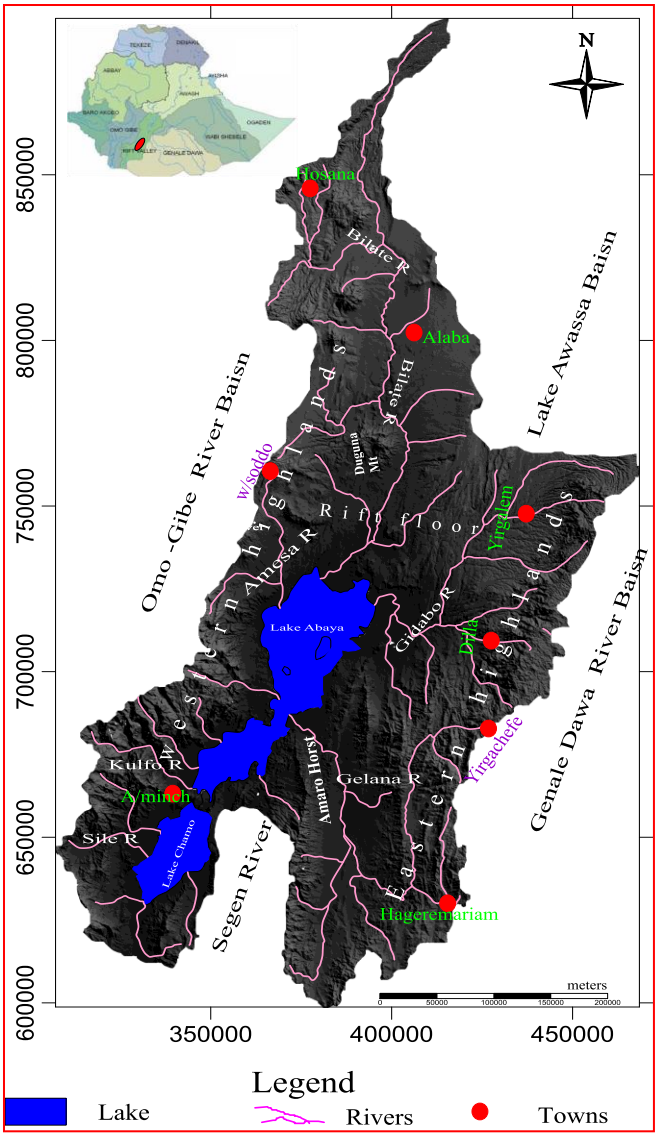

Fig 2- Location, physiographic and drainage map of Abaya Chamo Lakes basin

From Awasa Lake at about 1700masl the rift floor slopes down gradually to 0.8% in the south towards Lake Abaya and Chamo at an altitude of 1169 and 1110masl respectively (Fig 3). Thus the elevation of the rift floor is great in its central part in Awasa Lake. The Lakes aligned along the center of the valley following the rift axis are inland drainage basins which provide the ultimate discharge points for drainage from the escarpments, hills and valley sides.

The rift margins on both eastern and western sides of the Abaya Chamo Lakes basin are marked by distinctive rift fault escarpments with high relief (Fig.2). The eastern fault escarpments

continuously extend from the eastern face of Lake Awassa at NE towards Yirgachefe at SW. But towards the south of Lake Abaya, the rift splits into two narrow grabens namely: the Chamo and the Gelana grabens separated by Amaro Horst that both dying out and disappear at Latitude of 5^0 North. While the rift margin of western fault escarpment is not so clearly defined along the escarpment. In places, particularly south and north of sodo, and south of Hossana marginal faults are small or absent and the floor rises gently towards the plateau. The northern Hossana segment and Butajira plateau have sharp and very higher rift escarpment that splits into a series of smaller faults towards the rift floor. The area can be divided into three physiographic regions: the rift, a transitional escarpment, and highlands. The middle part of the basin is the rift floor bounded by highlands of southeastern and southwestern to the east and west respectively (Fig.2).

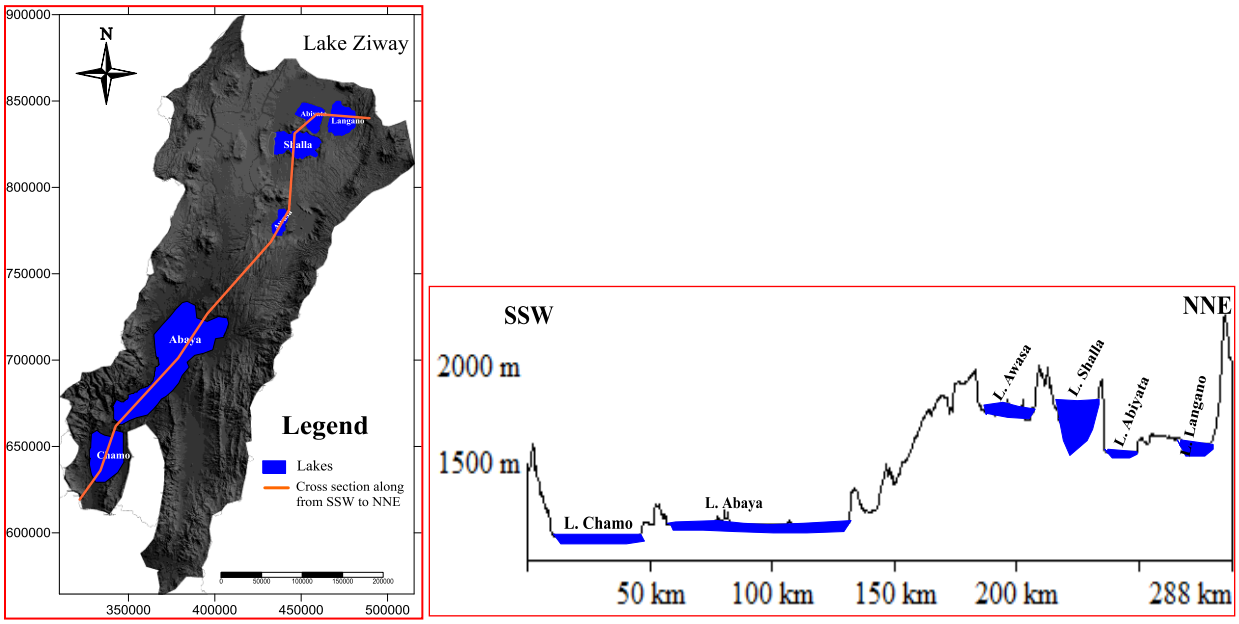

Fig 3 Physiographic profile of southern and central Ethiopian rift Lakes basins along SSW-NNE

The topography of the area strongly contrasts, ranging from Lakes and the surrounding rift floor to mountain ranges of western highlands side (west of Arbaminch to Hossana and its north) and eastern side (Hagere Mariam towards Hagereselam). There is a large topographic difference between the rift floor and the highlands. The altitude ranges from 2000 to more than 3000masl in most parts of the surface water divide in the plateau to 1169masl and 1110masl around Abaya and Chamo Lakes respectively. The lowest level of the basin is 1110masl at Lake Chamo but the highest peak is at the mountain of NW of Arbaminch and Guraghe at the northern tip of the

basin having an elevation of more than 3000masl. Escarpments are dominating landforms of eastern and western part of the basin with an elevation range of 1500masl to 2000masl at eastern and western sides of the basin. Most of them are very steep, broken only by gentle slopes made of secondary accumulation of mass waste. The escarpments are fault margins following NE-SW trends.

Isolated hills and mountains are either of volcanic centers or residues of the elevated block and are other common landforms in the area. The most examples are Amaro Horst and Damota and Duguna rhyolitic domes. The lowland plains occupy a major part of the area of the rift floor. These areas are almost flat to gently sloping plains. Within the rift floor, the system of horsts and grabens are very common as a result of tectonic processes. The topography is rolling down from the highlands towards the lakes from both sides of the Lakes.

The two main Lakes Abaya and Chamo are the result of volcano-tectonic effects having different characteristics discussed (Sileshi, 2001).

Table 1 Morphometric characteristics of Abaya and Chamo Lakes

(https://en.wikipedia.org/wiki/Lakes and Sileshi, 2001))

Phy para / Lakes	Altitude (m)	Area (km^2)	Lake area and islands (km^2)	Width (Km)	Depth (m) -maximum	Depth (m)-mean	Shoreline length (km)
Abaya	1,175	16342.2	1,162	20	24.5 (around the islands)	7.1	268.7
Chamo	1110	1857.2	317	13	14(near the middle)	14	108.1

2.3. Drainage

The contrasting topography (highlands, escarpments, and rift floor) of the study area converge the surface drainage from both sides towards the center of the basin to the Lakes (Fig 2). Bilate River flows towards south to Lake Abaya (1200masl) for a distance of about 185kms with a topographic slope of about 1% from Guraghe highlands (3000masl). Gidabo and Gelana are major Rivers that drain towards the Lakes from the eastern highlands (above 2000masl) with the slope of 2% and 0.95% respectively. Rivers flowing to the Lakes from western highlands Amesa, Kulfo and Sile flow for shorter distances and higher slopes of (54kms and 3.1%), (45kms and 4.6%) and (30kms and 6%) respectively.

The drainage systems of the basin are controlled by highland boundary older and deeper penetrative faults, Pleistocene fault scarps with calderas collapses and rift floor recent and deeper faults. These structures determine the intensity of drainage system, flow lines, drainage patterns, flow amounts and the route lengths of the Rivers. Radial, dendritic and parallel drainage patterns occur in the basin in places affected by elevation, tectonics, slope and lithologic units.

2.4. Climate

The climate of the Abaya Chamo Lakes basin like other parts of the country is largely controlled by the South - North movement of the Inter-Tropical Convergence Zone i.e. the zone of convergence of winds from northern and southern hemispheres. The marine wind flows from the Indian Ocean, humid, hot wind flows from the Atlantic Ocean through Congo basin and continental dry wind flows from Asia or Arabia govern the wind circulation system for the ITCZ (Gemechu, 1977; IRAT, 1977; Meskir Tesfaye, 2000). These wind sources control the occurrence of three rainfall regimes (uni-modal, short & long rains, bimodal) meeting in the study area. In spite of the convergence, the great variability of the climate elements, fluctuation in rainfall amount and seasonality occurs in the basin (Gemechu, 1977).

The westerly hot, humid winds from Atlantic Ocean enter south-west Ethiopia in March forming convergence zone with easterly less humid air mass flowing through Somalia and eastern scarp highlands that determine the first rainy season. Dry winds from high-pressure areas (Asia) produce short less rainy period in May. From July to September the southeasterly winds struggle with Indian Oceanfronts forming the convergence zone running above the western escarpment of MER giving the second wet season on Ethiopian plateau. October peak in regime C is due to the moisture form Indian Ocean supplying rain in south Ethiopia (IRAT; 1977, Daniel Gamachu, 1977) (discussed in section 4.2 and 4.7).

Abaya Chamo Lakes basin covers half of the southern main Ethiopian rift valley system where significant spatial rainfall variability is mapped using the long-term annual mean of 24 rainfall stations (Fig 9). Its spatial variation indicated that summer rainfall from the Atlantic Ocean is

stronger along western highlands and the northern portion of the basin whereas spring season rainfall is strong around eastern and western highlands of the southern part of the basin. The difference in source, distribution and amount of rainfall resulted in variation in the slope and D-excess of the LMWLs.

2.4.1. Rainfall data analysis

The interpretation of rainfall data of 24 rainfall station in the Abaya Chamo Lakes basin indicated seasonal and spatial variation of the long term average annual values. The altitude-rainfall relations of the long-term mean monthly Rainfall of stations indicated variability in correlations due to the prevailing wind direction and variation of altitude in the parts the basin (Table 2).

Table 2. Rainfall and altitude relation in different sectors of Abaya Chamo Lakes basin

s.no	Zone/Abaya Chamo Lakes basin	Equation	R^2	Remark
1	All stations	RF=0.44Alt+387	0.29	Effect of altitude, latitude and wind direction
2	Eastern escarpment	RF=0.05Alt+1090	0.01	Moisture receiving forests, altitude, latitude
3	Western escarpment	RF=0.5Alt+281	0.13	Effect of altitude, latitude and wind direction
	Wind ward	RF=4Alt-7534	0.94	Wind receiving mountains of Chencha,
	Lee ward	RF=0.44Alt+2225	0.1	Sparse vegetation and regime temperature
4	Rift floor	RF=0.74Alt-141	0.77	Altitude and escarpment moisture depletion

The amount of the rainfall received by different stations in different years is not consistent in different seasons (discussed briefly in chapter 4). The relation indicated that its correlation is significant only along windward of western side and along rift floor of the basin. The poor correlation in other parts is related to combined effect of altitude, latitude, wind trapping forests and seasonality of the rainfall.

The second factor that affects the distribution of the rainfall in the area is latitude. To south of the 6.3^0 degree latitude, which passes through north of Abaya Lake, the first peak rainfall period is in between March and June and the second peak in months of September and October with dry season from November to February. This tells that the area receives bimodal rainfall North of 6.30^0latitude, the peak rainfall period is in months between March to September with big rains in April, having one dry season from November to February (mono modal rainfall). The seasonal variability of the rainfall in the basin significant to the North and South of 6.30^0

latitude (Fig. 4 and 9). Bimodal rainfall pattern occurs in stations such as chencha, Geresse, and Yirgalem, whereas mono modal rainfall pattern occurs in stations such as Humbo, Wolayta soddo, and other stations on and around western escarpments.

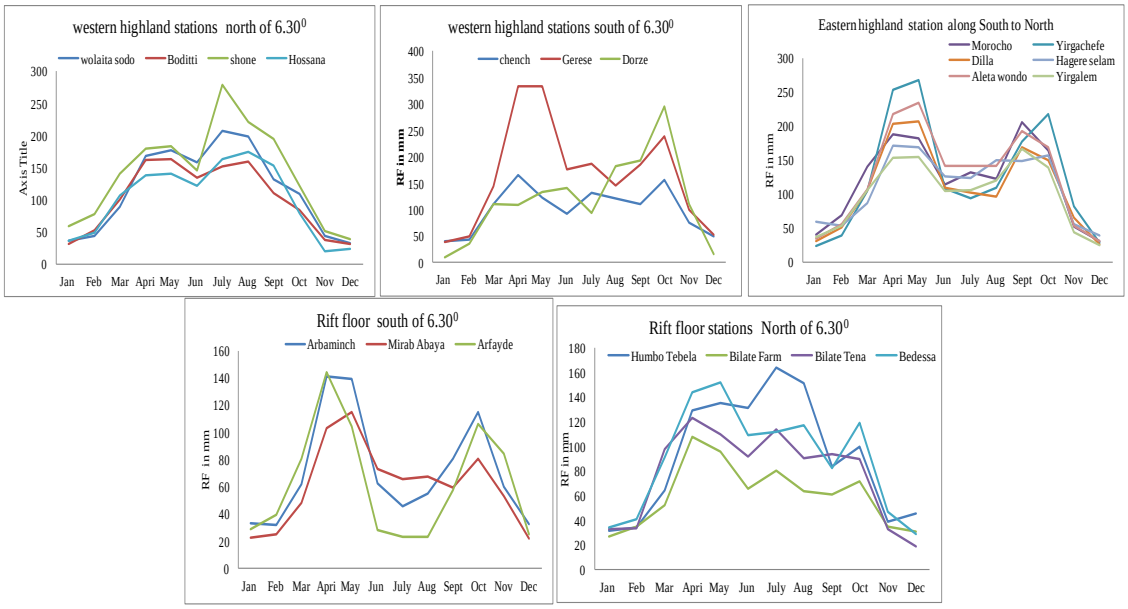

Fig. 4 a. Rainfall amount and Seasonality in the rainfall stations of Abaya Chamo Lakes basin

The basin gets minimum (693mm) and maximum (1985.2mm) amount of mean annual rainfall at Abaya (rift floor) and Gerese (South-west highland) stations respectively. The eastern and western part highlands and escarpments of the basin receive maximum rainfall amount of more than 1100mm but the rift floor and some associated areas, south of Hageremariam get less than 1100mm. Rift floor near to Lake Abaya get relatively less annual rainfall amount in between 690mm to 1000mm (Fig. 5). The annual rainfall amount of the basin is 1171mm and the seasonal proportion of annual rainfall in the Abaya Chamo Lakes basin in the summer, spring, and October to February is 47% (550mm), 35% (410mm) and 18% (211mm) respectively (Fig 13) (Annex 1).

2.4.2. Temperature

Long-term average minimum, maximum and mean monthly temperature is determined for thirteen stations in the basin (appendix 1.2). The temperature of the basin decreases with increased altitude (Fig.4b).the mean monthly temperature variation is small, but the maximum and minimum temperature showed variation with altitude. With the decrease of the altitude from

the escarpment towards the rift floor and from north to south, the temperature gradually increases. For example, at Mirab Abaya(1290 m.a.s.l.) annual mean maximum and minimum temperature is 30^{o}c and 16.5^{o}c respectively. While at Hagereselam (2700m.a.s.l.) the corresponding values are 18.8^{o}c and 8.4^{o}c (annex 1.2).

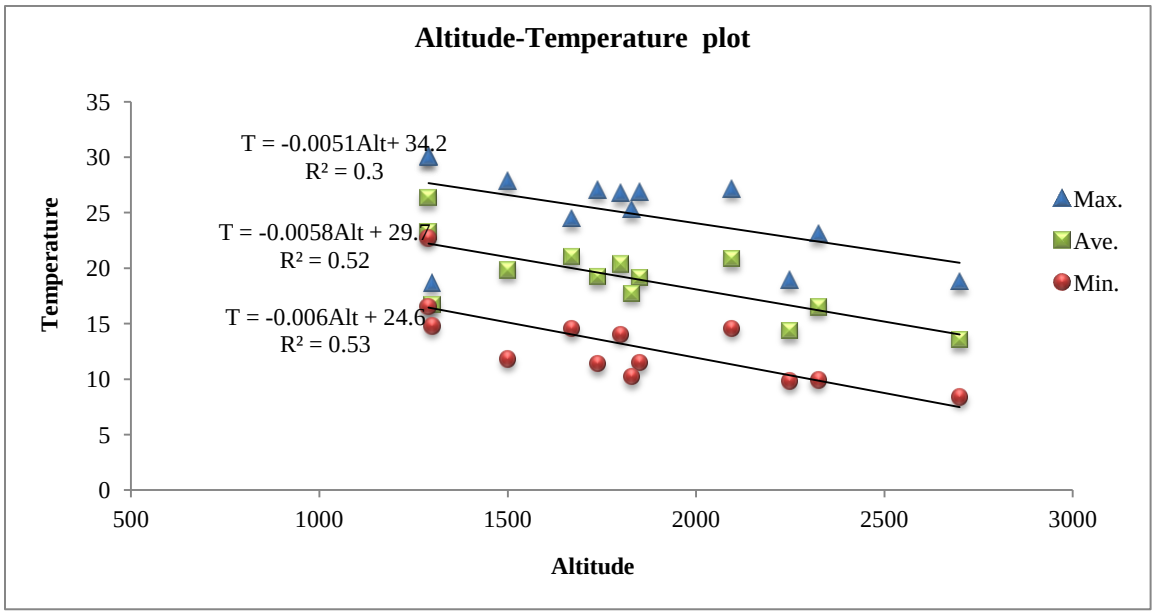

Fig 4b Altitude –temperature relation of some stations in the basin

3. GEOLOGY
3.1. Regional Geological Setting

The geological setting of the country and that of the Southern Main Ethiopian rift is briefly described based on a geological map of the Ethiopian main rift system (Merla et al., 1973; Kazmin, 1973) and its explanation and compilation (Mengesha et al., 1996). Accordingly, the Precambrian basement is the oldest formation found underlying all rocks in west, south and some areas in northern Ethiopia. The Paleozoic period is generally marked by non-deposition and erosion period, thus only a few units of this period as lower sandstone and claystone are observed in north, west and in the eastern Ogaden region (Alemayehu T, 2006). Following the Paleozoic period, land subsidence took place at the beginning of the Mesozoic period, which caused transgression of the sea to the land. This brought a vast accumulation of different types of continental sedimentary rocks, including limestone, sandstone, shale, mudstone, and marl over the Precambrian basement (Kazmin, 1979).

After the Mesozoic, stretching forces are driven by the very slow creep of rocks hundreds of kilometers deep initiated in Afro-Arabian landmass (Williams et al., 2004). This created the uplifting of Afro-Arabian continent with subsequent dissection and spreading of the landmass which resulted in the opening of the main rift in the Pliocene period (Coulie et al., 2003; Abebe et al., 2005; Chorowicz, 2005). This geologic venture starts from the Red Sea and the Gulf of Aden in the north and runs for about 6400 km southward. In Ethiopia, it forms a triangular depression of the Afar Triangle in the northeast and runs across the country splitting the central Ethiopian lands into eastern and western mountain blocks with a low-lying rift floor in the middle. As land dissection and spreading continued in response to tensional forces, extensive episodic volcanic eruptions took place, accompanied by a series of faulting which resulted in extensive extrusion of basalts along the tensional zones (Mohr and Wood, 1976; Abebe et al., 2005).

At the beginning of the Quaternary a huge ancestral Lake, stretching from the area around Chamo-Abaya lakes in the south up to Awash basin in the north existed until it separated into the present lakes by Late Pleistocene tectonic movement. Pleistocene–Holocene lacustrine sediments

cover a significant tract of ground and were deposited in a huge Lake whose level was 100 m higher during 3,500 to 2,100 years ago than today (Kazmin et al., 1980).

In early Pleistocene, mostly to the north of Lake Abaya, was filled with deposits from ash clouds, which poured from the cracks and gave rise to ignimbrites. In Quaternary, the alteration of the basic outpourings (alkaline basalts) and acidic outpourings (rhyolites, ignimbrites, obsidians, pumice, and ashes) occurred. During the Quaternary, after it had collapsed, the rift valley was covered with lacustrine stretches of which the present lakes are only remnants. Thus, the post-rift volcanic activity very often took place in the lacustrine environment and produced rocks with volcano-lacustrine facies (hyloclastic, rhyolite, and ignimbrite, diatomite, pumice, turfs, clays, etc.). Recent fractures began during the Holocene and are still considered as present day; they run NNE-SSW and have sheared all the earlier formations of the rift floor, especially in the centers. This fault belt is called Wonji fault belt (Mohr, 1967) and it is extremely dense in places. The present-day geology and landform of the Ethiopian rift in general and that of the study area, in particular, is as a result of a combined event of sedimentary (lacustrine), tectonic (faulting), and volcanic (effusive or explosive) activities.

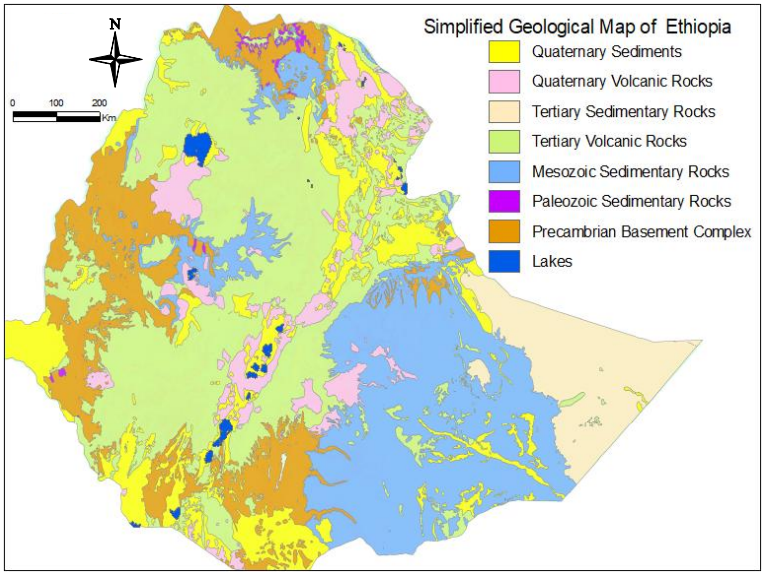

Fig 5a. Simplified geological map of Ethiopia (after GSE,1996)

3.2. Geology of Abaya-Chamo basin

Local geology of the study area and its lithostratigraphic profile is constructed from field visit and different previous works carried out in various parts of the basin, including: geological map of Dilla (Jiri et al, 2015), geological map of Hossana (Jiri et al, 2013), geological map of main Ethiopian rift (JICA, 2012), explanation of the geological map of Ethiopia (Mengesha et al, 1998), regional development plan (Halcrow *e*t al. 2008) and geological information from publications **(**Raphae¨l Pik et al. 1997; Abebe et al., 1998; Woldegeabriel et al., 1992; Giacomo Corti., 2009) and Geological Map of Omo River Project area (GSE, 1994 and GSE, 1983). The lithostrata of the basin consists older Tertiary volcanic units (Pre-Pliocene) that outcrop on the boundary/margin highlands or rift escarpment and the recent volcanic rocks cover the entire rift (Kazmin, et al 1980).

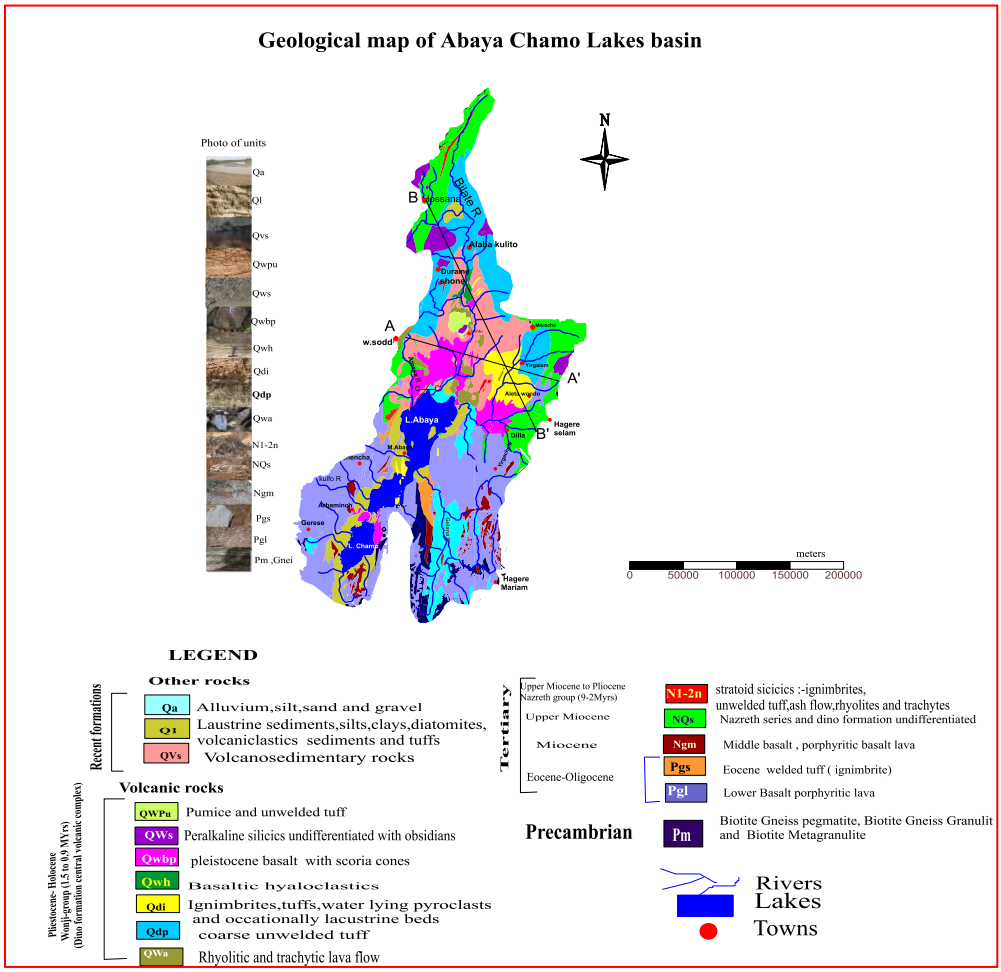

Fig 5b Geological map of Abaya Chamo Lakes basin with formations photo profile

Based on the correlation of different units of geologic formations from previous studies and missing fieldwork, there are sixteen units identified and described as follows (Fig. 4):

3.2.1. Precambrian strata

It is the oldest rock in the basin formed as a consequence of uplifting during the formation of Lake Chamo and Galena Graben (Harclow, 2008). Crystalline basement outcrops along the west of Gelana River (in N-S trend ridge Amaro Horst) in the southeastern part of the basin. It is high-grade metamorphic formation, including Biotite gneiss and related rocks. Basement crystalline rocks are formed in the Precambrian age of 960-370Ma (WoldeGabriel et al. 1990). This oldest unit covers a total area of about 1686km^2 within Abaya Chamo Lakes basin. Drilling in gneissic formation in Amaro showed that the top weathered part (3m) is underlain by the parent rock formation intercalated with clay and gravel up to the depth of 71meter. It is below 36m depth towards southeastern part of the basin (SWWCE, 2004).

3.2.2. Tertiary basalts and intercalated units (Pgl, Pgs, Ngm)

Tertiary basalts and associated formations classification consist of lower basalt, intercalated ignimbrites, and middle basalt. Different scholars correlated and classified this unit differently as Pre-rift Basalts with an age estimation of 12.6Ma - 44.9Ma (GSE, 1994). Pre-rift volcanic rocks consist Rhyolites, trachytes, ignimbrites with minor Tuff and basalt of Alaji formation at the type locality, or Aphyric and porphyritic Basalt and Salic flows covering the whole area (Halcrow, 2008) and or lower basalt which is porphyritic basalt lava (JICA, 2012).

Tertiary basalts with intercalations of ignimbrites are widely distributed in the southern half highlands both eastern (Dila – Yirgachefe) and western (along Chencha - Gerese) and escarpments of the basin (Fig.4). Tertiary basalt and associated ignimbrites cover the areal extent of about 4805km^2 towards the southern half of the Abaya-Chamo Lakes basin indicating that the southern part almost a quarter of the Abaya Chamo basin is covered by pre-rift Tertiary basalt whereas north of Lake Abaya is highly affected by recent tectonics in places pre-rift formations are not outcropped. Basalt lithology is dark gray to bluish gray porous or porphyritic lava which is weathered and as the result, olivine phenocrysts are altered into greenish brown to brown color

and plagioclase is visible. The unit has an onion-like-weathered surface (JICA, 2012). The unit is thick at places where mountains exist like in the southwest of Arba Minch, and east of Lake Chamo.

Drilling reports reveal that the depth of tertiary basalts in northwestern parts is (below 160 to 210mbgl) but exposed towards southwestern highlands (Fig.81) (SWWCE, 2004). Along the eastern highland the basalt is exposed to the south of Yirgalem through Aletawondo and towards the south. Within the rift floor where the top layers are recent formations of lowlands, from observation wells at Arbaminch and south of Lake Chamo, the lower basalt occurs at a depth range below 85m (1115mbgl) and 36m (1121mbgl) respectively.

3.2.3. Nazareth Group and Dino Formation (NQs) (Upper - Miocene)

According to (Meyer *et al*., 1978) cited in (Tefera *et al*., 1996) the name Nazareth Series was given to a thick succession of welded ignimbrites with fiamme, pumice, ash and rhyolite flows and domes with rare intercalations of basalt flows. This formation includes what was mapped by (Di Paola *et al*.. 1972) as basalts and ignimbrites of the plateau Trap Series. The Nazareth Group volcanic products are exposed to the surrounding areas along the rift margins and escarpments. The ignimbrite of the Nazareth series is considered to be products of eruptions mainly from marginal centers in the rift (Morbedelli *et al*. 1973). An age range of 9 – 3 Ma has been given to the Nazareth Series (Tefera *et al*. 1996).

Basalts and Nazareth Series are in most places overlain by green and gray ignimbrites with well-developed fiamme and water-lain pyroclastic (Dino formation) outcropping along the rift axis in the highlands and escarpments. The formation is mapped along the eastern and western highlands and escarpments covering the areal extent of about 2960sqkm. Along the eastern highland the unit outcrops at the highland periphery from southeast of Yirgachefe towards the south of Awassa and along the western part the unit is exposed to North West of Abaya Lake along highlands through wolayta sodo, Hossana and towards Guraghe highlands with some extension towards escarpment and rift in areas (Fig.4).

Boreholes drilled and screened through the formation in mapped areas revealed about the formation. Around Guraghe highland in an Adeb borehole (0412006E, 0892978N, and 3130masl) drilled for 102m depth, the underlying formation below 3m deep recent sediment deposits are dominated by fractured and weathered ignimbrites and pumice fall with intercalations of pyroclastic sand. Towards lower reliefs in Hossana, the formation is intercalated with basalt and gravel. Amacho well 7kms to the south of Hossana penetrated the formation of fractured and weathered ignimbrites and pumice fall for the drilling of 202meters (at 371477 E, 822577 N & 2186 masl). Deep wells at the northern corridor of the Gidabo River (208m) has a vertical column of composed of ignimbrites and pumices with acidic pyroclasts of Nazareth and Dino formation.

3.2.4. Stratoid silicic formation (N1-2n)

The unit is upper Miocene to Pliocene (9-2myrs) Nazareth group or the lower quaternary including silicic volcanic complexes: -ignimbrites, unwelded Tuff, ash flows, rhyolites, and trachytes. These volcanic complexes are situated along the axial zone of the Main Ethiopian Rift and are structurally controlled following the NNE-SSW direction of Tertiary major faults around north of Hossana towards Guraghe highland, east of shone and north of the Abaya Lake within the rift floor. The unit covers the extent of about 268sqkm area. The recent stages activity of the volcanoes is marked by obsidian flows, pumice, ignimbrite, rhyolites, Tuff and scoria eruptions. These structurally controlled units are major controls for the emanation of hot and warm springs.

3.2.5. Plio -Pleistocene Rhyolite (QWa)

Berhane *et al*., 1978 described Rhyolite as the remnant wall of the volcano-tectonic sub-circular collapse of the Pleistocene age. Rhyolitic flow outcrops in places along the rolling topography from sodo towards Abaya Lake (Fig.4). It is compact, porphyritic rhyolitic lava flows in association with obsidian intrusion and pumice ejecta and formed mainly from minerals such as pyroxene, olivine, and apatite (Gezahagn Y, 1980). The lithology consists of white to bluish brown rhyolitic tuff, white pumice, and hard tuff with rock chips of rhyolitic lava fragments of approx. 1 cm (JICA, 2012). In places, it is about 60m to 100m thick. Different studies correlate

the unit differently with Central Volcanic Complex (Halcrow, 2008) and also to Abaya Rhyolites (GSE, 2002). In most of the areas, this formation has less hydrogeologic importance.

3.2.6. Pleistocene coarse unwelded tuff (Qdp)

Coarse unwelded pumiceous pyroclastics constitute mainly of light tuff and ignimbrite that outcrop around northern (Bilate river basin and central part of Gidabo basin) (Fig.4). Coarse unwelded tuff covers the area of about 3000sqkmcwithin Abaya Chamo Lakes basin. From the borehole log reports, the vertical strata of the wells show that at Yirgalem town in the Aposto police collage compound well (0429701E, 0744125N, 1762masl) coarse unwelded formation is drilled up to the depth of 84m. But around shone and Alaba coarse unwelded pumice is drilled to the depth of more than 160meters deep (SWWCE, 2012).

3.2.7. Pleistocene Ignimbrite, Tuff, hyaloclastics and occasional lacustrine beds (Qdi)

The formation mainly occurs at Bilate River near Kulito, West of Yirga Alem, south of Mirab Abaya and its surrounding area along the fault line (Fig.4). The lithology consists of bluish-gray to green strongly welded rhyolitic - andesitic tuff. It is made up of a series of alternating ash, tuff and ignimbrite with highly weathered zones, alluvial deposits and sometimes Lacustrine materials covering an area of about 620sqkm. This formation hosts a number of hot and cold springs. At the Gidabo River west of Yirgalem the unit forms the wall rock of 30m high and is underlain by Yirga-Alem acidic volcano-sedimentary rocks by an unconformity (JICA, 2012, Sima et al, 2015). The unit is classified as Qdi at the type locality (Halcrow, 2008), and has a K-Ar age of 0.21±0.01My (WoldeGabriel et al. 1990). Deep well drilled through the formation at GPS location of (Grid zone 37N, 426114E, 7328751N and 1786 masl) shows that, after top 2m clay soil, the mixed formation continues up to the depth of 54m and below intercalation of clay and sand occur with the pyroclastic deposits (SWWCE,2012).

3.2.7. Basaltic hyaloclastics (QWh)

The Lithology mainly consists of dark brown tuff, volcanic sand, dark brown to black basaltic tuff breccia. The dark brown basaltic tuff breccia is distributed along the Bilate River to SSW of

Alaba (Fig.4). These strata correspond to Rhyolites, trachytes, ignimbrites with minor tuff and basalt of Alaji Formation (Halcrow, 2008). In localities, the basalt pyroclasts overlie the alternating beds of tuff, and related rocks including scoria and scoracious basalts.

3.2.8. Pleistocene basalt with scoria cones (Qwbp)

Pleistocene basalt outcrops mainly NW of Dila, north of Lake Abaya and in between Abaya and Chamo Lakes forming the bridge of God. Around Dilla, Pleistocene basalt is thick at quarry sites along rivers and overlies rhyolites and ignimbrites (Halcrow, 2008). It covers an area extent of about 1100sqkm within the Abaya Chamo basin. Pleistocene basalt is Dark brown to black in color and is massive basalt lava. This formation is strongly weathered with onion structure and is characterized by plagioclase like a strip of paper at Dila on the east side. Due to its extreme weathering, it is very difficult to recognize the layer as lower and middle basalts. Along Bilate River to the north of Lake Abaya, porous and joint developed in the layer. Artesian hot observation well drilled in the rift floor towards the 40kms north of Lake Abaya in Pleistocene basalt formation showed that the basalt is highly fractured and jointed (JICA, 2012). The narrow bridge of land divides Lake Abaya from Lake Chamo is formed by faulted blocks of basalts trending N 10°-20° E and tilted to the east. The basalts of the bridge of God are thought to be Quaternary by (Levitte et al., 1974). The basalt flows are either fine-grained or porphyric. The most recent volcanic rocks are scoriaceous basalt flows and rarely trachytic tuffs emitted from the faults; often they cover the lowest part of the hills. Pleistocene basalts of Lowlands between Abaya and Chamo where Arbaminch springs discharge at (0664748 N, 340536 E, 1279masl) are highly faulted, jointed and fractured.

3.2.9. Undifferentiated Peralkaline silicics with obsidian (Qws)

Undifferentiated Peralkaline silicics (Qws) formation is distributed within the basins where there are quaternary volcanic centers forming huge mountains (Fig.4). Undifferentiated silicic formations from Central Volcanic Complex (Qws) covers the highland areas of type localities. It is formed from alternating units of acidic lava flows and pyroclastic flow deposits of both acidic and basic origin. The main units are tuff, rhyolite, scoria, pumiceous tuff and pumice (the topmost units). The Central Volcanic Complex formation to the north of Durame overlies the

Dino formation. The Rhyolite quarry situated in the southern part of the mountain is assumed to be directly overly Dino Formation. This unit pinches out in the southern part after a short distance. The wells drilled in the SE valley of the mountain show that this unit is absent. NE-SW faulting and rifting probably defining the contact between the Dino Formation and the Ambericho Central Volcanic Complex unit. Well drilled at the top high elevation of the mountain (at Serera GPS location of 0368736E, 0808334N, and altitude of 2470masl) showed that for the depth of 280m (2190mbgl) the whole formation is alternating weathered and fresh Rhyolite after the top 40m topsoil and ignimbrite.

3.2.10. Holocene Pumice and welded tuff (QwPu)

Holocene volcanics include lithologic units consisting of pumice fall, pumice flow, brown rhyolitic lava and obsidian originated by Dugna volcanic and the surrounding uplifts and volcanic centers in the north of Lake Abaya (Fig.4) The uplifts have rhyolite lava with obsidian, fine pumice fall to the upper part. In the mapped area the unit has area cover of 130sqkm. The strata overlay acidic volcano-sedimentary rocks by an unconformity. The recent basalts are formed associated with pumice and obsidian and in places, there are hot grounds and gas emanating from the uplifts (Halcrow 2008). The Holocene pumice unit is about 400m thick at Duguna from the top of the Bitena village towards Bilate river base. Deep well drilled at Duguna Damot Shinka to the depth of more than 250mts penetrated Holocene pumice and Tuff intercalation and the water disappeared after conducting pump testing due to highly permeable pumice layer that could not retain the water (SWWCE, 2012).

3.2.11. Acidic Volcano-Sedimentary Rocks (QVS)

The Acidic volcano-sedimentary rock unit has a different grouping by different studies. Strata around the flat plain area around Hossana to Amacho correspond to Qdi and N1_2n（Stratoid Silicics (Halcrow, 2008) and to rift Floor Ignimbrite and colluvial-alluvial gravel, sand, silt and pyroclastic（EWTEC, 2008) and to Dino Formation and Qvs in GSE (2003). For this study, it is grouped to as QVS (volcano-sedimentary rock) which cover the plain areas of about 1910sqkm. This formation is classified as other rocks formed on the surface of Holocene volcanics. It is the product of tuff with the white pumice flow, their alternations, and Lake land environment

formation. The unit covers widely in the southern rift floor of the area to the north of Abaya Lake. The rock unit is mainly distributed in wide flat plains along the Bilate River from west of Alaba kulito towards the mouth of Lake Abaya and along the tributaries of Gidabo river. A volcano-sedimentary rock is characterized by eroded topography over a wide area. From the well lithologic log reports and site visit, the formation is a volcaniclastic rock with pumice lamination, clastic sand and silt alternation by an unconformity. Deep wells drilled in the piedmont plains south of wolaita Soddo town (Fig.4) show that wells have strata composed from tuff, pumice, and other volcanic rocks which become sand and silt or volcaniclastic rock to the depth up to 180meters.

3.2.12. Lacustrine deposits (Ql)

The mode of origin of lacustrine deposits could be related to ancient lake deposits, water deposited volcanic ejects, or coarse sediments intruded into the lake by flooding (Tenalem Ayenew, 1998). The lacustrine sediments are intercalated with Pliocene to Pleistocene ignimbrites both on the rift floor and rift shoulders and re-deposited volcanic ash and tuffs and are mainly represented by sand and silt. The major components of the sediments are volcanic in origins such as pumice and volcanic ash, obsidian, Rhyolite and basaltic rock fragments (Tsegaye et al., 2005; Bevenuti et al., 2002). In the rift floor inter-layering of primary air fall pyroclastic deposits and lacustrine deposits are common. The oldest sediments are lacustrine diatomite, tuffaceous clays, and silts interbedded with basal ignimbrites of the Nazareth group. These deposits are commonly exposed as lacustrine environment deposits adjacent to the Lake Abaya and Chamo which have physical characteristics of soft, powdery, easily erodible, and whitish in color and light in weight. They can be either ancient (older) or recent (younger) lacustrine deposits. The recent lacustrine deposits constitute the plain areas which are situated on the edge of the Lake Abaya and Chamo. In places where the lacustrine deposits occurred, the plains are separated each other by the structural basaltic ridge, running NNE-SSW or N-S. Lacustrine deposit underlies various older volcanic formations and overlies the recent alluvium. Except in places where the tectonically controlled rocks occur. Drilling reports in the lacustrine environments, including Arbamich University, shelle, and lowlands of Burji areas reveal

lacustrine sand for depth up to 110meters in lower reliefs. But towards rift escarpment, the depth of the lacustrine formation is shallower.

3.2.13. Recent surface formations-Alluvium, silt, sand and gravel (Qa)

Recent deposits in the area include soils and alluvial sand deposits. The floodplains of the Rivers overlie the pyroclastic flow or fall deposits. The river basins draining the mountains surrounding the lakes have discharged colluvial and alluvial deposits into the rift valley in the form of piedmont slopes and large alluvial fans. The material of the Piedmont slope is fairly coarse and angular. The alluvial deposit consists mainly layers of silt, sand, gravel, and pebbles with clay and silts dominating in the deltaic area. This formation has gradually pushed toward the center of the valley and has probably covered the lacustrine deposits in many places along the Lakeshore. The lacustrine deposits are chiefly composed of silts and clays. In places, the alluvial sediments occur together with lacustrine where the river meanders. Recent formations (Alluvium and Fluvial deposits mainly occur in the lower course of the Bilate River along its gentle slope, joining Abaya Lake, the major downstream courses and floodplains of the Gidabo River and its tributaries. Colluvial and outwash debris is found widespread in the area, particularly along the foothills of the major fault scarps forming a drainage line along the Galena River and around lowlands of Gidole (Fig.4).

3.3. Geological structures

Uplift, Doming and eventual rupture of the Afro-Arabian region resulted in the formation of the East African Rift system oriented in the NE–SW and NNW–SSW directions. The initial sagging of the Main Ethiopian Rift began around 15 to 14 million years (Ma) ago. An important event in the rift development took place around 10 Ma ago (Kazmin et al., 1978; Davidson, 1983). This development caused faulting of the pre-rift volcanic succession. Ethiopian main rift valley lakes basin margin and rift floor are known by its NNE-SSW fault systems (WoldeGabriel et al, 1990). Fault system in the northern Rift Valley Lakes Basin is characterized by the development of continuous major faults which has a big displacement with minor parallel faults and fault zones associated with volcanic activity in the rift floor. While Precambrian and Neogene fault system

in southern Rift Valley Lakes Basin is neither continuous nor regular. It indicates that the basin is well developed in the northern part and poorly developed in the southern part.

In southern Ethiopia, the rift valley is distinctly separated from the adjacent plateau by series of normal step faults which have large throws with steep fault planes usually trending parallel to the NNE-SSW rift axis. Within the study area, the rift valley is 70 to 90kmts wide. The normal faults displaced from 200 to 600mts mostly from the rift margin highlands towards escarpments and lower reliefs along the western part and from 500 to 1000mts along the eastern margin of the Abaya-Chamo basin. Along the western margin, higher displacement towards lower reliefs occurred around the north tip (Guraghe highlands) and the displacement decrease towards the south.

Different sets of fault systems occur within the study area, including NNE-SSW, N-S, NNW-SSE and semi-circular collapse faults (Fig.31). The NNE-SSW and N-S trending fault systems are the dominant main border tertiary faults which extend for long distances up to hundreds of kilometers. Tertiary tectonics in the western side of the study area includes long boundary NNE-SSW faults (West of Lake Chamo to North tip of the basin). Parallel trending tertiary faults run from west of Lake Chamo through Arbaminch along the west margin of Lake Abaya forming the lake boundary (Fig.4). To the north of Hossana towards Guraghe highlands, the main border tertiary fault is almost continuous. Where there is an interruption of main boundary faults there is a minor boundary fault aligned in the same direction. The interruption of the boundary major tertiary fault could be related to the formation of big volcanic centers like along western highlands. Minor boundary faults aligned N-S direction clearly observed towards the southeast and north of Lake Abaya. The eastern margin of the Abaya lake basin is well developed and it is defined by a more or less continuous NNE-SSW system of boundary faults from SE of Lake Awassa along towards Dilla. The major boundary fault from south of Dilla is bifurcated by the N-S striking Amaro Horst bounded by N-S major faults. Amaro Horst separates the Ganguli basin in the west of the Gelana depression in the east. The minor escarpment and boundary faults in the eastern face align both along a NNE-SSW and N-S faults. The N-S fault systems penetrated much of Gelana basin and pass towards the western face of Lake Abaya with interruption where the NNE-SSW fault system cut Gidabo basin delta areas (Fig.31).

NE-SW and perpendicular NNW-SSE Precambrian, Eocene and Oligocene fault systems are mainly distributed in the margin and the faces of the lakes where fault systems making the Lake boundary and align the islands. These fault systems control the development of the drainage basin of Gelana, the appearance, and disappearance of some streams in Lake Chamo basin and Amaro Horst. The highland and escarpment of faults of these times are responsible for the recharge of the highland rainfall and emanation of small and medium cold springs. Quaternary tectonic system (Pleistocene to Holocene Fault System) in the area includes sub-circularcalderaa collapses and wonji fault en-echelon swarm fault series.

The sub-circular collapses are observed in the basin (Fig.31 and Fig.39) and in places cutting the Pleistocene ignimbrites with the displacement of 60-200meters. These collapses are aligned along the direction of NNE-SSW fault systems. The rift floor is marked by intense and fresh faulting (active wonji fault belt) (Mohr, 1967). The northern part of Lake Abaya is very densely affected by recent tectonics and volcanic eruptive centers. The basalt cliff that forms the NNW shore of Lake Abaya is one of the Holocene rift floor faults. Within the rift floor fault belt, there are minor Horst and Graben structures " rift-in-rift" structures with vertical escarpments varying from few to 50meters and determining the occurrence of young volcanic centers. Hot springs and fumaroles emanate from the foot of these structures. Another set of rift floor faults that are responsible for the groundwater exchange from Gidabo basin and Awassa lake basin towards Lake Abaya basin. Tectonics below the Lake bottom could be understood from the islands and land surface tectonics around the Lake. The two islands of Lake Abaya are aligned along the boundary fault direction (NNE-SSW) and N-S. The southern end of the Lake down throws to the north (Jiri, 2014). These intensive tectonics occurred within the lake bottom could be the cause of relatively high salinity of the Lake as a result of emanation of hot springs through open faults and fractures feeding the Lake. In between the two Lakes (Abaya and Chamo), quaternary volcanics form the so-called "bridge of God" spaced about 4 to 6kms in different parts of the bridge. A different set of tectonics occurred in the area, including the eruptive centers and NNE-SSW trending wonji fault belt systems.

4. CHARACTERIZATION OF THE STABLE ISOTOPIC *(ὁ^{18}O AND ὁ^{2}H)* COMPOSITION OF RAINFALL AND ITS SPATIAL VARIABILITY

4.1. Background

The investigation of surface and ground water hydrology initially requires the understanding of the origins of the rainfall. The stable isotopic composition of rain waters (Ő^{18}O and Ő^{2}H) is used in the characterization of the composition and compare the variety of precipitation moisture sources and its derivative processes. The difference in the sources and processes results in the variation of isotopic effects for local stations. Several scholars undertook scientific study of the Ő^{18}O and Ő^{2}H composition of rainfall waters of the IAEA/WMO stations in Ethiopia (Dansgaard, 1964; Rozanski et al., 1993; Levin et al., 2009; Kebede, 2004; Kebede and Travi, 2011) with special emphasis on the anomalous Ő^{18}O and Ő^{2}H composition of Addis Ababa rainfall compared to other stations of neighboring countries in the region.

But the isotopic signals of precipitation, its origins and variations in different physiographic sectors of the Abaya Chamo Lakes basin are not dealt. Therefore, the organization of the stable isotopic (Ő^{18}O and Ő^{2}H) composition of the rainfall waters in Abaya-Chamo Lakes basin and its environs, assessing the comparative relationship with the prevailing moisture sources and characterization of the rainfall based on its isotopic effects deal with this particular study to gain the insight of the sources of the recharged water in the basin.

For this purpose, the precipitation isotopic composition of (Ő^{18}O and Ő^{2}H) of the IAEA/WMO stations (in years 1999/2000) in and around the study basin (annex 1.2) is used. The isotopic composition of (Ő^{18}O and Ő^{2}H) shallow groundwaters (Edmunds et al, 2001) and River waters (Kendall and Coplan, 2001) are used as a proxy for rainfall isotopic composition in places when the long-term data set are not available.

4.2. Source of precipitation to Ethiopia and southern rift valley areas

The rainfall regime of Ethiopia is under the influence of two major ocean monsoons of the Indian and Atlantic (Graffits, 1972; Gemechu, 1972). Several convergence zones are regionally superimposed and the variability of sea surface temperature in different seasons associated with

Lakes, topography and maritime that makes the distribution of the rainfall pattern complex and change rapidly over a short distance (Nicholson, 1996). The seasonal and annual rainfall variations are the results of micro-scale pressure systems and monsoon flows which are related to changes in pressure systems (Chamberlin, 1996). The moisture-bearing winds enter into Ethiopia in different seasons and the complexity of the Ethiopian topography makes the distribution of rainfall highly variable due to the formation of local convective activities along the wind and lee wards (Nicholson, 1996; Kebede, 2004). As a result, the climate regime of Ethiopia is distinct compared to similar latitude regions due to its location between the Sahel and equatorial Africa, the proximity of Ethiopia to Indian ocean and /or continental rainfall sources and Orographic enhancement of rainfall amount (Kebede, 2004; Kebede and Travi, 2011).

However, separate seasonal sources of rainfall in Ethiopia from from the Indian Ocean, humid and hot wind flows from the Atlantic Ocean through Congo basin, and continental dry wind flows from Asia or Arabian govern the wind circulation system. The intertropical convergence zone (ITCZ) governs the zone of convergence of winds from northern and southern hemispheres (IRAT, 1977; Gemechu, 1977; Meskir T., 2000; Chamberlin and Okoola, 2003). The characterization of Ethiopia into three seasons as autumn “Bega’ (October to January = ONDJ), spring ‘Belg’ (February/March to May=MAM) and summer ‘keremt’ (June to September=JJAS) is based on the monsoon from these sources (NMA, 1996).

The northwestern plateau (NWP) gets annual average rainfall of 75% and 25% during the summer and spring seasons respectively (Kebede, 2004; Kebede and Travi, 2011) whereas the southern Ethiopia rift valley (Abaya-Chamo Lakes basin) gets 47%, 35% and 18% of annual rainfall during summer, spring and OND seasons respectively. This indicated the difference in the distribution of the rainfall in the area as a result of the variation in the migration of the intertropical convergence zone (ITCZ) and associated wind pattern behavior (Telford, 1998) (Fig. 5 and Fig.6).

Understanding the heterogeneity in the source and rate of rainfall, and classification of similar variability areas could be used for regional water resources management and rainfall prediction in the area (Abiy G. et al., 2014). In this part of the thesis the variations in isotopic composition

of the rainfall in the Abaya Chamo Lakes Basin are traced for its moisture sources and mechanism of the migration of winds along different topographic settings.

a. Spring season (March April May)

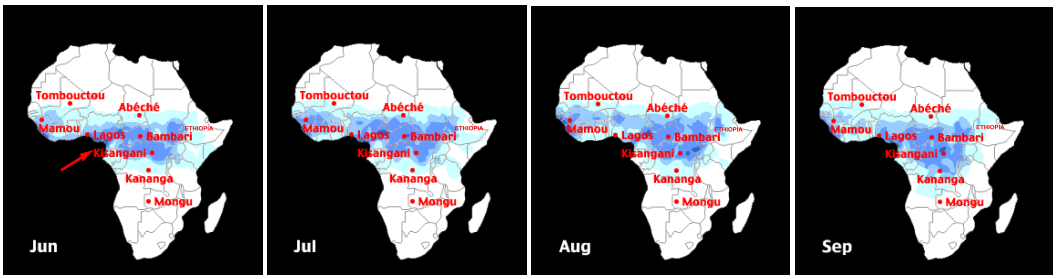

b. summer season (June, July, August and September)

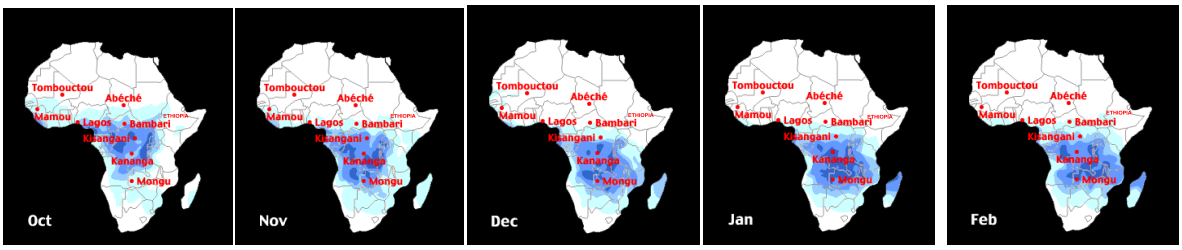

c. October to February (Autumn) season

Fig 6 a - spring season, b - summer season and c- autumn season migration of the intertropical convergence zone (ITCZ) in East and central Africa shows seasonal precipitation patterns across the continent and in Ethiopia. The blue shading on the map shows the areas of highest cloud reflectivity, which correspond to the average monthly position of the ITCZ and the red arrow showing the wind migration direction (http://people.cas.sc.edu/carbone/modules/mods4car/africa-itcz)

The annual rainfall distribution of Ethiopia (Fig.9) is the admixture of the three seasons. In spring (March, April, May) the ITCZ is moving from south to North crossing Ethiopia (Fig. 5a). The hot, humid winds from the northern Indian Ocean enter south Ethiopia in March. Winds from the northern Indian Ocean, which is less humid air mass flowing through Somalia and eastern highlands of the southern main rift valley determine the first spring rainy season in March to May and extend its influence to the western face of the main Ethiopian rift (Fig.6) boundary of Indian Ocean influence. During the spring season, southern Ethiopian rift valley and

the southwestern parts of the country is influenced and gets the annual proportion of about 35% in the southern Lakes basin (Fig.12).

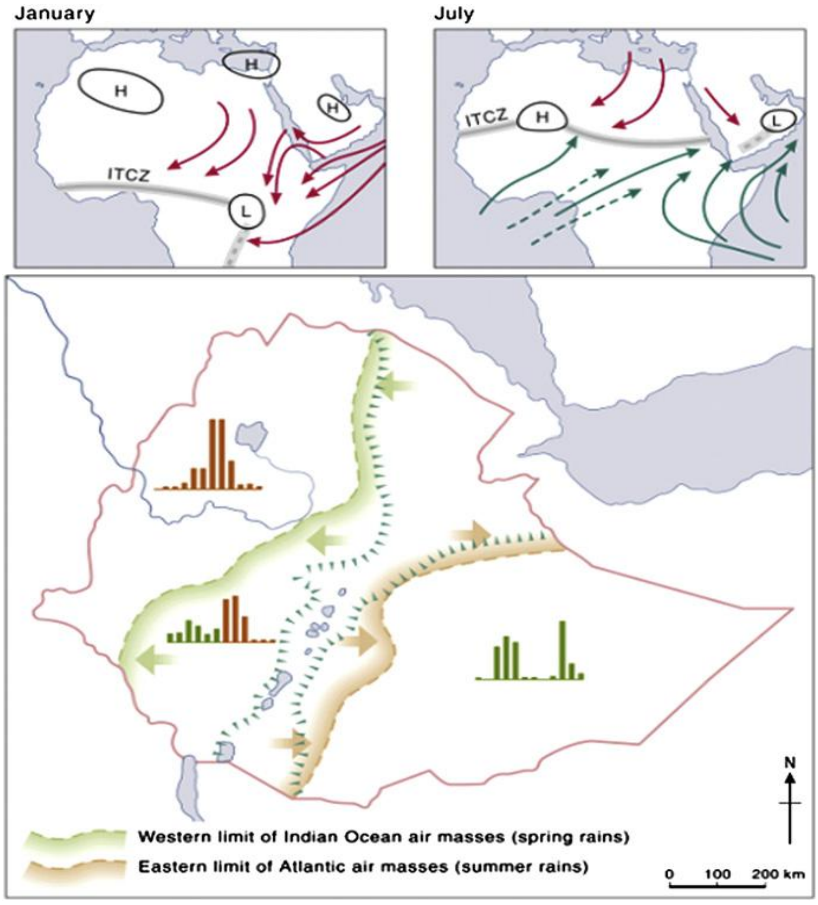

Fig 7 Seasonal migration of the Inter-tropical convergence zone (ITCZ) and associated wind pattern in Ethiopia (Telford, 1998).

In summer (June, July, August, September) the ITCZ is located in northern Ethiopia and the region is under the influence of the southwesterly and southerly monsoon flows (Fig 5 and Fig.6). The southwesterly and southerly flows bring moisture from three sources, including: low-level moisture pulled from the Congo vegetation basin, from the Atlantic Ocean and partly from the Equatorial Indian Ocean (Gemechu, 1977; Kebede, 2004). Open continental water bodies (such as tropical lakes and Lake Victoria) may also play an important role in feeding the low-level southwesterly flows (Kebede and Travi, 2011). Southern Ethiopia rift valley including Abaya-Chamo Lakes basin gets almost 47% of the rainfall during this season (Fig.12).

Between October and February, the ITCZ is located south of Ethiopia (Fig.5c). This results in a northerly flow of dry and cold air from the Arabian continent (Kebede, 2004). The southward flow brings some moisture from the Arabian Sea and Northern Indian Ocean to the eastern lowlands bordering the South Eastern highlands and passes to southwestern highlands producing rainfall. October peak rain in the southern rift valley is due to the moisture from the northern Indian Ocean and cold air from northerly supplying rain to southern Ethiopia (IRAT; 1977, Gamachu, 1977). During these months the southern rift valley gets about 18% of the annual rainfall (Fig.12).

4.3.Spatial distribution of rainfall and its variability in Abaya-Chamo Lakes basin

4.3.1. Altitude – Rainfall relation

Abaya Chamo Lakes basin covers half of the southern main Ethiopian rift valley system where significant spatial rainfall variability is mapped using long-term annual mean of 24 rainfall stations (Fig.7 and Fig.9). The basin gets minimized (693mm) and maximum (1985.2mm) amount of mean annual rainfall at Abaya (rift floor) and Gerese (south-west highland) stations respectively. This showed that the eastern and western part highlands and escarpments of the basin receive maximum rainfall amount of more than 1100mm but the rift floor and some associated areas to the south of Hageremariam get less than 1100mm. Lower lands near to Lake Abaya get relatively less annual rainfall amount in between 690mm to 1000mm.

The relation of rainfall to altitude in three sectors (eastern highlands, western highlands, and rift floor) of the basin (Fig.8) indicates that the spatial distribution of rainfall is controlled not only by altitude but also the latitude and prevailing wind direction carrying moisture to the basin affect it. The 24 rainfall stations in the basin showed the altitude-rainfall relation is RF (mm) = 0.52 ALT (m) + 256 with a correlation coefficient of R^2=0.5. The correlation of the rainfall to altitude along eastern highlands and western highlands is very poor, but it is strong where R^2=0.77 in rift floor.

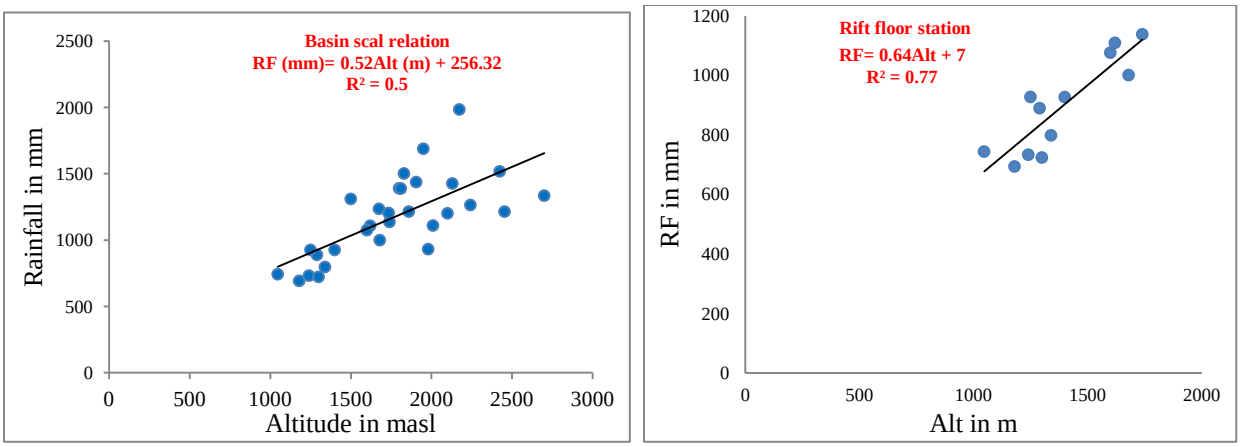

Fig 8 Relation of Altitude to rainfall of the entire basin and rift floor stations

4.4.Seasonal variability of the rainfall distribution in Abaya-Chamo Lakes Basin

Abaya Chamo Lakes basin gets a seasonal proportion of 47%, 35% and 18% of annual rainfall in summer, spring, and October to February respectively (Fig.12). The variability in amount could be related to the difference in moisture sources and variation in elevation. Eastern highland of Abaya Chamo Lakes basin gets bi-modal rainfall along its N-S transect (Fig.7 and Fig.9, annex 1.1) from Morocho towards Hageremariam (153mm to 268mm) during April and May. The second peak in these areas is in September and October (148mm to 217mm). In the area, the summer (JJAS) rainfall (93mm to 142mm) is relatively lower than the spring (MAM) and October peaks. The spring rainfall is dominant in the eastern highlands and escarpments where the humid moisture-bearing winds from the northern Indian ocean climb to the highlands of the basin through Somalia lowlands (Fig.5, Fig.6) and influence Omo-Gibe basin to the west of Southern Ethiopian rift valley (Telford,1998).

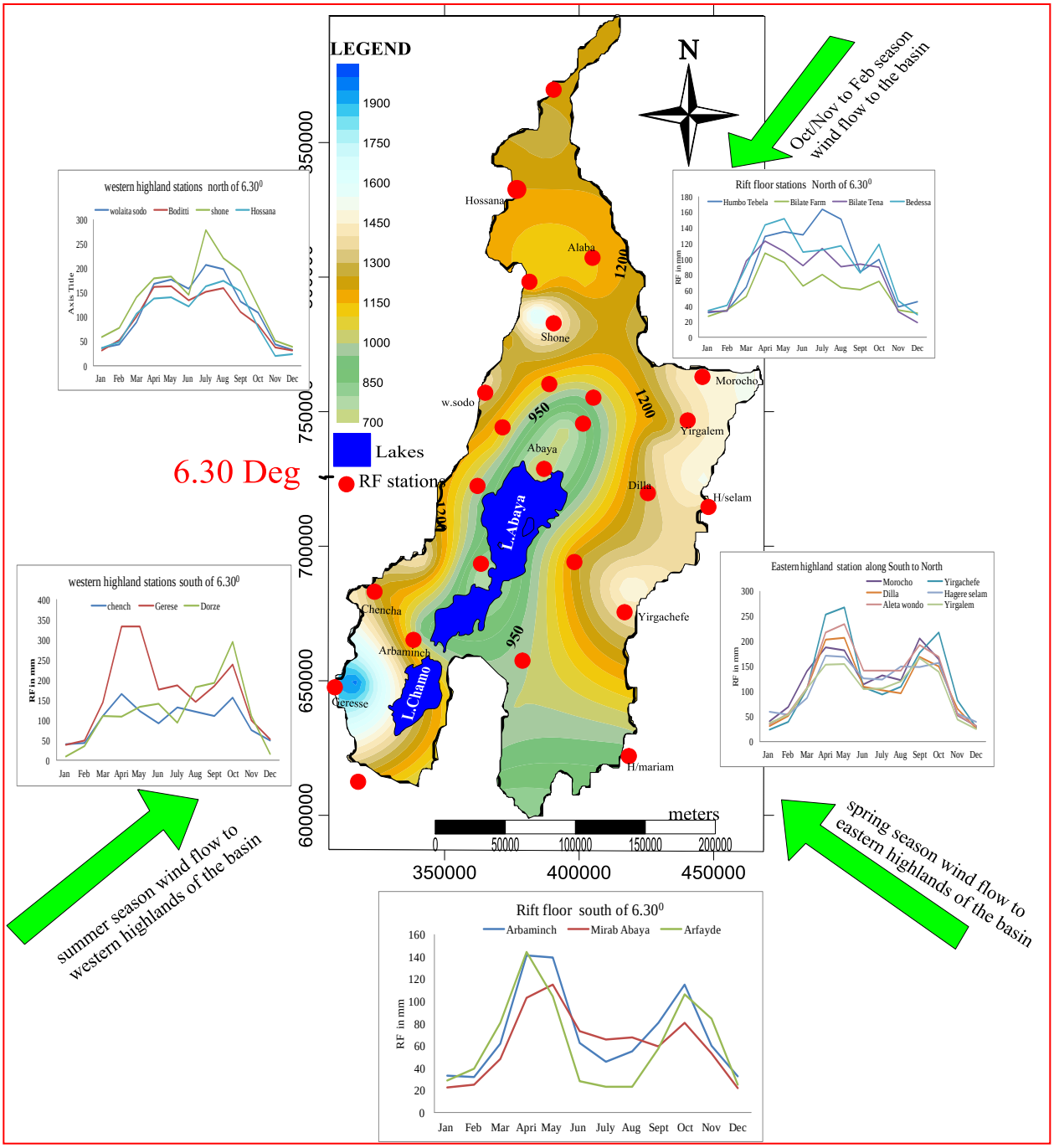

Fig 9 Spatial distribution of annual rainfall amount in Abaya Chamo Lakes basin with prevailing wind direction arrows and inset variable annual average plots of different areas (***to North of 6.30⁰ uni-modal rainfall pattern in eastern and western parts, and South of 6.30⁰ bimodal rainfall pattern in eastern and western part, rift floor stations also show bimodal pattern***) .

Spring rain mainly concentrates on the highlands of southwestern and eastern parts of the basin and generally decreases northwards. This is related to the period when the ITCZ begins to influence south and southwest Ethiopia in its south-north movement (Fig.10). The spring season

rain descends west to the rift floor of the basin and more pronounced to south of 6.30^0 latitude where the summer rainfall is lower (Fig.11) and ascend to southwestern highlands of the basin (Gerese and Chencha) to condence and supply with high seasonal rainfall of 810mm greater than even at Yirgachefe (626mm). This is related to the effect of the high elevation of the southwestern highlands where the level of cloud condensation is higher.

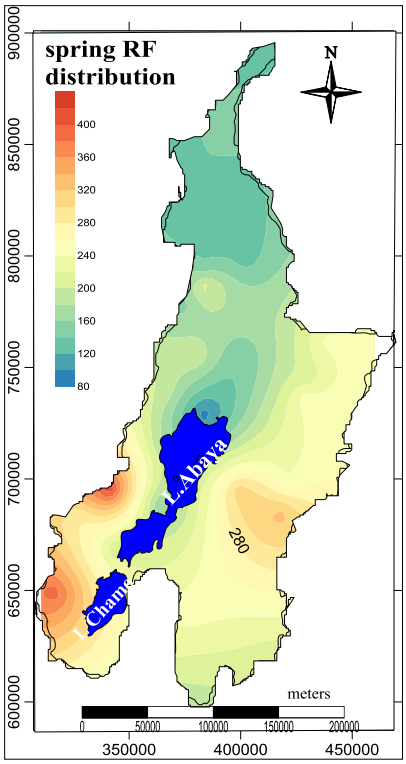

Fig 10 spring rainfall distribution

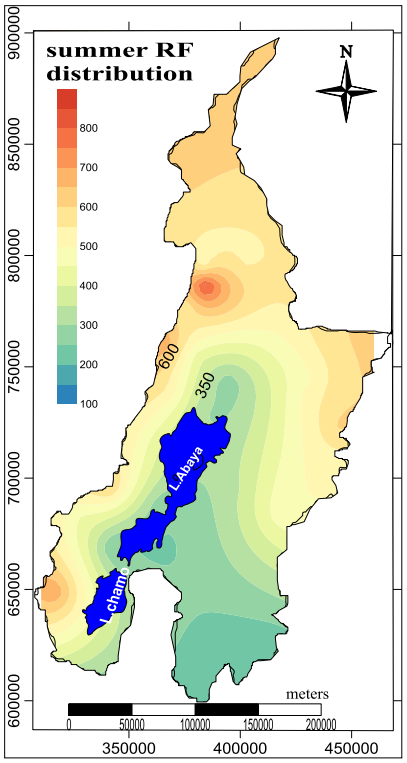

Fig 11 summer rainfall distribution

During the summer season, the southwesterly and southerly moisture from the Atlantic Ocean and the equatorial Indian Ocean enter towards southwestern highlands of Abaya Chamo Lakes basin extending towards east to the western face of Genale Dawa highlands through southern main Ethiopian rift floor (Telford, 1998). The south-west equatorial westerlies ascend over the southwestern highlands and produce the main rainy season over most parts of highland Ethiopia. The southerly winds from the Indian Ocean, despite the fact that they lose their moisture over the East African highlands, are blowing over the eastern lowlands of Ethiopia, where their influence on rainfall is minimized due to the effect (Kassahun 1999). Rainfall stations along western highlands and escarpments of Abaya Chamo Lakes basin get a higher proportion of annual rainfall during summer (JJAS) (Fig.12) than the spring season (MAM). The peak period is in July and August and sometimes extends into September. To the south of

6.30^0 latitudes along western highlands and the escarpment of the basin, the summer rainfall is lower compared to north of 6.30^0 latitudes (Fig.11) related to orographic effect. Summer rainfall is higher on Southwestern highlands, but it becomes less towards rift floor and eastern highlands (Fig. 12). The extreme low JJAS (summer) rainfall amount of southern and eastern stations Arfaide, Burji and Amaro Kelle is related to the prevailing summer wind , the low altitude and re-evaporation of the rainfall.

The October to February rainfall is less in proportion (18%) in the Abaya Chamo Lakes basin and its distribution is more or less similar except in some highland stations (Fig.12). This could be linked to the position of entry of dry and cold air from the Arabian continent and the southern Indian ocean (Kebede, 2004) where the position of the ITCZ is to the south of Ethiopia (Fig.5 and Fig.6c).

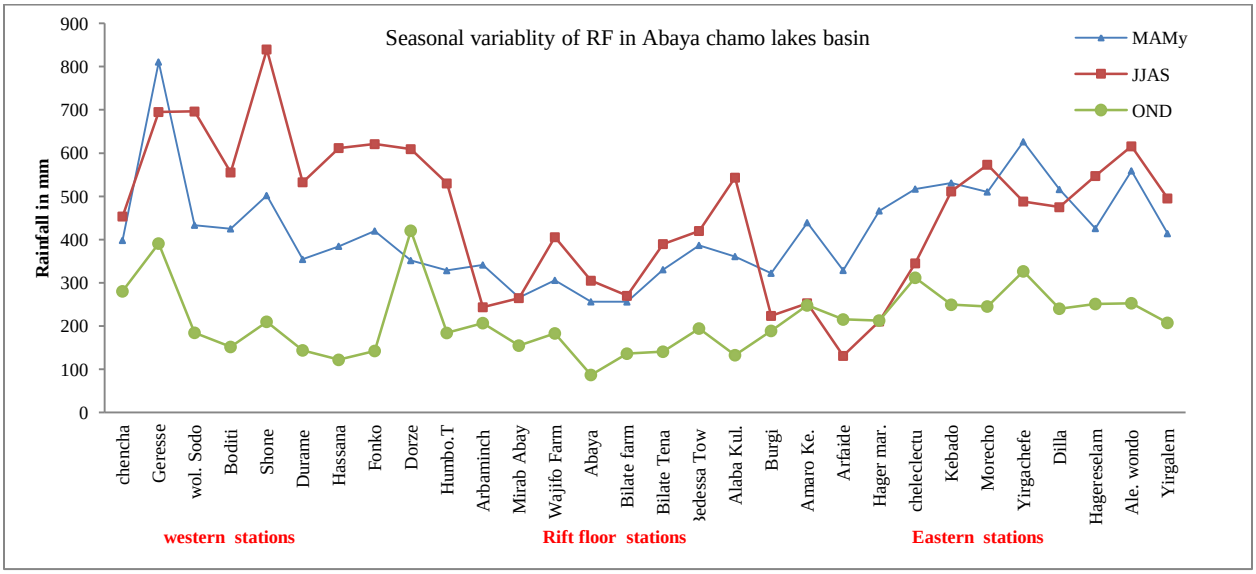

Fig 12 the proportion of seasonal variability of rainfall in stations of Abaya-Chamo Lakes basin

The North Western Ethiopian Plateau (NWP) gets much of its rainfall during the Sahel summer (JJAS) and little rain during spring (MAM) with the annual average of 75% and 25% rainfall respectively (Kebede, 2004). Abaya Chamo Lakes basin gets rain during Sahel summer, spring and October to December with the average proportion of 47%, 35% and 18% of annual average rainfall (Fig.12). The scenario in two areas indicates the difference in controls for the amount

and distribution of the rainfall in the country that further shows the complex and hybrid of moisture sources (the humid and arid climates) and orographic enhancement (Nicholson, 1996).

4.5.Isotopic composition (ŏ^{18}O and ŏ^{2}H) of Rain waters in Abaya Chamo Lakes basin

Scientific principles used in the hydrological investigation with stable isotopes of ŏ^{2}H and ŏ^{18}O indicated the concept of meteoric water line and the isotope effects (Gat, 1981). The stable isotope composition of precipitation from different parts of the world resulted a linear line (δ^{18}O‰ versus δ^{2}H‰) called the Global Meteoric Water Line (GMWL) or Craig line (Craig, 1961) with the equation $\delta\ ^{2}H = 8\ \delta\ ^{18}O + 10‰$ VSMOW (Fig.13).

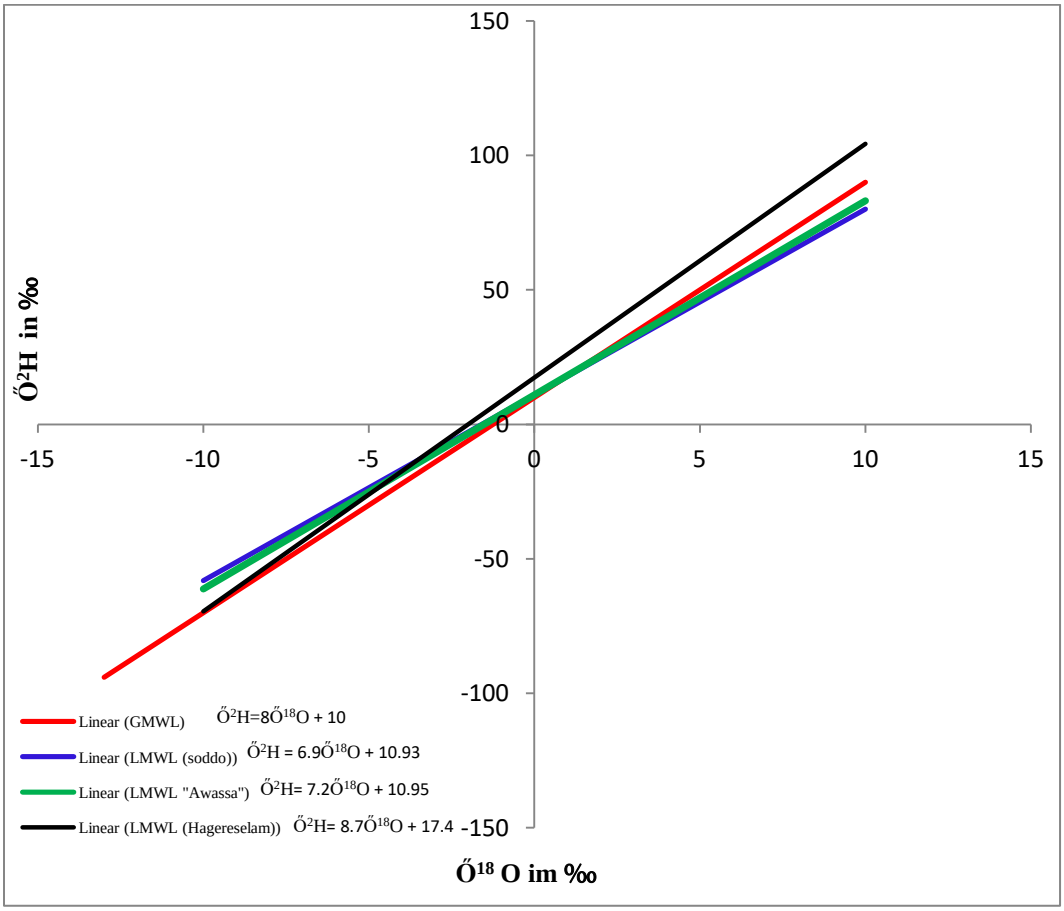

Fig 13 Linear relation of δ^{18}O‰ vs δ^{2}H‰ of precipitation at three GNIP station (Data 1999/2000, IAEA), the red regression line represents the Global Meteoric Water Line (GMWL), the blue, green and black regression lines represent the Local Meteoric Water Lines (LMWLs) at Sodo, Hawassa and Hagereselam stations respectively.

The local meteoric water lines (LMWLs) are made based on the relation (δ^{18}O‰ versus δ^{2}H‰) of one year GNIP data from three local precipitation stations of the western highlands (Sodo),

eastern highland (Hagereselam) of Abaya Chamo Lakes basin and rift valley (Hawassa) nearby basin of the study area (IAEA , 1999/2000). The rainfall stable isotopic composition could be traced using $\delta^{18}O$ and $\delta^{2}H$ as proxies from cold springs (Edmunds et al, 2001) and Highland River waters (Kendall and Coplan, 2001) and (Mekenzie, 2001) to understand the spatial distribution of isotopic composition.

The average values of ($\delta^{18}O$‰, $\delta^{2}H$‰) of one-year local precipitation stations of Hagereselam (-1.97‰, 0.27‰), Awassa (-0.72‰, 5.83‰) and wolaita sodo (-1.44‰, -0.96‰) showed deviation from GMWL average (-4‰, -22‰). The GMWL and three LMWLs (Fig.13) intersect at the ($\delta^{18}O$‰, $\delta^{2}H$‰) axes at different points. The slope and D-excess of the yearly precipitation for the stations of Hagereselam (8.7 and 17.4‰), Awassa (7.2 and 10.95‰) and wolaita sodo (6.9 and 10.93‰). The variation in average isotopic composition, slope, and D-excess of each LMWLs with the GMWL is related to the change in isotope value of the source and/or season, the rate of evaporation of source, the isotopic evolution of air mass and relative humidity during precipitation (Gat, 1996; Kebede and Travi, 2011). The difference in D-excess may reflect a higher kinetic (non-equilibrium) effect during evaporation of the moisture along the trajectory of the two main moisture sources of the region: the monsoon from the Atlantic and Indian oceans to southern Ethiopia. The regression lines for the stations of sodo and Awasa are plotted to the right of the GMWL because of substantial evaporative enrichment except for Hagereselam which is at highlands (2600masl). The average values of the rainfall stable isotopic composition of the GNIP stations of Abaya Chamo Lakes basin do not show significant variation to understand the moisture source and the isotopic effects along the moisture trajectory directions. Therefore characterization using isotope effects and its seasonal variation is preferred to show the variations.

4.6. Isotopic effects for rainfall characterization

4.6.1. Amount effect

The dependence of isotopic composition on the amount of rain describes the amount effect where greater monthly precipitation amounts result in more depleted $\delta^{18}O$ and $\delta^{2}H$ values (Dansgaard, 1964). This could be related to the formation of clouds yielding heavier rains with depleted heavy isotopes favored by lower ambient temperature (E. Mazor, 2004). The relation of monthly

rainfall amount to the monthly average stable isotopic composition of precipitation of the wolaita sodo and Hagereselam GNIP stations for year 1999/2000 (IAEA, 2000) are available to understand the variations using amount effect.

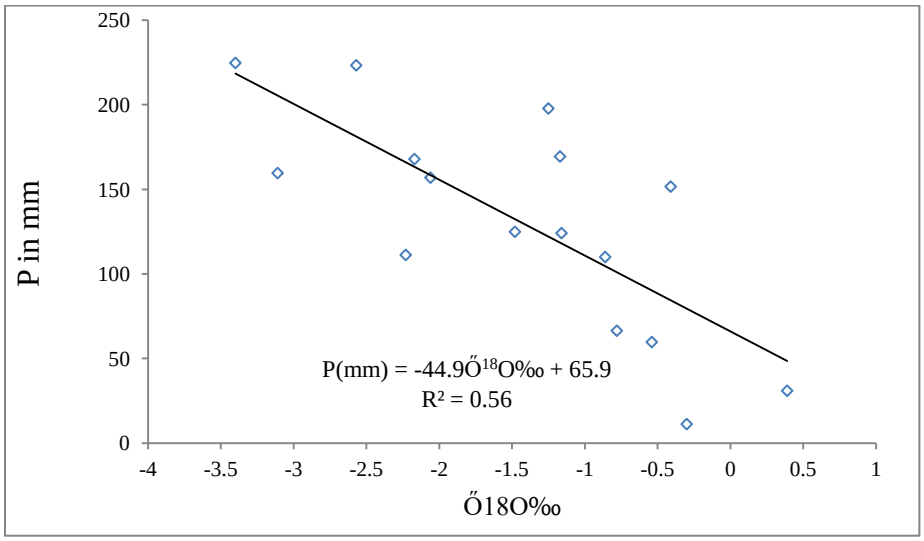

Fig 14 Amount effect for all seasons of wolaita sodo station

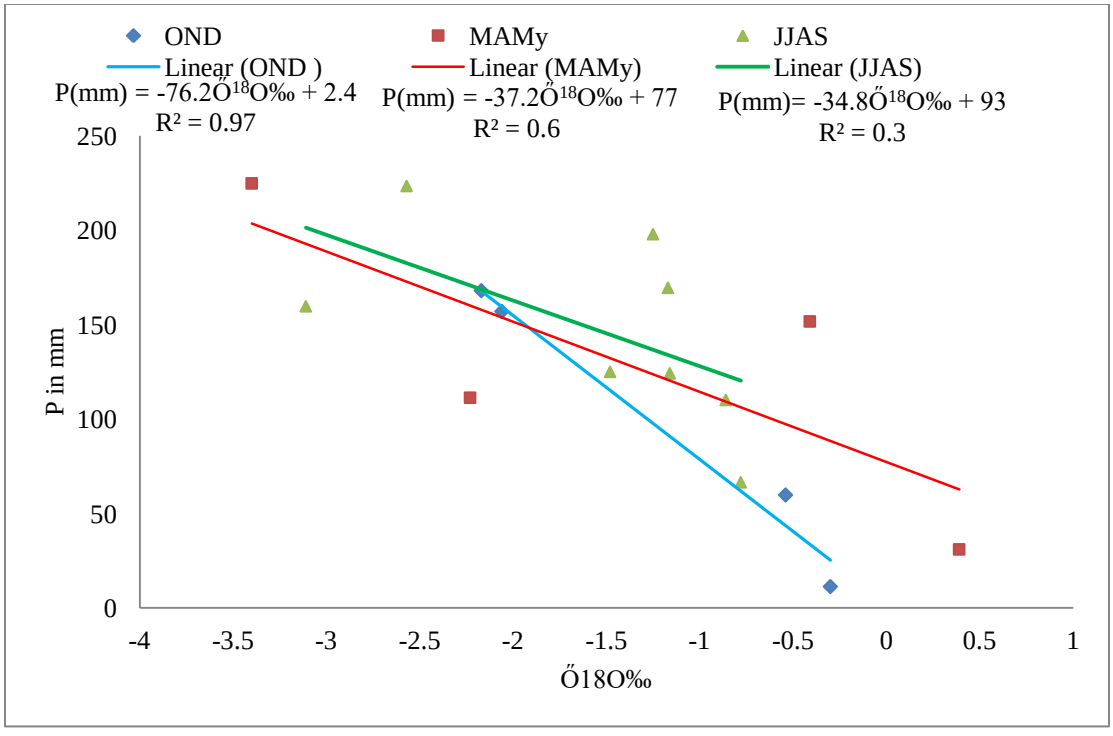

Fig 15 Rainfall amount and $\text{Ő}^{18}\text{O}$ variations for three segregated seasons of wolaita sodo station

Wolaita sodo station GNIP data showed a relatively weak correlation (R^2 = 0.56) (Fig.14 and Fig.15) for the amount of rainfall and $\H{O}^{18}$O‰ on a yearly basis. The amount effect of major rainfall season (JJAS) showed a weak relation (R^2 = 0.3), the spring (MAMy) season (R^2 = 0.6) and the October peak (OND) season (R^2 = 0.97) with the δ^{18}O of the respective months. This indicates that the amount effect is visible only for small rains and cannot explain isotope variation in fully developed monsoon season of major rainfall events where the meteorological parameters such as (humidity and temperature) are almost uniform. This is because, in small rain drops, the amount of rainfall becomes important to overcome the re-evaporation of rain waters. During low rainfall, re-evaporation of rainwater leads to enrichment and therefore a clear and relatively high correlation (R^2 = 0.97) of δ^{18}O to rainfall amount exists.

4.6.2. Altitude effect

As the clouds rise up to higher altitudes, heavier isotopes are depleted and the residual precipitation gets isotopically lighter. The altitude effect is locally variable and turns out to be an effective tool in tracing groundwater recharge (E. Mazor, 2004). The spatial variation of stable isotope could be explained by the altitude effect that leads to the difference in composition of ($\H{O}^{18}$O, Ő2H, d-excess) precipitation. The rate of depletion of summer rainfall of Abaya Chamo varies differently in parts of the basin. It showed the depletion rate of $\H{O}^{18}$O‰ per 100m to be -0.2‰ in windward of southwestern, -0.07‰ in northwestern and -0.05‰ in eastern parts of the basin. The value is consistent with the altitudinal variation of $\H{O}^{18}$O = -0.1‰/100m on the Northwestern Ethiopian plateau (Kebede, 2004) especially for summer rainfall in windward.

Using the highland cold springs isotopic compositions as proxies, the altitudinal variation in the southwestern part of the Abaya Chamo Lakes basin is -0.5‰/100m (McKenzie et al., 2001), which seem inconsistent with that of the North-Western plateau and the present southwestern highland of the basin. The inconsistency could be related to the effect of evaporated cold springs and Rivers to the leeward part of the area where rift microclimate controls the hydrology. The variation in d-excess with altitude (Fig.16) could also be used to characterize the processes for a different rate of depletion per 100m. Evaporative enrichment of the rainfall beneath the cloud base is higher towards lower altitude where the d-excess is lower. But along areas where the

inter-mountains affect the wind flow to leeward of the summer rains, the d-excess varies greatly (Fig.24).

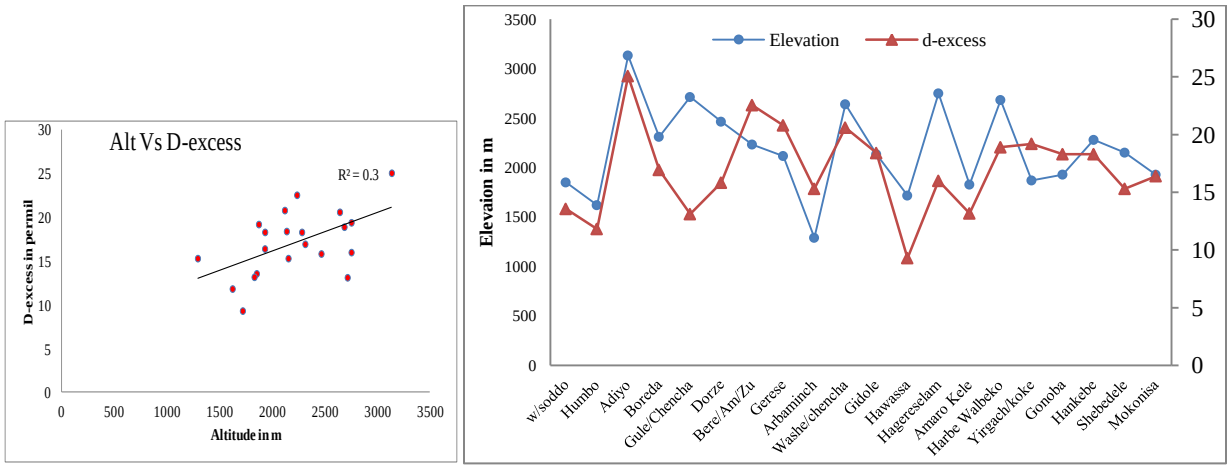

Fig 16. The variation of d-excess with altitude

It is understood that evaporation is lower around highlands where the temperature is lower. But , some highland rainfall stations and proxies cold highland springs showed poor correlation of Altitude with the d-excess (R^2=0.3) in the basin. Highlands of Chencha and Dorze showed less d-excess due to evaporation from shallow unconfined aquifers. The higher d-excess of Gerese for comparatively less altitude could be related to cold and depleted wind entering into the south western highlands through Gerese highlands during summer. Other crossing relations are also related either to evaporation or wind direction (Fig.16).

Highland cold springs and highland River streams sampled during summer season reflect the isotope value of precipitation. Based on this, recharge altitude of springs and wells of the lowland area of Arbaminch are developed (Mekenzie, 2001). In the recent study, a relation of elevation and $\delta^{18}O$‰ is developed to be Elev (m) =-855 $\delta^{18}O$‰ - 876 resulted in an elevation effect of approximately –0.12‰ $\delta^{18}O$/100m rise. The relation describes that Arbaminch Springs with the $\delta^{18}O$‰ composition of -3 is recharged from the surrounding highlands of Chencha and Gerese above 2100masl (Fig.17). Slight enrichment is revealed from relatively lower d-excess = 15.3‰ of Arbaminch springs (at 1200masl rift floor) compared to that of Chencha and Gerese cold springs (d-excess above 20‰).

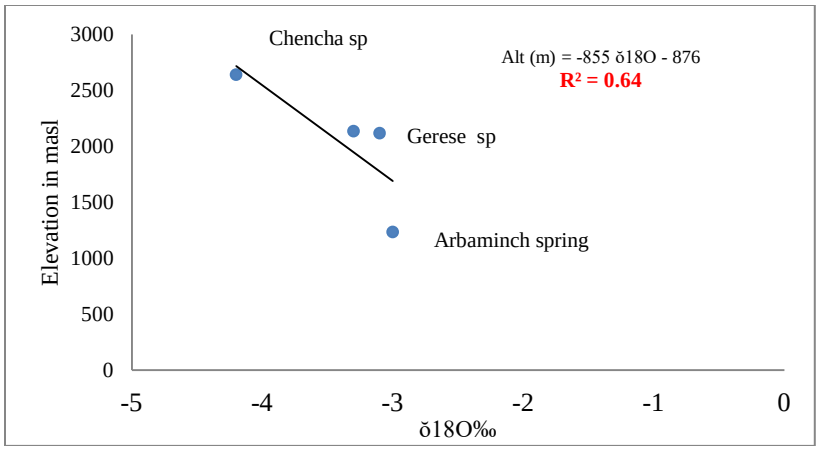

Fig 17 Recharge altitude of Arbaminch area springs

4.6.3. Temperature effect

Temperature is the major parameter in determining the isotopic values of precipitation as the formation of precipitation mainly depends on the evaporation of oceanic water into the air and condensation at which clouds and rain or snow are formed (Dansgaard,1964). The temperature effect is the powerful tool in hydrology and is responsible for tracing the large variation in the isotopic composition of groundwaters. Seasonal differences in the composition of precipitation are also traced to identify the spring and summer fronts (E. Mazor, 2004). The relation of temperature to stable isotope composition ($\delta^{18}O‰$, $\delta^{2}H‰$, and d-excess‰) in the Abaya Chamo Lakes basin display the equation of $\delta^{18}O‰ = 0.13Ta-4.8$ and $\delta^{18}H‰ = 0.65Ta- 15.03$ where Ta is the air temperature of the sample areas. This indicates that for the increase of $1^{0}c$ of temperature the precipitation is enriched by 0.13‰ of $\delta^{18}O$ and 0.63‰ of $\delta^{18}H$ in the basin.

The relation of temperature versus $\H{O}^{18}O‰$ of precipitation (Fig.18) showed a characteristic pattern of wind source and portions of the basin. Southwestern stations such as Chencha, Gerese, Gidole, and Arbaminch (Fig.23) showed relative depletion even for increasing air temperature. But for almost similar air temperature, Hagereselam rainfall is relatively enriched than Chencha related to the effect of summer moisture source that passes through rift valley and climbs again to the eastern part of the basin (Hagereselam).

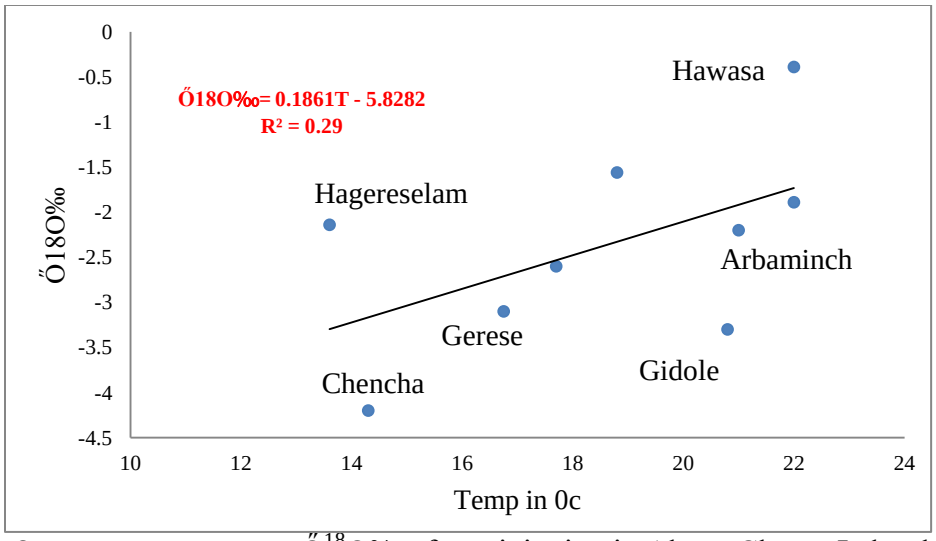

Fig 18 Temperature versus $\delta^{18}O$‰ of precipitation in Abaya Chamo Lakes basin

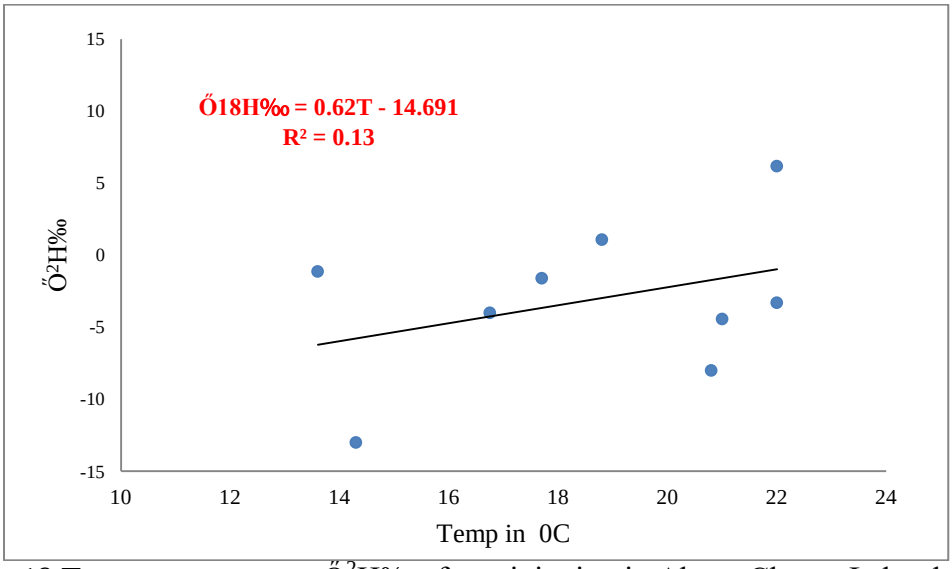

Fig 19 Temperature versus $\delta^{2}H$‰ of precipitation in Abaya Chamo Lakes basin

The variation in d-excess (Fig.20) showed that precipitation received by southwestern highlands of the basin is relatively depleted. But these stations of the eastern part of the basin and the rift valley (Hawassa and Humbo) are relatively evaporated. The low d-excess of rift valley stations is related to evaporation of the rainfall beneath the cloud base favored by low relief higher temperature. The ascension of summer depleted residual cloud to the eastern highlands of the basin from the rift valley gives relatively depleted rain compared to lower reliefs.

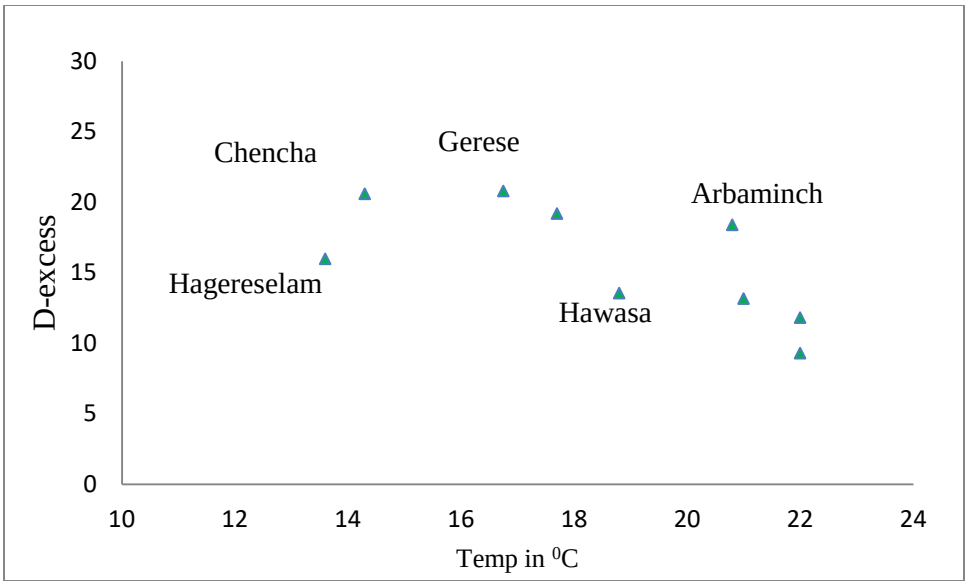

Fig 20 Temperature versus D-excess of precipitation in Abaya Chamo Lakes basin

4.7.Isotopic characterization of different moisture sources in Abaya Chamo Lakes basin

When seasonal air mass leaves its source, it is exposed to the most frequent processes of condensation and evaporation. Water evaporation leads to enrichment (increase in heavy isotope content with respect to the light) in the stable isotope composition in the residual water fraction. Every precipitation event depletes the vapor remaining reservoir. Water with heavier $^{18}O/^{16}O$ and $^{2}H/^{1}H$ ratio forms the initial water droplets of rains and as vapor mass continues to lose its heavy isotopes it becomes more depleted in heavy isotopes. Meteoric water in a given environment when it undergoes phase changes related to hydrological processes, its isotopic composition changes accordingly (Fig.21). The most important isotope effects of these changes used in hydrologic investigations are altitude, latitude, amount, evaporation, seasonality, temperature, continentality and paleoclimate effects (Gat, 2001; Gat et al., 1994).

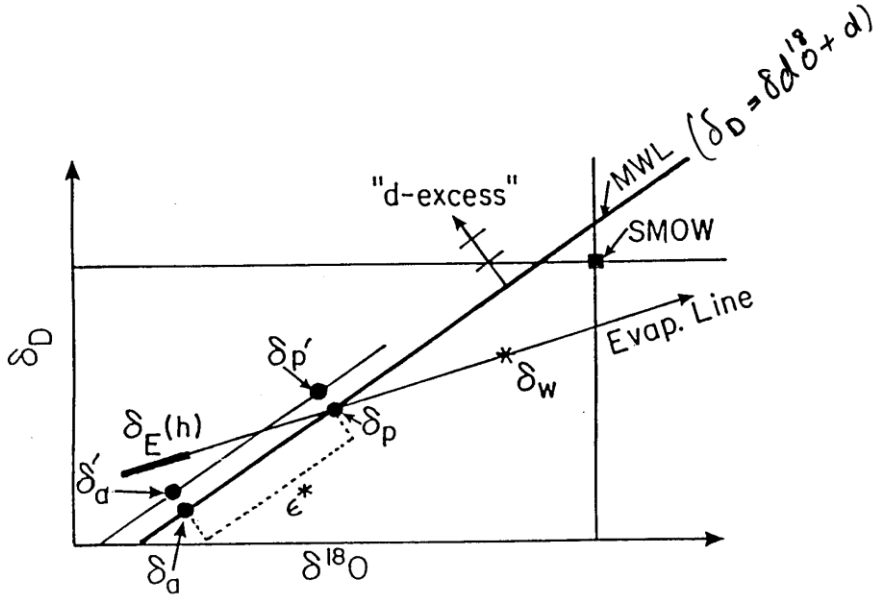

Fig 21 Isotope composition of evaporated surface water (δw), the original precipitation prior to evaporation (δp), and the evaporated vapor (δE), all plotted along the same evaporation line. Both precipitation (δp) and atmospheric vapor (δa) in equilibrium condition are plotted along the MWL separated by the enrichment factor for the environmental temperature (ε*). When the evaporated water (δε) mixes with the local atmospheric vapor (δa), a new vapor (δ'a) is formed that plots above the MWL. If rain later condenses from this vapor, it would plot along a new line parallel to the MWL but with a higher d-excess value; after Gat et al., (1994).

The isotopic signal of precipitation in the source water regions is transported to local topographic conditions and further altered with additional condensation/evaporation processes according to the local climate (Jeff B LANGMAN, 2015). (Kebede, 2004) indicated that seasonal variation in $\delta^{18}O‰$ and d-excess of rainfall in Ethiopia reflected principally the differences in sources of moisture and the rain derivation mechanism. The seasonal variation of $\delta^{18}O‰$ and d-excess in the Abaya Chamo Lakes basin is more easily viewed through comparison of isotopic characteristics of stations (Fig.21). The maps reflect differences in source waters, evaporation/condensation (temperature effect) and inter-isotope fractionation (d-excess generation). A larger evaporation effect is apparent for the spring season as indicated by slightly enriched $\delta^{18}O‰$ and smaller d-excess compared to the summer season. This is consistent with the rainfall amount that summer rainfall mainly originated from the Atlantic ocean and southern Indian ocean during cold months has a higher amount, but that of the spring season rainfall originating from Indian ocean has a lower amount during the hotter months (March to May) (Fig.22).

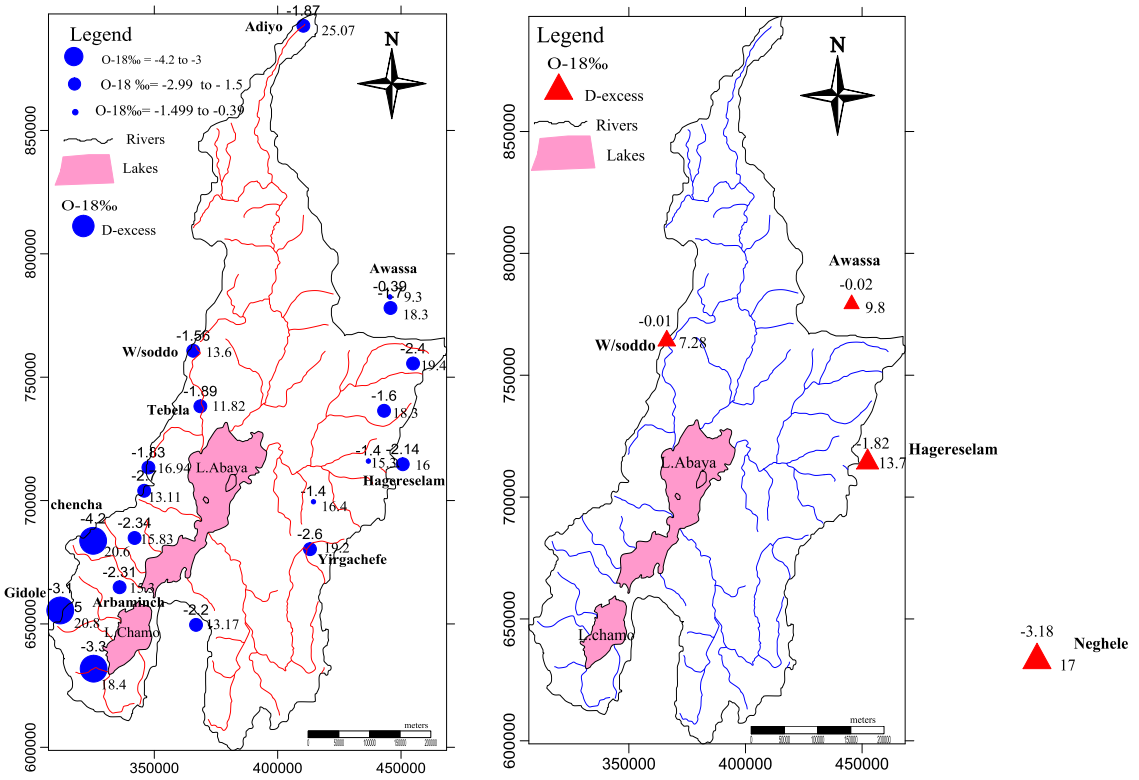

Fig 22 Spatial distribution of the summer season (right) and spring season (left) $\delta^{18}O‰$ and d-excess of rain water from GNIP stations (IAEA, 1999/2000) and proxy sample sites. Spring season samples represented by red rectangles all from GNIP stations.

$\delta^{18}O‰$ and $\delta^{2}H‰$ compositions of short-term monthly rainfall were measured at a few Ethiopian rift valley stations. One year monthly average of the three GNIP Stations Data (1999/2000, IAEA), 15 cold springs of highland and escarpment areas and 2 highland River/stream samples of summer months (JJAS) isotope ($\delta^{18}O‰$ and $\delta^{2}H‰$) of the Abaya Chamo Lakes basin are used in the characterization of the source and migration of the wind. The data showed relative depletion with $\dot{o}^{18}O‰$ to southwestern ranging from -4.2‰ at Chencha to -0.39 ‰ at Awassa and d-excess‰ in between 9.3 at Awassa and 25 at Guraghe highland (Fig.23).

The global distribution of annual mean $\dot{o}^{18}O‰$ of precipitation based on GNIP data indicated that there is a general trend of enrichment from the southern hemisphere ($\dot{o}^{18}O$=-8‰) towards northern Ethiopia and Sahel zone ($\dot{o}^{18}O$=+2‰). The Abaya Chamo Lakes basin is situated in the range of 0 to +2‰ on the map (Gat, 2001). The 1969 summer (JJAS) precipitation of Kenya (Kericho) GNIP station data has $\dot{o}^{18}O$ ranging from -0.7‰ to +0.8‰ and d- excess range of -

8.84‰ to 12.8‰ (Fig.24). This implied that the summer precipitation is relatively enriched to the south of Ethiopia.

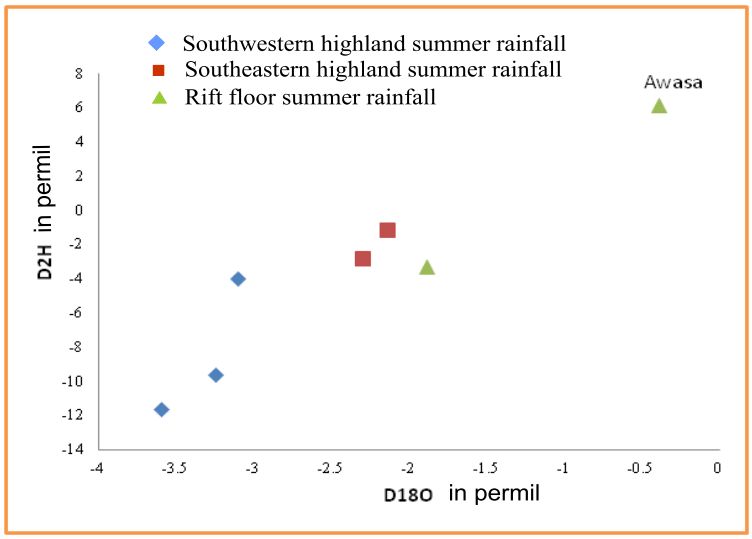

Fig 23 Summer rainfall isotopic composition along different sectors of southern Ethiopia.

However, when the cold summer season precipitation originated mainly from the Atlantic Ocean enters into south Ethiopia, it ascends to southwestern highlands of the Abaya Chamo Lakes basin (Gidole, Gerese, chencha) and undergoes condensation at higher altitude (>2500masl) (Fig. 22, 23,24,). During the processes of gradual condensation of the cloud to higher altitudes, equilibrium isotopic fractionation makes the remaining vapor and the latter precipitation become more and more depleted in $\delta^{18}O$ and $\delta^{2}H$ (Gat, 2010).

NNW highlands in Ethiopia (Addis Ababa) getting 75% of annual rainfall in summer from the Atlantic and Indian Oceans admixture (depleted in $\delta^{18}O$‰) (Kebede and Travi, 2011), Abaya Chamo Lakes basin similarly gets depleted ($\delta^{18}O$‰) intensive (about 50%) of annual rainfall in the wet summer months (JJAS). The relative higher depletion in the summer season of southwestern highlands of the Abaya Chamo Lakes basin ($\delta^{18}O$=-4.2‰ and $\delta^{2}H$=-13‰) (Fig.22) is related to Rayleigh distillation of moisture sources during the ascension to highlands through the coast of Congo and Kenya (Kericho) (Fig. 24).

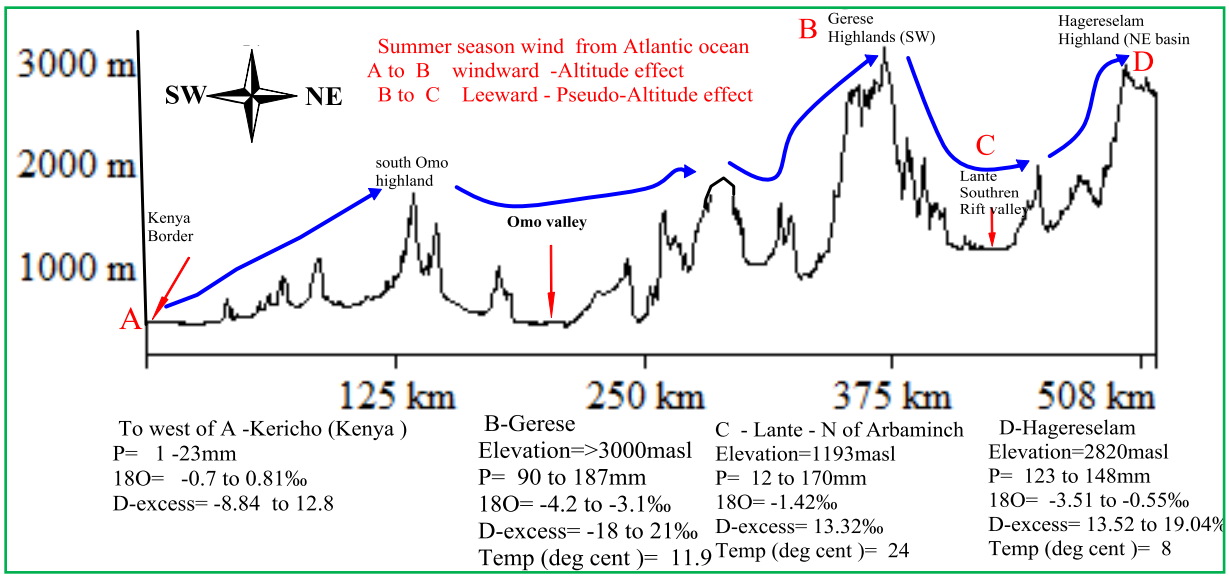

Fig 24 simplified conceptual profile of the summer moisture bearing wind flow from Atlantic ocean along the SW-NE direction of Abaya Chamo Lakes basin indicating altitudinal variation in $\delta^{18}O$ and d-excess of GNIP stations (Kericho, Hagereselam) and proxy groundwaters of Gerese and Lante localities. The letters A, B, C, and D represent localities and the arrows point to moisture bearing wind flow direction. P and T are mean annual rainfall and temperature respectively during isotope data analysis

The moisture continuously depletes in heavy isotopes ($\delta^{18}O$) as it moves over the western face of the southwestern highlands of the Abaya Chamo Lakes basin because of the altitude effect (-0.2‰ per 100m) which almost agrees with that of NNW plateau. The moisture descends over the leeward face of Gerese Mountain to the southern rift floor around Arbaminch with pseudo-altitude effect (-0.12‰ per 100m). The descending moisture gets warmer and evaporated while rainfall in leeward enriching the rainfall by 0.12‰ per 100m elevation drop. The enrichment of $\delta^{18}O$ is 0.23‰ per 1°C increase in air temperature towards the rift from southwestern highlands (Fig.24). The influence of summer Atlantic Ocean moisture trajectory extends to the eastern highlands of the Abaya Chamo Lakes basin (seasonal migration of ITCZ) and hence the moisture bearing wind passes the rift floor and ascends over the face of eastern highlands. The air that condenses yields relatively depleted rainfall at Hagereselam station (average summer $\delta^{18}O$ = -2.14‰ and d-excess = 16‰) with the altitude effect of -0.05‰ per 100. The relatively less depletion towards eastern highlands could be related to evaporation while rainfall, a complication of the enriched warm North Indian Ocean monsoon entering to eastern face during summer and a lesser amount of summer rainfall received by the area. When the moisture passes further to the north of the basin, it becomes relatively enriched ($\delta^{18}O$ = -0.39 ‰ at Awasa) and

eastern escarpments. The relative enrichment is related hotter temperature favoring evaporation from rainfall beneath the cloud base where the air mass is undersaturated (Fig.23). It is also linked to the size of the precipitation drop and its intensity that lower sized and less intensive rains are enriched with heavy stable isotopes (Gat, 2001).

Spring season (MAMy) is hotter than summer in the southern Ethiopian rift valley. As described in the above sections of this chapter, the spring season rainfall is originated from hot humid winds of the northern Indian Ocean. When it enters to southern Ethiopia in March, it influences both eastern and a western part of the basin as ITCZ migrates to the north. In addition to the rift, the spring season moisture bearing wind influences both Omo-Ghibe and the Blue Nile basins.

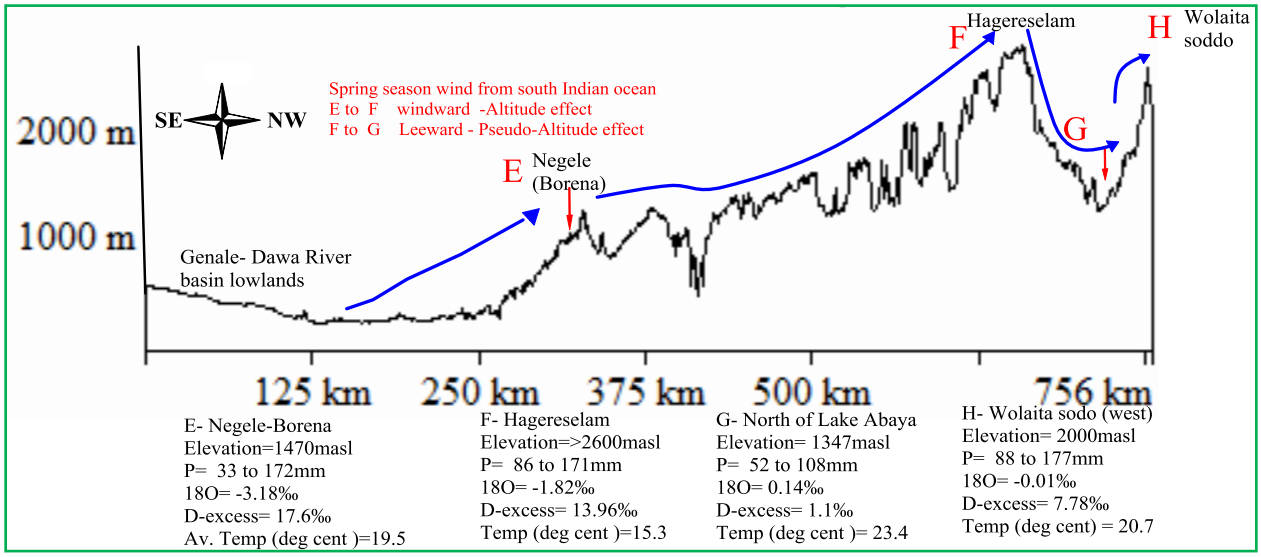

Fig 25 simplified conceptual profile of the spring season moisture bearing wind flow from the southern Indian Ocean along the SE-NW direction of Abaya Chamo Lakes basin indicating the altitudinal variation in $\delta^{18}O$ and d- excess of GNIP stations (Negele Borena, Hagereselam, and Wolaita soddo). *The letters E, F, G, and H represent localities and the arrows point to moisture bearing wind flow direction. P and T are mean annual rainfall and temperature respectively during isotope data analysis)*

When the moisture bearing wind flows over the eastern windward face of the eastern highlands of the Abaya Chamo Lakes basin, the rainfall showed progressive enrichment from the Neghele Borena GNIP station ($\delta^{18}O$ =-3.18‰ and d-excess = 17‰) towards Hagereselam and other Northwest stations (Fig.25) with the altitude effect of -0.1‰ per 100m. This showed the enrichment of $\delta^{18}O$ by 0.1‰ for elevation rise of 100m. The moisture continues to descend to leeward NW face of Hagereselam (Fig.25) progressively enriched with the pseudo-altitude effect of -0.15‰ per 100m. It becomes more enriched in streams of rift floor at G North of Lake

Abaya. This is related not only due to increasing temperature favoring heavy isotope enrichment rate of 0.24‰ per 1^0c to rift floor but also warmer moisture coming into the basin. Further flow of the spring wind source towards northwestern highlands of Abaya Chamo Lakes basin produced slightly depleted rain at Wolaita sodo. The spring wind ascends and condenses with altitude effect of – 0.02‰ per 100m. The enrichment of spring season rain waters and proxies regardless of increased altitude could be related to the decreased amount of rainfall and a hotter season that eases evaporation of rainfall beneath the cloud base towards Northwest (Fig.22). It also could be related to justification by (Kebede and Travi, 2011) that there are three factors for the enrichment of the spring season rainfalls: (a) nearness of the area to Northern Indian Ocean favoring initial stage of condensation, (b) high temperature and low humidity and (c) high sea surface temperature over the northern Indian Ocean.

The association of the rainfall isotopic composition and movement of the ITCZ in Abaya Chamo Lakes basin is generally observed in three seasons of the year. But the detailed characterization is done in two major seasons (summer and spring). The formation of depleted rainfall in May of the spring season, July and August of the summer season and October month is associated with strong convection and high altitude condensation within air column. During spring season higher rainfall is received, especially in the eastern part of the basin in May where the ITCZ moves to North and moisture-bearing air from Northern Indian ocean condenses at higher altitudes and giving depleted rainfall at Hagereselam (Average $\delta^{18}O$ =-1.8‰) and wolaita sodo. In the summer months (July and August) Abaya Chamo Lakes basin gets intensive rainfall from Atlantic and South Indian oceans when the ITCZ is in northern Ethiopia providing depleted rainfall in the basin ($\delta^{18}O$ =-3.21‰). Likewise, in October when the ITCZ is located to the south of Ethiopia, dry and cold convective air from Arabian continents also converges at highlands of the basin and give depleted rain.

The effect of local climatic factors on the variation in the isotopic composition of rainfall and proxies in and around Abaya Chamo Lakes basin is observed from seasonal altitude and pseudo-altitude effects and amount of D-excess. The altitude and pseudo-altitude effects in the windward and leeward respectively of the basin (Table 3) vary greatly. The variation of windward altitude effects of summer and spring seasons is due to the difference in sources of moisture, temperature

sea surface and climatic condition of the wind trajectory. The pseudo-altitude effect of summer and spring rains is almost similar enriching towards the rift floor from both sides of the highlands attributed to the wind migration to high-temperature low relief areas that facilitate evaporation of rainfall beneath the cloud base. The residual winds of summer and spring months ascending to both eastern and western highlands low-temperature areas respectively, showed low altitude effect with the sign of depletion.

Table 3 summary of altitude and pseudo-altitude effects of moisture sources in the Abaya Chamo Lakes basin.

Moisture sources to Abaya Chamo Lakes basin	Windward Altitude effect per 100m		Leeward Pseudo-altitude effect per 100m		Residual wind ascending after leeward Altitude effect per 100m	
SW-NE wind from Atlantic ocean (summer)	-0.2‰	Depletion	-0.12‰	Enrichment	-0.05‰	Depletion
SE-NWwind from north Indian ocean (spring)	-0.1‰	Enrichment	-0.15‰	Enrichment	-0.02‰	Slight depletion

Generally, variation in moisture sources, micro-climate effects, physiography of Abaya Chamo Lakes basin and the distances of moisture sources from the basin determined the isotopic composition of the rainfall. The groundwaters in the basin could either be sourced from direct recharge from local rainfall or regionally linked with other basins.

4.8.Tracing Groundwater recharge in the Abaya Chamo Lakes basin with ^{18}O and D-excess

The rainfall isotopic composition changes in space and time in response to the rainout and the isotopic effects such as temperature, amount and altitude (Clark and Fritz, 1997). Seasonal shifting of the moisture sources, mainly between the Indian Ocean and the Atlantic Ocean during spring (March to May) and summer (June to September) respectively in the Abaya Chamo Lakes basin and its surroundings is the major cause for the variability of the rainfall isotopic composition. The relation between $\delta^{18}O$ and $\delta^{2}H$ of precipitation, groundwaters, Rivers, and Lakes (Fig.26) indicates variation in the source and mechanism of recharge to the hydrogeological systems in the basin. The Local Meteoric Water Lines (LMWL) drawn based on 1999/2000 one year GNIP stations data of IAEA (Wolaita soddo, Hagereselam and Hawassa) showed variation in the d-excess and slope values (Fig.13) compared to that of the GMWL $\delta^{2}H‰=8\delta^{18}O‰+10$ (Craig,1961). This reflects the sign of evaporation for the LMWL at the right side of the GMWL (lesser D-excess) and depletion at left side in station of Hagereselam (high D-excess).

The ŏ^{18}O‰ and D-excess composition of groundwaters in Abaya Chamo Lakes basin range in between -6.82 to 6.54 and -11 to 52 respectively. Compared to the isotopic composition of summer rainfall (ŏ^{18}O‰=-4.2 to -0.39 and D-excess‰ =9.3 to 25) and spring rainfall (ŏ^{18}O‰=-2.6 to -0.01 and D-excess‰ =7.28 to 17), most of the groundwaters circulating within the depth range of 0 to 180mbgl along the highlands, escarpments and rift aquifers towards escarpments are recharged from modern rainfall. The dominant portion of the recharge is from summer rainfall by percolation through fractures and fault blocks as local and regional flow systems. However, the source and mechanisms of recharge are briefly discussed in the section covering Isotope hydrology.

Groundwater from western highland wells (WHW), western highland cold springs (WHC), and highland River streams (Fig.26) plot close or above the LMWLs indicating waters of high D-excess when evaporation prior recharge is less. The relative depletion of southwestern water points compared to the EHCs is that WHCs is directly recharged more from summer depleted rainfall in addition its altitude effect and the evaporation prior recharge is less due to cold temperature of the summer months. But eastern cold springs (EHCs) are recharged more from spring rainfall during hotter months when the evaporation prior the recharge is higher. This could also be associated with the source of summer rainfall to the basin from the Atlantic Ocean though Congo basin continental sources.

Some groundwaters from eastern highlands, western highlands and rift floor plot at the range of modern rainfall, but below the LMWLs showing evaporative fractionation before recharge (reduced D-excess). This shows that the recharge source of these waters is more from spring rains coming from the southern Indian Ocean during hotter months (March to May). Groundwaters plotted to the right side of LMWLs at the initial stage of evaporation line are recharged either directly by the highland rainfall and evaporated from upper unconfined sources or indirectly through Rivers beds by vertical leakage and side flows. Groundwaters aligned along evaporation line (D-excess‰ up to -11) are recharged either from Lakes directly or evaporated rivers nearby.

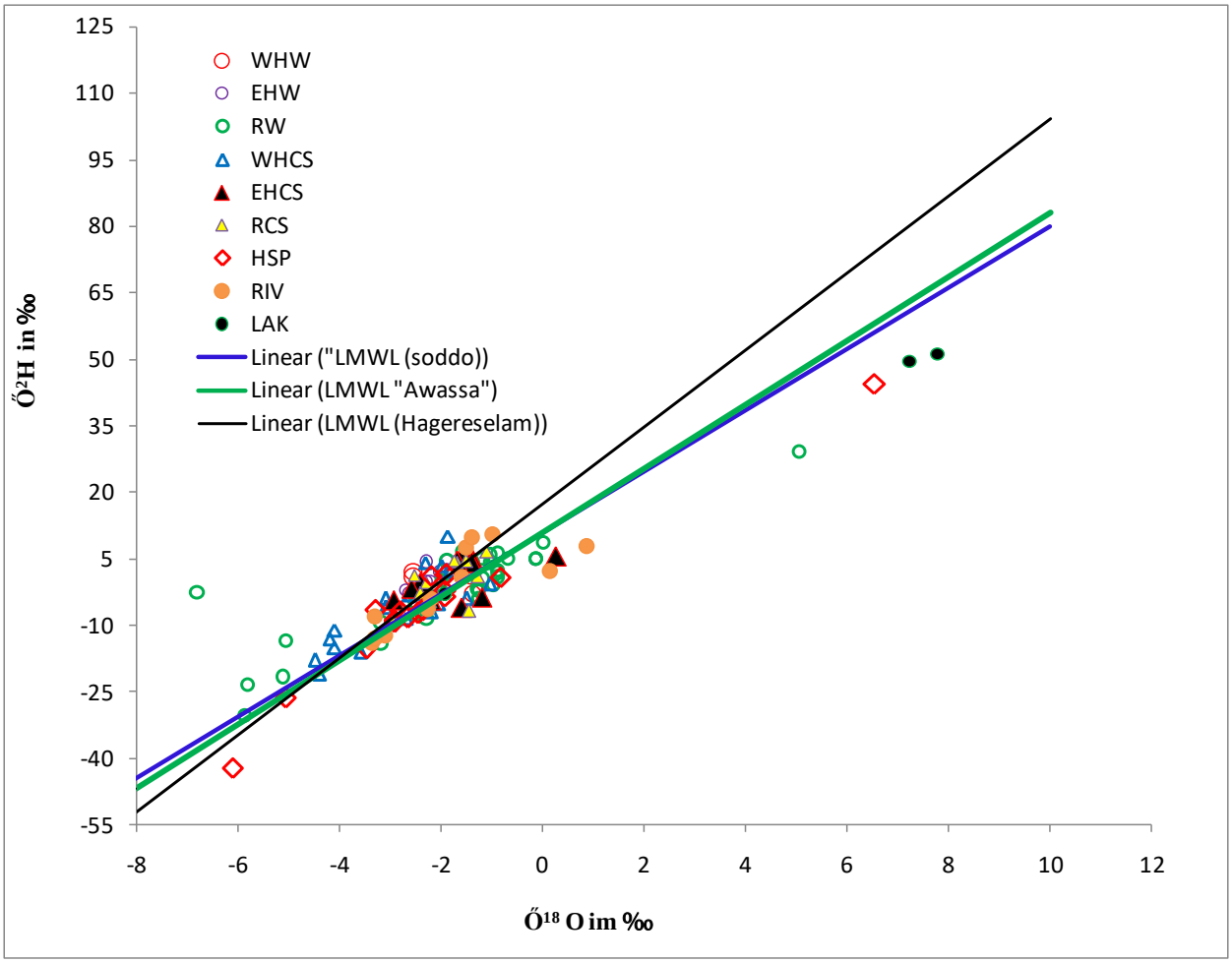

Fig 26 Plot of different waters on LMWLs of Abaya Chamo Lakes basin (WHW- western highland wells, EHW-Eastern Highland wells, WHCS-Western Highland Cold springs, EHCS-Eastern Highland Cold springs, RW-Rift Floor wells, RCS-Rift Floor Cold springs, HSP- Hot Springs, RIV –Rivers and LAK –is lakes samples)

Relatively highly depleted groundwaters with ŏ^{18}O‰ below -4.2 occur in deeper rift floor aquifers 150 to 400mbgl (Fig.26). This shows that the aquifers are recharged by older waters than recent rain. Based on ^{14}C (Kebede and Travi,2011) justified that the recharge source of relatively highly depleted groundwaters for aquifers of the southern Addis Ababa and the rift valley to be late Holocene rains recharged in the highlands and currently discharging in rift floor. The work also indicated that during late Holocene humid phases the moisture penetrated inland into western Ethiopian mountains. For relatively depleted rift floor waters of the Abaya Chamo Lakes basin, the major source could be humid Holocene south Indian moisture too. The recharge source of older waters plotted at the depleted end below the LMWLs with low D-excess ‰ (6.68 to16) indicating the relatively evaporated recharge source and the second category of older

waters plotted above LMWLs with D-excess ‰ (19.5 to 52) indicate waters which had been recharged by high-intensity local rainfall during past wet climate times.

South Indian Ocean is the major source of recent enriched spring rain to southern Ethiopia. The relatively depleted ($\check{o}^{18}O$ <-4.2‰) deeper rift floor waters of the Abaya Chamo Lakes basin indicate that there is significant variation in the isotopic composition ($\check{o}^{18}O$, $\check{o}^{2}H$, and D-excess) of late Holocene moisture and the recent moisture coming into the basin from the same source in the same season. This could be linked to the change in climate due to natural and human-induced effects of the continents.

The D-excess amount of groundwaters from wells and springs located near the River channel indicated that there is the interaction of surface and groundwater systems as identified based on values (4.8‰ to 9.9‰) (Fig 27 left). Groundwaters represented by (RW3, RW4, WHW3, HSP10, HSP11, HSP12) in the Bilate River basin, RCS2 in the Amesa River catchments, (WHCS19, RW9, RW10, RW11) in Chamo Lake catchments, (EHCS9, EHCS10) in the Gelana River basin and (RW17, RW21, RW29, RW40, EHW17) in the Gidabo River basin (Fig. 27) showed the sign of almost similar range of enrichment in $\check{o}^{18}O$‰ and D-excess values to the respective River's waters. This could be related to the migration of the enriched River waters from the channel to the groundwater systems through the permeable river bed or the sides of the River channel.

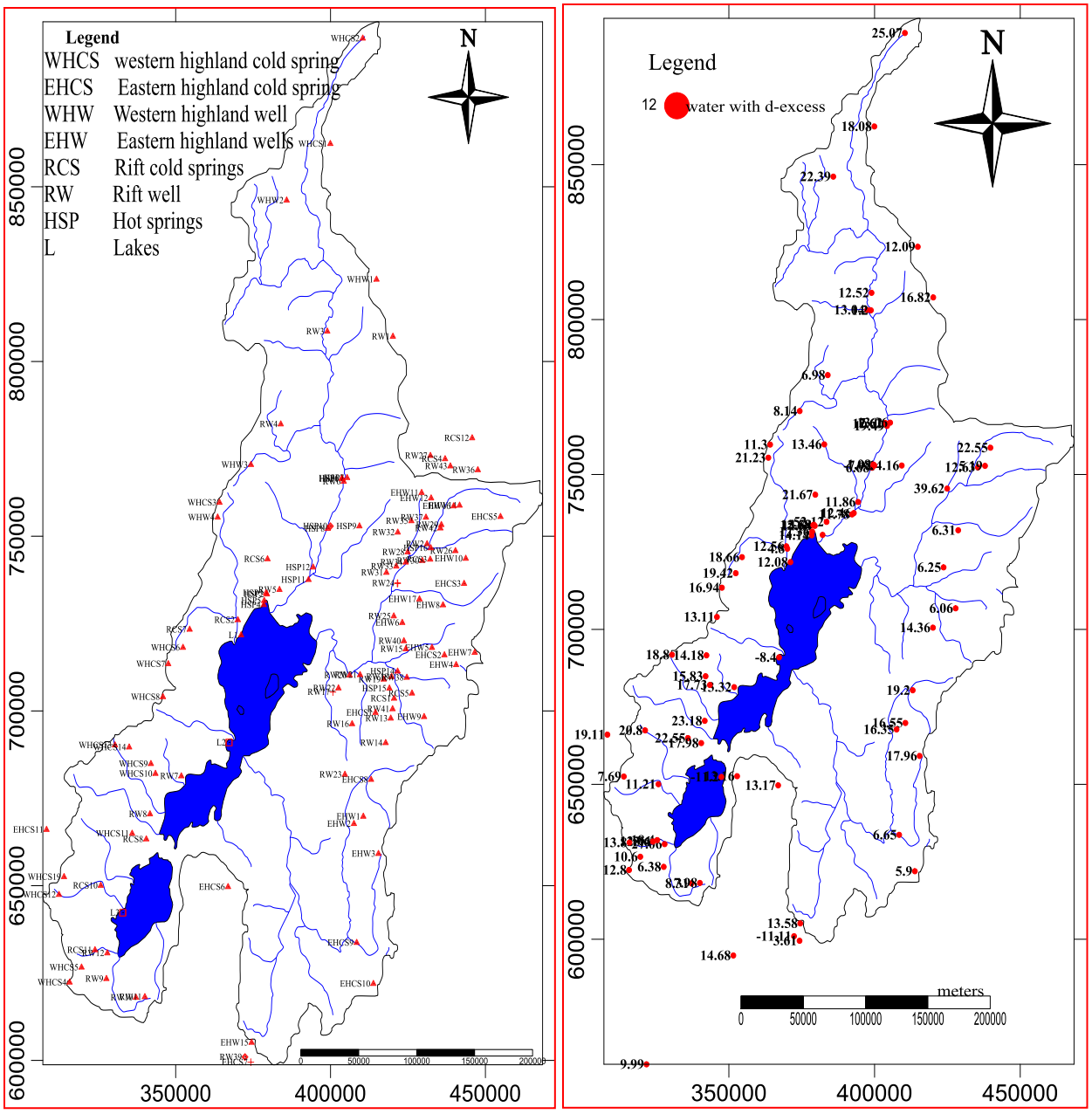

Fig 27 Groundwater points for isotopes (right) and d-excess (left) of Abaya Chamo Lakes basin

Generally, the higher D-excess of groundwaters, clustering of the waters along the LMWLs towards summer rainfall isotopic composition range and the discharge variability of cold and hot springs in the Abaya Chamo Lakes basin makes the groundwaters meteoric in origin. It is also indicated from (Fig.28) that direct recharge from precipitation is the most important source supplying water to the hydrogeological system of the basin and is enriched in SSW to NNE trend.

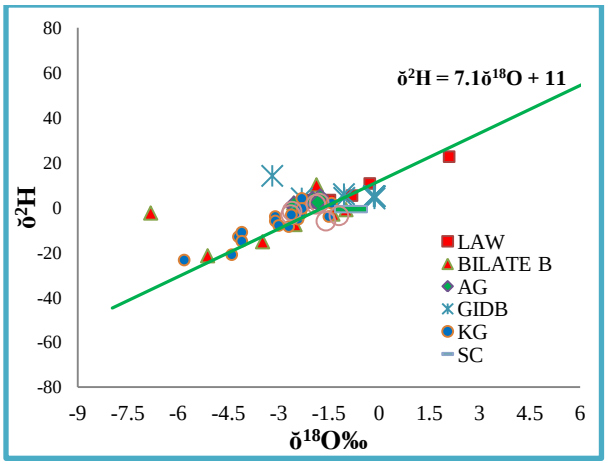

Fig 28 The general SSW–NNE enrichment trend of groundwaters in River basins of Abaya Chamo Lakes basin (*LAW- Lake Awassa, Bilate B- Bilate, AG- Amessa Gurucho, GIDB- Gidabo, KG- Kulfo Gidana, SC- Sile Chamo and GELA- Gelana*).

However, the basin scale isotopic analysis of tracing the recharge sources indicated that direct infiltration of precipitation in all parts of the basin, seepage from Rivers and Lakes, old waters joined the groundwater system during Holocene, and mountain block recharge are four sources of recharge to the hydrogeological systems of the basin.

5. CONFIGURATION AND HYDRAULIC PROPERTIES OF VOLCANIC AQUIFERS

5.1. Introduction

The knowledge of the well characterized aquifer system is essential to solve scientific and community problems in a given area and hence effective groundwater resources location, development and management are possible when the hydrogeological systems framework and dynamics of flow are well understood (Singhal and Gupta, 2010). The configuration of volcanic aquifers and the groundwater circulation at different depths is controlled mainly by physiographic, geologic units and tectonics that determine the hydraulic characteristics of aquifer units. With depth, the porosity and permeability tends to close, thus sufficient secondary porosity should be developed for such rocks to be considered as aquifers (Vernier, 1993). Because of its partly acceptable chemical constituents of waters in it, volcanic aquifers are one of the most exploited aquifers in Ethiopia (Alemayehu, 2006) providing water through wells and springs.

Different geological formations originated in the basin as a result of various geological processes occurred in the past. The early tertiary volcanics are dominantly localized in the highlands and Late Tertiary volcanics (rift Series) mostly confined within the rift floor. Fissural volcanism primarily forming rhyolitic ignimbrites and voluminous flood basalts. The recent rocks consisting alluvial, lacustrine and volcano-sedimentary formations covered around the Lakes, along the plains and river deltas in the rift (Woldegebriel et al., 1990). Temporal processes of occurrence of rock units and spatial variability in deposition are the reason to a different degree of weathering and fracturing Thus, differently deposited strata vary much in their appearance and composition depending on the condition under which they are formed and their cooling process. They are generally marked by low original porosity but can form important aquifers when exposed to weathering processes by post-depositional faulting and fracturing. The frequency and extent of weathering, jointing, fractures and flow contacts are the most hydrogeological factors imparting porosity and permeability of volcanic aquifers. Due to different eruptions and time gap in between them, the rocks formed prior have been weathered and /or eroded with subsequent

deposition of alluvial materials giving rise to layers of paleosoils. These rocks are groundwater reservoirs hosting both cold and thermal waters.

The hydraulic properties of major aquifer units in the basin is due to scoria deposit and gas vesicles, columnar joints, lava tubes, faults, geological contacts, weathered media, fractures, and lineaments. These structures are important in the groundwater circulation and the flow within volcanic rocks. The permeability and porosity vary depending on spatial and vertical extent of formation and mode of deposition. Based on this, extrusive volcanic rocks of highlands are generally massive /weathered to the top and have low primary porosity whereas the volcanic pyroclastics in the rift floor have high primary porosity.

5.2. Major Hydrostratigraphic units in Abaya Chamo Lakes basin

The complex nature of the rift volcanics in the basin and lack of enough quantitative data on yield, permeability, and aquifer thickness for each specific hydrostratigraphic unit makes the preparation of hydrogeological map difficult and hence characterization of the hydrostratigraphic unit is done for major aquifer units. Broadly, the hydrostratigraphic units of the Abaya Chamo Lakes basin could be classified based on the regional aquifers permeability into fissured, porous, mixed fissured and porous ,and units essentially of no groundwater resources. Having these major classifications as background and field information of surface geology, borehole lithologic log data, basic hydrostratigraphic units within the basin is classified into five major groups. These include: 1) Low productive fissured Basement complex hydrostratigraphic units, 2)Moderate to locally highly productive fissured Tertiary basalt and associated units, 3) Moderate to locally highly productive fissured upper Tertiary to Pleistocene acidic volcanic units, 4) Moderate to locally highly productive fissured and mixed porous Pleistocene basalts and associated units, and 5) Moderately to highly productive porous sedimentary and volcano-sedimentary units (Fig.31).

5.2.1. Low productive fissured Basement complex

A high grade metamorphic Gneissic rock (Pm) of the Abaya Chamo Lakes basin is less fractured and devoid of primary porosity and is classified under low productive fissured aquifers. The

water bears in the weathered top portion and are characterized by very low secondary porosity and permeability. The aquifers are unconfined in Amaro shallow drilled wells (≤ 50m) and confined in a deep well (>60m). The weathered top unconfined shallow aquifer of the unit has a thickness of about 10 to 15meters , but in deep wells it is up to 25meters of weathered columns. The static water level is from near surface to 34meters in the unconfined shallow aquifer and in confined aquifer, it is up to 60meters. Small unconfined cold springs and wells discharge up to 4lit/Sec. The drawdown in wells is higher which could reach even up to a final depth of wells (SWWCE, 2004; 2009).

5.2.2. Moderate to locally highly productive fissured Tertiary basalt and associated units

The aquifer portions of lower basalt, middle basalt, and associated middle welded Tuff/ignimbrite are classified under extensive aquifer of fissured permeability covering the southern half of basin in the eastern and western highlands, escarpments and extending towards lower reliefs (Jiri, 2015). The unit exhibits columnar joints, fracturing, strong weathering and /tertiary faulting and hence is the major aquifer for shallow wells, deep wells, and springs of the area (Fig.31). The weathering of Tertiary formations is due to its position receiving higher amounts of highland rainfall (above 1300mm).

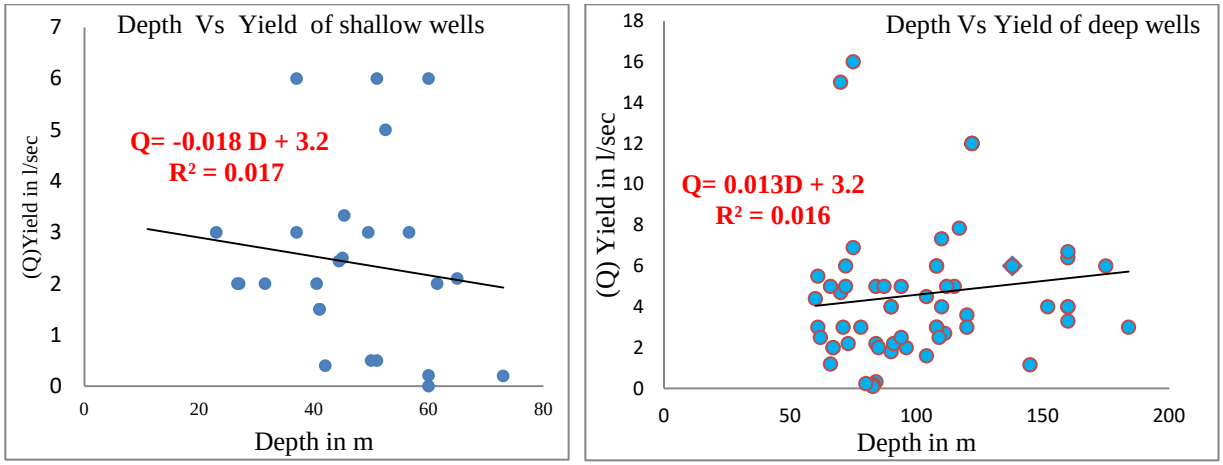

Fig 29 Relation of Depth to yield of shallow wells (right) and deep wells (left) in tertiary basalts and associated units

The thickness of the formation is more than 1600m from highlands of Chencha towards wells in Arbaminch but vary in places where the basement rocks are near to the surface and overlying acidic volcanic bury it (Jica, 2012). The unit forms confined to unconfined aquifers. Along River valley of Gelana and nearby Lakes, it forms unconfined aquifers while the weathered and fractured media of the unit form confined aquifer.

The spatial distribution of cold springs in tertiary basalts and associated formations (Fig.37) indicated that high yield cold springs (8 to more than 200l/Sec) are aligned along fractures and near scarps of the big faults (NNE-SSW). The depth to yield relation plot (Fig.29 right) of shallow drilled wells in the Tertiary basalts and associated units indicated that the wells discharge up to 6lit/Sec in the depth range of 60meters and in places, smaller discharging wells occur due to its location away from fractures and the extent of weathering becomes low with depth. However, weathered strata of older basalts are important sources of shallow water mostly in the southern half of the basin. The slope is negative for shallow wells depth–yield relation with poor R^2 supports the spatial heterogeneity of the yield and the low extent of weathering with depth.

Deeper wells drilled in Tertiary basalts showed slight increase of yield with depth though the correlation is very poor. Increased well discharge (up to 16lit/Sec) and static water level of artesian to 69meters occurs in the unit. Artesian wells flow from Tertiary basalts of lower reliefs of Arbaminch plains is related to the increased fracturing to store water (SWWCE, 2015) and converging flows towards the area. But in places, the potential of the Tertiary basalt aquifer is less (Fig.29 left) which could be associated with the massiveness or low fracturing of the formation in localities like west of Lake Abaya (Fig.31) where wells drilled for 200m in massive basalt become nonproductive.

5.2.3. Moderate to locally highly productive fissured Tertiary to Pleistocene. acidic volcanic units

These units of fissured and sometimes mixed aquifers consist hydro strata of upper tertiary Nazareth series rocks, stratoid-silicics (ignimbrites, tuff, trachytes, Rhyolite), and lower

Pleistocene rocks. The units form extensive aquifer of fissure permeability occurring along the eastern and western highlands, escarpments, piedmont plains and rift floor of the basin. The hydrogeological characteristics of the units depend mostly on the age, tectonic and geomorphological settings. The distribution of large Tertiary faults, Pleistocene sub-circular caldera, rift floor faults, fractures, geological contacts and weathered portions of the units mainly control the depth of drilling and discharge of wells and springs.

Ignimbrites and related acidic volcanic rocks have discharge in the range of (1.4 to 20l/Sec) for the drilling depth range of 80 to 253m within the formation thickness of more than 2000meters. In places along the River and fault/fracture lines, weathered portions and piedmont plains where these units occur, the aquifers are unconfined while confined in other localities (Fig.30, 31). Aquifer discharge from the thickness of 12m to 66m having a drawdown of 3.96 to 96meters (annex 2). The higher well discharges and large yielding cold and hot springs (35 to 120lit/sec) are exploited along Tertiary fault, Pleistocene caldera wall and quaternary fault zones indicating that the formation is highly productive as a result of its secondary fracture porosity and permeability. Therefore, the local investigation is essential to determine the available yield and the extent and depth of the groundwater resources in acidic volcanic rocks especially in ignimbrites and tuffs (Fig.30). It is true in the case of 20l/s discharging deep well (104m) drilled in fault/fracture zone at Guraghe highland (3130masl) (SWWCE, 2015).

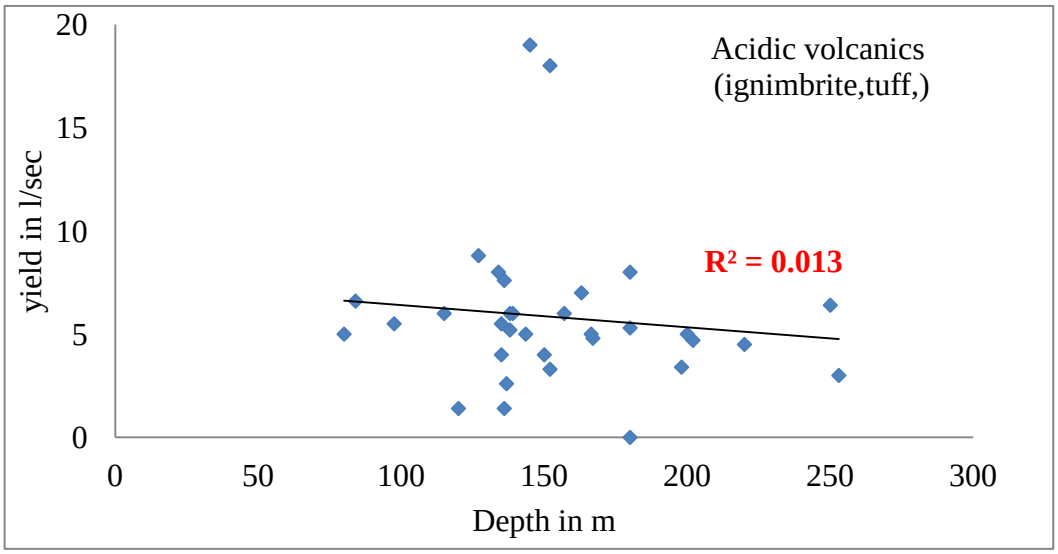

Fig 30 Depth versus yield of deep wells in acidic volcanics

Lamarbe cold spring (northern tip of Bilate River basin) flowing towards the Lake Shalla Basin and Loke cold spring flowing towards Awassa Lake Basin from the upper Gidabo Basin (Mulgeta M., 2007) indicates the regional groundwater transfer of deeper groundwaters from this unit. Hot springs are also related to undifferentiated per alkaline silicics forming volcanic uplifts initiated deeper faults ascending hot spring (Q=50lit/Sec) as in Arto to the west of Alaba Alaba areas (Fig. 37).

The poor correlation of depth to yield plot of deep well in acidic volcanics (Fig. 30) could be related to the age of the rocks, rate of weathering and extent of fracturing/faulting. Highly departed yield values of wells could be related to their location along regional buried older faults filled by volcanic sediments or near the faults facilitating the regional flow of the groundwater.

5.2.4. Moderate to locally highly productive fissured and mixed porous Pleistocene basalts and associated units

Pleistocene basalts and associated hydrostratigraphic units are classified as moderately productive and locally highly productive fissured and mixed porous aquifers of rift floor. Pleistocene basalts occur with basaltic hyaloclastics, peralkaline silicics undifferentiated with obsidians and overlying pumice (Fig.4 and Fig.31). Mixed inter-bedding of basalts with porous scoria and pumice makes the unit multilayer aquifer. Secondary permeability is enhanced in this formation because of strong weathering and development large escarpment faults, joints and fractures of rift floor (Jiri, 2016). The formation is distributed mainly south of Dila, along with the River Bilate both northern and southern parts of Dimtu and in between lakes Abaya and Chamo forming the bridge of God (Halcrow, 2008).

Deep wells of rift floor drilled in Pleistocene basalts and associated formations penetrated to the depth range of 70 to 160meters discharging 3.5 to 12lit/Sec from the aquifer thickness of 18 to 24m. These wells exploit groundwater from upper aquifers recharged by highland rainfall. The drawdown in the aquifer unit is almost insignificant in highly permeable Pleistocene basalts up to 32meters. The aquifers are confined in most of the cases, but unconfined in places where rift faults facilitate the emergence of cold and hot springs (SWWCE, 2015). The occurrence of hot springs from unconfined aquifers in rift floor, especially to the north of Lake Abaya forming

Abaya geothermal field. In some localities, turbulent and fast horizontal flow of cold spring waters (Arbaminch) and vertically flowing hot springs (North of Lake Abaya) indicated the different orientation of faults and fractures. The flow of a hot spring is weak and the wells give a low yield through a higher drawdown in localities where the fracture apertures are filled by either recent sediments or pyroclasts and geyserites, The alignment of scoria cones along the rift floor plains shows recent uplift along the fault line determining the direct recharge to the system and the discharge of wet season small local springs.

Associated with young basalts Holocene obsidians form aquiclude in the rift floor in the north of Lake Abaya. The outcrops of obsidian show well-developed fracturing. The fractures are usually open and are not filled with clay which leads to rapid infiltration of rainwater. All the small seasonal springs emerge at the massive basalt river bank of Bilate show the flow of infiltrating groundwater flows along these fractures and emerge as intermittent springs and where the obsidian flows are thick with joints filled with silts or/and clay, the unit develops long-lasting seasonal and even perennial springs.

Deeper aquifers (>150meters) of the rift floor below basaltic layers are mainly composed of sand and gravel. This aquifer is highly productive in rift floor with well discharge range of 12 to 26lit/sec and drawdown of 2.5 to 48.9meters. Its distinction from the upper aquifer in recharge source and mechanism is briefly discussed in the section of isotope hydrology.

5.2.5. Moderately to highly productive porous sedimentary and volcano-sedimentary units

Volcanic and sedimentary rocks generally form volcanoclastic strata associated with volcanic eruptions having the characteristics of sedimentary materials. The strata are dominated by clastic sediments of volcanic origin, lacustrine sediments occurring with either tuff or Quaternary deposits and alluvial, colluvial, elluvial sediments units. The units are distributed along piedmont plains, River valleys and surrounding the Lakes of the basin. The remnant sediments of the Lakes reach a significant thickness particularly around the Lakes and in marshy areas along Bilate (Boyo), Gidabo and Gelana rivers (Fig.31).

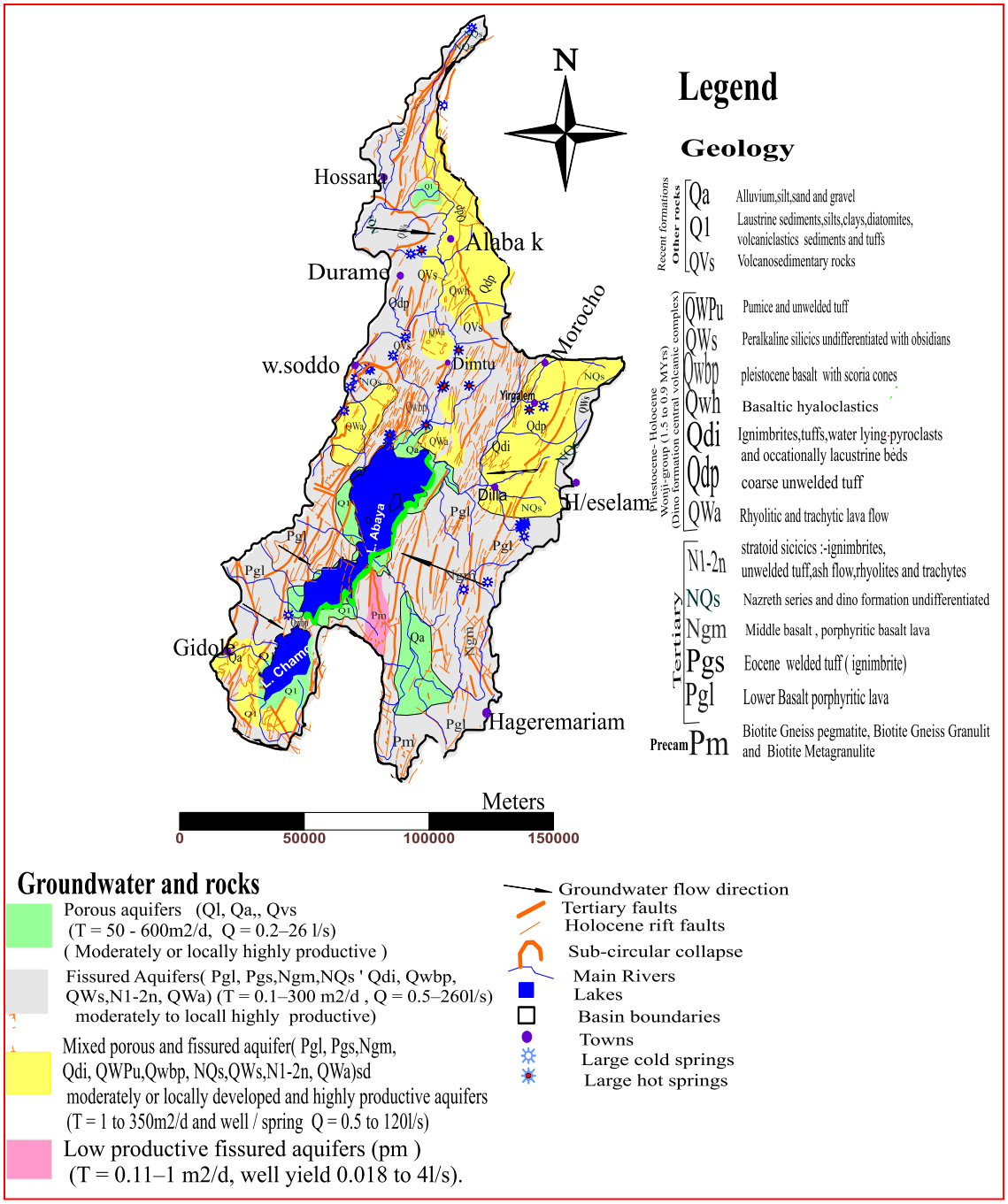

Fig 31 Hydrogeological map Abaya Chamo Lakes basin

The aquifer is a very good source of groundwater depending on the thickness, sorting and recharge conditions. Groundwaters drilled along west of Lake Abaya towards Arbaminch in unconfined aquifers of alluvial and lacustrine sediments are providing usable water in depth range of 50 to 200meters. The yield of boreholes drilled varies from 1 to 6l/s (SWWCE, 2015). These rocks are characterized by the texture of sediments (clay to sand and gravel, ash, tuff and

diatomaceous materials). The dominant materials are silts inter-bedded with tuffs. Volcano-sediment deposits where reworked, poorly sorted, rounded to sub-rounded shape are characterized to be moderate to locally highly productive confined aquifers in piedmont plains and lower reliefs.

5.3.The role of geological structures in groundwater occurrence and flow

Physiographic setting of the Abaya Chamo Lakes basin resulted from past geologic and tectonic activities (Bekele et *al.,* 1992) controls the nature of water-bearing rocks, the occurrence and distribution of groundwater and its flow condition. The study basin is the most reworked part of the country by tectonic and volcanic processes through the occurrence of features like Tertiary volcanic uplifts and border faults, escarpment normal faults, sub-circular caldera collapses, Rhyolite domes, cinder cones and rift floor en-echelon step faults. These structures in places broadly determined the hydrogeological Characteristics of the basin through recharging the groundwater system and variably discharging as wells (0.2-26l/sec) and springs (0.06-260lit/sec). There are four tectonic features that control the occurrence and flow of groundwaters in the area.

1. Highland area (>1800masl) of the two sides of the basin is highly affected by Tertiary NNE-SSW faulting/fracturing and deep weathering responsible for the shallow and deep circulation of groundwaters. Groundwaters emerge as springs along contacts, fractures and slope breaks. Large faults forming rift escarpments are responsible for the discharge of large springs (Tamiru A., 2003). The weathered strata of Tertiary basalts and acidic volcanic are major sources of shallow waters. The frequent intercalation of tuff, pumice, weathered and fractured ignimbrites and older basalts in places along the highlands, escarpments and Intermountain complexes of lower reliefs determine low discharging shallow wells and cold springs (≤6.3lit/sec) (Fig.37) and the difference in hydraulic properties in wells. Localities affected by tertiary faults and its vicinities are endowed with a higher quantity of waters more than 60l/s of springs and 25l/s of deep wells (Abrham A,2006).

2. Pleistocene Circular and sub-circular caldera occurred in areas north of Lake Abaya where recent tectonics heavily affected. Two adjacent Sub-circular caldera collapse to the NE and SSE of wolaita soddo is responsible for the origination of more than ten larger yields (3 to 35lit/sec) cold springs along the caldera wall. Deep wells drilled above the caldera wall for 260m deep have a discharge of 2.6lit/sec indicating that the flow is more governed by caldera structure in the area. The variability in the discharge of springs along the caldera wall is related to variability in recharge, rock type, fracture aperture and higher topographic differences, (Abrham A, 2006). To the north 40kms away from Lake Abaya, smaller caldera structures occur on Duguna volcanic ridges (Jica, 2012) in rift floor has walls with low discharge ≤ 2lit/sec cold springs.

3. The N-S and NNE-SSW rift floor Holocene wonji fault belt system faults control the discharge of different magnitude of cold and hot springs. In places where fractures and faults penetrate deeply, high heat from the deep crust affect the upper aquifers in deep wells and hot springs, but colder spring emerge where separate fracture or fault system occur (Fig.37).

4. Volcanic springs and steam particularly NNE of Abaya adjacent to the lake with a temperature of 96ºc are deep source originated from magma or juvenile water rich in silica (433mg/l) (Teclu, 2007). But the hot springs of lesser silica is of shallower aquifers in contact with highly heated rocks which is the case in chewkare hot spring (42^0c) (Gezahagn Y, 1980).

5.4. Groundwater head and flow direction

A water table contour map of an aquifer is a very vital tool in groundwater studies as one can derive from it the gradient and the direction of the groundwater flow. It is a graphic representation of the hydraulic gradient of the potentiometric surface. Hence the direction of the groundwater flow, being perpendicular to the equipotential lines, can be directly deduced from these maps. Furthermore, an effluent (gaining) or influent (losing) from a source (upper lands or River) and artesian effect can be determined using these maps (Freeze and cherry, 1979). The groundwater head of the Abaya Chamo Lakes basin is constructed for local, intermediate and regional flow systems. Small and medium springs and shallow wells of depth less than 60

meters are assumed to represent local or intermediate flow systems and large springs (> 6lit/Sec) and deep well's depth greater than 70 to 400meter represent regional flow/deeper aquifers. For this purpose shallow drilled well, smaller and medium springs, deep wells and large springs are used (annex 3). The resulting groundwater level maps (Fig.32) indicate that shallow groundwater level in aquifers of highlands (east and west boundaries of the basin) more or less follow the topography and flowing towards the rift floor from almost all parts of the basin.

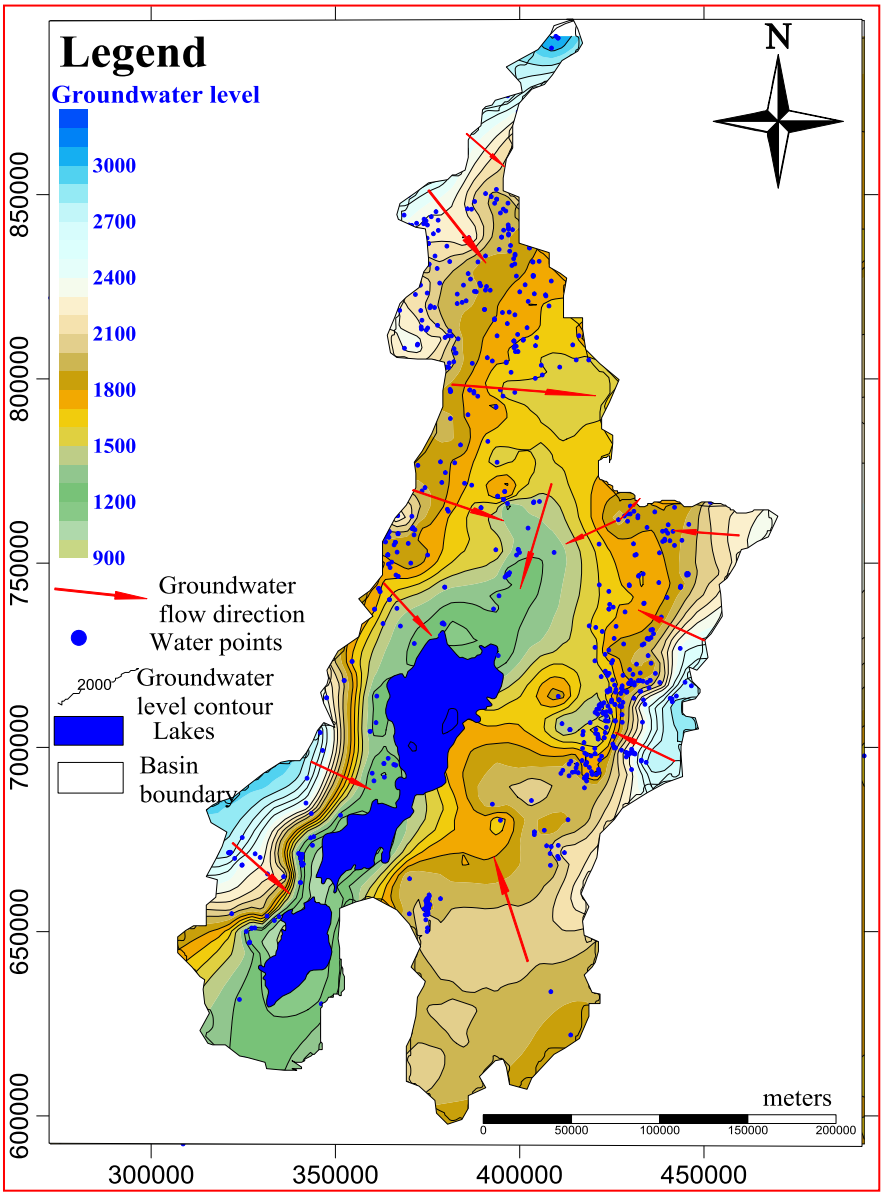

Fig 32 Groundwater level and flow in Abaya Chamo Lakes basin (*constructed from shallow wells, deep wells, springs. The water level index is given as legend on the map*)

In areas of the eastern part of Bilate basin where thick pumice drilled to the depth of more than 360m, regional groundwater flows out of the study basin. The groundwater outflows to Lake Awassa or Lake Shalla Basin from the eastern part of the Bilate River basin which is in the opposite direction to flow of surface water from the western boundaries of Lakes Basin towards the Bilate River basin. The regional groundwater flow pattern of deeper aquifers is convoluted in places where geologic structures and local barriers dislocate aquifers and consequently also depth to static water level and flow. This revealed that as in basins highly affected by Tertiary tectonics in the north of Bilate basin changed the flow direction of deeper aquifers. In North of Gidabo River basin, the outflow of groundwater from deeper aquifers is facilitated by bigger faults. To the east of Lake Abaya towards escarpments, the flow is also complex due to tectonic structures.

The depth to groundwater level (static water level) is increasing towards the rift floor from both sides of the highlands. Although the regional groundwater flow direction is towards the rift floor from both sides; topographic gradient, local barriers, lithology, and structures are responsible for the complex deeper flow pattern.

5.5. **Hydraulic properties of volcanic rocks in Abaya Chamo Lakes Basin**

5.5.1. **Transmissivity (T) distribution**

Aquifers are natural systems having a high degree of variability, that makes the description of its hydraulic properties difficult. Understanding of the hydrogeological and hydraulic properties of aquifers using a proper groundwater pump tests assist in the development and efficient management of groundwater resources (Neven kresic, 2009). Transmissivity is a measure of the capability of the aquifer to transmit groundwater through a unit-wide saturated area over its full depth, under a unit gradient. Transmissivity estimated from pumping test measures how much water can be transmitted horizontally. It is the product of the hydraulic conductivity and the thickness of the aquifer (Driscoll, 1986) and is employed in most groundwater flow equations to understand the flow dynamics (Freeze & Cherry, 1979).

Pumping tests in the available wells of Abaya Chamo Lakes basin were conducted for the purpose of water supply from 24 to 48hrs to determine the discharge and estimate the pump

capacity/position and hence the chance to get appropriate data is associated with full penetration of the aquifer materials, careful logging of the well, proper screening of the aquifers with provision of observation wells and conducting accurate pumping test which further require selection of appropriate pump for the test, accurate measurement of well yield, drawdown and well recovery. These activities require experienced expertise from data collection up to analysis to identify defined aquifer system. As a result, hydraulic data obtained from such traditional wells are often less relevant.

In this study, the effort is made to investigate the spatial distribution and correlation of aquifer parameters of the volcanic aquifers of the Abaya Chamo Lakes basin. Empirical relations of the specific capacity and transmissivity values helped in the estimation of the hydraulic properties of aquifers (Jalludin and Razack, 2004; Huntley et al., 1992; Razack and Lasm, 2007; Yitbarek, 2009 and Sandra K. Richard et al, 2016). The approaches by the above researchers used easily available aquifer parameter specific capacity (S_c) of a well, which is the ratio of pumping rate (Q) to drawdown (s) in the well for quantification of transmissivity (T) and is an area and formation specific. The fact that S_c is correlated with hydraulic-flow properties (Theis, 1963) can simplify parameter estimation mainly because S_c values are more abundant in groundwater databases than values of T or hydraulic conductivity (K), and offer another approach to estimate hydraulic parameters of aquifers.

Pumping test data of 99 domestic wells from different formations in the Abaya Chamo Lakes basin from which transmissivity is for 59 and specific capacity is for 89. For both wells have measured depth, static water level, yield and aquifer thickness are collected from different sources and organized. The methods for the analysis of pumping test data are described in (Kruseman and De Ridder, 1991). The transmissivity values unmeasured are calculated from specific capacity using a simple linear regression which was performed on both the actual data and log-transformed data to obtain an empirical relation (Fig.35). The pump test based analysis for transmissivity (T) and specific capacity (Sc) is log-transformed to obtain an empirical relation for 59 wells in the basin. The relation showed

$$T = 0.65\ (Sc)^{1.13} \qquad (5.1)$$

Where T is the transmissivity and Sc specific capacity are in m^2/day having a log-log correlation coefficient of R^2=0.63.

The 59 pairs of data of Sc and T in the Abaya Chamo lakes basin has R^2=0.63 (Fig.33) showing low correlation compared to Ashange basalts and Awash volcanic complex terrains. This could be related to the utilization of T and Sc data of wells drilled for water supply purpose whose relevancy of data collection, monitoring and analysis has many limitations. In addition, the partial penetration of wells and the heterogeneity of volcanic aquifer materials of the complex rift Abaya Chamo Lakes basin.

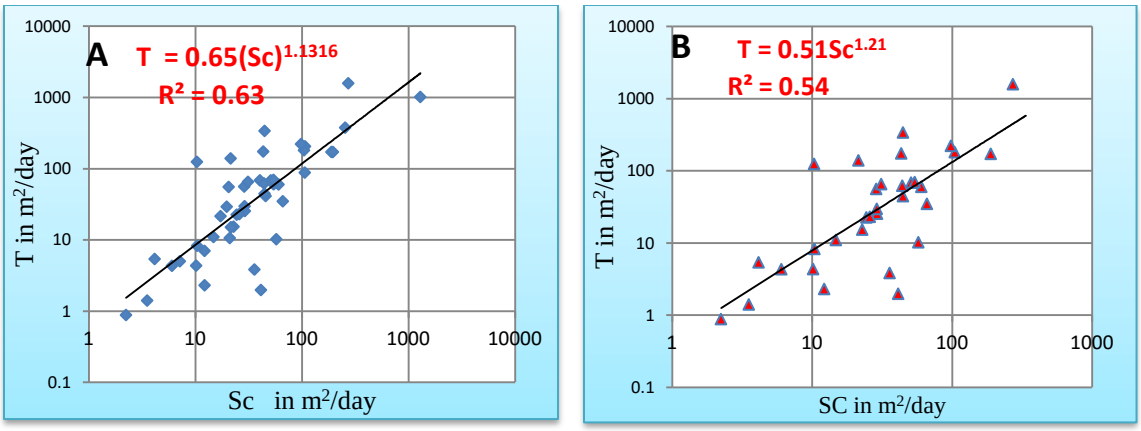

Fig 33 Relation of Sc (m^2/d) and T (m^2/d) analyzed from pump test results of A) 59 data points from different aquifer formations and B) 30 data points from weathered and fractured ignimbrite and tuff aquifers Abaya Chamo lakes basin

The heterogeneity is more reflected in fractured and weathered ignimbrite and tuff of Abaya Chamo lakes basin as

$$T = 0.51\ (Sc)^{1.21} \qquad (5.2)$$

Where T is the transmissivity and Sc specific capacity are in m^2/day with a log-log correlation coefficient of R^2=0.54.

Table 4 Comparison of the empirical relations obtained from different studies

The empirical relation between T and Sc	Aquifer	R^2	study source
$T = 11(Q/S)^{0.93}$	Ashange basalts Ethiopia	0.99	Seid G. 2011
$T= 1.25(Q/s)^{1.003}$	Upper Awash volcanics Ethiopia	0.97	Yitbarek,2010
$T=0.33(Q/s)^{1.30}$	Fractured crystalline, Ivory Coast	0.93	Razack and Lasm,2007
$T = 15.3(Q/sw)^{0.67}$	Alluvial deposits Morrocco	0.63	Razack and Huntly,1992

$T = 0.65 (Q/Sc)^{1.13}$	volcanic rocks in Abaya chamo, Ethiopia	0.63	present work

The data showed that the aquifers of the Abaya Chamo Lakes basin have a less magnitude of Transmissivity compared to the others described in the table (Table 4). The differences in the transmissivity of the volcanic aquifers in the table could be due to the heterogeneity in the age, the rate of faulting/fracturing and weathering, infilling of the fractures/fault openings and inter-bedding of differently erupted volcanic strata of the volcanic rocks that determine the differences in permeability and porosity.

The correlation coefficient of $\log_{Sc}$ and $\log_T$ of Ignimbrites and tuff aquifers ($R^2 = 0.54$) is more heterogeneous than basalts and volcano-sedimentary rocks ($R^2 = 0.63$) of Abaya Chamo Lakes basin. The specific capacity of Tertiary basalts in the Abaya Chamo Lakes basin is in the range between 5.28 to 551.55m^2/day. This variability is related to the difference in depth of aquifer penetration (60 to 175m), nearness to major faults collecting to discharge areas and lower drawdown from fractured and weathered tertiary basalts. Relatively higher variability in specific capacity of Ignimbrites and tuffs as potential aquifers of the basin could be related to multi-layer aquifer nature, partial penetration of aquifer, paleosols as inter-bedding materials and wide fractures and joints controlling deeper circulation.

A small number of data points of hydraulic properties (T and K) could not be spatially representative. Therefore the use of empirical relation $T = 0.65 (Sc)^{1.13}$ to calculate transmissivity from specific capacity is found to be very important to understand the spatial variation of Transmissivity (Fig. 35) though the calculated and the measured values do not show such a strong relation (Fig. 34). The low correlation of the T measured and T calculated could be basically related to the heterogeneity of the rocks and variable source data.

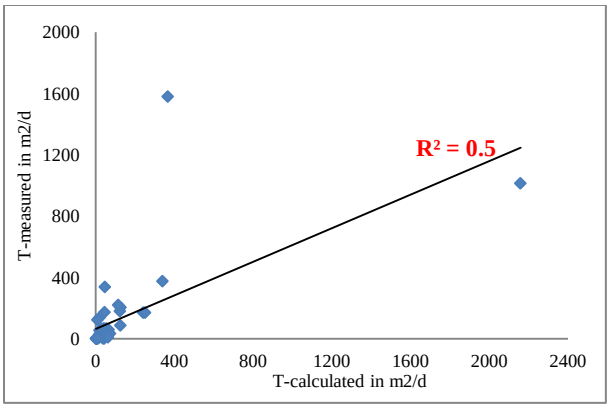

Fig 34 T-calculated versus T-measured in wells of the basin

Tertiary formations at the eastern and western highland boundaries and escarpments of the basin showed transmissivity (T up to 350m^2/d) in depth range of 60 to 253mbgl. Deep wells drilled in the aquifers of high (T = 150 to 350m^2/d) are aligned along major boundary faults but T values below 200m2/d could be related to less recharge (high drawdown), interbedding, filling of fractures or fault openings by weathered materials and its position away from major fractures (Fig 31, Fig 35).

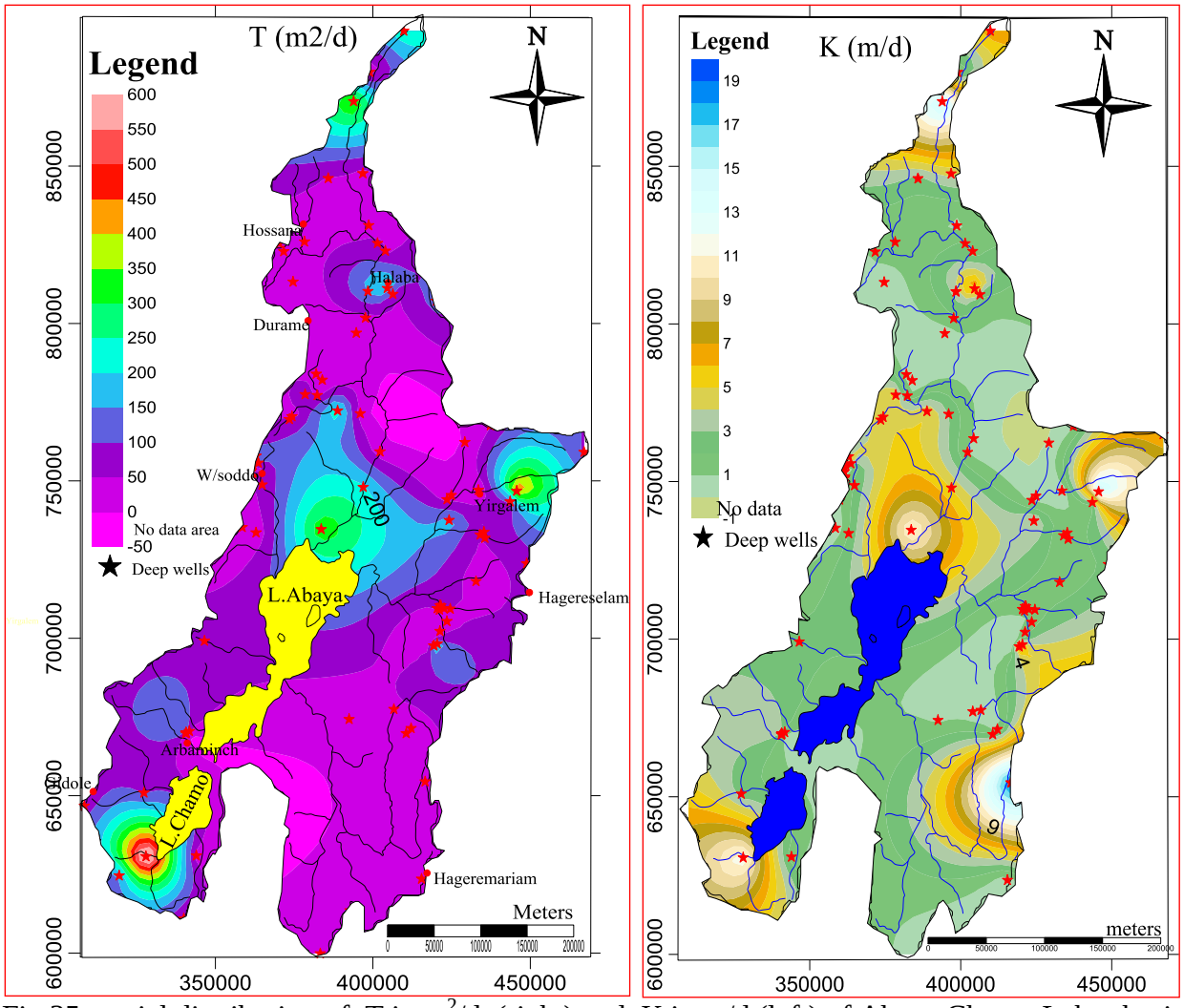

Fig 35 spatial distribution of T in m^2/d (right) and K in m/d (left) of Abaya Chamo Lakes basin

Rift floor aquifers of the higher T up to 800m2/d) in faulted and fractured areas in the north of Lake Abaya and south of Lake Chamo could be related to deeper rift aquifers composed of sand/gravel and higher recharge source other than rain (Refer section 7 isotope hydrology recharge source and mechanism). Such aquifers have materials formed under the condition that easies the groundwater flow. High discharging cold and hot springs could also be related to large boundary and rift faults or slope breaks. There is a general increase of T towards rift floor indicating that the degree of fracturing, their interconnections (networks) and aperture increases from highlands and escarpment towards

5.5.2. **Hydraulic conductivity (K) distribution**

Volcanic rocks are characterized as both sedimentary and fractured rocks. As sedimentary rocks, it occurs as stratification of lavas, tuff, breccias, alluvial intercalations with fossil soils on top of volcanic deposits. Its occurrence as a fractured rock is in the form of polygonal cooling joints in basalt and fractures in ignimbrites and welded tuff. The hydrological behavior of volcanic rocks, therefore, depends on the combination of geological nature and selection of the model for understanding the groundwater movement and flow (UNESC0, 2004).

Hydraulic conductivity k is the constant of proportionality in Darcy's Law and indicates the quantities of water that will flow through a unit cross-sectional area of a porous medium per unit time under a hydraulic gradient of 1. It is governed by the size and shape of the pores, the effectiveness of the interconnection between pores, and the physical properties of the fluid. If the interconnecting pore is small, the volume of water passing from pore to pore is restricted and the resulting hydraulic conductivity is quite low. It is commonly calculated by using the formula (K=T/b) where T is the transmissivity in m^2/d of the aquifer and b the aquifer thickness in m. Wells data of areas in the country as a whole and Abaya Chamo Lakes basin, in particular, lack basic parameters of groundwater data which limit the estimation of hydraulic conductivity.

The hydraulic conductivity of the Abaya Chamo lakes basin was estimated from the empirically calculated and pump test analyzed transmissivity values of 85 deep wells plotted on a map (Fig. 35). The calculated and pump test evaluated hydraulic conductivity are highly correlated (R^2=0.7) (Fig 34). Hydraulic conductivity estimates range from 0.071 to 19.44 m/d implying low values. Highland older weathered aquifers of the basin are represented by lower ranges of hydraulic conductivity (1 to 4m/day). This relates to the filling of weathered materials into the fractures and pore spaces of aquifers along highlands of the basin. It agrees with (David and Deweist,1966) that hydraulic conductivity and porosity of volcanic rocks tend to decrease slowly with geologic time due to filling and compaction of secondary minerals into fractures. But the spatial distribution of hydraulic conductivity K along eastern highlands and the northern part of the basin is relatively higher in places affected by boundary faults guiding the flow. The K values are also higher in rift floor deeper aquifers (sand and gravel) affected by Holocene faults, particularly to the south of Chamo and north of Lake Abaya (Fig.31 and Fig.35).

Generally, the hydraulic properties of the basin depend on secondary structures (faulting and fracturing) and weathering. In the aquifers of highlands, the role of NE-SW tertiary faults is higher in controlling the movement and flow of the groundwater (Fig.31). But the higher rate of weathering of the upper parts of older rocks of highlands (Basalts, Ignimbrites, trachytes, rhyolite) and subsequent discharge to fractures and fault scarps reduce the size of fractures and other openings with a consequent progressive decreasing of the permeability. The increased hydraulic conductivity of rift floor in the north of Lake Abaya related to deep penetrative faults giving rise to a high value of K in aquifers of geothermal field.

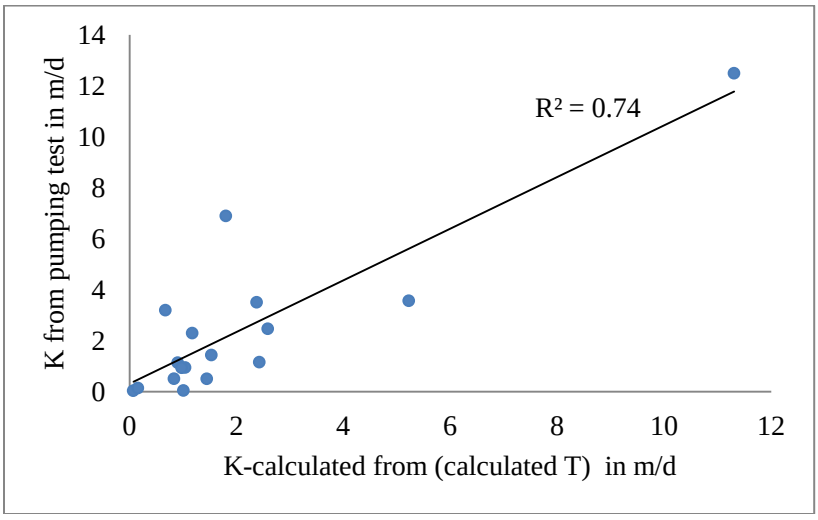

Fig 36 correlation of calculated and evaluated values of hydraulic properties (*The K evaluated is the value form pumping test but the K calculated is the value of T//b where the T value is calculated from the relation of T and Sc. The T calculated divided by the aquifer thickness gives the calculated K*)

5.5.3. **Distribution of Spring discharge and its variability**

The richness in groundwater resources of the Abaya Chamo Lakes basin is indicated by the existence of diverse spring types (depression, contact, fault, fracture and joint) with discharge varying from 0.036 to 260lit/sec. Based on the temperature of the reservoir the springs could be cold and thermal/volcanic. Field investigation on discharge measurement of 282 cold springs and 14 hot springs ranging between 0.036lit/sec to 260lit/sec helped to classify the springs according to the magnitude of their discharge. 268 springs (89%), 15 springs (5.1%), 2 springs (0.7%) and 7 springs (2.4%) have discharge rate ranges of 0.036 to 10lit/sec, 10.01 to 25lit/sec, 25.01 to 50lit/sec and 50.01 to 260lit/sec respectively (Fig 37). Less discharging (0.036 to 4 lit/sec) cold

springs of the eastern and western highlands and escarpment are either contact (highly permeable weathered and fractured rocks overlying less permeable rocks) or depression (short breaks in topography along the slope).

The elevation distribution of springs discharge (Fig 38) displayed that Shallow circulating small springs with discharge (< 5 lit/Sec) are concentrated in the highlands and escarpments (>1700masl) unconfined to semi-confined aquifers (sediments and weathered rocks) in places receiving maximum rainfall (1300mm and above). Larger cold springs LMSP (>100lit/sec) as in the northern tip of the basin highland (Fig 37) could be related to deeper aquifers of inter- basins. Other cold springs in this range of discharge (>10lit/sec) in the highlands and escarpments are associated with deep cutting faults and fractures (LKMSP, AWSP, LMSP). Cold Springs (AMSP) in rift floor (<1200masl) in between Abaya and Chamo Lakes to the western side is highest discharging spring (260lit/sec) in the basin. Hot springs are clustered along the rift floor and have variable discharge rates related to fault/fracture openings or infilling of fractures by recent pyroclastics or sediments.

Many of the low discharging cold springs (<1lit/Sec) in the highlands are used for domestic water supply in the basin and are less stable. They are assumed to be fed by groundwater from a small reservoir susceptible to seasonal changes or even get lost during extended dry months. However, the investigated springs decrease their discharge, but do not dry up in dry months. Smaller cold and thermal springs of rift floor occur due to local direct and indirect recharge of aquifers. High discharging cold and hot springs of different groups are observed to be stable and have almost maintained their discharge throughout the year which suggests a regional flow through wide fractures or faults.

The distribution of high discharging cold and hot springs is more in the northern half of the basin compared to the southern half related to the effect of Pleistocene and Holocene tectonics which was intense in the northern part of the basin. Hot springs with a discharge 5 to 76lit/sec cluster along the rift floor in the direction of recent rift faults flow throughout the year suggesting its regional flow system.

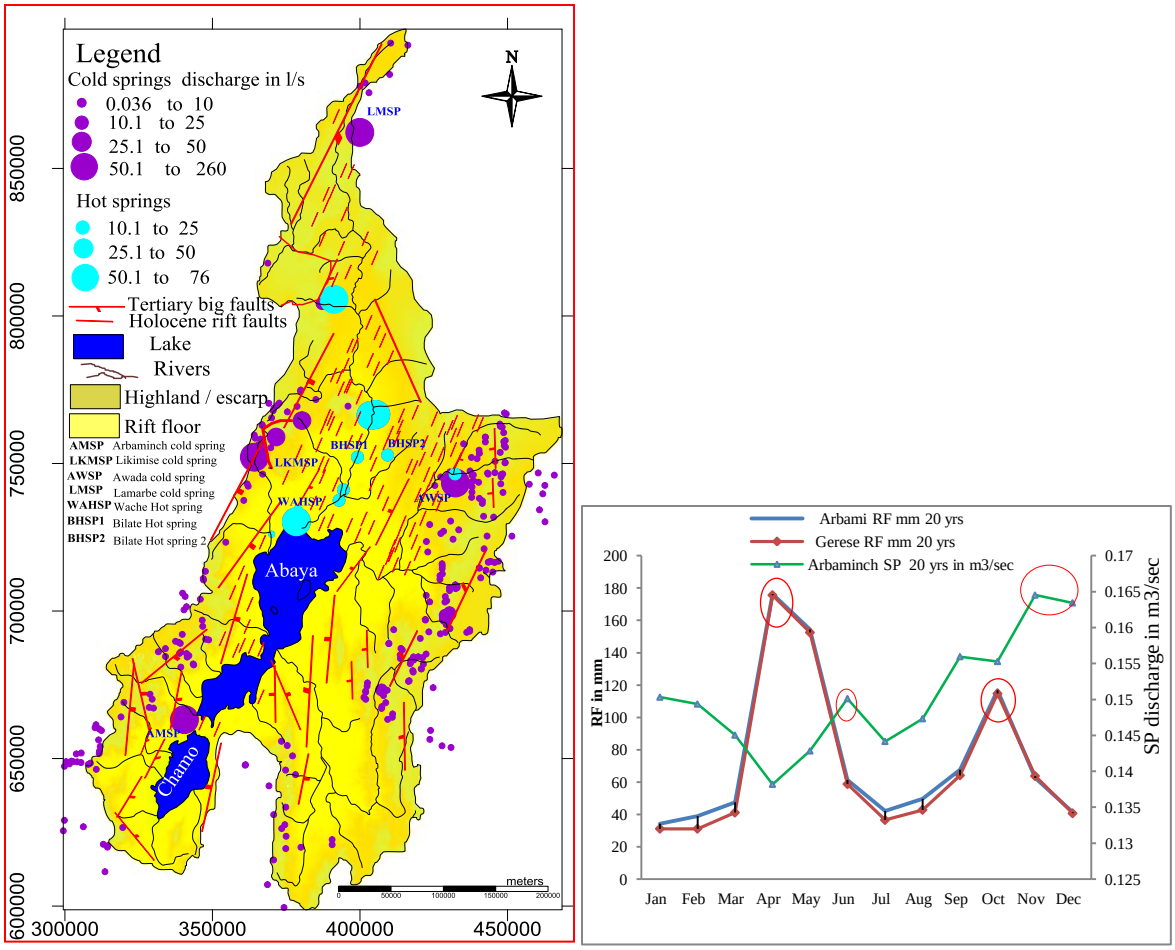

Fig 37 Distribution of cold and hot springs in Abaya Chamo Lakes basin (right) and relation of Arbaminch (AMSP on map) spring discharge to nearby rainfall stations (left)

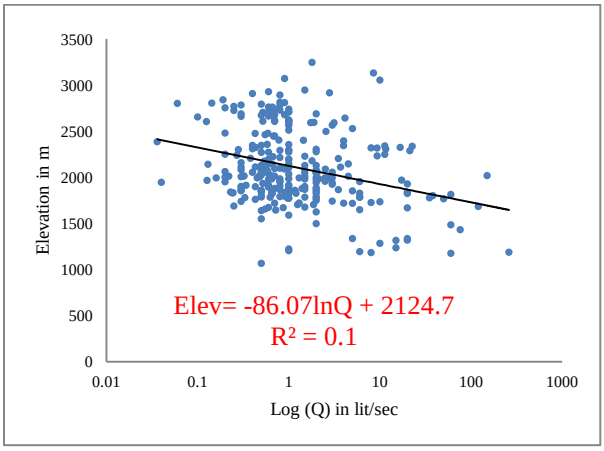

Fig 38 Elevation distribution of springs discharges

April and October peak mean monthly rainfall of Arbaminch areas plotted against Arbaminch spring discharge showed the estimated lag time for the recharged rain water to appear at spring

discharging points (residence time). The June peak discharge of the spring is the consequence of April peak rainfall and the November highest peak discharge of the spring is the effect of October peak rainfall of the recharging catchments. The two cases showed that the April peak rainfall recharges the groundwater and appears at spring discharging point after two months, but the October peak rainfall cumulatively appears after one month. This indicated that the residence time of the spring water takes longer period during dry seasons and shorter as rainfall and spring discharge increases.

5.6.**Conceptualization of aquifer systems and groundwater dynamics**

Aquifer systems of Abaya Chamo Lakes basin is conceptualized based on the evidence obtained from geomorphological, hydrological, geological, tectonic features, hydraulic, hydrochemical and isotopic data (Fig.39, 81, 82, 83, 84). The geomorphological nature of Abaya Chamo Lakes basin is characterized by elevated mountains surrounding the eastern and western boundaries, its fault escarpments and the rift valley floor where the Rivers drain from both sides to and the Lakes lie (Fig.2). Based on the synergized indicators, the aquifer systems of the three physiographic sectors (highland, escarpment and rift floor) have been conceptualized.

5.6.1. ***Highland aquifer systems***

Highland aquifer systems are composed of older Tertiary formations (basalts, ignimbrite, trachy-ignimbrites and weathered deposits in Piedmont plains and inter-mountain gullies of the plateau) mainly in the eastern and western parts the Abaya Chamo Lakes basin above 2000masl bounding the rift floor. The area is characterized by a series of giant tertiary border faults each producing large volcanic uplifts radially fractured and steep escarpment. Sub-circular caldera collapses, Rhyolite domes and Post-depositional structures (cooling joints, cracks, and shallow weathered strata) control widely the occurrence and distribution of highland groundwaters. Highland aquifers are characterized by the fissured or mixed fissured and porous permeability (Fig.31). It determines the accumulation and circulation of shallow groundwater over deep as evidenced by the existence of numerous small springs along the highlands in both sides (Fig.37, 39, 82). Shallow aquifers (0 to 60m) are unconfined to confined near the surface and in places affected by faults/fractures, but with increased well depth (60 to 253m) it becomes confined.

Aquifer systems in the highland area are directly recharged by depleted (ŏ^{18}O‰=-4.2 to -0.39) highland rainfall with the amount of above 1300mm/year (Fig.9). Direct recharge amount of about 290mm to 400mm adds to the groundwater system of highlands aquifers (Michael et al., 2016; Tesfaye, 2010; Abrham, 2006 and Arbaminch University, 2010). Shallow groundwaters and streams of the highland area indirectly recharge the system by means of percolation through fractures and fault blocks as local and regional flows (Fig.26). In localities where the surface and groundwater divides coincide, the mountain blocks bound the lateral continuity of the aquifers as indicated from drilling reports of the dry well (depth > 300m) in the triple junction Guraghe highland Lake Abaya (SWWCE, 2016).The composite (shallow and deep) groundwater head of in the highland aquifers of the basin follows more or less topography with perpendicular flow direction towards rift except in places laterally connected by faults and fractures (Fig.32). The aquifers are represented by lower ranges of hydraulic properties (T=50 to 350m^2/d) and (K=1 to 13m/day) in the wells with a depth range of 60 to 253mbgl. Localities of higher hydraulic properties are aligned along major boundary faults whereas lesser values are linked with the filling of weathered materials into fractures and pore spaces of aquifers, interbedding and its position away from the major fractures (Fig 31,35).

Highland groundwaters are Ca-HCO3 to Mg-Na-HCO3 type (Fig.54, 55) and are diluted as waters undertook low rock-water interaction, low isotopic fractionation and low residence time assisted by its fast flow through open fractures/faults under higher hydraulic gradient. The richness of Ca and Mg in waters related to the minerals of Anorthite ($CaAl_2Si_2O_8$) and Forsterite (Mg_2SiO_4) respectively in host rocks (Hem, 1985). The dominance of HCO_3^- in highland waters is due to its derivation from upper soil zone (Ayenew, 2005) and unequal dissolution of silicate minerals in places covered by volcanic rocks (Appelo and Postma, 1993). With increased depth in the highlands, the waters become rich in EC, Na, and Cl.

5.6.2. ***Escarpment aquifer systems***

Escarpment aquifer systems provide transitional groundwater with an elevation range of 1500 to 2000masl between highlands and rift floor (Fig.32, 83). Dominant escarpment aquifer units are composed of weathered and fractured ignimbrite, pumice and tuff; volcano-sedimentary rocks, Pleistocene fractured basalt, and recent sediments. Gneiss and old basalts of the southern

escarpments of the basin are in places cut by Tertiary and Pleistocene faults. Escarpment fault systems of the basin determine the change in aquifer configuration and topography. Both fissured, porous and mixed fissures and porous permeability determine the aquifers in the escarpment (Fig.31, 39). The scale of normal faults and dip direction of faults have great impact on groundwater flow. The existence of thermal springs, wetlands, and swamps is related to the east dipping direction acting as both (leaky) barriers to the horizontal flow and conduits parallel to the fault plane (Fig.39, 81,82,83,84). Westward dipping escarpment faults facilitate the transfer of highland recharged groundwaters towards Lake Abaya and also facilitate the flow of large cold springs in places like Awada plain.

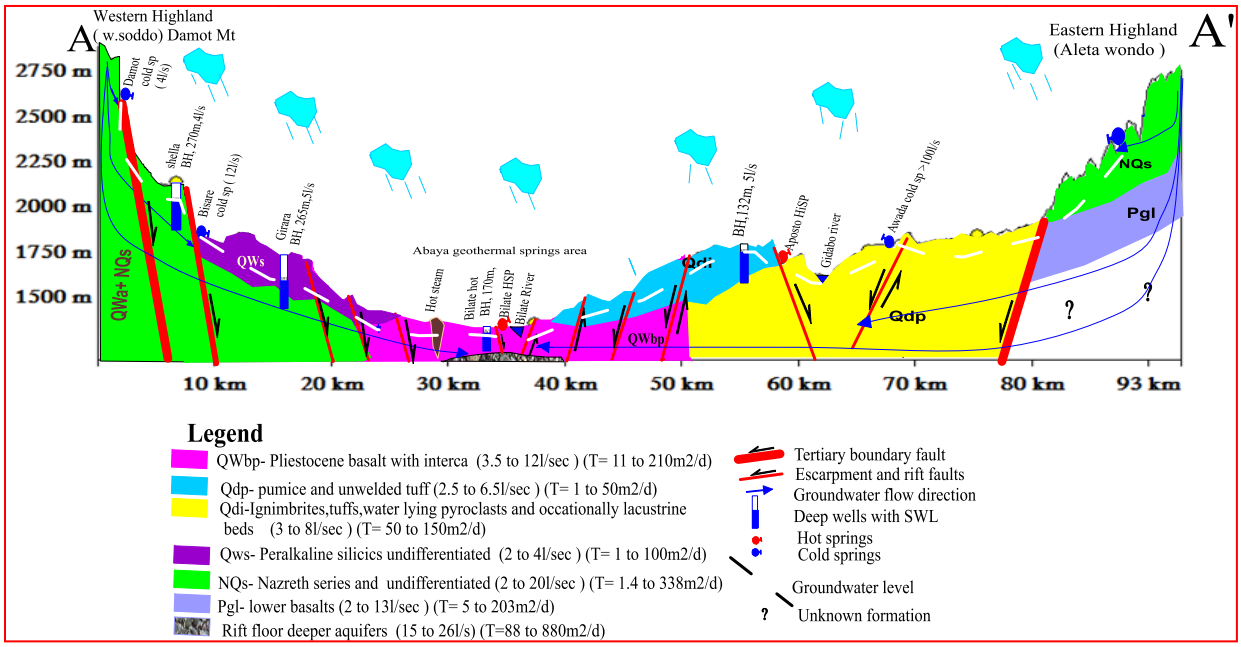

Fig 39 Hydrogeological conceptual model (E-W) of the Abaya Chamo Lakes basin to the north of Lake Abaya- Section A-A' is shown in the hydrogeological map and the Geothermal field is further conceptualized for deeper thermal source emanation and its distribution to other aquifers

Marshy Plains, buried faults/fracture area, and Rivers side of escarpments are rich in shallow groundwater (15 to 55m). In the escarpment areas, direct recharge is about 10% to 20% of rainfall amount (1000 to 1300mm) as indicated in previous studies (Fig.9) and indirect recharge from rivers and wetlands are used as local sources of waters in unconfined to semi-confined aquifers of the central Bilate, Gidabo, and Gelana basins (Fig.37, 39). Deep wells drilled to depths (110 to 265m) are recharged from both local and intermediate flows of the highlands.

Compared to the highland wells, the average depth is shallower but the average discharge of aquifers in escarpments increases for deep wells and springs. Deeper aquifers are confined, but along or near fracture lines it forms unconfined. (Fig.37).

Depleted escarpment groundwaters (ȯ^{18}O ‰= -3.2 to -0 99) of the basin is supplied by the highland and escarpments rainfalls though the degree of depletion varies in the eastern and western sides of the escarpment (Fig.26). This relatively similar isotopic composition to highland waters could be related to fast percolation of highlands rain waters favored by high hydraulic gradient and open fractures connecting highlands with escarpment areas. The regional groundwater flow pattern of escarpments is complicated in localities due to the presence deep cutting faults. These faults not only control the gushing out large perennial large cold and hot springs (up to 120l/s) but also connecting inter basins of the Awasa Lake basin to Abaya Lake basin manifested as hot springs discharging northwest of Dilla (Fig.37, 39,58).

The inland NNE-SSW faults affecting the eastern escarpment River basins (Gidabo and Gelana) evolved the composition of groundwater to Na-Ca-HCO_3 though Mg-Ca-HCO_3, Mg-Na-HCO_3 are dominant escarpment groundwaters. The transmissivity value (T= up to 250m^2/d) and Hydraulic conductivity ((K=1 to 6m/day) of escarpment aquifers (Fig.35). This indicated that escarpment aquifers are more permeable compared to highland aquifers.

5.6.3. ***Rift floor aquifer systems***

Rift floor lies between a surface elevation of 1100 to 1500masl is marked by intense and fresh Holocene faulting (Mohr, 1967). The occurrence and distribution of groundwaters in this sector of the basin are mainly controlled by the flow dynamics occurring in highlands, escarpments and rift floor. Water-bearing strata in rift floor is formed of Pleistocene basalts, young pumice, and ignimbrite, scoria, fluvial and lacustrine sediments, volcaniclastic rocks, sand and gravel. The rift valley floor comprises the NE–SW right stepping NNE–SSW ‘‘rift-in-rift" faults. Intensive cutting by Holocene faulting resulted in close en-echelon swarm faults and recent active eruptive centers. Obsidian cones and the Lakeside faults determine the discharge of hot steams and vertically flowing hot springs respectively especially to the north of Lake Abaya. Two major aquifers occur in the rift floor. The upper aquifer with hydrostrata of Pleistocene basalt, Lacustrine sediments, recent acidic and basic volcanic occurs in depth range of 60 to 160m

whereas the lower aquifer in-depth range of 150 to 400mts is sand and gravel. Shallow aquifers near River delta, Lakes sides and fault controlled springs from the unconfined aquifer, but aquifers in other formations are confined. Porous permeability is the major aquifer, especially around Rivers and Lakes though fissured and the mixture of fissure and porous occur on the rift floor (Fig. 31, 37, 39).

The aquifers of the rift floor of the basin are recharged by both direct and indirect recharge from different sources. (1) Direct recharge of about zero to 5% of annual precipitation of the rift floor (800mm to 1100mm) as indicated in previous studies and (2) Indirect recharge of highlands and escarpment shallow groundwaters through open faults and fractures. High yielding cold and hot springs discharging in rift floor are recharged from highland rainfall. The rift waters are relatively having similar depletion to higher elevation groundwaters and are less evolved. Along the groundwater evolution and flow direction, both shallow and intermediate groundwater flow systems form the indirect recharge (all inclusive recharge) and the preferential direct recharge of present meteoric waters contribute to the rift groundwater flow system including highly fractionated thermal springs towards the northern mouth of Lake Abaya (Fig.37). Progressive increase in spring discharge towards the rift floor from the highlands is related to the rift boundary and escarpment Pleistocene and upper Tertiary faults. This is supported by (Tamiru A., 2003) that the occurrence and flow of numerous high yielding cold spring in the rift is via open faults of highlands and escarpments (section 5.5.3). (3) Indirect recharge from Lakes and Rivers as indicated from some enriched groundwaters (section 8.3.5) and (4) groundwaters directly recharged under wetter and cooler climate to sand and gravel deeper aquifers of the rift floor (Fig.39, 40, 77).

The composite groundwater level in rift floor (Fig.32) indicates that the flow system is complex in rift aquifers of Bilate and Gidabo River basins in places the flow is controlled by rift faults and thick permeable pumice layer. The deeper groundwater flows towards the east (Lake Awassa Basin) from Bilate due to deeper water strike in the sand layer below thick pumice. Two kinds of groundwater flow occur in the rift floor: converging flows across the rift from eastern (E-W) and western (W-E) sides and parallel to the rift (N–S). The eastward-dipping faults of the rift floor is acting as a major barrier for the groundwater coming from the recharge areas of the basin and

drain parallel to subparallel to the rift axis and favor the occurrence of thermal springs. “Rift in rift” structure control swamps and hot grounds in the rift floor of the area. Highly mineralized waters to the NNW flank of Abaya Lakes basin (Wache thermal spring) (Fig.37) is fault controlled thermal springs (96^0c) and rich in bicarbonate indicates it deep source through faults acting as a hydraulic conduit connecting shallow and deeper circulating groundwaters.

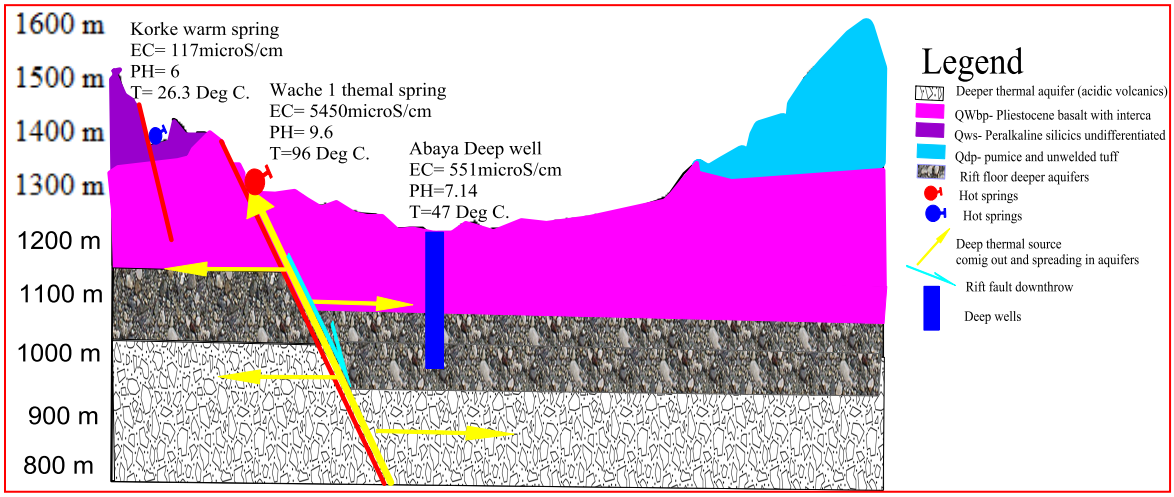

Fig 40 C-C’ section on a geologic map showing rift faults as a conduit to emanate thermal water which thermally affects the other aquifers especially to the lower reliefs (location of faults in Abaya Geothermal field on the Geologic map)

Hydraulic properties (T=50 to greater than $600m^2/d$) and (K=3 to 15m/day) in wells with a depth range of 60 to 400mbgl represent the rift floor aquifers. Higher hydraulic properties in rift aquifers are related to deeper sand and gravel aquifers and fracture permeability (Fig.31,37).

But a good hydraulic connection is assumed to exist because of tectonic events/ deep-seated faults affected the basin during various geologic times still recent. Highly evolved thermal waters from deeper sources uprise towards near-surface aquifers through deep faults and affect the groundwater composition and amount. Groundwaters are Ca-HCO3 to Na-HCO3 and Na-Cl type in rift floor (Fig.58). Higher residence time in flat hydraulic gradients of the area, deeper faults ascending geothermal gradient, a higher temperature heating the upper aquifers and higher rock-water interaction in the geo-media makes the rift waters highly evolved in the basin.

6. HYDROGEOCHEMISTRY

6.1. Introduction

In Abaya Chamo lakes basin, hydrochemistry is used as an important tool in the understanding of aquifers and analysis of hydrogeological systems so that distinct groundwater systems have a representative and variable chemistry which is acquired as a result of chemical alteration of the meteoric water recharging the system (Back 1966). Local variations in meteoric water composition are related to variation in atmospheric composition resulted from the activities of humans, plant and animal metabolism, and gases from volcanoes and other geothermal sources (Toth, 1963). Particulate matter carried into the air by wind discharged from smokestacks, or entering the atmosphere from outer space provides constituents such as CO, SO_4, O_3, and NO_2 or other nitrogen-containing gases may play important roles in air pollution and may influence the composition of rainwater (Hem, 1989).

The composition of groundwater is controlled by factors such as: source and chemical composition of recharge water, lithological and hydrological properties of geologic units, chemical reactions taking place within the geomedia, the amount of residence time, biochemical factors within the soil and water and the influence of humans (Hem, 1989 and USGS, 2002). The net effect of antecedent factors determines the number and amount of solutes present in groundwater through dissolution, alteration of previous components, precipitation or other processes (Freeze and Cherry, 1979). Though no much detail work has been done in the basin, in this study hydrochemistry can be interpreted to understand the major hydrogeological systems based on hydrochemical signature and key processes that have occurred in the aquifers with the integration of the isotopic signatures of waters.

6.2. Chemistry of different Waters

6.2.1. Rainwater chemistry

Abaya-Chamo lakes basin gets maximum rainfall during summer when the ITCZ is in northern Ethiopia and moisture from the Atlantic Ocean and partly from the Equatorial Indian Ocean (Gemechu, 1977; Kebede, 2004) feed the basin (section 4.2). To understand the geochemical evidence for the source of moisture and composition of rainfall, summer rainfall chemistry of

five stations is used. The water samples from all sources such as rain, Lake, River and groundwater are analyzed in in the regional laboratory are checked for the for its fits accurate ionic balance as also described in part 1.4.

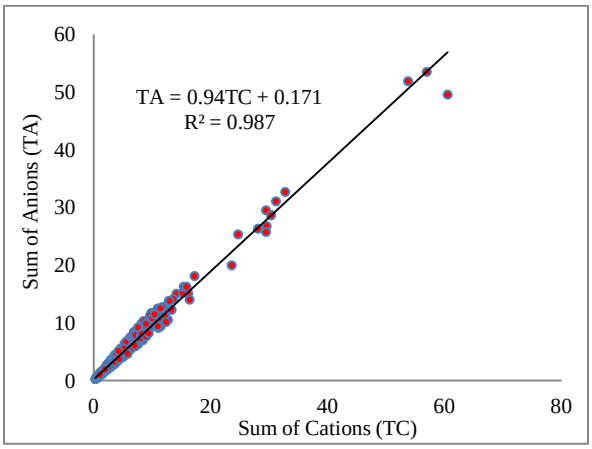

Fig 41 The relationship between the total cation and total anion

The chemical composition of the rain waters of the stations showed that the Ca and HCO3 are dominant ions of the rain and the waters are Ca-Na-HCO3 to Ca-HCO3-Cl type. The ratio Na/Cl of summer rainfall chemistry of western highlands and rift floor areas of the Abaya Chamo Lakes basin indicated that it is higher at highlands like the wolaita sodo station but lowest in near rift floor Lake Abaya areas. The highest amount of ions in rainwater indicates that the rainfall is under less continuous clean up of the atmosphere and hence particles in rainwater are higher. The variations in the ratio of Na/Cl also indicated that the moisture sources of summer rain and the nature of rainfall formation is variable for the parts of the study area which is briefly discussed in part chapter 4.

6.2.2. Rivers water chemistry

The chemistry of stream/ River waters mainly depends on processes including: anion retention of catchment soils, Weathering of minerals in catchment soils as a source of base cations (calcium, magnesium, sodium, potassium), adsorption and cation exchange in soils, buffering of soil solution pH by weak organic acids (e.g. humic and fulvic acids) and by weak inorganic acids (e.g. Al hydroxides and carbonic acid), formation of Al complexes with fluoride (F) and sulfate ions and with organic compounds, biologically mediated transformations and uptake of cations

and anions, generation of acid neutralizing capacity (ANC) by dissociation of carbonic acid with subsequent exchange of hydrogen (H) ions for base cations (B.J. Cosby et al, 2001). The River water chemistry is, therefore, can be understood as an input-output process of the catchment through atmospheric inputs (rainwater), hydrologic processes and anthropogenic /human-induced processes which respond differently under changing catchment conditions (Ababu, 2005). To understand the catchment processes in the basin, major ion chemistry data of some 15 Rivers samples are collected from laboratory of Arbaminch University and south water bureau.

The river water samples indicate that there are three major groups and are mainly Calcium, Magnesium, Sodium, and Bicarbonate rich. River water samples designated as 11 to 35 (Fig.42)) are calcium, Magnesium, Sodium, and bicarbonate dominant consisting water types of Ca-Mg-HCO_3, Ca-Na-HCO_3, Ca-Na-Mg-HCO_3, Ca-Na-HCO_3-SO_4, Mg-HCO_3, Mg-Ca-HCO_3, Mg-Na-HCO_3. Na-Ca-HCO_3, Na-Ca-HCO_3-SO_4, Na-HCO_3, and Na-HCO_3-SO_4.

The Ca, Mg and HCO_3 rich Rivers water samples (11, 12, 14, 21 and 22) could be related to the weathering of basaltic rock minerals in catchment soils around highlands or escarpments. Streams and Rivers from highland areas of the basins (Gidabo, Gelana, Kulfo, and Hare) escarpments/lowlands of (Amesa and Gelana) (Fig.42) are originating and flowing over basaltic basic formations have a percent ionic composition of Ca^{+2} (30% to 53%), Mg^{+2} (14% to 41%), Na^{+1} (4% to 37%) and HCO_3^- (60% to 99%). The higher proportion of HCO_3^- in River samples of the highlands is attributed to dissociation of carbonic acids in soil (B. J. Cosby et al, 2001). The samples show lower EC but as in the samples (14), the EC is higher (440µS/cm) due to the mixing of hot springs along Gidabo near Yirgalem. The bicarbonate and chloride content at the same site is also elevated as result mixing of thermal waters.

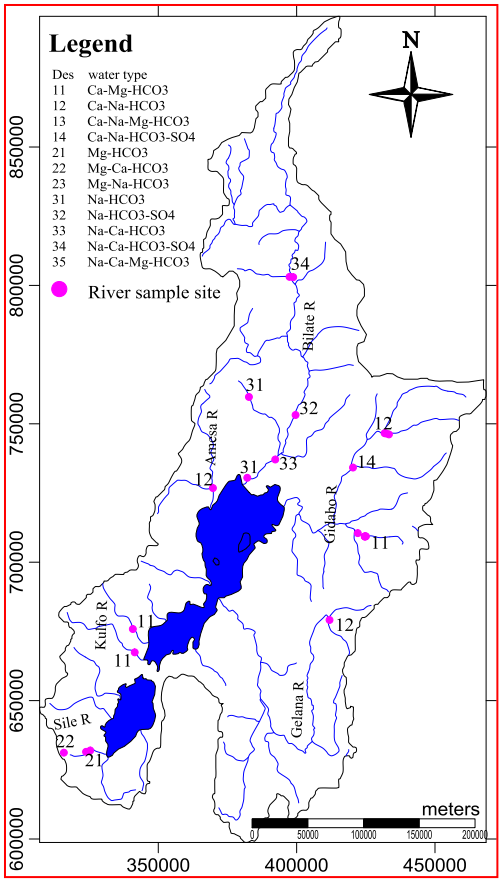

Fig 42 Chemical composition and water types of River waters in the Abaya Chamo Lakes basin

The proportion of magnesium is higher in River water samples (21,22) of Sile area in the southwest of Chamo Lake compared to Calcium content. The laminar flow and relatively more residence on the less sloppy flat channel of Rivers over basaltic formations facilitate evaporation at lower reliefs resulting in higher EC (540 µS/cm) and alkalinity.

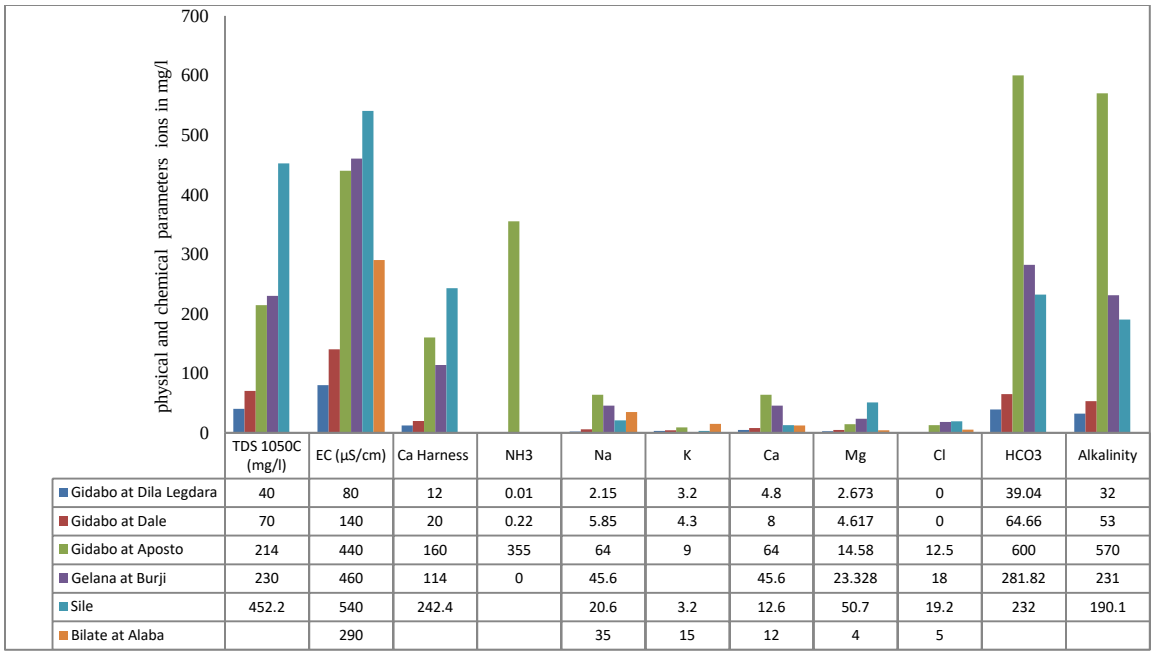

	TDS 1050C (mg/l)	EC (µS/cm)	Ca Harness	NH3	Na	K	Ca	Mg	Cl	HCO3	Alkalinity
Gidabo at Dila Legdara	40	80	12	0.01	2.15	3.2	4.8	2.673	0	39.04	32
Gidabo at Dale	70	140	20	0.22	5.85	4.3	8	4.617	0	64.66	53
Gidabo at Aposto	214	440	160	355	64	9	64	14.58	12.5	600	570
Gelana at Burji	230	460	114	0	45.6		45.6	23.328	18	281.82	231
Sile	452.2	540	242.4		20.6	3.2	12.6	50.7	19.2	232	190.1
Bilate at Alaba		290			35	15	12	4	5		

Fig 43 variations in the chemistry of representative Rivers samples of the basin

Na^+ and HCO_3^- are dominant ions in River water types (31, 32, 33 and 34) along the Bilate River basin. River samples along the flow directions indicated that it has evolved from a Na-Ca-HCO3-SO4 type in 34 to Na-HCO3 at 31 near the area of the entry to Lake Abaya (Fig.42). This is attributed to weathering of acidic rocks/soil in the catchments and mixing of the River with more evolved thermal springs along the course. Higher salinity and electrical conductivity towards the lower reaches of Abaya Lake is related to higher evaporation from marshy lands and mixing of thermal waters.

Bicarbonate is the dominant contributor of alkalinity in River waters of the basin. The water chemistry of the Rivers samples of the basin (Bilate, Gidabo, Gelana, Kulfo, Hamesa, and Sile) is influenced by the capacities of the respective catchments to retain the H^+ ions and in return exchange it for Calcium, Magnesium, and Sodium. The Rivers contain higher concentrations of bicarbonate and the equivalent divalent Calcium and Magnesium ions followed by Sodium and Potassium. The silicate weathering of the parent rocks provides these solutes concentrations to the River waters.

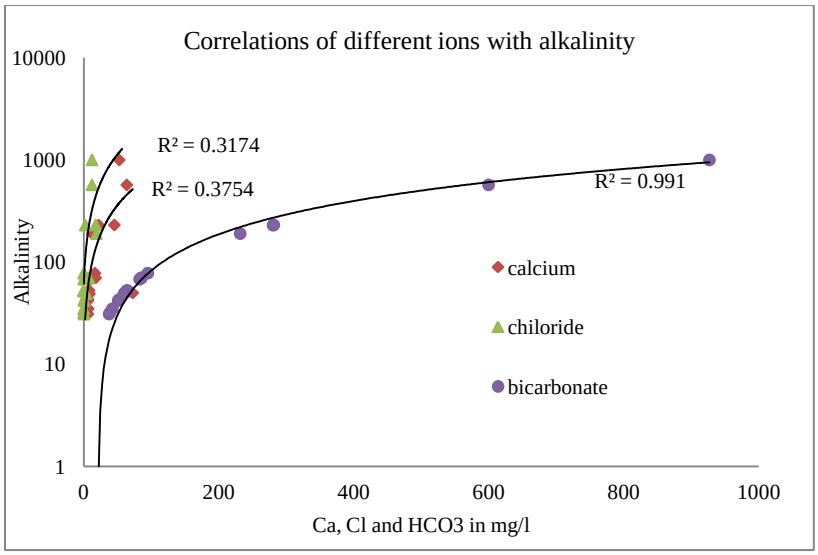

Fig 44 correlation of alkalinity with ions

Chloride concentration of Lower lands of Sile River (19.2mg/l) and Gelana areas at Burji (18mg/l) is also related to increased evaporation around lowland plain that might lead to increased storage of chloride which is leached down the soil and appears as an inter-flow. Rivers chemistry of the Abaya Chamo lakes basin is therefore mainly controlled by the input precipitation and catchment land use and geology of the area and interaction of River-groundwaters along the flow lines.

6.2.3. Lakes water chemistry

Ethiopian Lakes become a center of research since the 1960s. Northern and central Ethiopian rift Lakes basin system was one of the highly researched parts including the bounding highlands and escarpments. Differences in hydrogeological setting, mode of origin and prevailing climatic conditions make the Ethiopian Lakes highly variable (Tenalem A., 2009). But only a few fragmented works were done in the Abaya Chamo Lakes basin. The recent work, therefore tried to collect existing Lakes water samples to identify the Lakes water types, temporal Lakes water chemistry trends and its interaction with groundwater.

Dominant ions in the Lakes waters are Na^+, HCO_3^- and Cl^-. The water type is Na-HCO_3 and Na-HCO_3-Cl in Lakes Abaya and Chamo respectively. But the main differences in the waters of the

two lakes are that the concentration of major ions in Lake Chamo is higher than that of Lake Abaya.

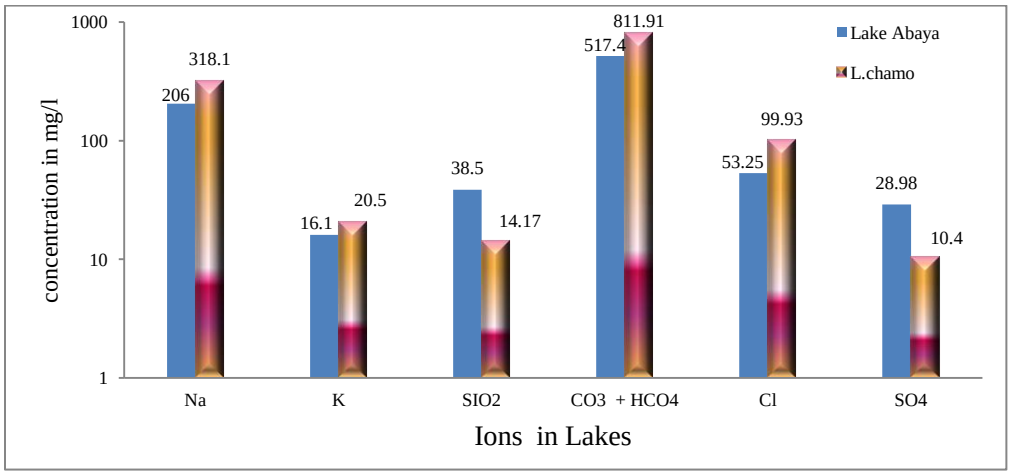

Fig 45 Average concentrations of ions in Lakes Abaya and Chamo

The concentration of Na^+ ranges 177.1mg/l to 239.66mg/l in Lake Abaya whereas in Lake Chamo it ranges from 209.3mg/l to 420mg/l. Bicarbonate in the waters of Lakes Abaya and Chamo ranges (384.3mg/l to 603.9mg/l) and (573.4mg/l to 1004.06mg/l) respectively. The water of Lake Chamo has a Cl^- concentration almost double compared to Lake Abaya (Fig.45).

The PH value of the rift Lakes ranges from 8 to 10 and have higher sodium, bicarbonate, and chloride (Tenalem, 2009) and the two southern rift Lakes (Abaya and chamo) are also in these ranges. Generally, the measured values of the physical parameters and the sum of ions of Lake Chamo are relatively higher than that of Lake Abaya.

This could be linked to the tertiary and Quaternary period basaltic formations of the area, higher bicarbonate concentrations of the low lying Rivers (Fig. 42), increased exchange of Cations (Sodium, Calcium, and Magnesium), residence time of the waters in Lakes reservoir, the less amount of inflow/outflow to/from the Lakes, the length, and area of the Lake, mixing of inflowing waters, higher evaporation from Lake surfaces and Lake waters contribute to the higher ion concentration and salinity of the lakes in common compared to Lake Abaya (Table 5).

Table 5 Average chemical parameters of the Lake waters

Lakes	PH	EC (µS/cm)	Sum cations	sum anions	Salinity (g/l)	Ca (mg/l)	Mg (mg/l)	Na (mg/l)	K (mg/l)	SIO2 (mg/l)	HCO3 (mg/l)	Cl (mg/l)	SO4 (mg/l)
L.Abaya	8.86	1015	10.3	10.95	0.825	14.33	3.76	206	16.1	38.5	517.4	53.25	28.98
L.chamo	9.128	1567.92	15.275	15.6	1.27	11.5	10.14	318.1	20.5525	14.17	811.91	99.9325	10.416

6.2.3.1. Temporal variation in the hydrochemistry of Abaya and Chamo Lakes

The chemical analysis results of the monthly Lakes water (Abaya and Chamo) samples in 2004 presented that the chemistry of the two Lakes vary based on seasonal changes in precipitation and temperature. Though the variation follows seasonal changes, the change in parameters such as PH is more discernible in Lake Chamo than Lake Abaya related to the seasonal effect of rain and dilution which is less in Lake Chamo (David W C and James O Sickman, 1999; Ababu, 2005). As such, short-term Lake water chemistry monitoring cannot show the variability over a long period of time, and since there is no regular Lake water chemistry monitoring system in the country in general and in the study area in particular, some attempt is made to collect hydrochemical results from previous works with the concern of Limnology, water quality and geothermal investigation (Ababu, 2005; Kebede E. et al, 1994; Otterbach L., 1995; Zinabu G et al., 2002; UNDP,1977). The concentration of the ions of the Lakes sampled starting from 1961 for Lake Abaya and 1964 for Lake Chamo is used for comparison of the Lakes. The results showed an increased trend of ions.

The strong temperature effect on the hydrogen-ion behavior has considerable geochemical significance and majorly hydrolysis and oxidation influence the amount of PH in the natural waters (Hem, 1985). The PH of Lake Abaya showed an insignificant amount of increase, whereas Lake Chamo water samples showed an increase from 8.9 to 9.23 for 40 years from 1964. The electrical conductivity of the two Lakes also indicated that for the last 40 years Abaya showed annual increases of 7.6µS/cm but Lake Chamo showed more than double (16µS/cm). This indicated that the difference in the presence of charged ionic species as a result of local hydrologic conditions. This is more pronounced in Lake Chamo than Lake Abaya and the following plots described which concentration favors more the electrical conductivity of the Lakes (Fig.46). Sodium, bicarbonate, and chloride are important contributors for higher EC.

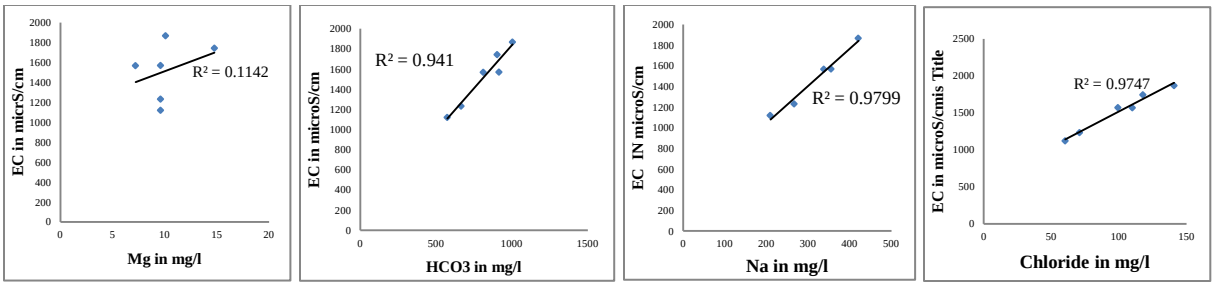

Fig 46 the relation of different ions to the electrical conductivity of the Lake Chamo

The salinity accumulation trend of Lake Chamo is greater than that of Lake Abaya owing to an aggregate of contributing factors: less inflow into the Lake, the greater salinity of the inflowing Rivers, greater evaporation from the Lake, less precipitation over the Lake and greater retention time in Lake Chamo than in Lake Abaya.

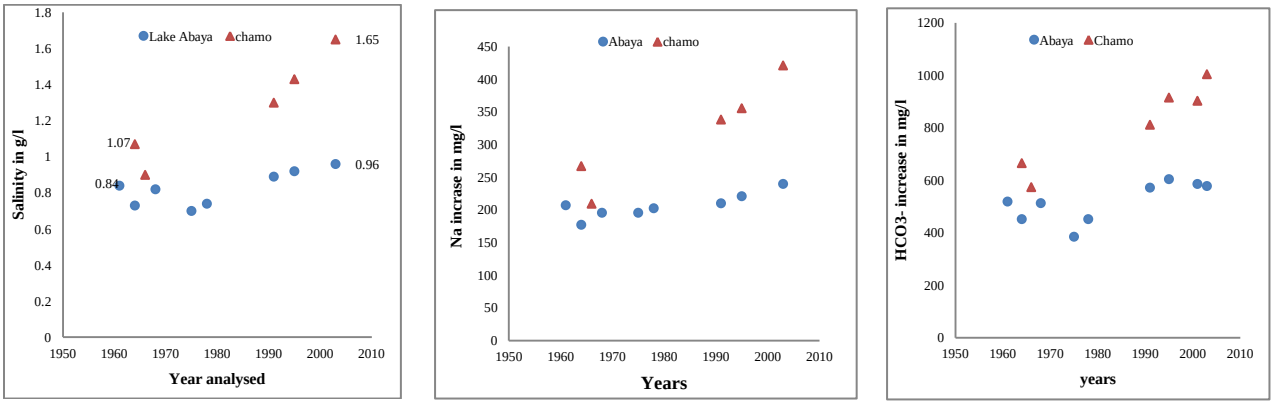

Fig 47 the trend of salinity, sodium, and bicarbonate the two Lakes over 40 years.

The plots (Fig.47) showed an almost similar trend of increment for salinity, Sodium, and bicarbonate for the two Lakes sampled at different times starting from 1961. It is apparent at a glance of the data that there is an upwards significant rate of increase in the concentrations of most of the ions for both Lakes. Particularly over recent years, both Lakes face increasing salinity, sodium, and bicarbonate. Lake Chamo faces a greater rate of Increase in salinity which amounts to more than 50% over the past 40 years. The trend in salinity increase of Lake Abaya started after 1976 and is still increasing at a moderate rate (14%). The decrease of salinity in 1970's and its increase afterwards could be apparent from related mainly to the rainfall cyclic

effects. It become apparent from 50 years rainfall data of Wolaita sodo that salinity increased for the less rainfall moving average years and decreased for the more rainfall years.

The trend of increment of major ions such as Na, HCO3, and Cl in Lakes water facilitate for the increment of salinity. This could be linked to increased runoff and sedimentation of lower reliefs towards Lakes (Degalo, 2007), enhanced leaching of anions retained in catchment soil, weathering of minerals and exchange of cations to the Lakes (B.J. Cosby et al, 2001) and increased evaporation over the Lake water's surface.

Quality problems related to irrigation water include salinity, specific ion toxicity, and SAR (Sodium Absorption Ratio) (Tamiru A and Tenalem A., 2001). Due to increasing salinity, concentrations of dissolved salts the SAR (Sodium Absorption Ratio) trend also increased (Fig.48).

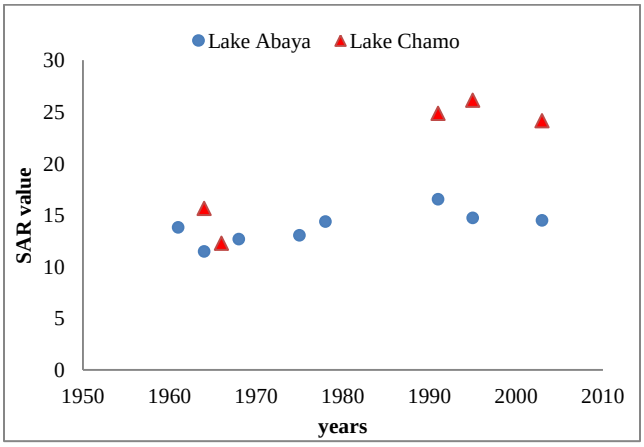

Fig 48 the trend of SAR for Lakes water

The increasing trend of SAR in both Lakes after 1970's is related to decreasing rainfall and increasing evaporation in the basin contributing to the Lakes. Problems related to excess sodium in irrigation water relative to calcium and Magnesium have an adverse effect on soil structure and reduce the rate at which water moves into and through the soil (infiltration & permeability). Based on the relation (Hem, 1985), SAR valves of less than 3 is considered to cause no difficult effect on agriculture, SAR in between 3&9 cause slight effect, and SAR values greater than 10 causes a severe effect. SAR values trend of Lake Abaya is in the range of 11 to 14.7 whereas for

Lake came it ranges between 12.3 to 26.1. The values indicated that both the lakes can cause an adverse effect on soil and plants if used for irrigation (Fig.48).

6.2.4. Groundwater chemistry

Successful groundwater resources location, development, and management are possible when the aspects of groundwater recharge sources, mechanisms and dynamics of flow in the aquifer are well understood (Kebede et al. 2005, B. B. S. Singhal and R. P. Gupta 2010). Analysis of hydrogeological systems using hydrochemical signatures complemented with environmental isotopes is used as a tool that provides sources and mechanism of the recharge and the flow systems in aquifers (Ayenew et al., 2008, Kebede et al. 2005, Kebede 2013). Various scholars conducted scientific studies in main Ethiopian rift Lakes using hydrochemistry in the analysis of hydrogeological systems of central Ethiopian rift lakes basin and geothermal resources (Ayenew, 1998; Berhanu, 1996: Fikre, 2006; UNDP, 1973; Craig et al., 1977; Mackenzie, et al., 2001; Teclu, 2007; and Chernet, 1993).

Hydrogeological system analysis of Lake Abaya Chamo basin using hydrochemical signatures is is a new study in the basin, focusing mainly on the distribution of the water types and evolution of the groundwater along the flow direction, circulation of the groundwater in different hydrogeological systems and the use ionic relations for an understanding of hydrogeochemical processes that occur within the systems.

The study used the chemical analysis results of the water samples (Fig.49) for which the techniques of water sampling and analysis of the samples indicated is discussed in the methodology section.

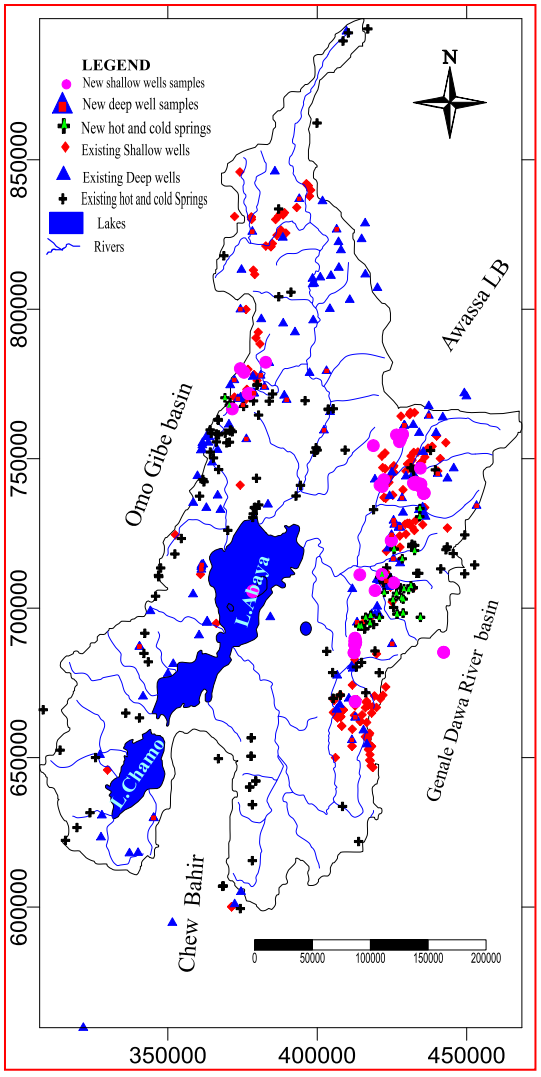

Fig 49 Groundwater sampling sites

6.2.4.1. Variability of physical parameters of groundwater

PH

PH is the measure of acidity or alkalinity of waters with a scale of 0 to 14, 0 being extremely acidic and 14 being extremely alkaline. PH of natural waters is governed by factors such as CO_2/ $HC0_3^-$ / CO_3^{-2} equilibrium, dissociation of acidic solutes, H^+ ion consuming species such as silicates and reactions forming precipitation and oxidation (Hem, 1989). The PH value of 484 representative groundwaters samples in the Abaya Chamo Lakes basin is the range of 5 to 9.64 (Annex 4).

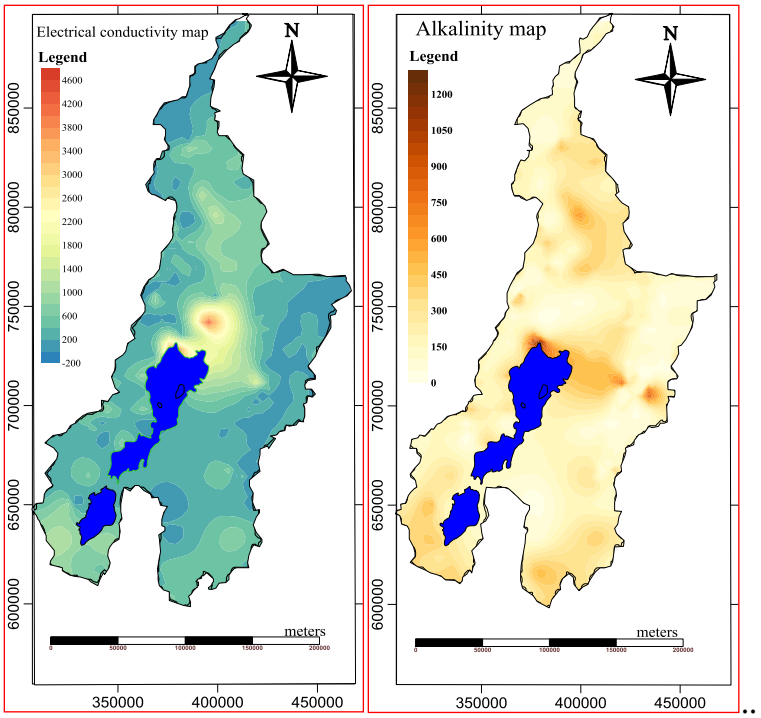

Fig 50 Electrical conductivity and Alkalinity maps of groundwaters in Abaya Chamo Lakes basin

The eastern and western highlands of the basin have Lower PH values (< 6.5). This could be linked to wet climate favored oxidation of older highland acidic rocks such as Ignimbrites releasing CO_2 into the water. The higher PH values for waters in lowland area are related to higher residence time in host rocks and the reaction with Geo-media under a higher temperature, that consume H^+ (higher alkalinity) along the flow path (Table 6).

Field PH monitoring/measurement during production well pump testing at the southern plain of Wolaita sodo town (NW of Lake Abaya) showed variability until end of the 31st hour when the water is pumped from mixed lower and upper aquifers to the water level of 53.8m (Fig. 51). This indicates that vertical leakage from shallow mixed aquifer formations of different depths has a variable value of PH whereas deeper aquifer from volcaniclastic aquifer showed an almost constant scenario of PH after 31st for a continuous drop of the water level. This also implies that mixed waters from various shallow strata were recharging the system and are under varying chemical processes.

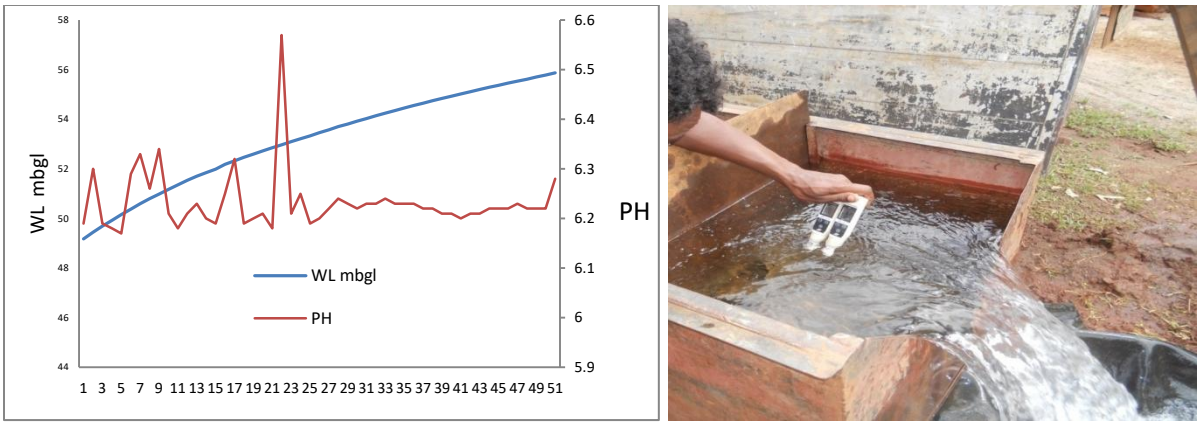

Fig 51 PH variability for a water level drop of wolaita sodo well (right) and photo during field pump testing (left).

Electrical conductivity (EC)

Electrical conductivity is a measure of the ionic strength of water; it is related to the nature and extent of dissolved substances or mineral content of water and their relative and actual concentration. Mostly it is given in unit µS/cm (micro Siemens per centimeter) and is measured at a standard temperature of 25^0c (Hem, 1989).

Groundwaters at different physiographic set up of the basin are identified based on the EC map (Fig.50 (right), 52 and Table 5). Highland waters are less mineralized with average EC=324 µS/cm. But some hot springs emerging at the foot of highlands towards escarpments, small spring waters, hand dug wells exposed to evaporation from shallow depth and deep wells drilled in Gneissic rocks are moderately mineralized in the areas with EC up to 1592 µS/cm. Escarpment waters are more or less similar to highland waters due to the fast flow of groundwater from highlands towards escarpments through wide fractures and have less residence time and contact with the rock media. Rift floor waters are evolved and highly mineralized with the EC range of (147 -2960) µS/cm. The low EC rift floor ground waters such as Arbaminch springs is also related to highland recharging open faults and fractures towards discharging points.

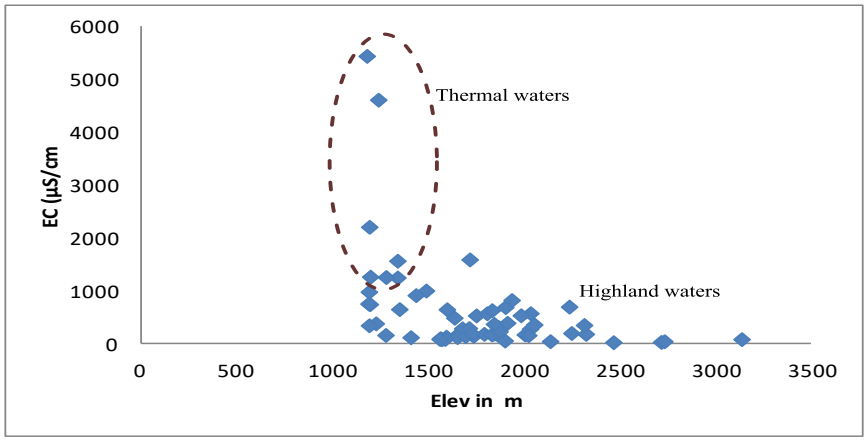

Fig 52 EC plot with altitude

Table 6. Physical parameters of waters different setups

Group	Variables	PH	Temp	EC	Sp No	Physiography
I	Min	5.1	15.8	2.7		.
	Max	8.8	40.6	1592	323	Highland waters
	Mean	6.9	23.4	324		
II	Min	5.6	16.3	32		
	Max	8.6	34.2	940		Escarpment waters
	Mean	6.9	22.6	237	46	
III	Min	5	17.3	147	182	Rift waters
	Max	9.6	94.3	2960		
	Ave	7	26.9	447		.
IV	Min	8.2	90	4620		Rift thermal waters
	Max	9.6	96	5450	2	
	Ave	8.9	93	5035		

Exceptionally mineralized groundwaters at the north of Lake Abaya are thermal waters under a higher deeper temperature of the gradient. Higher EC in deep wells of the lowlands and hot springs is due to increased temperature. While water circulates within considerable depth, it attains a higher temperature than the water near the land surface. Since higher temperature raises the rate of dissolutions and solubility of most of the rock minerals, hot thermal springs and deep boreholes in rift center have higher EC and TDS.

Alkalinity

The alkalinity of a solution may be defined as the capacity of the solute that water has to react with and neutralize the acid. The property of alkalinity must be determined by titration with a strong acid, and the endpoint of the titration is the pH at which virtually all solutes contributing

to alkalinity have reacted. Titration of strong acids to its end point PH (the experimental point at which the rate of change of pH per added volume of titrant (dPH/dV acid) is at a maximum) and the color indicator evaluates the property of alkalinity. It evaluates the potential of the solution for some kinds of water-rock interaction whereby the dissolved carbon dioxide species, bicarbonate, and carbonate are substantially enriched from soil zones and aquifers (Hem, 1989).

In the Abaya Chamo Lakes basin, alkalinity varies in the range of 4.2 to 1440mg/l (Fig.50). This could be related to various reactions taking place in the soil and rock media of the catchments. Lower alkalinity (up to 350mg/l) in the highlands of the basin could be related to relatively less rock-water interaction and as a result weak silicate weathering of aquifer materials. Higher values of alkalinity of groundwaters (1440mg/l) in the rift aquifers of the basin indicated the higher rock-water interaction under higher temperature gradient (up to 96^0c), longer residence time, and the effects of bigger faults that facilitate higher temperature gradients to non-thermal aquifers near the surface. Bicarbonate is the dominant contributor of the alkalinity in the basin as indicated from springs, shallow and deep wells (Fig.53 right). Alkalinity increase with depth where alkalinity of shallow wells plots below to that of deep wells (Fig.53 left)

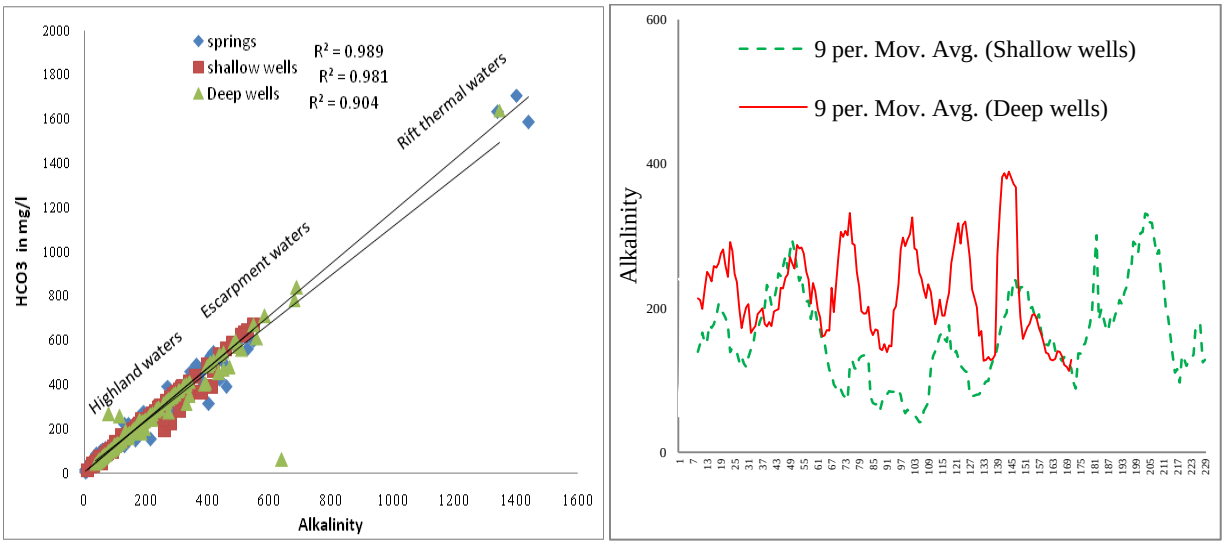

Fig 53 the relation of Bicarbonate to alkalinity and alkalinity to a depth

6.2.4.2. The chemical composition of groundwaters and its spatial variability

Hydrochemical data of different groundwater samples were employed to identify water types, mechanism of recharge, groundwater flow and evolution within aquifer systems in different parts of the world (Plummer and Glynn, 2005). 608 groundwater samples (Fig.49 and annex 4) are used to understand the water types and its distribution, the groundwater evolution and flow direction in the different physiographic regimes (highland, escarpment, piedmont plains and rift floor) (Fig.58). Piper diagram (Fig. 54, 55, 56, 57) also showed that Na^{+1}, Ca^{+2}, Mg and HCO_3^- are dominant ions in most parts of the basin.

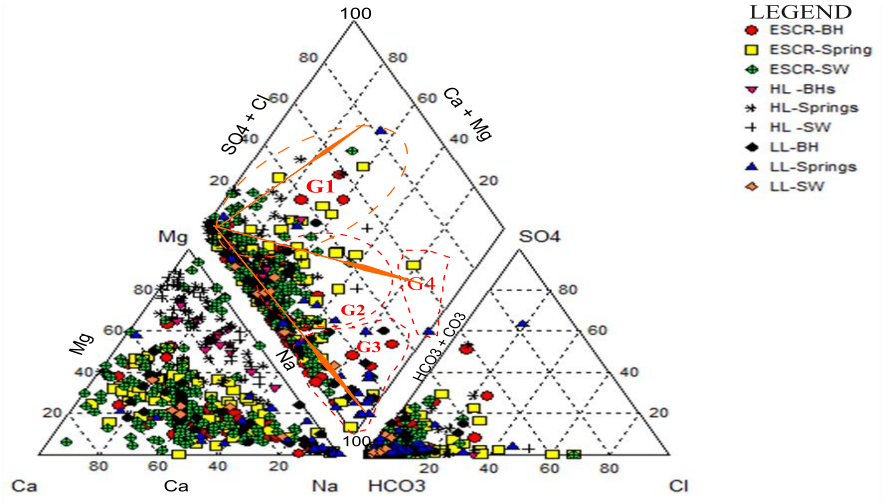

Fig 54 Piper plots of hydrochemical samples. G1, G2. G3. G4 represent water groups and symbols indicate water sources.

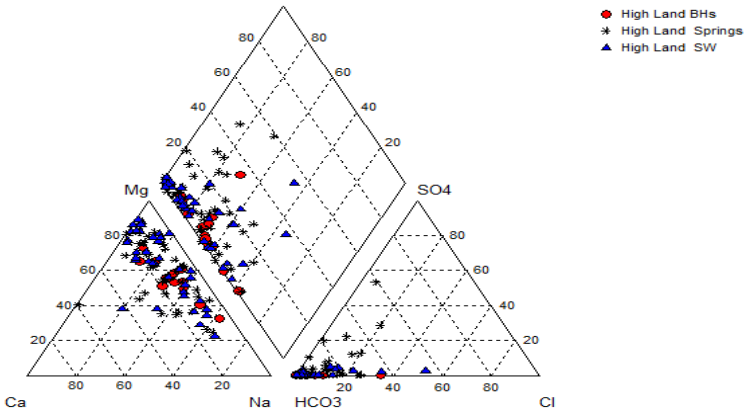

Fig 55 Highland (G1) groundwaters

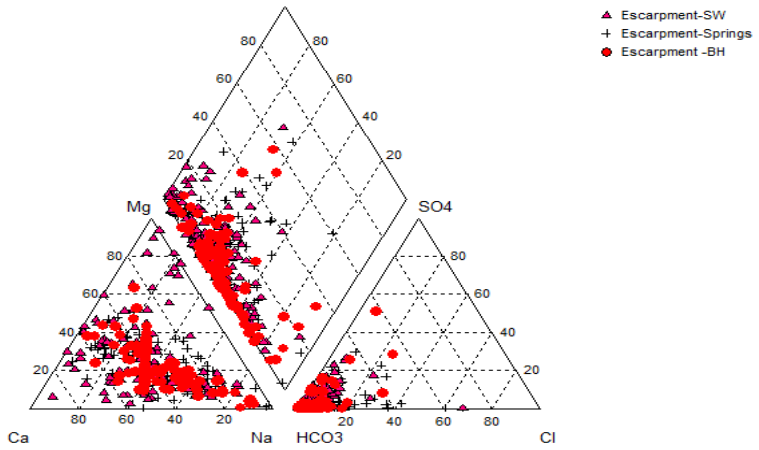

Fig 56 Escarpment (GII) groundwaters

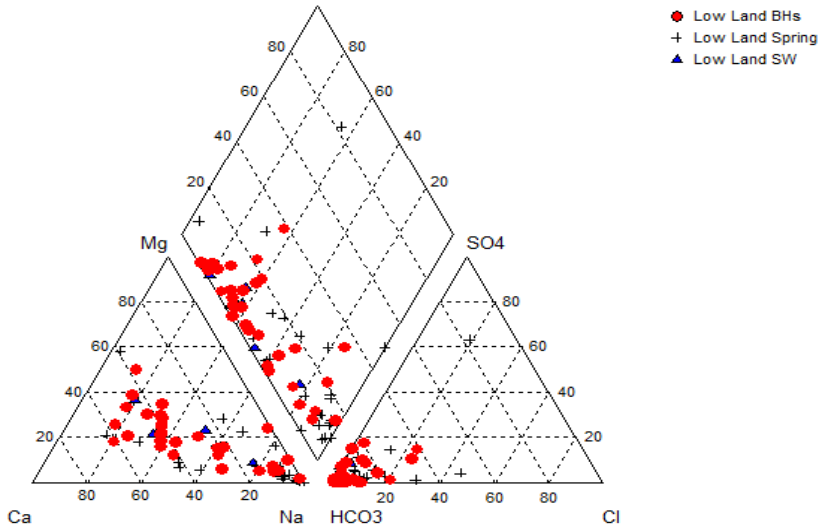

Fig 57 Rift floor groundwaters (G3 and G4)

The plots and maps assisted to categorize the waters into four dominant groups in the basin. The basic distinction of these water types is the difference in the degree of variation in elevation, EC, Temperature, Na^{+}, Ca^{+2}, Mg^{+2}, Cl^{-}, HCO_3^{-} and other minor ions. Based on the variability of parameters: Ca-HCO_3, Ca-Mg-HCO_3, Ca-Mg-Na-HCO_3, Ca-Na- HCO3, Ca-Na-HCO3-Cl, Mg-Ca-HCO3, Mg-Na-HCO3, Na-Ca-HCO3, Na-Ca-HCO3-Cl, Na-HCO3, Na-HCO3-SO4 and Na-Cl (HCO3) types of waters are identified.

Waters rich in Ca^{2+} and HCO_3^{-} are represented by Ca-HCO_3, Ca-Mg-HCO_3, and Ca-Na-HCO_3 which are dominant in the highlands and towards escarpment recharge areas covered dominantly by tertiary formations (Fig.39, 58). These water types have three major subgroups (S11, S12,

S13) based on the variability of major ion concentration (Fig 59,60). Mg^{2+} and HCO_3^- dominating sub-groups Mg-Ca-HCO3 and Mg-Na-HCO3 mainly occur in the piedmont plains, inter-mountain areas, and along the channels of Rivers. Na^+ and HCO_3^- rich water types of lower escarpment and rift floor have four subgroups (Fig.58) representing rift floor thermal waters mostly in localities west of Dilla and north of Lake Abaya along a NNE-SSW or N-S trending deep rift Holocene faults. Highly evolved Na-Cl water type Wache thermal (annex 3) is with a little proportion of HCO_3^- outlier rift floor volcanic water.

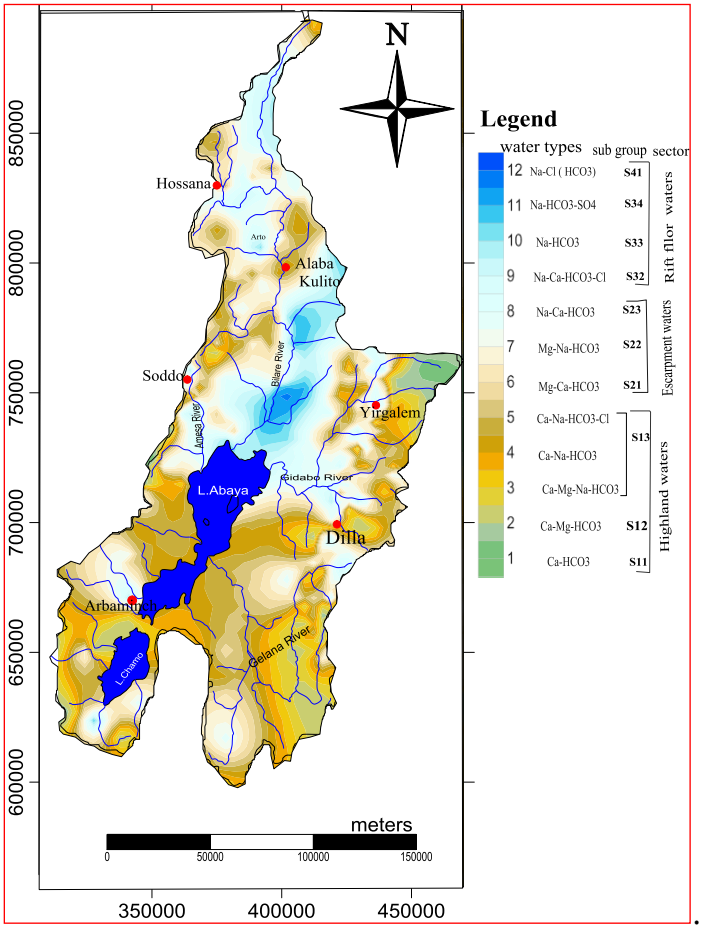

Fig 58 Spatial distribution of water types, major groups with subgroups along the physiographic regimes

The extent of groundwater evolution is lower in the southern half of the basin, particularly in the Gelana River basin and west of Lakes Abaya and Chamo basin mainly in Tertiary basalt and recent alluvium aquifers (Fig.58). Highland waters recharged in fractured and weathered media of Tertiary formations are dilute and are shallow circulating. The dilute low EC cold spring

waters of Group 2 and 3 waters in the rift floor indicates the occurrence of local recharge through faults as in the rift floor of the southern half. The degree of spatial consistency among the groups /subgroups of major water types across the rift valley suggests that there is a distinct pattern of the changes between the principal hydrochemical facies defining hydrochemical evolution. This indicated that highland waters Ca and a HCO3 rich group of waters (Fig.55) having average EC=324µS/cm is evolved to Na-HCO3 of average EC=467µS/cm) in escarpments and rift floor waters and further evolution to Na-Cl (Table 7) having average EC of (5450µS/cm) with increasing rock-water interaction. The evolution of waters on piper diagram showed that some waters of both rift floor and escarpment waters plot together with highland waters and near the escarpment indicating highland aquifers are connected to rift and escarpment aquifers. The details of each group and subgroups is discussed in the following sections.

6.2.4.3. Multivariate statistical analysis of clusters and its relation to hydrogeological systems

Investigation of statistical relationships of dissolved constituents of water samples and its hydrogeological systems (aquifers) could be possible using multivariate statistics (Drever, 1997). Statistical associations do not necessarily establish cause-and-effect relationships, but do present the information in a compact format as the first step in the complete analysis of the data and can assist in generating hypothesis for the interpretation of hydrochemical processes (C. Güler, 2002). The hydrogeological and statistical concept of the classification of groundwater chemistry with detailed technical description is given in (Güler et al., 2004, WARD, 2003). The advantage of the multivariate statistical analysis over different graphical methods such as Piper diagram is that it is an effective solution for analysis of the large mass of data with many variables generated from groundwater hydrochemical data (Join et al., 1997). In this study, Hierarchical Cluster Analysis (HCA) and Principal Component Analysis (PCA) were used to classify waters into objective groups based on their similarity and understand the groundwater systems. A Microsoft Excel @ add-in module XLSTAT 2017 was used to conduct the HCA and PCA.

Table 7 Descriptive statistics of hydrochemical variables in mg/l

Variable	Observations	Minimum	Maximum	Mean	Std. Deviation
EC (µS/cm)	608	2.700	5450.000	373.405	430.988
PH	608	5.000	9.640	6.968	0.758
Na	608	0.100	1300.000	52.324	121.649
K	608	0.000	156.000	7.366	10.007
Ca	608	0.000	133.760	26.378	22.534
Mg	608	0.100	65.000	10.018	9.833
F	608	0.000	46.000	1.325	4.013
Cl	608	0.000	762.000	10.877	44.566
NO3	608	0.000	120.980	3.548	7.426
Alkalinity	608	4.200	1440.000	182.461	174.266
HCO3	608	5.120	2830.000	235.970	265.650
SO4	608	0.000	230.000	7.299	20.296
PO4	608	0.000	78.800	2.658	7.992

To determine the relationship between water samples, the standardized data matrix was imported into the statistical package. The statistical clusters are analyzed for spatial coherence confirming that the clusters have a geological basis corresponding to flow paths. On the other hand, PCA also called R-mode factor analysis is used to determine the association and sources of variation between parameters.

The variability of the hydrogeological systems and groundwater composition in the Abaya Chamo Lakes basin is mainly related with geological, tectonic, topographic and other human-induced factors. This is revealed through the interpretation of the above factors using inter-variable relationships of hydrochemical parameters. Descriptive statistics of 13 major hydrochemical variables of 608 observations (Table 7) are used for cluster analysis in the Abaya Chamo Lakes basin.

6.2.4.3.1. Hierarchical cluster analysis (HCA)

Statistical classification of hydrochemical data from Q-mode hierarchical cluster analysis (HCA) according to their parameters has been proven to provide a suitable basis for objective classification of water composition into hydrochemical facies (Güler et al., 2002, Güler and Thyne, 2003; Kebede et al., 2005; Ayenew et al., 2009) with the assumption of analysis techniques including homoscedasticity (equal variance) and normal distribution of the variables

(Alther, 1979). HCA is a powerful tool in the classification of groundwater chemistry into consistent clusters (groups and subgroups) using some measure of similarity or Euclidean distance. The package examines the available combinations of similarity/dissimilarity measurements using Euclidean distance (straight line distance between two points in c-dimensional space defined by c variables) as similarity measurement with Ward's method for linkage (Güler et al., 2002). This produces typical hierarchical tree having distinctive groups where each member of the group is more similar to its fellow members than to any member from outside the group. The result from HCA was used to understand the major controls for the clusters in association with a spatial map of water types (Fig.58) and the principal component analysis (PCA) (Fig.61).

The meaningful descriptions of the groundwater systems of each cluster in the Abaya Chamo Lakes basin are given through the organization of the different species according to common variables to conceptualize the groundwater systems. For this classification 13 variables (EC, PH, Na^{+}, K^{+}, Ca^{+2}, Mg^{+2}, F^{-}, Cl^{-}, $NO3^{-}$, Alkalinity, $HCO3^{-}$, $SO4^{-2,}$ and $PO4^{-3}$) of 608 groundwater samples (232 shallow wells, 171 deep wells and 205 cold and hot springs) are clustered in the dendrogram (Fig.59).

The groups and subgroups clustered in the dendrogram are ordered from Group I towards the outer Group IV from left to right along the groundwater evolution direction. Along with this direction EC, PH, Na^{+}, K^{+}, T, HCO_3^{-}, Cl^{-}, SO_4^{2-}, and F^{-} increase, but Ca^{2+} and Mg^{2+} decrease except for the Group II cluster which occurs along Intermountain, piedmont plains and River valley of escarpment areas of the basin. Group I water occurs along the highlands in Tertiary formations. Group III subgroups are located in the rift floor, but get an additional indirect recharge from the highlands and escarpments. The outlier Group IV clustered away from other groups is one Wache volcanic spring located at NNW flank deep fault of Lake Abaya which showed distinct high chemical evolution.

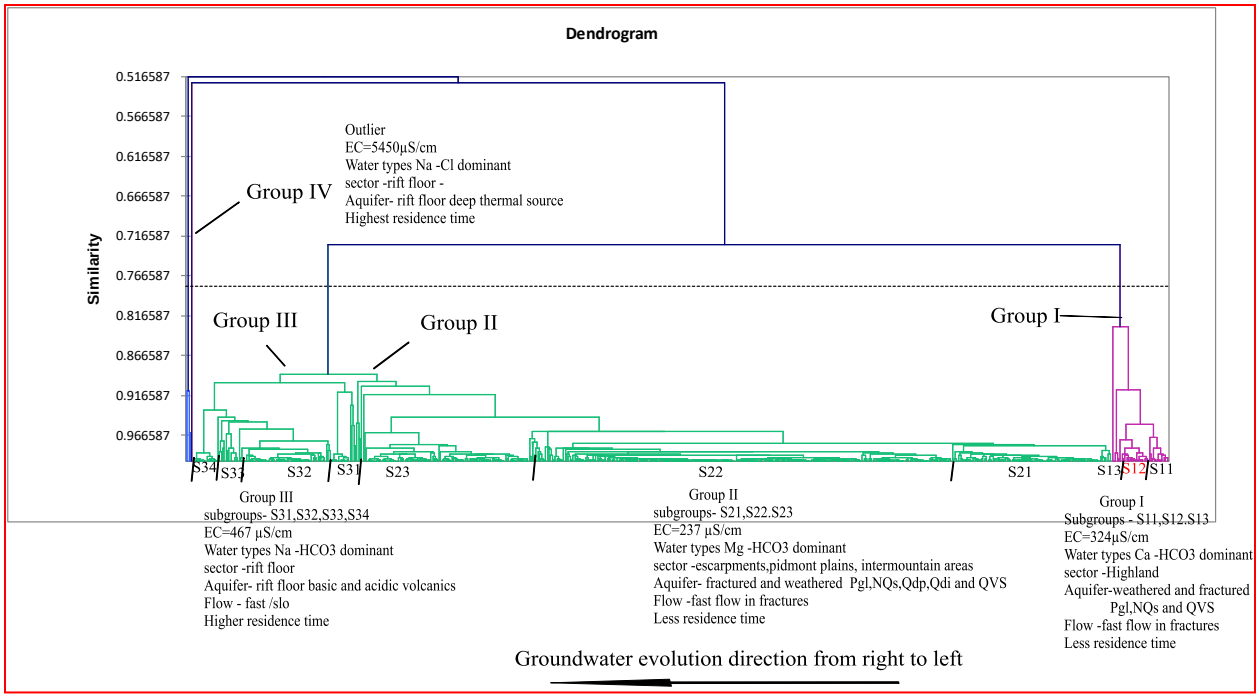

Fig 59 Dendrogram of the HCA with the 'phenon line' of similarity index=0.774

Based on the representation of water types on the piper diagram (Fig.55, 56, 57), spatial mapping of the clustered subgroups (Fig.58), statistical clustering of the subgroups (Fig.59, 60) and (Table 8 and 9); the description of the different groups/subgroups and its correlation with the hydrogeological system is discussed below.

Group I (G1) Ca^{2+} and HCO_3^- rich water types have three subgroups S11 (Ca-HCO3), S12 (Ca-Mg-HCO3) and S13 (Ca-Na-HCO3). The subgroups are dominant in aquifers of highland and towards escarpment recharge areas in the basin. Ca and Mg are derived from basic volcanic rocks (basaltic and sediments of basaltic origin) minerals Anorthite ($CaAl_2Si_2O_8$) and Forsterite (Mg_2SiO_4) respectively (Hem, 1985). The dominance of HCO_3^- in highland waters is related to its derivation from upper soil zone (Ayenew, 2005) and unequal dissolution of silicate minerals in places covered by volcanic rocks (Appelo and Postma, 1993). The average proportion of ions of the G1 waters is Ca (52%)>Mg (22.8%)>Na (18.9%) and HCO3 (85.39%). Ca-HCO3 Water-type evolves to Ca-Mg-HCO3 and Ca-Na-HCO3 water types from both eastern and western highlands towards Escarpments and Ca^{2+} rich waters towards the Lakes are related to sediments of basic rock's origin. The variability in the composition of the subgroups of Group I (G1) waters is related to the increase of (EC, T, Na^+, K^+, Mg^{2+} and HCO^-_3) and decrease of Ca^{2+} from S11

(Ca-HCO3) to S13 (Ca-Na-HCO3) which is associated with difference in the depth of groundwater and evaporation from shallow aquifers of the highlands.

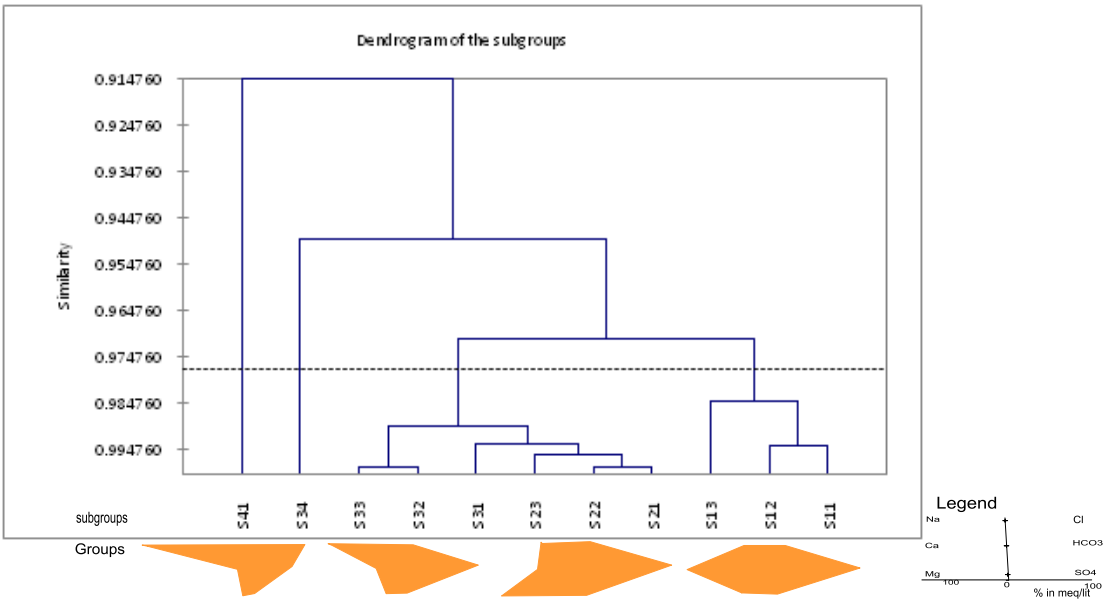

Fig 60 Dendrogram representing groups and subgroups in the stiff diagram

Group I water types are circulating in shallow depth (up to 150m) and dilute having less residence time and short groundwater flow paths within weathered and fractured media of Gneiss, tertiary basalts, trachytes, ignimbrites and mixed volcaniclastic rocks (Fig.39 and 58). These waters are recharged by highland rainfall and have low EC (2.7 to 1592) µS/cm (average EC of 324µS/cm and temperature of 23.4^0c) (Table.8). Higher variability of EC among samples in a group is related to the occurrence of the waters in Genesis rocks (BH98), waterlogged marshy areas (SW77, SW120, SW200, SW221, and SW224). Higher EC of deep wells is related to increased depth and temperature, facilitating the rate of weathering. Some low relief waters (SP79) of Arbaminch spring at an elevation of 1189masl has almost equal EC and Ca to SP88 of the western highlands at an elevation of more than 1900masl which could be related to fast fracture flow from highland recharge areas (annex 4).

Along the fault-controlled Gidabo and Gelana River channels, the Ca and HCO_3 rich waters occur due to River bed recharge as indicated by the difference in water type. Most of the highland shallow wells and small springs are Ca-HCO3 water types, but deep wells and higher

yield spring are Ca-Mg-Na-HCO3 waters. Though highland waters have lower ions concentration, averaged physical and some chemical (Na, HCO3, F, Cl) parameters of waters increase from shallow to deeper flow regimes (Fig.55) where acidic volcanic occur at depth in areas affected by recent faults.

Table 8 statistical summary of hydrochemical parameters of groundwaters for 608 samples clustered based on the distribution of water types within three physiographic regimes *(temperature in ^{0}C, EC in µS/cm; cations and anions in mg/l;; STDEV is the standard deviation and % is averaged ionic percent relative to corresponding major ions)*

Group	Variables	PH	Temp	EC	Na	K	Ca	Mg	F	Cl	HCO_3	SO_4	Water type
I	Min	5.1	15.8	2.7	0.2	0.5	2.7	0.46	0	0.5	5.12	0	Ca-HCO3
	Max	8.8	40.6	1592	116	97	134	63.8	6	144	783.2	87	Ca-Mg-HCO3
	Mean	6.9	23.4	324	24	6.2	32.6	10.3	1	7.5	195.5	5.2	Ca-Na-HCO3
	STDEV	0.7	2.79	257	23	7.1	24.7	9.04	1	13	149.6	11.5	
	% ions				19		52	22.8		6.4	85.39	3.07	
II	Min	5.6	16.3	32	0.1	0.6	5	1.7	0	1	12.81	0	
	Max	8.6	34.2	940	80	20	80	55	3	20	600	39.3	Mg-Ca-HCO3
	Mean	6.9	22.6	237	17	6.3	16.7	18.6	1	5.1	173.1	2.1	
	STDEV	0.7	2.98	181	18	4.2	18.1	13.4	1	5	133.7	6.08	Mg-Na-HCO3
	% ions				20		23.7	48.3		5.7	85.94	1.33	
III	Min	5	17.3	147	3.5	1	0.2	0.24	0	4	10.25	0	Na-Ca-HCO3
	Max	9.6	94.3	4220	713	41	101	65	22	104	1708	230	
	Ave	7	26.9	467	93	7.9	18.2	7.5	2	10	301	11.1	Na-HCO3
	STDEV	0.8	11	476	137	7.2	14.5	8.3	4	19	334.3	30.5	
	% ions				57		22	14		5.6	84	2.7	Na-HCO3-Cl
IV	Max	9.6	96	5450	1300	156	1.1	0.1	46	762	2830	89	Na-Cl/HCO3
	% ions				95		0.05	0.01		43	52	3	

Group II (G2) is Mg^{2+} and HCO_3^- dominating groups consisting three sub-groups of water types occurring on piedmont plains, inter-mountain and River channels of the escarpments. Some water types of escarpment areas are also Na^+ and HCO_3^- dominating towards upper margins of the lowlands. Subgroups consist S21 (Mg-Ca-HCO3), S22 (Mg-Na-HCO3) and S23 (Na-Ca-HCO3) water types occurring in aquifers composed of weathered and fractured Tertiary basalts and welded tuff (cut by older faults and Pleistocene caldera), Pleistocene basalts, scoria and mixed volcano-sedimentary rocks (Fig.31,39). These aquifers have Ca^{+2} (23.7%), Mg^{+2} (48.3%), Na^+ (20%) and HCO3 (86%) indicating slight evolution of Ca^{+2} to Mg^{+2} towards the escarpments (Table 7,8,9). The proportion of Na^+ increases towards the lower parts of the escarpment up to 57%, which make the separate clustering of S23 (Fig.59, 60).

The mixed (Mg, Ca, Na) HCO_3 waters are shallow circulating and less mineralized with lower EC (32 to 940) µS/cm and average EC=237 µS/cm showing less resident highland waters with fast fracture flow. The average EC and PH of the subgroups of Group II waters are lower than that of the subgroups of Group I and HCO_3^- almost equal, indicating that fast flowing and shallow circulating highland waters mix with the escarpment recharged groundwater and are at

regional scale at an early stage of geochemical evolution that undergone less rock-water interaction (Kebede et al, 2005) (Fig. 55,56). The composition of Group I and Group II subgroups generally depends on the reaction of rainwater with older basaltic and acidic highlands and escarpment rocks yielding (Ca, Mg, Na) HCO_3 waters and altered rocks.

Table 9 statistical summary of hydrochemical parameters of groundwaters for 11 subgroups *(temperature in ^0C, EC in µS/cm; cations and anions in mg/l*

Group	Sub group	SP.No	EC (µS/cm)	PH	T ^0c	Na+	K+	Ca+2	Mg+2	F-	Cl-	HCO_3-	SO_4	d18o	d2H	D-excess	water type
	S11	22	297	7.1	21	8	4.9	39	6.6	0.5	4.4	161	5.5	-2.04	1.79	18.11	Ca-HCO3
G1	S12	121	267	6.7	23	11.5	4.6	29	11	0.4	5.2	163	2.6	-1.93	-2.3	13.14	Ca-Mg-HCO3
(270)	S13	127	346	7	41	28.8	6.7	33	9.7	0.6	5.1	217	3.5	-1.42	1.96	13.32	Ca-Na-HCO3
	S21	39	237	7	23	15.7	6.4	19	18	0.6	5.7	170	2.3	-2.59	-1.2	19.48	Mg-Ca-HCO3
G2	S22	43	237	6.5	23	19.7	5.8	10	21	0.3	3.4	183	1.5				Mg-Na-HCO3
(203)	S23	121	337	6.9	24	47.2	6.3	21.4	7	0.9	3	212	2.3	-1.54	1.3	13.62	Na-Ca-HCO3
	S31	52	412	6.8	27	70.5	6.4	16.8	11.2	1.12	25.3	212	7.45	-2.34	-4.65	14.07	Na-Ca-HCO3-Cl
	S32	50	744	7.3	30	267	11.6	11.3	6	4.51	6.2	712.2	17.5	-3.74	-14.1	15.82	Na-HCO3
G3	S33	24	935	7.4	59	223	12.6	11	3.6	5.7	17.6	484.8	84.1	-4.54	-8.1	28.22	Na-HCO3-SO4
(134)	S34	8	1117	7.5	58	374	21	12	3.4	17.4	132	728	46	-1.48	-5.1	6.74	Na-HCO3-Cl
G4 (1)	S41	1	5450	9.6	96	1300	156	0.2	0.1	46	765	1450	89	-2.93	-9.3	14.14	Na-Cl (HCO3)

Group III (G3) waters occurred in localities west and north of Dilla and north of Lake Abaya along a NNE-SSW or N-S trending deep rift faults are rich in Na^+ and HCO_3^- (Fig.58). This Group also occurs within recent basic and acidic rocks, volcano-sedimentary rocks and rift floor lacustrine and fluvial sediments surrounding the Lakes and River courses reworked by recent volcanic activities. It represents rift floor cold and thermal waters having four sub-groups S31 (Na-Ca-HCO_3-Cl), S32 (Na-HCO_3), S33 (Na-HCO_3-SO_4) and S34 (Na-HCO_3-Cl) (Table 8,9). This group of water is highly mineralized exclusively representing the thermal springs and wells with EC (147 to 4220µS/cm and have average EC=467 µS/cm). Water temperature ranges from 17^0c to 94.3^0c mostly in lower relief below 1400masl. Low EC cold groundwater samples of the group result from local recharge in shallow aquifers of the rift floor. Faulted midlands and escarpments have high-temperature hot springs as in Yirgalem, Dila and Halaba Arto hot spring (94.3^0c) confirmed by (Ayenew, 2005) as the thermal waters in the Ethiopian rift and adjacent escarpments are characterized by high Na^+ and almost exclusively dominated by a single HCO_3^- anion. Each subgroup of the group has a unique water type associated with its aquifer lithology and tectonics. S31 (Na-Ca-HCO3-Cl) subgroup is along the lower margin of the escarpment and is relatively less mineralized compared to S34 (Na-HCO3-Cl) which is from most recent fault affected rift floor.

Along the evolution path, the most important trends are increasing in Na^{+}, HCO_3^{-}, T, Cl, and EC towards the rift and the reverse in Ca^{+2} and Mg^{+2} as one goes down from S32 to S34 (Fig.58 and Table 9). The good coherence among mean values of the subgroups can be clearly explained in terms of the hydrochemical characterization of groundwater circulations. Samples that belong to the same subgroup are located in close proximity to one another, suggesting more or less the same hydrogeochemical processes (evolution) and/or flow paths. Subgroups S34 are highly evolved waters towards the rift floor where HCO3 start to be replaced by SO4 and Cl. The NNE-SSW alignment of Na^{+} and HCO_3^{-} rich groundwater connecting Lake Awassa basin to the southern part of the Gidabo River basin (Dilla area) reflects the inland connection of the groundwater system by recent rift faults. The deflection of Gidabo River flow line near north of Dilla also reveals the existence big faults connecting the basins.

The fourth group (G4) water is highly evolved Na-Cl/HCO_3^{-} type volcanic water represented by one thermal spring with average EC (5450µS/cm) and an average temperature of 96^{0}c. SP49 thermal water occurs along NNW-SSE and N-S trending recent faults cutting extensive Ql, N1-2n, and QWbp rock units (Fig.31). Other thermal springs in the area, especially north of Lake Abaya are also highly evolved such as SP57 but major ions anions vary significantly. SP49 and SP57 have high variability in the concentration of Cl^{-} (762,126) mg/l and HCO_3^{-}(1450, 2830) mg/l and PH (9.6,8.2) indicating that SP49 thermal springs are discharging from a highly evolved deep high-temperature reservoir (Fig.59, 60). (Teclu,2007) indicated that the reservoir temperature of SP49 and SP57 thermal springs is 250ºC and 180ºC respectively, which might suggest that there is no seawater intrusion. This group of water is highly evolved where Ca and Mg is almost totally precipitated and replaced by Na in the waters because of Na-silicate minerals weathering reaction and mixing with highland and escarpment converging waters facilitated by high temperature.

6.2.4.3.2. Correlation among Parameters

The hydrochemical relationship of the different clusters of water types could be distinguished using correlations among hydrochemical variables (Table 10). Some ions including Na^{+}, K^{+},

HCO_3^-, F^- and SO_4^{2-} were significantly and positively correlated with EC but Ca^{2+} and Mg^{2+} correlate insignificantly.

Table 10 statistical correlation matrix

Variables	EC (µS/cm)	T 0 c	PH	Na	K	Ca	Mg	F	Cl	NO3	Alkalinity	HCO3	SO4	PO4
EC (µS/cm)	**1**													
T 0 c	**0.624**	**1**												
PH	0.420	0.325	**1**											
Na	**0.721**	**0.683**	0.292	**1**										
K	**0.654**	**0.569**	0.282	**0.638**	**1**									
Ca	0.263	-0.024	0.268	-0.005	0.003	**1**								
Mg	0.274	0.023	0.243	0.037	0.110	**0.582**	**1**							
F	**0.685**	**0.804**	0.349	**0.808**	**0.660**	-0.072	-0.036	**1**						
Cl	0.491	**0.622**	0.261	**0.665**	**0.639**	0.035	0.048	**0.699**	**1**					
NO3	0.054	0.008	-0.111	0.061	-0.074	0.107	0.107	-0.030	0.107	**1**				
Alkalinity	0.502	0.144	0.317	**0.509**	0.207	0.479	0.432	0.231	0.045	0.070	**1**			
HCO3	**0.743**	**0.557**	0.352	**0.881**	**0.522**	0.336	0.354	**0.640**	0.415	0.044	**0.760**	**1**		
SO4	**0.506**	0.327	0.244	**0.583**	0.373	0.049	0.055	0.445	0.362	0.071	0.346	0.485	**1**	
PO4	0.053	0.006	0.093	0.039	0.061	0.132	0.066	0.014	0.039	-0.092	0.046	0.041	0.020	**1**

This implies that these ions increase in concentration along the groundwater evolution direction in aquifers from highlands towards rift center. Higher correlation of Na^+ with HCO_3^- *(r^2=0.881)* and F^- *(r^2=0.808)* is related to increased silicate weathering in the rift whereas Cl^- *(r^2=0.665)* and SO_4^{2-} *(r^2=0.583)* is related to the emanation of deep thermal sources. Highland groundwater clusters are rich in Ca^{2+} and Mg^{2+} showing poor correlation with Na^+ and K^+ due to the removal of divalent cations (ion exchange) through precipitation along the flow direction. HCO_3^- has a strong positive correlation with EC, T, Na^+, F^-, and alkalinity indicating bicarbonate alkalinity.

Principal components analysis (PCA

Principal Components Analysis (PCA) is a statistical method that takes a multivariate dataset and reorients it in such a way that the axis of greatest variance becomes the first principal component (PC1), and the axis of second-greatest variance becomes the second (PC2), and so on. A bivariate plot of PC1 vs. PC2 will thus summarize the greatest amount of variance in the dataset and be a more comprehensive summary of that dataset than a plot of any two of the original variables (Grunsky et al., 2014, Yousef Nazzal et al., 2015). Thus PCA is used to reduce a large set of geochemical datasets into few factors (new variables out of a set of existing original variables) that allow interpretation of variance within datasets and reveal high-level data

structures that cannot be detected using univariate or bivariate methods. It presents meaningful interpretations through groupings of samples with no a prior knowledge of their spatial relationships to each other.

The first principal component (F1) absorbs and accounts for the maximum possible proportion of the total variance in the data set and the second component (F2) absorbs the maximum of the remaining variance and so on. The maximum number of principal components is equal to the number of variables. The total variance accounted by all the Fi's will be equal to the number of variables because each standardized variable has variance equal to 1. For interpretation, only a few numbers of Fi are retained in the analysis. The number of principal components to be retained in the analysis is based on Kaiser Criterion. As per this criterion, principal components (Fi) having latent root or Eigenvalue (denoted by λi) greater than one are considered essential and are retained in the analysis. Factor loading (Yousef Nazzal et al., 2015) is the standardized values of the original number of variables. High factor loadings (value of a close to ±1) indicate a strong relationship (positive or negative) between the variable and the factor. The factor loadings matrix is rotated using varimax orthogonal rotation to maximize the relationship between the variables and some of the factors. This rotation results in high factor loadings for the variables correlated with the factor and low loadings for the remaining variables. The suitability of the dataset for PCA is tested by Kaiser–Meyer–Olkin (KMO) which is a measure of sampling adequacy. A value of KMO that is >0.5 indicates PCA can be performed. In this study, PCA was carried out in the standardized data sets and sorted by using Eigenvalues greater than 1.0 as these are considered significant influences towards the hydro-geochemical processes (Sahu et al. 1998; Panigrahy et al. 1999; Sundaray et al. 2006; Sundaray, 2010; P.K.Mohopatra et al,2011).

The PCA was performed on the standardized data set of fourteen hydrochemical variables having KMO measure of sample adequacy is 0.633. Three principal components (PC1, PC2, and PC3) accounting for 65.2% are retained having Eigenvalues greater than unity out of 14 where 11 have Eigenvalues less than unity (PC4 to PC14) (Table 11).

Table 11 Eigenvalue of PCs before varimax rotation

	PC1	PC2	PC3	PC4	PC5	PC6	PC7	PC8	PC9	PC10	PC11	PC12	PC13	PC14
Eigenvalue	5.7	2.1	1.2	0.97	0.9	0.7	0.6	0.43	0.4	0.37	0.19	0.14	0.13	0.006
Variabili (%)	41.12	15.7	8.4	6.9	6.44	5.03	4.26	3.12	2.85	2.64	1.40	1.03	0.96	0.05
Cumulative %	41.12	56.83	65.2	72.19	78.6	83.67	87.93	91.06	93.91	96.56	97.96	98.99	99.95	100.0

The factor loadings obtained after varimax orthogonal rotation from the data set of 14 variables and processes which have been interpreted from the factor loadings are given in (Table 12). The factor includes both positive and negative loadings. Loadings close to ±1 indicate a strong correlation between a variable and the principal component. Loadings higher than ±0. 75 are considered strong correlation, loadings between ±0. 5 and ±0. 74 are considered moderately correlated and loadings approaching 0 indicate weak correlations (P. K. Mohopatra et al, 2011). Based on the significant factor loadings (greater than ±0. 5), each principal component is assigned a process which the significant variables are likely to be associated with the component.

PC1

PC1 is strongly loaded with EC, Na, K, F and HCO_3 that accounts for 71.6% of the variability in the dataset. This principal component has a significant positive loading for EC, Na^+, F^- and HCO_3^- and moderate positive loading for K^+, Cl^-, Alkalinity, and SO_4^{-2}. The other loadings in this PC are all positive less than 0.5 and have a weak correlation (Table 11). Substantial positive loading of EC, Na^+, F^- and HCO_3^- indicated highly evolved groundwater of the basin. The least positive loading of Ca^{2+} and Mg^{2+} compared to Na^+ and K^+ is related to increased ion exchange along the groundwater evolution direction. Elevated temperature and rock-water interaction in aquifers facilitates the release of Na^+ and K^+ to groundwater and precipitation of Ca^{2+} in aquifer matrix. This also tends to increase HCO_3^- towards the rift floor.

The difference in the loading of Na^+ and K^+ is related to the resistance of K-minerals to hydrolysis /weathering in solution (Hem, 1992) and hence K^+ is lower. Increase in F^- is related to lower Ca^{2+} in the waters. Increased $SO4^{2-}$ and Cl^- in the solution could also be related to thermal activities of the rift floor where the highest concentration of Cl^- is analyzed at the thermal spring

(SP49) is 762mg/l (annex 4). The hydrogeochemical process assigned to this component is silicate weathering /hydrolysis responsible for the formation of Group III and Group IV clusters in rift floor. The clusters are highly mineralized where the groundwater of the basin has undergone maximum evolution.

Table 12 PC loadings obtained after varimax orthogonal rotation

	PC1	PC2	PC3
EC	**0.868**	0.095	0.001
T ^{0}c	**0.765**	-0.331	-0.041
PH	0.489	0.229	-0.391
Na^{+}	**0.913**	-0.166	0.122
K^{+}	**0.749**	-0.241	-0.133
Ca^{+2}	0.222	**0.800**	-0.059
Mg^{+2}	0.255	**0.742**	-0.013
F^{-}	**0.849**	-0.367	-0.038
Cl^{-}	**0.703**	-0.342	0.022
$NO3^{-}$	0.045	0.137	**0.761**
Alkalinity	**0.557**	**0.624**	0.116
$HCO3^{-}$	**0.875**	0.267	0.096
$SO4^{-2}$	**0.609**	-0.034	0.167
$PO4^{-3}$	0.070	0.138	**-0.596**
Eigen value	5.7	2.1	1.2
Proportion	0.716	0.139	0.001
% proportio	71.59	13.900	0.100
Cumulative	71.591	85.491	85.492
Interpretation process	silicate weathering of rift formations and ion exchange	silicate weathering of tertiary formations	weathering or anthropogenic pollution

PC2

PC2 explains 13.9% of the variability and has a strong positive correlation with Ca^{+2} and Mg^{+2} and moderate positive correlation with Alkalinity. Other parameters show poor correlation. Negative and low correlation of Na^{+} and K^{+} indicate the reduction of ions influenced by the increased concentration of Ca^{+2} and Mg^{2+} in the water. The increment of Ca^{+2} and Mg^{2+} is due to silicate weathering of Anorthite and Forsterite respectively in aquifers of highlands and escarpments. Low loading of F^{-} is due to enriched Ca^{2+} trapping the ion from the solution in PC2. Aquifers of the highlands and escarpments have low temperature and less chloride derived from the rain. PC2 represents the formation of Group I and Group II clusters, as a result of silicate weathering of highland and escarpment area rock minerals, which are less mineralized having low EC at an early stage of hydrochemical evolution.

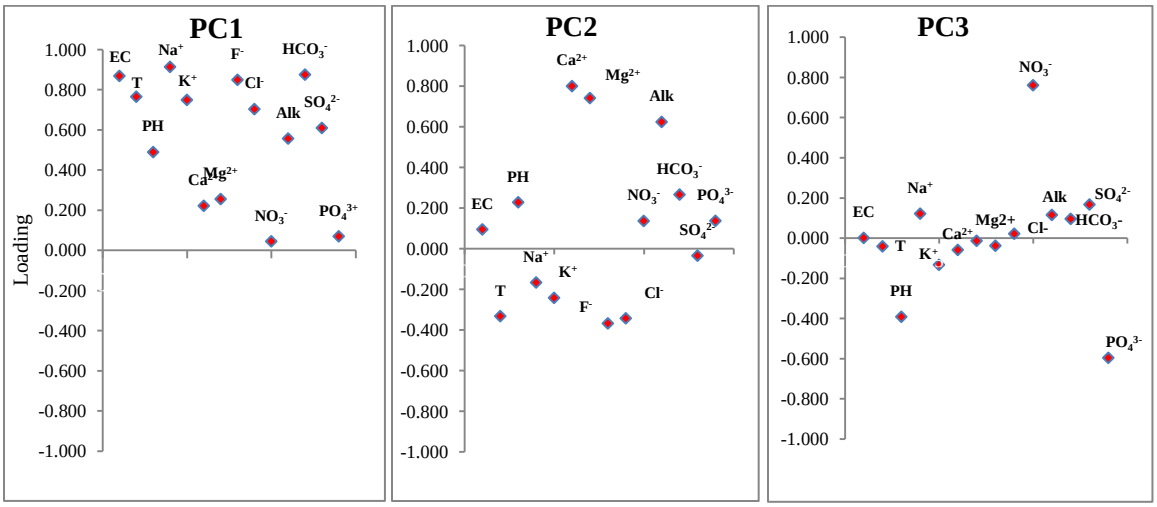

Fig 61 presentation of correlations of hydrochemical variables on PCs

PC3

PC3 showed positive, strong correlation with NO_3^- and moderate negative correlation with PO_4^{3-}. Though this PC has an insignificant proportion of variability in a data set (0.1%), it explains important correlations with respect to the groundwater contamination in the basin. All other variables are poorly correlated that plotted around 0. A positive sign of NO_3^- suggest increased concentration as a result of weathering or anthropogenic pollution. High load of NO_3^- occurs in BH91 (45,7mg/l), BH97 (120.9mg/l), SW38 (64.2mg/l), SW172 (62mg/l) and SP10 (65mg/l). This PC mainly showed oxidation of domestic wastes and weathering of nitrate bearing rocks that released NO_3^- to the groundwater system in these localities.

The presentation of PC1 Vs PC2 on the unit circle (Fig.62) indicated that Na^+, EC, F^- and HCO_3^- are positively correlated with the first component, PC1 (the horizontal axis) where variables are plotted on the unit circle close to 1. This indicated that the variables showed better variance when close to 1 and poor when closer to 0 as $NO3^-$ and PO_4^{3-} for both PC1 and PC2. Ca^{2+}, $Mg^{2+,}$ and alkalinity are positively correlated to the PC2 (vertical axis) as also indicated on PC2.

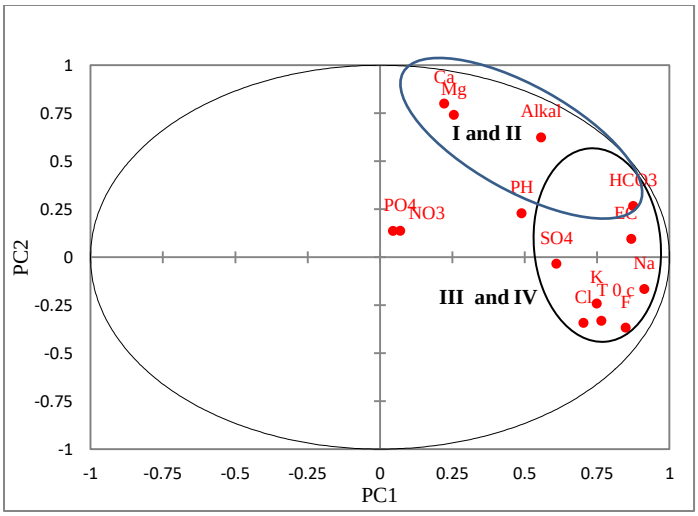

Fig 62 presentation PCs on unit circle

The unit circle PC1 vs PC2 viewed dominant ions of Abaya-Chamo Lakes basin groundwater systems representing clusters together as Group III (Na-HCO_3) and Group IV (Na-Cl) types at the positive strongly correlating side of PC1. These types are evolved groundwater occurring on the rift floor. Group IV water represents highly concentrated thermal water as discussed in PC1. Group I (Ca-HCO_3) and II (Mg-HCO_3) types dominantly circulate within the aquifers of highlands and escarpments are diluted that occur under the early stage of evolution and are evolved to be Na-HCO_3 in lowlands through silicate weathering facilitated by higher temperature and ion exchange and precipitation as discussed in PC1. Generally, the groundwater in Abaya – Chamo Lakes basin evolves from Ca-HCO3—Mg-HCO3—Na-HCO3 — Na-Cl which is aligned on the unit circle from the strong positive part of PC2 to strong positive part of PC1.

6.2.4.4. Chemical stratification of aquifers

Aquifers of the different episodes (Precambrian to extrusive volcanic rocks and recent formations) of the Abaya Chamo Lakes basin are exposed to different degrees of weathering and fracturing. Between the different eruption time periods, the rocks have been weathered and eroded with subsequent deposition of alluvial materials resulting in multi-layer aquifers with a range of unconfined to semi-confined and confined layers. As a result, the aquifers of the area show spatial and vertical heterogeneity (Fig.31 and 81).

The relation of averaged physical and chemical parameters of groundwater samples with depth in different parts of the basin (Fig.63) indicated that the values of EC, Na^{+}, Cl^{-} and HCO_3^{-} increase with depth from a highland shallow well to lowland rift floor deep well. Shallow groundwater in the basin occurs in upper unconfined/semi-confined dilute aquifer of the localities. Deeper groundwaters showed increased concentration for some parameters mentioned above and decrease in amount for Ca^{2+} and Mg^{2+}.

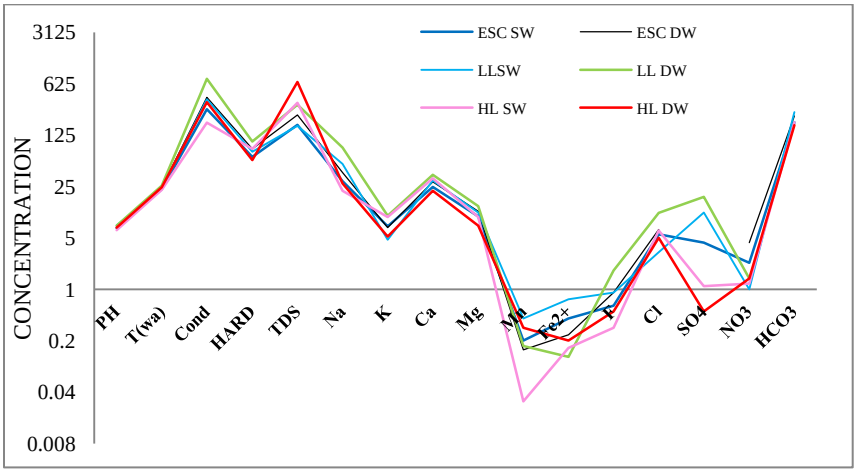

Fig 63 The relation of averaged physical and chemical parameters of groundwater samples with depth (shallow and deep wells) in different parts of the basin (*HLSW-highland shallow well, HL DW-highland deep well, ESC P SW- escarpment and plain shallow well, ESC P DW-escarpment and plain deep well, LL SW- lowland shallow well, LLDW- lowland deep well*).

The physiographic setup of the different sectors, shallow and deep well lithologic logs, hydrochemical data of aquifers and the tectonic setup of the areas are used to understand the hydrogeologic and hydrochemical nature of shallow and deep aquifers of Abaya-Chamo lakes basin using 2D cross-sections across the basin in selected representative areas (Fig. 39,40,81). This obtained a clear picture for the variability of the groundwater origin, flow, and type.

Spatial map of water types and piper diagrams display that the composition of groundwater in shallow and deep aquifers in the highlands, escarpments and rift floor sectors are interconnected and evolve with depth. Highland waters are rich in Ca and HCO_3 but shallow unconfined /semi-confined aquifers (0 to 60mbgl) and deep confined (up to 253mbgl) showed evolution from Ca-HCO_3 type to Na-Ca-HCO_3-Cl types, Highland wells showed increment in some parameters as EC (185 to 349 µS/cm), Na^{+} (19 to 60%), Mg^{2+} (16 to 19%) and HCO_3^{-}(90 to 92%) but

decrease in Ca^{2+} (59 to 32%) and Cl^{-} (7 to 2.1%) with depth. The variation in the proportion of major ions and distinction of water types is related to the variation of hydrogeochemical processes within aquifer systems such as the dissolution of silicate minerals (Appelo and Postma, 1993) and reactions taking place in soil zones of shallow aquifers (Ayenew, 2005). This case could partially work in places where faults connect faster and less evolving flow systems of highlands and rift floor.

Along escarpments (large fault margins and associated piedmont plains) of the basin, the groundwater is moderate to highly evolve with depth. In Intermountain areas filled with recent sediments, shallow groundwater is a Mg-HCO3 type, but deeper aquifers of the escarpment area have Na-HCO3 and Na-HCO3-SO4 types. Though the range of difference between the maximum and minimum ionic concentration values varies, the average (EC, Alkalinity, PH, Na, Ca, Mg, HCO3, and Cl) of shallow and deeper wells in escarpment aquifers showed a slight increment with depth (Fig.63 and Table 9). The intensity of tectonics is more in the northern half of the basin (GSE, 2000), and in places along the escarpment, the eastern dipping faults are responsible for the emanation of thermal springs (Fig 81). These thermal springs are the result of deep artesian aquifers intersected by NNE-SSW trending normal faults. The faults obstruct the general groundwater evolution consistency from the highlands towards the rift both spatially and vertically by emanating deep mantle sources and evolve the nearby aquifers through the interstices and fractures.

Lacustrine and fluvial deposits that filled in the Boyo Graben (Fig.81) modified the shallow and deeper groundwater composition of the escarpment. This indicated on the water type map more evolved groundwater of Yirgalem (Mg-Na-HCO3) and Dilla hot springs (Na-Ca-HCO3) aligned along the eastward dipping fault from Lake Awassa towards the north of Dilla blocking the continuity of Ca-Na-HCO3 waters (sees a water type map). The faults act as a conduit for the flow of hot springs along the eastern escarpment (Yirgalem hot spring T= 45.3^{0}c) and the barrier (to the opposite of W-E shallow and deeper groundwater flows) along the western escarpment (Arto hot spring T= 94^{0}c). The hydrochemical signatures show that shallow and deeper aquifers of the rift floor have characteristic EC, and major ions.

In deeper aquifers (sand and gravel) of the rift floor in the monitoring deep wells (depth 151m at north of Lake Abaya to 400m at Alaba), there is depleted groundwater originated not from the recent rainfall, but recharged during past climate (see chapter 8) whereas shallow rift floor groundwaters in rift volcanic rocks are mostly recharged by recent rainfall of rift and surrounding highlands and affected by thermal gradient through Holocene tectonics (Fig. 40, 84).

7. THE USE OF IONIC RELATIONS IN UNDERSTANDING HYDROGEOCHEMICAL PROCESSES AND SOURCE OF IONS IN THE ABAYA CHAMO LAKES BASIN

7.1. Introduction

The interaction between groundwater and aquifer minerals result in various water types and its chemistry depends on different hydrogeochemical processes that the hydrogeological system undergoes over space and time (Hussien B.M. and Faiyad A.S., 2016). The processes determining the composition of the groundwater are controlled by natural or anthropogenic factors (Hem, 1985). Different scholars used major ion ratios relations for understanding hydrogeochemical processes. Some of the works consisting: mechanisms controlling world water chemistry (Ronald J. Gibbs, 1970), the use of ion chemistry to identify salinization of coastal aquifers of the Sabarmati River Basin in India (Kumari Rina et al., 2013), modeling the hydrogeochemical processes and source of ions in the groundwater of aquifers within Kasra Nukhaib Region in West Iraq (Hussien, B.M. and Faiyad, A.S. , 2016), Studies on Major Ion Chemistry and Hydrogeochemical Processes of groundwater in Port Harcourt City of Southern Nigeria (H. O Nwankwoala and G.J Udom,2011), geochemical characteristics of shallow groundwater in Datong basin of northwestern China (Huaming Guo and Yanxin Wang ,2005), a geochemical approach to determine Sources and Movement of Saline Groundwater in a Coastal Aquifer in the San Diego area of California (USGS,2013) used the chemistry of major ions and their ratio to understand the hydrogeochemical processes occurring in the aquifers.

Based on the above scientific backgrounds, analysis and identification of the hydrogeochemical processes occurring in hydrogeological systems of the Abaya Chamo Lakes basin are done using groundwater chemistry and ionic relations (annex 4). Properties such as electrical conductivity, pH and major ion concentrations (Ca^{2+}, Mg^{2+}, Na^{+}, K^{+}, Cl^{-}, HCO_3^{-}, and SO_4^{2-}) of groundwater were taken into consideration. The spatial variation of these ions and the proportion of their abundance are discussed in hydrogeochemical facies part above. Hydrogeochemical processes governing the groundwater chemistry in the Abaya Chamo Lakes basin using hydrochemical indices are discussed below.

7.2. Hydrogeochemical processes

7.2.1. Silicate weathering

Groundwaters occurring in the hard rock formation generally have a high concentration of major ions controlled by silicate weathering of rocks (Meybeck 1987). Weathering and hydrolysis of silicate minerals such as feldspars are suggested to be major chemical processes determining the hydrochemistry of rift floor groundwater (Darling et al., 1996; Gizaw, 1996; Rango et al., 2009; Seifu et al, 2011). Silicate weathering is the dominant process in determining the concentration of major ions, especially HCO_3^- and corresponding cations in the water with increasing residence time and water-rock interaction (Herczeg and Edmunds, 2000). In highly weathered, fractured and faulted basic and acidic origin hard formations of the Abaya Chamo Lakes basin the sources of major ions is predictable from the analysis of the ionic ratios relations.

A Ca^{2+}/Mg^{2+} ratio greater than 2 may represent the dissolution of silicate minerals into the groundwater (B. G. Katz et al., 1997, Katz et.al., 1998, Tahoora Sheikhy Naran et al, 2014). Groundwater samples in an Abaya Chamo Lakes basin with a Ca^{2+}/Mg^{2+} ratio higher than 2 showed the dissolution of silicate minerals in areas (Fig.64) contribute calcium and magnesium to the groundwater. The plot of Ca^{2+}/Mg^{2+} (Fig.65) also reveals that most of the groundwater samples are clustered around and below the 1:1 line which indicates the predominance of carbonate and silicate weathering. Most areas of the basin with aquifers of basement rocks, Tertiary basalts to the south-west of Abaya Lake, Pleistocene basalts north of Lake Abaya, peralkaline rocks and Tertiary ignimbrites have Ca^{2+}/Mg^{2+} greater than 2 indicating the weathering of silicate minerals. Areas of north and south of Dilla and north of Hageremariam showed higher of rate weathering of silicates from older basalts (Fig.4, 31, 64).

Ca–Mg–Na–HCO_3 type waters evolving from the highlands towards escarpments are most probably a result of weathering of olivine, Diopside, and plagioclase which are major components of basalts of the study area (Peccerillo et al., 2003; Kersten, 2009). Dissolution of Anorthite and Forsterite yields calcium and magnesium as to the reaction:

$$CaAI_2Si_2O_8\ (\text{Anorthite}) + H_2O + 2H^+ = AI_2\ Si_2\ O_5\ (0\ H)_4 + Ca^{2+} \quad 7.1$$

$$5Mg_2SiO_4\ (\text{Forsterite}) + 8H^+ + 2H_2O = Mg_6(OH)_8Si_8O_4 + 4Mg^{+2} + H_4SiO_4 \quad 7.2$$

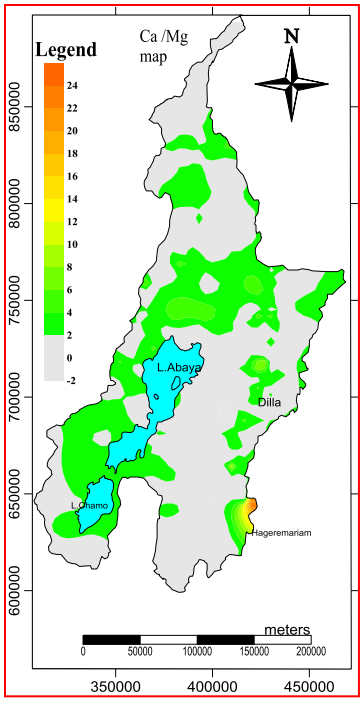

Fig 64 Spatial distribution of Ca/Mg ration

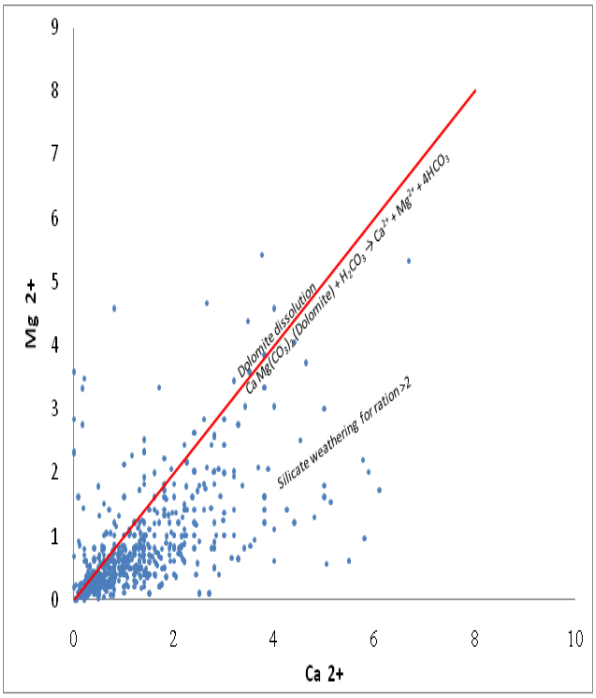

Fig 65 plot of Ca^{2+} versus Mg^{2+}

The majority of the samples showed a Na^{+}/Cl^{-} ratio equal to or greater than 1 may represent sodium, which had been released from the silicate weathering process (the reaction of the feldspar minerals with the carbonic acid in the water where cations and bicarbonate as a dominant anion form in the groundwater) (Meybeck, 1987). Silicate weathering is also the most sources of HCO_3^- in addition to soil zone.

$$2NaAlSi_3O_8+2H_2CO_3+9H_2O \Rightarrow Al_2Si_2O_5(OH)_4+2Na^{+}+4H_4SiO_4+2HCO^{-}_3 \qquad 7.3$$

(Albite) (Silicate weathering) (Kaolinite)

Groundwaters of Na^{+}/Cl ratio greater than or equal to 1 indicates that the dominant process for the formation of Na^{+} ion is silicate weathering (Stallard and Edmond, 1983). The extent of silicate weathering is higher towards lowlands and lower at highlands (Fig.66). The lowland groundwater (elevation vs Na/Cl) has a higher ratio greater than 1. Rift floor groundwater, especially hot springs have a higher ratio indicating the high weathering rate facilitated by thermal temperature gradient and/or evaporation.

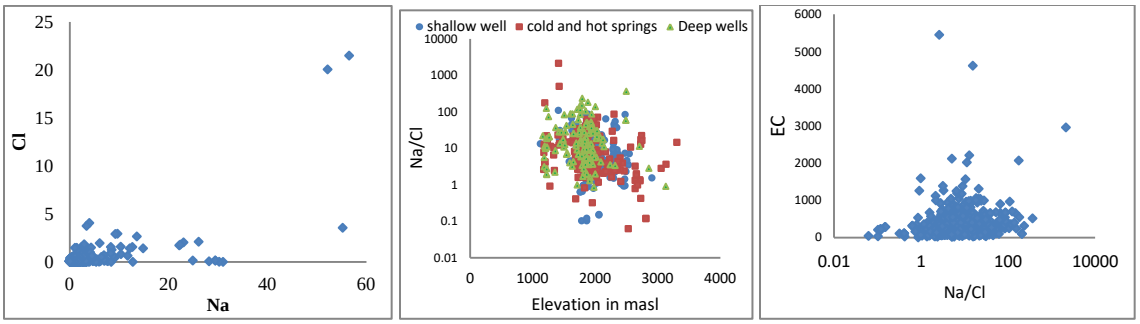

Fig 66 the ratio of Na/Cl and its relation with elevation and EC (electrical conductivity) for groundwaters

The relation of Na^+/Cl^- Vs EC trend indicated two processes involved in the formation of new: such as higher EC groundwaters with a low ratio of Na/Cl indicating evaporative process, whereas low EC waters of almost constant Na/Cl ratio indicate silicate weathering in highland, escarpments, and rift floor waters. Within Abaya Chamo Lakes basin this could be noted as a a lower ratio (Na/Cl <1) highland and escarpment waters (Fig.66 middle) have lower EC. Most groundwater samples (1<Na/Cl<100) located in both highlands, escarpments and lowlands are rich in Na^+ ion formed due to silicate weathering in moderate waters (EC < 2000 µS/cm). Deep wells and hot springs have higher EC related to elevated temperature favoring silicate weathering (Fig.66 left). The occurrence of the Na–HCO3 type waters mainly found in the Rift floor aquifers (Fig.58) is attributed to the increase in Na^+ concentrations partly to the dissolution of Na-feldspars from acidic/rhyolitic rocks. Such silicate hydrolysis are aided by the high CO2 partial pressure observed in the Main Ethiopian Rift (Darling et al., 1996; Gizaw, 1996).

7.2.2. Ion exchange process

The process in which the ions attracted to a solid surface may be exchanged for other ions in aqueous solution is known as ion exchange process. It is simply defined as the exchange of ions in rock aquifers by the ions in the aqueous solution or groundwater. Cation exchange modifies groundwater quality and is one of the most important geochemical processes taking place in aquifers (Hussien, B.M., and Faiyad, A.S., 2016). Cation exchange of Ca^{2+} for Na^+ on clay minerals such as smectite and illite, as well as secondary carbonates is responsible for a change in relative cation contents in rift groundwaters groundwater (Rango et al., 2009).

The examination of the binary plots of (Ca^{2+}+Mg^{2+}) versus (HCO^{3-}+$SO4^{2-}$) is used to study the relative importance of ion exchange and different weathering processes. If Ca, Mg, SO_4, and HCO_3 are derived from a simple dissolution of Calcite, Dolomite, and Gypsum, a 1:1 stoichiometry of (Ca+Mg) to (SO_4+HCO_3) should exist (McLean et al., 2000). If the ion exchange process dominates over the reverse ion exchange, the groundwater samples in the plot of Ca^{2+}+Mg^{2+} versus HCO_3^- + $SO4^{2-}$ have a tendency to shift to the right due to the excess of $HCO3^-$ + $SO4^{2-}$. Otherwise, water samples are positioned on the left due to a large excess of Ca^{2+} + Mg^{2+} over $HCO3^-$ + $SO4^{2}$ (Kozłowski M., Komisarek J. 2017). Based on the scientific background, the average ratio of Ca^{2+} + Mg^{2+} versus HCO^{3-} + $SO4^{2-}$ of almost more than 95% of groundwater samples in Abaya Chamo Lakes was less than 1 or (0.7) which shifted to HCO_3^- + $SO4^{2-}$ direction indicating ion exchange occurring during silicate and carbonate weathering. The spatial distribution of the ratio relation (Fig.67) indicated that most aquifers in the basin undergo ionic exchange where the ratio is less than 1. The ratio is greater than 1 in few localities where it is shifted in the direction of Ca^{2+} + Mg^{2+} indicating higher concentrations of Ca^{2+} + Mg^{2+} relative to HCO_3+SO_4 can be a result of a reverse ion exchange process where the Ca and Mg in the aquifer matrix have been replaced by Na at favorable exchange sites and has accounted for the dominance of Ca and Mg ions in groundwater over Na. Reverse ionic exchange hydrogeochemical process for the maximum Ca and Mg cations occurs in gneissic aquifers to the SSE of Lake Abaya. The ion exchange reaction for samples shifting towards anions may be explained as follows:

$$Ca^{+2} + Na\ (exchanged) \leftrightarrow 2Na^{+} + Ca\ (exchanged) \quad 7.4$$

$$Mg^{2+} + 2Na\ (exchanged) \leftrightarrow 2Na^{+} + Mg\ (exchange) \quad 7.5$$

and for some few samples plotting above the 1:1 line the ion exchange is the reverse as

$$2\ Na - Clay_2 + Ca^{+2} \rightarrow 2Na^{+} + Ca - Clay \quad 7.6$$

Significant lowering of Ca^{2+} and Mg^{2+} concentrations in Rift floor groundwaters (Fig.58) is related to precipitation and ion exchange contributed considerably to the evolution of Ca-dominated to Na-dominated groundwaters. These processes are particularly pronounced in the

thermal groundwaters sampled from hot springs in fault zones and active volcanic centers especially in the north of Lake Abaya.

Chloro-alkaline index (CAI) is one of the indices used to understand the ion exchange between the groundwater and its host environment (Schoeller, 1977) and is expressed by:

CAI1=Cl-(Na+K) /Cl and 7.7

CAI2=Cl-(Na+K) /(SO4+HCO3+CO3+NO3) 7.8

Where (All values of ions are measured in meq/l)

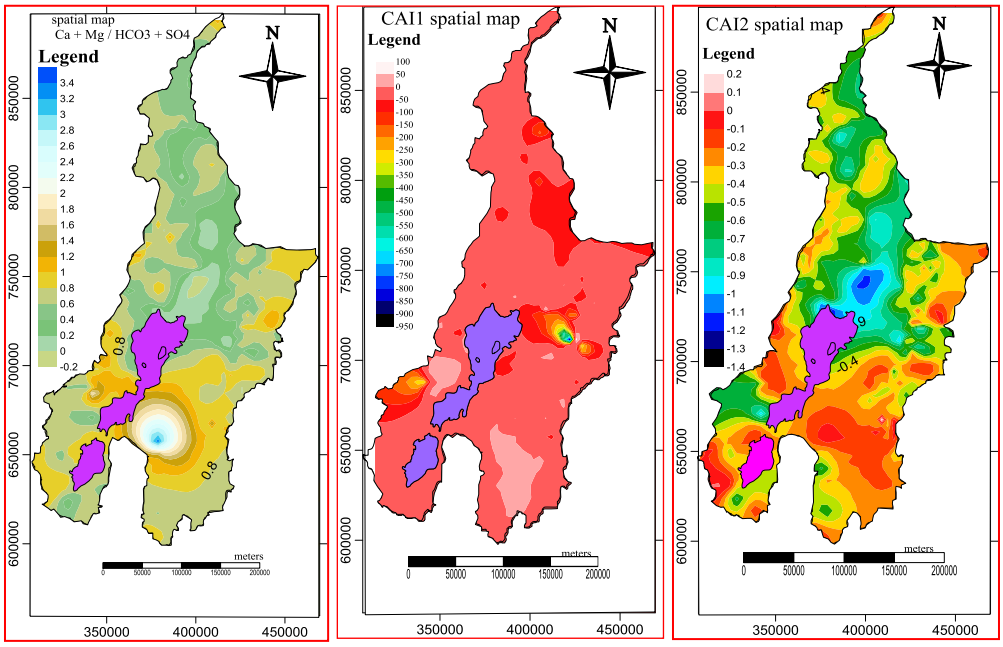

Fig 67 map of $Ca2^{+}$ + Mg^{2+}/ HCO_3+SO_4 Fig 68 map of CAI1 Fig 69 map of CAI2

From the above relations when the result of both CAI1 and CAI2 indices are negative, there is an exchange between Ca and Mg in the groundwater with Na and/or K in the aquifer material during the interaction, and if the CAI1 and CAI2 indices are positive, there is the reverse ion exchange (an exchange between Na and/or K in the groundwater with Ca and Mg in the aquifer material through the interaction).

Groundwater systems in the Abaya Chamo lakes basin have variable CAI1 and CAI2 that assist in the identification of localities where ion exchange or reverse ion exchange occurs. It also

indicates the extent of ion exchange variability in clarifying the rate of rock-water interaction. The ranges of indices are indicated in (Fig.68, 69). The spatial distribution of the CAI1 and CAI2 indicate that in most part of the basin ion exchange is the dominant hydrogeochemical process. Ion exchange is lesser along highlands and southern half of the basin, but its extent is higher in localities north and northeast of Lake Abaya where the degree of rock-water interaction is higher facilitated by elevated temperature of rift floor thermal aquifers. In this case, in thermal systems, almost all Ca and Mg are exchanged by Na and K.

Reverse ion exchange is identified in some localities east of Lake Chamo in recent deposits aquifer of Gelana basin to the southern part, weathered and transported clastics of Tertiary formation origins and lacustrine deposit aquifers in the western part of Lake Abaya area (Fig.68). In this case, the reverse ion exchange (exchange between Na and K in the groundwater with Ca and/or Mg in the aquifer material) is dominant where the water types are Ca-HCO_3 (Fig.58).

Generally, the ratio relation maps (Fig.67, 68,69) suggest that the extent of ion exchange along the highlands, escarpments, and rift floor is variable. Aquifers in the highlands and localities where Ca and HCO3 are dominant components of groundwater composition, the extent of ion exchange is less (Fig.58). The ion exchange highly increases along the direction of groundwater evolution towards the rift floor. This indicated that along the direction of evolution, the rock-water interaction is higher in aquifers where there is higher residence time and as result the amount of Na and HCO3 in water dominate. (Seifu et al, 2011) suggested such developed geochemical evolution can be explained by their circulation in active fault zones (Abaya geothermal field) where CO2 rises up from mantle sources whereby during such deep circulation Ca2+ may be removed by hydrothermal alteration.

7.2.3. Evaporation process

The evaporation process is a common phenomenon, not only in surface water, but also in groundwater systems (T. Subramanian et al, 2009). Evaporation is one of the hydrogeochemical processes that play a significant role in altering the quality of water, especially in regions that experience dry and semiarid climate. To understand the dominating hydrogeochemical processes

within Abaya-Chamo Lakes basin, groundwater samples from different sectors are plotted on the Gibbs diagram (Gibbs, 1970, 1971) that recommended a simple plot of TDS versus the weight ratio of $Na^{+}/(Na^{+} + Ca^{2+})$ and Cl/ (Cl + HCO3) to differentiate the influences of rock-water interaction, evaporation and precipitation as dominant processes on water chemistry (Fig.70).

The low TDS (<100mg/l) groundwater samples occur in eastern and western highlands of the Abaya Chamo is rainfall dominated. This implies that low TDS waters of highlands recharged during the rainy season and stored in shallow unconfined aquifers mostly occur as small seasonal springs and shallow hand dug wells. Most of the groundwater sample plot in the region of the major hydrogeochemical process of rainfall and rock–water interaction dominance fields. Groundwaters of escarpments and some rift floor are in this field along groundwater flow/evolution where TDS is increasing. A few samples of high TDS showed the process of evaporation. Higher evaporation increases the TDS and samples tend to move from rock dominance to evaporation zone. Some hot springs around Dilla area and thermal springs to the north of Lake Abaya having TDS >1000mg/l plotted on the evaporation dominating field could be related to either evaporation prior recharge or evaporation from groundwater in high surface and near-surface temperature gradient of the rift floor.

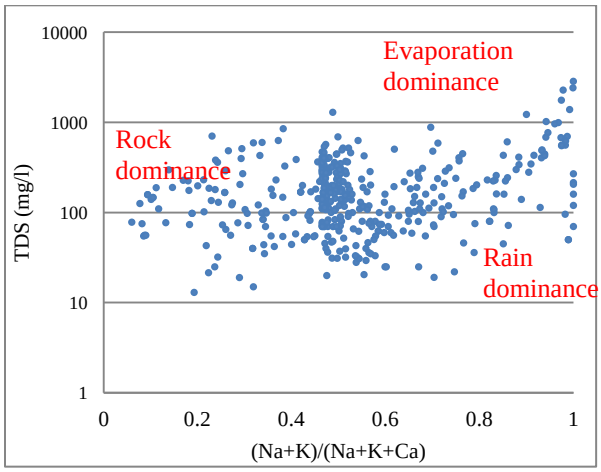

Fig 70 the Gibb plot of water samples

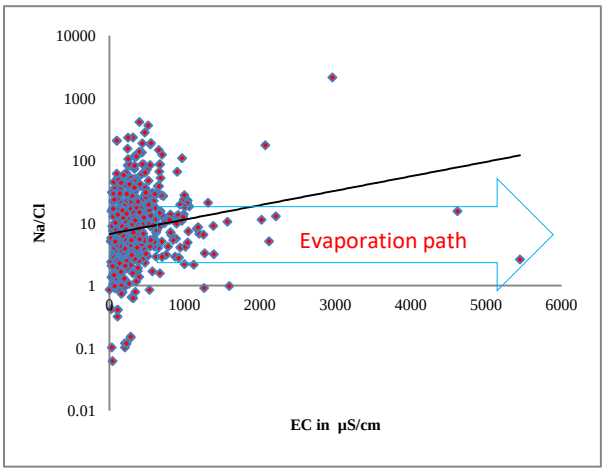

Fig 71 EC versus Na/Cl of water samples

The relation of EC Vs Na^{+}/Cl^{-}indicates two processes involved in the formation of Na: such as higher EC waters with a constant lower ratio of Na/Cl indicating evaporative process in rift floor waters (Jankowski and Acworth 1997) and a molar ratio greater than 1 indicating silicate

weathering. The EC vs Na/Cl scatter diagram of the groundwater samples of the basin (Fig.71) shows that the trend line is inclined towards the direction of Na/ Cl, and Na/Cl ratio increases with increasing salinity (EC) which seems to be the addition of sodium by ion exchange reaction. This indicated that evaporation may not be the major geochemical process controlling the chemistry of groundwater in the rift floor, but also dissolution and ion exchange dominate over evaporation which is also justified in Gibbs diagram. Low EC waters of variable Na/Cl ratio in the highlands are dominated by silicate weathering, but rift floor hot springs have higher EC related to elevated temperature favoring evaporation in addition to silicate weathering.

This is also supported by the Cl^-/HCO_3^- ratio that may show the influence of increasing salinity due to saline water, mixing to the groundwater systems (Bayan Muhie Hussien and Abed Salih Faiyad, 2016). The influence of salinity is directly linked with evaporation from the surface or groundwater systems. Localities around Lakes Abaya Chamo and Basement terrain SSW of Lake Abaya have groundwater samples with $Cl^-/HCO3^-$ ratios in the range between 0.5 – 1.9 which showed that the water was slightly or moderately affected by salinization (Fig.72). Except for these areas, groundwater samples in the Abaya Chamo lakes basin have a ratio of $Cl^-/HCO3^-$ less than 0.5 indicating that ground waters are fresh or unaffected by salinity.

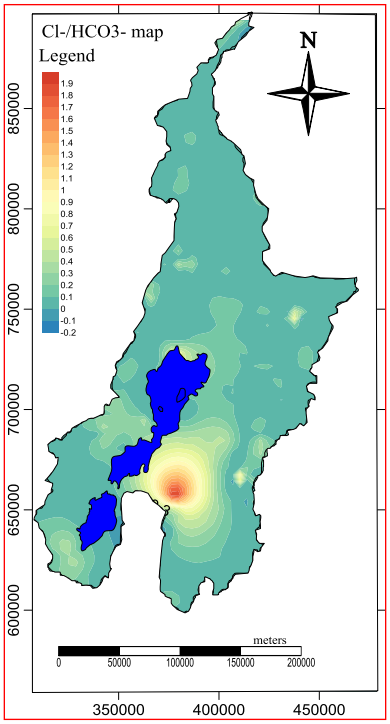

Fig 72 spatial distribution map of $Cl^-/HCO3^-$ indicating evaporation dominating localities.

8. ISOTOPE HYDROLOGY

8.1. Introduction

Isotope hydrology is an important tool in understanding hydrological processes such as recharge rate and recharge mechanism, surface water-groundwater interaction, the time scale of processes, origin of pollution (Craig, 1961; Gat, 1980; Fritz and Fontes, 1980; Gonfiantini, 1986; Fontes, 1980; Fontes and Edmunds, 1989; Coplen, 1993; Gat, 1996; Mazor, 1997; Clark and Fritz, 1997, Cook and Herczeg, 2000). The science of Isotope hydrology by now is also growing and becoming more powerful in understanding the hydrology of arid and semi-arid regions of Ethiopia in providing much desirable knowledge for groundwater resources management (UNDP, 1973; Ayenew, 1998; Mackenzie, 2001; Kebede, 2003; GSE, 2007; Jica, 2012; Kebede, 2013).

Stable isotopes of hydrogen and oxygen are an integral part of the water molecule (Dansgaard, 1964). Oxygen has three stable isotopes: ^{16}O, ^{17}O, and ^{18}O; and hydrogen has two stable isotopes: ^{1}H and ^{2}H (deuterium). The relative abundances of the lighter isotopes of hydrogen (^{1}H=0.999) and oxygen (^{16}O=0.997) are naturally high. Variations in the relative abundance of stable isotopes due to their differences in mass change the isotopic composition by a transition (evaporation, condensation, sublimation, freezing, and geochemical reactions) of a compound in different hydrologic compartments (water bodies) are important phenomena in hydrological studies. These phenomena (Isotope fractionation) depend mainly on the temperature that allows using the isotopic variations in nature as tracers in hydrological processes. Stable isotopes of ^{18}O (oxygen-18) and ^{2}H (deuterium) are most commonly used in studying hydrological processes and the basin behavior, including tracing the history of water, its recharge location, movements and interaction (mixing) along the flow path and aquifers in addition to hydrochemistry and water level measurements.

The concentration of isotopes in water is extremely small and as a result, the determination of specific isotopes in a water sample is very difficult. Therefore, isotopic ratios are used to determine the abundance and are commonly reported as δ values in units of parts per mill (‰) relative to a standard of known composition. The ratio R is given by

$$R = \frac{\text{Abundance of rare (heavy)isotope}}{\text{Abundance of abundant (light)Isotope}}$$

Practically R is a very small number to use and the isotopic compositions are given as delta (δ) in per mil (‰) deviated with respect to standard values. These deviations are denoted by δ^2H for deuterium and $\delta^{18}O$ for ^{18}O and expressed as:

$$\delta^2H(^o/_{oo}) = \frac{\left(\frac{^2H}{^1H}\right)_{sample} - \left(\frac{^2H}{^1H}\right)_{standard}}{\left(\frac{^2H}{^1H}\right)_{standard}} x\,1000$$

$$\delta^{18}O(^o/_{oo}) = \frac{\left(\frac{^{18}O}{^{16}O}\right)_{sample} - \left(\frac{^{18}O}{^{16}O}\right)_{standard}}{\left(\frac{^{18}O}{^{16}O}\right)_{standard}} x\,1000$$

δ ‰ value can be positive or negative depending on the amount of the isotopic content of a sample relative to VSMOW standards ($1.5575x10^{-4}$ for $^2H/^1H$ and $2.0052x10^{-3}$ for $^{18}O/^{16}O$). A positive δ value means that the isotopic ratio of the sample is higher than that of the standard, whereas a negative δ value denotes the isotopic ratio of the sample is lower than that of the standard.

The application of these environmental isotopes (δ^2H and $\delta^{18}O$) in hydrological investigation to understand the processes in a catchment follows basic principles, including 1) Waters recharged at different times, in different locations, or that followed different flow paths are often isotopically distinct; 2) Unlike most chemical tracers, environmental isotopes are relatively conservative in reactions to catchment materials. This is especially true for oxygen and hydrogen isotopes in water. This means that meteoric waters retain their distinctive fingerprints until they mix with waters of different compositions and in the case of isotopes of dissolved species there are reactions with minerals and fluids which involve isotope fractionation. 3) Solutes in catchment waters that are derived from atmospheric sources are commonly isotopically distinct from solutes derived from geologic and biologic sources within the catchment. 4) Both biological cycling of solutes and water-rock reactions often change isotopic ratios of the solutes in predictable and recognizable directions; these interactions often can be reconstructed from the isotopic compositions. 5) If water from an isotopically distinctive source (e.g., rain with an

unusual isotopic composition) is found along a flow path, it provides proof for a hydrologic connection, despite any hydraulic measurements or models to the contrary. Details on the use of the stable isotopes in the hydrological investigation are given in previously listed references above in this section.

8.2. Stable isotopic (δ^2H and $\delta^{18}O$) composition of precipitations

A hydrologic investigation using stable isotopes of δ^2H and $\delta^{18}O$ based on the scientific principles indicated the concept of meteoric water line and the isotope effects. The stable isotope composition of ^2H and ^{18}O of precipitation from a different part of the world give a linear line ($\delta^{18}O‰$ versus $\delta^2H‰$) called the Global Meteoric Water Line (GMWL) or Craig line (Craig, 1961) with the equation: $\delta\ ^2H = 8\delta\ ^{18}O$ + 10‰ VSMOW. The local meteoric water lines (LMWLs) (Fig.73) are made from the relation ($\delta^{18}O‰$ versus $\delta^2H‰$) of three local precipitation stations from the western highlands (sodo), eastern highland (Hagereselam) of Abaya Chamo Lakes basin and rift valley (Awassa) nearby basin of the study area from one year GNIP data of the stations (Data 1999/2000, IAEA).

The monthly average values of ($\delta^{18}O$, δ^2H) of one-year local precipitation stations Hagereselam (-1.97‰,0.27‰), Awassa (-0.72‰,5.83‰) and sodo (-1.44‰, -0.96‰) indicate deviation from GMWL average (-4‰, -22‰). The GMWL and LMWLs intersect at the different ($\delta^{18}O‰$, $\delta^2H‰$) points (Fig.73). The variation in average isotopic composition of the rainfall and their intercept points at the GMWL is related to the change in isotope value of the source, the rate of evaporation of the source, the isotopic evolution of them air mass, relative humidity during precipitation (Gat. 1996). The difference in intercept may reflect a higher kinetic effect during evaporation (non-equilibrium evaporation) of the moisture along the trajectory of the moisture sources of the area (the Atlantic and Indian oceans). The regression lines for the stations of sodo and Awasa plotted to the right of the GMWL because of substantial evaporative enrichment except for Hagereselam (at 2600masl).

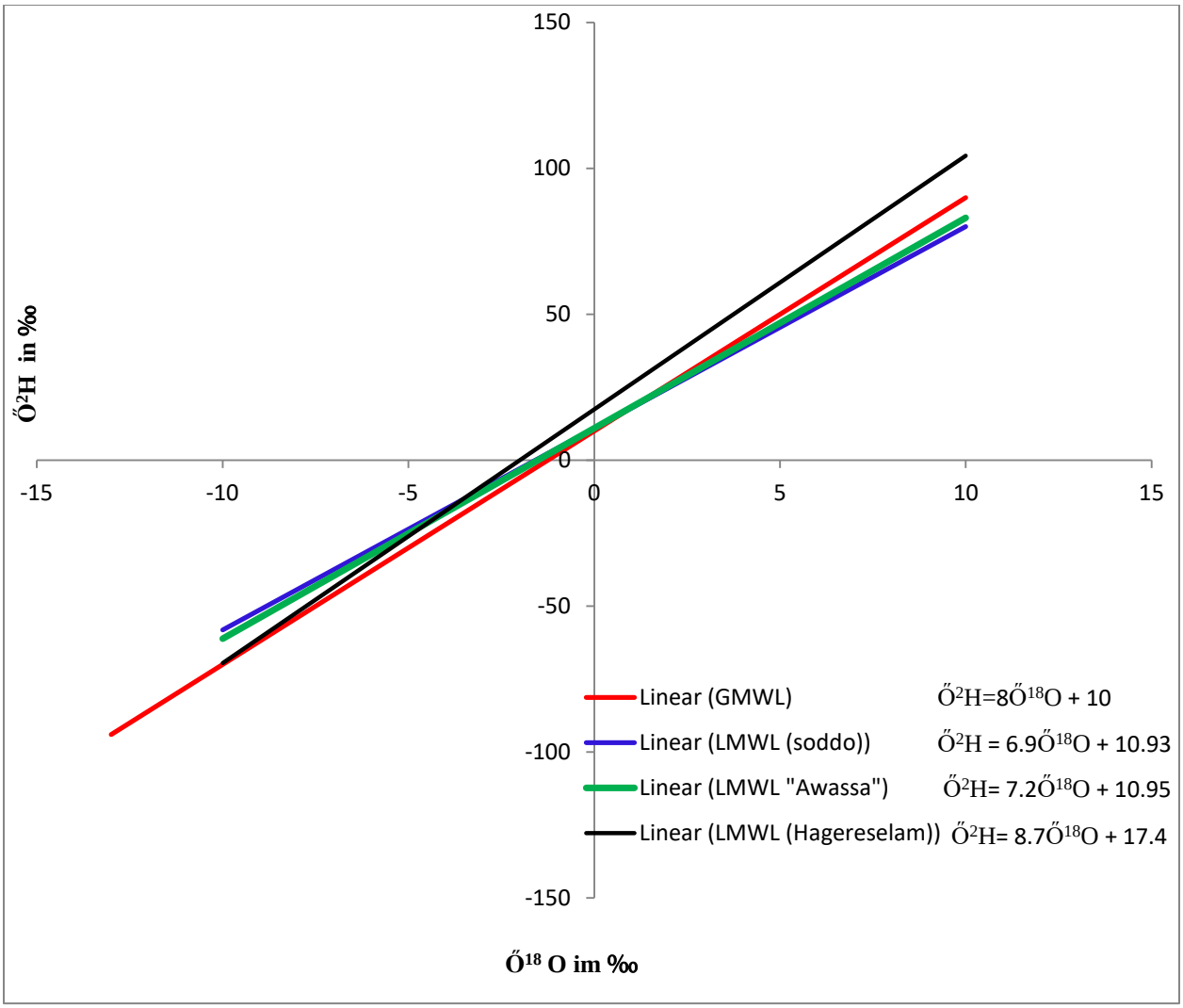

Fig 73 linear relation of $\delta^{18}O‰$ vs $\delta^{2}H‰$ of precipitation at three GNIP station (*Data 1999/2000, IAEA), the red regression line represents the Global Meteoric Water Line (GMWL), the blue, green and black regression lines represent the Local Meteoric Water Lines (LMWLs) at sodo, Awasa and Hagereselam stations respectively*)

When the air mass leaves its source, it is exposed to the most frequent processes of condensation and evaporation. Water evaporation leads to enrichment in the stable isotope composition in the residual water fraction (increase in heavy isotope content with respect to the light). Every precipitation event depletes the vapor remaining reservoir. Water with heavier $^{18}O/^{16}O$ and $^{2}H/^{1}H$ ratio forms the initial water droplets of rains and as vapor mass continues to lose its heavy isotopes it becomes more depleted in heavy isotopes. Meteoric water in a given environment when it undergoes phase changes related to hydrological processes, its isotopic composition also changes accordingly (Fig. 74 a and b). The most important isotope effects used in hydrologic

investigations are altitude, latitude, amount, evaporation, seasonality, temperature, continentality and paleoclimate effects.

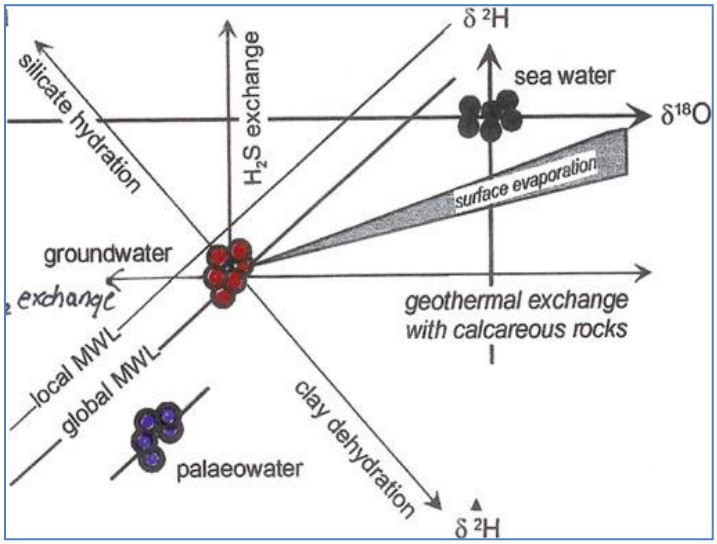

Fig 74. LMWL, GMWL and isotopic composition modifications accompanying hydrological and geochemical exchanges in the hydrologic compartment (after Kebede, 2013)

8.3. Spatial variation in isotopic (^{18}O and ^{2}H) composition of groundwaters in Abaya Chamo Lakes basin

The altitudinal variation of ȯ^{18}O‰ of rainfall on Ethiopian plateau is -0.1‰/100m (Kebede and Travi, 2011) whereas within the Abaya Chamo basin, it is -0.33‰/100m and -0.36‰/100m along eastern and western highlands respectively. Southern highlands and rift floor get relatively more depleted rainfall than the central rift valley and highlands as indicated from Arbaminch (ȯ^{18}O= -3‰ at 1200masl) to Awasa (ȯ^{18}O= -0.72‰ at 1700masl) showing northward higher altitude enrichment trend.

To understand the variability of hydrogeological systems in the Abaya Chamo Lakes basin, the isotopic composition of (ȯ^{18}O, ȯ^{2}H and d-excess) of groundwater samples (62 wells, 41 cold spring and 16 hot and warm springs) and surface water samples (12 River samples and 3 Lakes) are used. The data (ȯ^{18}O and ȯ^{2}H) are gathered from previous studies (UNDP, 1973; Mekenzie, 2001; GSE, 2007; Jica, 2012 and Abraham et al, 2016). As far as the original data is concerned, the especial emphasis is given to the data set of newly drilled observation wells in rift zone and associated data collected from existing water schemes in the basin in the research period for the

rift valley master plan in collaboration with southern Ethiopian water bureau. For the proposed study objective and also to see the aquifers variability, the data set is found to be more valuable as presented in (Fig.75).

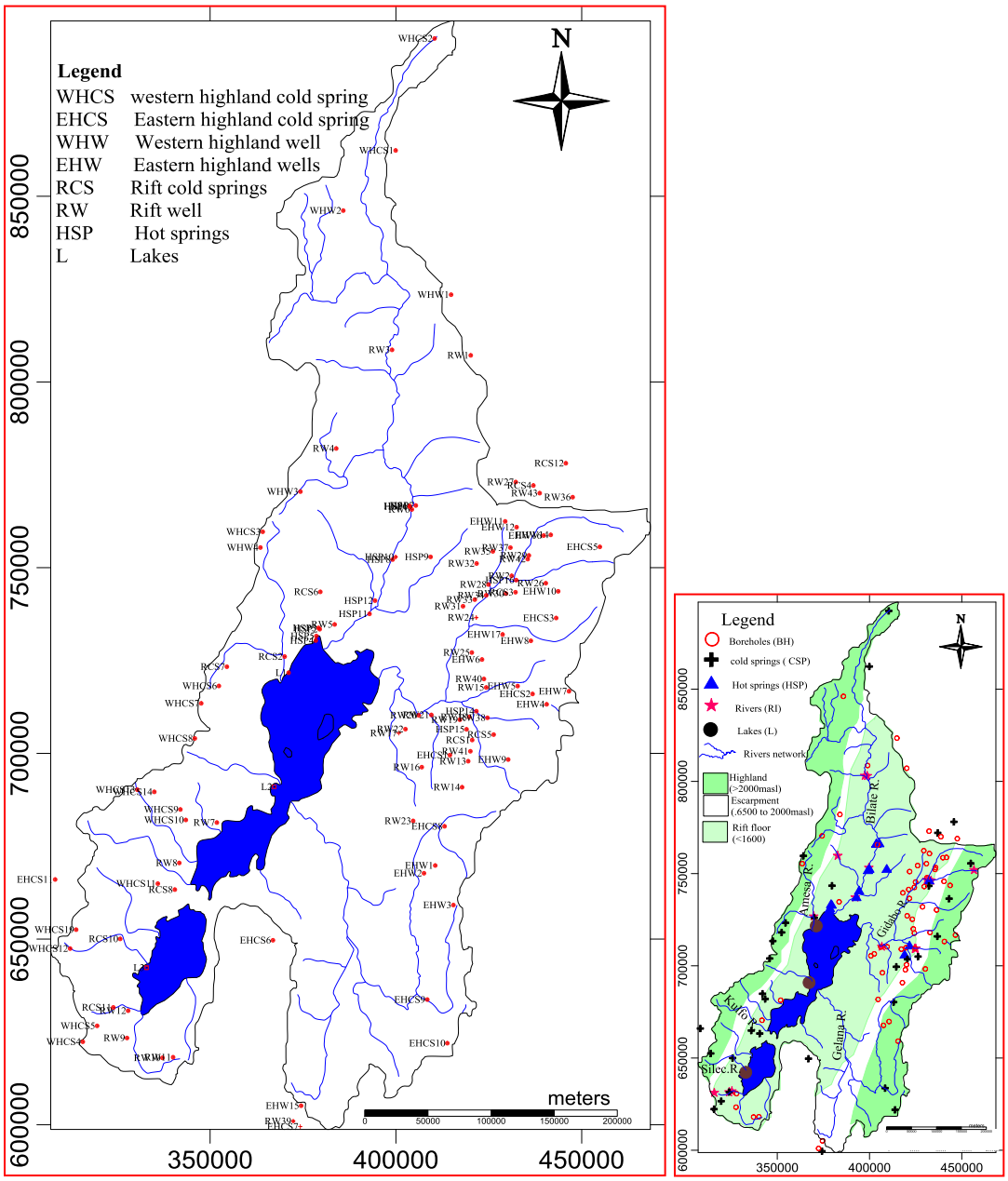

Fig 75 The spatial distribution of stable isotope data of different waters along three different physiographic regimes of Abaya Chamo Lakes basin

The results from the water isotopes are used to gain an insight into the groundwater recharge source and mechanism (Rozanski et al., 1993), groundwater flow and evolution direction

(Edmunds et al., 1992; Fausto et al., 2006), lake –groundwater relations (Kebede et al, 2002) and isotopic effects such (mixing and evaporation) in different sectors of the basin. This is possible because of the existence of spatial and seasonal variation in $\delta^{18}O$ of rain falls, the difference in the d-excess of rainfall waters along the three sectors of the basin and the enrichment of lakes in $\delta^{18}O$ and $\delta^{2}H$.

The major sources of groundwaters in Abaya-Chamo Lakes basin could be directly from rainfall or indirectly from other sources such as interconnected aquifers, Rivers and Lakes. But the major sources of recharge are rainfall as indicated on the plots of LMWLs and groundwaters (discussed in chapter 4). The averaged LMWL of the three GNIP rainfall stations ($ó^{2}H‰=7.14ó^{18}O$ ‰+12) and the ($ó^{18}O$-$ó^{2}H$) regression line for highland groundwaters of the basin ($ó^{2}H‰= 5.2\ ó\ ^{18}O‰$ +9.74). The intersection of the two linear lines is at ($ó^{18}O$, $ó^{2}H$) = (-1.32,2.84) which indicated that the average stable isotopic composition of the surface water before recharge is relatively depleted with respect to $ó^{18}O‰$ according to (J. R. Gat, 2010).

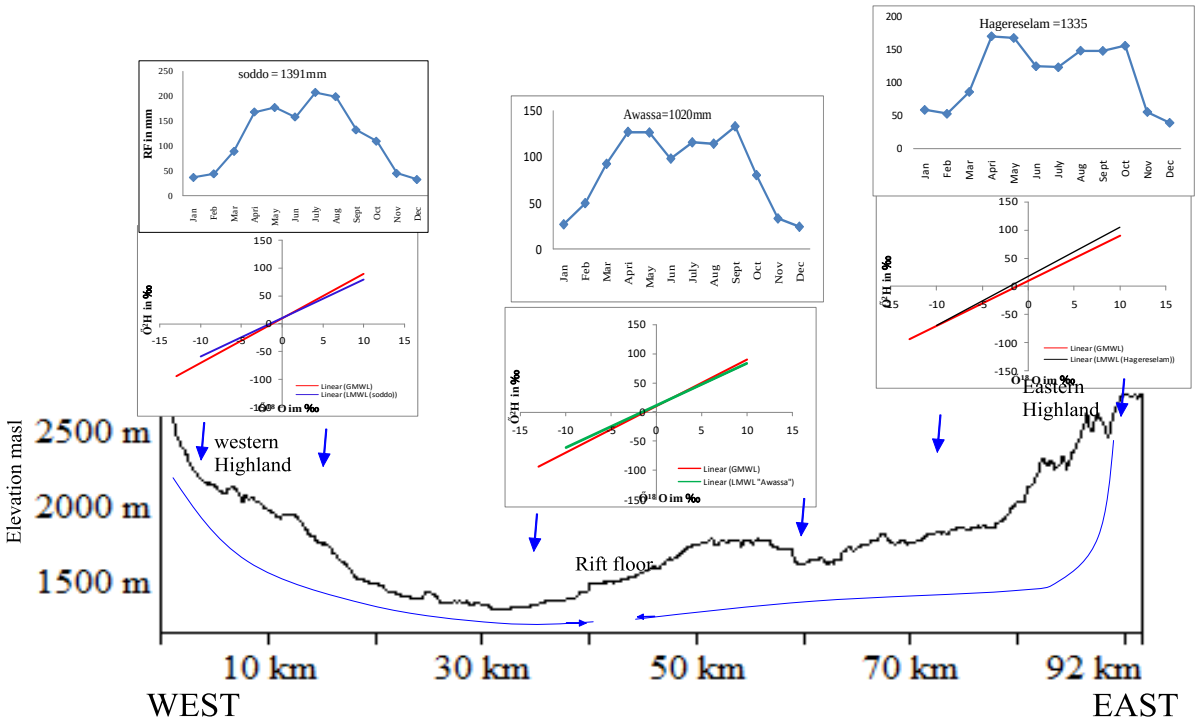

Fig 76 profiles of the amount and isotopic composition of recharging rainfall across the basin

However, the average surface water isotopic composition before recharging of different parts of the basin is variable. The local meteoric water line could be constructed from highland springs

and Rivers with low TDS and analogous chemistry of precipitation (Mekenzie, 2001). Based on this, the local meteoric water line (LMWL) of southwestern highlands is $\dot{o}^2H=8.1\dot{o}^{18}O+19$ and a coefficient of 0.73. The regression line of groundwaters of southwestern highlands ($\dot{o}^2H=5.84\dot{o}^{18}O$ +10) and the LMWL intercept at ($\dot{o}^{18}O$, $\dot{o}^2H$) of (-3.8, -12). Similarity, the regression lines of cold springs and locally flowing groundwaters of the eastern highlands ($\dot{o}^2H‰=7.6\dot{o}^{18}O‰+16.5$) and Hagereselam LMWL ($\dot{o}^2H‰=8.7\dot{o}^{18}O‰$ +17.4) intercept at (-0.82,10.3) whereas that of the rift floor locally flowing groundwaters ($\dot{o}^2H‰=3.3\dot{o}^{18}O‰+4.7$) and Awassa LMWL ($\dot{o}^2H‰=7.2\dot{o}^{18}O‰+10.95$) have (-1.6,-0.54) intercept in common. The above relations obtained variable intercepts (stable isotopic composition of the surface water before recharge) indicated the eastward enrichment from the southwestern part of the basin. This pattern is similar to the summer rainfall enrichment trend as discussed in chapter 4. It is linked to the variability in the humidity of the vapor forming the rainfall and the re-evaporation during rainfall that further caused the kinetic fractionation (Dansgaard, 1964). The extent of weathering and fracturing of the geologic units and fast flow through faults and fractures could also be also a factor in areas of higher depletion.

The stable isotopic composition of 120 groundwaters samples (Fig.75 and Table 13) is summarized based on their physiographic areas. Though the minimum and maximum values of the isotopic composition of groundwaters vary, the average isotopic composition ($\dot{o}^{18}O$, $\dot{o}^2H$, and D-excess) of groundwaters in the highlands/escarpments and rift floor is almost highly related. This indicated that the source of recharge for most of the groundwaters is rainfall and interconnected aquifers of the highlands, escarpments, and rift floor

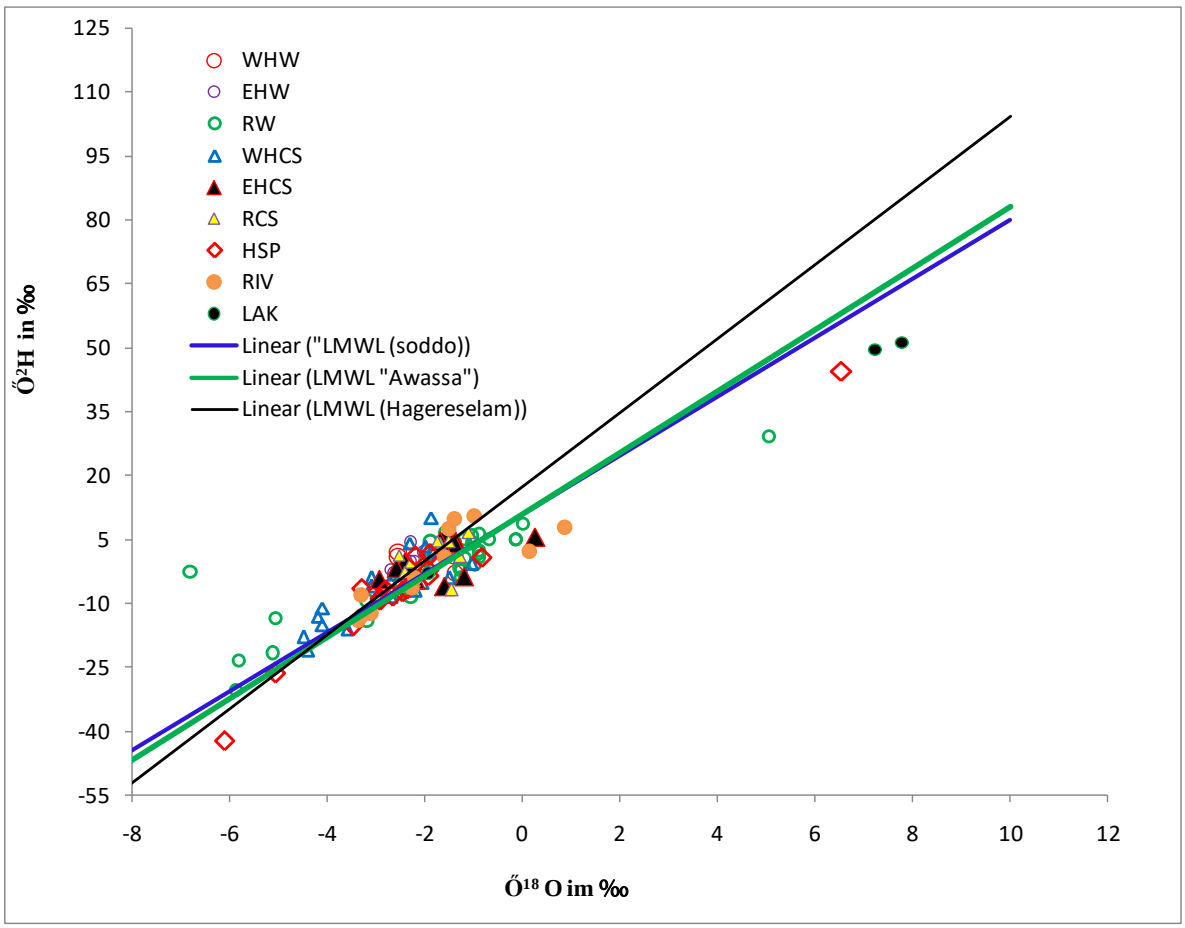

Fig 77 Plot of different waters on LMWLs of Abaya Chamo Lakes basin (*WHW- western highland wells, EHW-Eastern Highland wells, WHCS-Western Highland Cold springs, EHCS-Eastern Highland Cold springs, RW-Rift Floor wells, RCS-Rift Floor Cold springs, HSP- Hot Springs, RIV –Rivers and LAK –is lakes samples*)

Table 13 statistical summary of Environmental isotopes and D-excess of groundwater, Lakes and Rivers samples *(GW-EB - groundwaters in entire basin, WHW- western highland wells, EHW-Eastern Highland wells, WHCS-Western Highland Cold springs, EHCS-Eastern Highland Cold springs, RFW-Rift Floor wells, RFCS-Rift Floor Cold springs, HSP- Hot Springs)*

Water	(ὸ^{18}O‰			ὸ^{2}H‰			D-excess			
category	Min	Max	Av	Min	Max	Av	Min	Max	Av	samples
GW-EB	-6.82	6.54	-2.06	-42	44.4	-2.1	-11.1	52.1	14.6	120
WHW	-2.55	-1.38	-1.96	-2.9	1.99	0.2	8.14	22.4	16	4
EHW	-2.7	-0.16	-2	-7.8	5	-0.1	6.31	22.6	16.4	17
WHCS	-4.2	-1.05	-2.8	-21	10.1	-6	7.7	25	16.5	19
EHCS	-2.93	0.26	-1.7	-6.07	5.6	0.43	3.6	19.2	14	11
RFW	-6.82	5.04	-1.78	-30.3	29.2	-1.1	-11	52.1	13.8	42
RFCS	-3	-1.1	-1.93	-8	6.5	-0.06	4.8	21.7	15.3	11
HSP	-6.11	6.54	-2.2	-42.2	44.4	-5.9	-7.92	20	12.2	16
Lakes	-1.91	7.8	4.38	-3.2	51.2	33	-11.2	12.1	-2.51	3
Rivers	-3.38	0.85	-1.8	-14	10.5	-1.57	1.08	21	13.15	12

Based on the isotopic signatures of the groundwater systems in the Abaya Chamo Lakes basin are grouped into five (Fig.78).

8.3.1. Group I (Highland and escarpment hydrogeological systems)

Group I represents highland and escarpment areas groundwaters system having isotopic signature of ὁ^{18}O‰ (-4.5 to -1.4), ὁ^{2}H‰ (-21 to 10.1) and d-excess ‰ (10.6 to 25.1) in the basin. Water samples of group I include WHW2, WHW4, EHW1, EHW2, EHW3, EHW4, EHW5, EHW6, EHW7, EHW8, EHW9, EHW10, EHW11, EHW12, EHW13, EHW14, EHW15, EHW16, WHCS1, HCS2, WHCS3, WHCS4, WHCS5, WHCS6, WHCS7, WHCS8, WHCS9, WHCS10, WHCS11, WHCS12, WHCS13, WHCS14, WHCS15, WHCS16, WHCS17, EHCS1, EHCS2, EHCS3, EHCS4, EHCS5, EHCS6, EHCS8, and EHCS11 which are plotted towards depleting side along the LMWLs of the basin (Fig.75, 77 and annex 5).

The highland and associated hydrogeological systems are recharged directly by depleted highlands and escarpments summer rainfall (ὁ^{18}O ‰= -4.5 to -0 3) under cold air condition. But the degree of depletion of rainfalls varies from south to north on both sides of the basin due to basin scale microclimatic variability as discussed in section 4. Low EC and depletion with respect to heavy isotopes of the group indicated that the waters are formed due to fast percolation of highland rain waters favored by high hydraulic gradient and open fractures where the residence time, rock-water interaction and isotopic fractionation are very low. In places where big faults and wide fractures connect highland aquifers with lowland discharging areas, the groundwater (RCSP 8) (Fig.75) is less evolved (EC = 347 µS/cm) and depleted with respect to heavy isotopes (ὁ^{18}O‰= -3, ὁ^{2}H‰= -8 and d-excess ‰ = 16). This indicated that the spring at an elevation of 1189masl in south rift is recharged in cooler climate condition (higher d-excess) at recharge altitude greater than 2000masl. The turbulent and fast flow of the spring via big fault scarps down throwing young Pleistocene basalt for more than 200mts also reveals less residence time from point of recharge altitude. The residence time could be one month of summer and two months of spring season rains to reach to spring discharge points as indicated from the relation of average spring flow and rainfall of the nearby stations (Fig. 37 left)

8.3.2. Group II (mixed waters)

This group of water is constituted of both from wells, cold springs, hot springs, Rivers, and Lakes. Samples from the highlands, escarpments and the rift floor plot below LMWLs towards the enrichment direction of ó^{18}O and ó^{2}H around the intersection of Line of evaporation. The waters have ó^{18}O‰= (-2.47 to 0.27), ó^{2}H‰ = (-8.3 to 8.8), d-excess ‰ (1.08 to 10) and T^{0}c of (20.3 to 40) and EC in the µS / cm of (143 to 847). Groundwaters and river samples of the group is represented by WHW3, EHW17, RW2, RW4, RW9, RW10, RW11, RW17, RW21, RW29, RW32, RW35, RW40, WHCS18, WHCS19, EHCS7, EHCS9, EHCS10, RCS2, HSP6, R3 and R4 (Fig.75 and 77).

The isotopic composition of the mixed waters is relatively enriched compared to the highlands and escarpments. Shallow groundwater circulation is dominant along the highlands where depleted unconfined and semi-confined aquifers are sometimes susceptible to evaporation from the shallow water table, causing relative enrichment in heavy isotopes of small springs (WHCS18, WHCS19, EHCS7, EHCS9, and EHCS10) (Fig.75). This implies that within the same localities, shallow and deeper aquifers could be either recharged in different ways or affected by evaporation which is well described for southwestern highlands (Mekenzie, 2001). Other waters like WHW3, EHW17, RW2, RW4, RW9, RW10, RW11, RW17, RW21, RW29, RW32, RW35, RW40, RCS2, HSP6, R3, and R4 are located closer to Rivers or its tributaries are enriched due to its interaction. River samples along Bilate, especially towards the rift, are evaporated (d-excess around 1‰). The range of isotopic composition of this group shows the mixture of relatively depleted groundwater and evaporated Rivers with average ó^{18}O‰=0.5, ó^{2}H‰=5.1. This is true as water types along the River courses (Fig.58) are more evolved Na-HCO3 compared to other sources evaporating from the surface (higher EC). Vertical leakage and side flow of the river to the groundwater systems ease the River-groundwater interaction through extensional tertiary and Holocene faulted/fractured zones. This enhances the enrichment of the groundwater of this group.

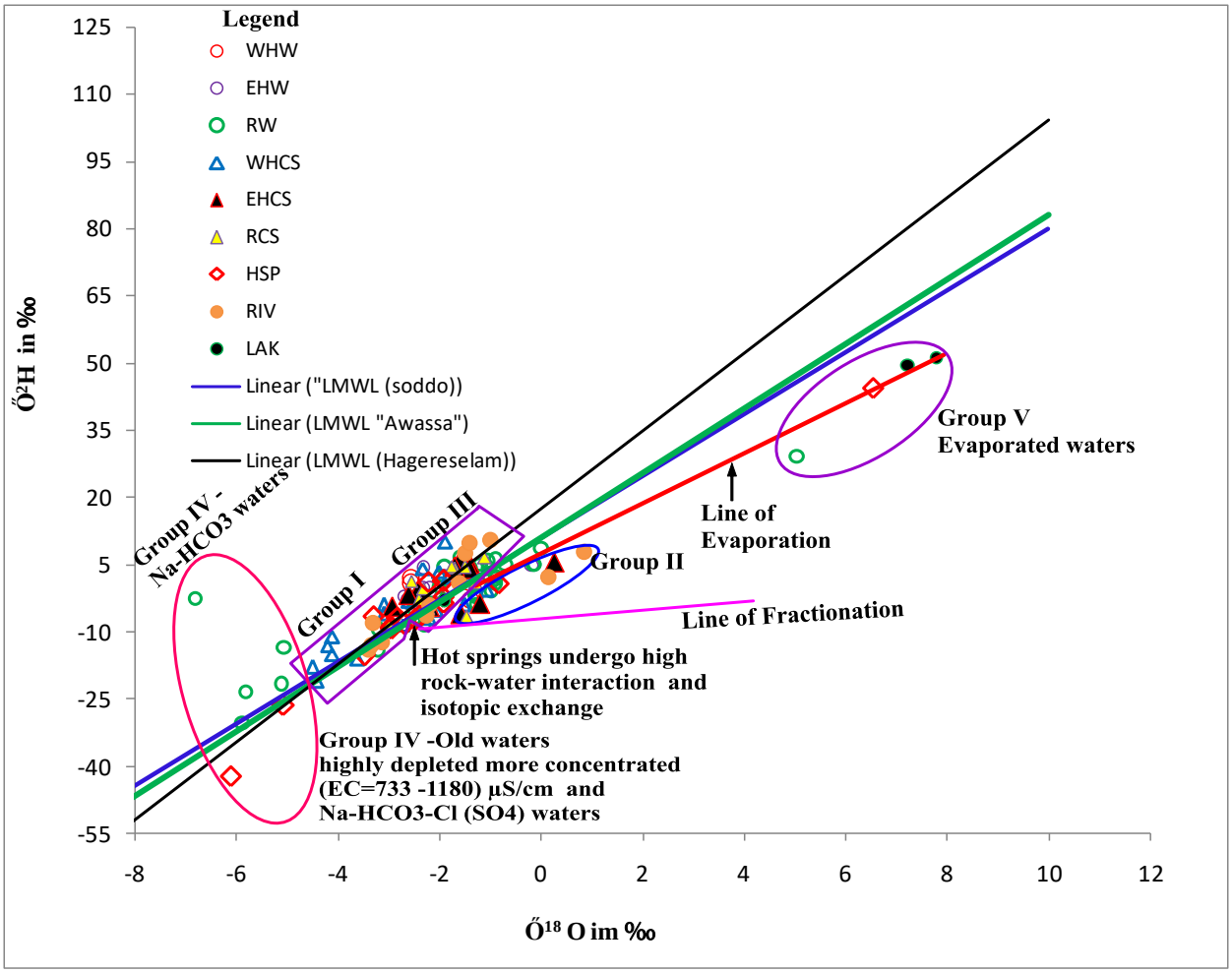

Fig 78 stable isotope-based groups of waters in Abaya Chamo Lakes basin

8.3.3. Group III (Relatively depleted and concentrated rift floor waters)

Rift floor wells, cold and hot springs of Abaya-Chamo Lakes basin is classified under Group III based on their stable isotopic composition and d-excess. The waters have a high range variation of stable isotopic ȯ^{18}O‰ (-3.48 to -0.9), ȯ^{2}H‰ (-15.2 to 6.5), and d-excess ‰ (11.2 to 21.6). Variations in chemical composition of this group are also significant, ECµS/cm (117 to 5450), T^{0}c (20 to 96), Na^{+} mg/l (12 to 1300), HCO_3^{-} mg/l (30.7 to 2830) and Cl^{-} mg/l (0.9 to 762) indicative of the differential geochemical reactions in the aquifers. Group III waters are represented by RW3, RW16, RW18, RW20, RW25, RW26, RW27, RW28, RW30, RW31, RW33, RW34, RW36, RW37, RW41, RCS1, RCS3, RCS4, RCS5, RCS6, RCS7, RCS8, RCS9, RCS10, RCS11, HSP1, HSP2 ,HSP3, HSP4, HSP7, HSP11, HSP12, HSP13, HSP14, HSP15 and HSP16 (Fig.75 and annex 5). These

water samples are clustered along the LMWLs towards the enriched side and differ from Group I depleted highland and escarpment waters in its higher temperature, EC, major ions and relative enrichment in heavy isotopes. The waters are highly evolved Na-HCO3, Na-HCO3-Cl, and Na-Cl type mainly occurs on the rift floor (Fig.31).

Higher d-excess (>10‰), discharge variability of rift cold and hot springs during wet and dry seasons and the clustering of group III waters along the LMWLs at the enriched side make the rift floor waters meteoric in origin. Highland and escarpment rains recharge this system in the form of regional flow and rift floor rains of summer and spring recharge locally.

The deep geothermal gradient to the upper aquifers and mixing of the thermal and meteoric sources favor higher hydrochemical evolution in rift tectonic zones. The isotopic plot of meteoric originated thermal groundwaters showed drifting towards the right with a higher positive oxygen shift from LMWLs (Fig.78). Thermal spring Wache1 (HSP4) (Fig.75) at the NNW flank of Lake Abaya has a high temperature of 96^0c and is characterized by its positive ^{18}O-shift in order of 1.5‰ indicating an exchange of ^{18}O with rock having an $^{18}O/^{16}O$ ratio with respect to an original water source (high circulation period). Under this condition of rock-water interaction along the flow path, some ^{18}O is transferred from the rock to the water and some ^{16}O from the water goes to rock. This selective enrichment (Drever, 1982) relates to the alteration of silicate minerals such as feldspars to clay minerals that cause a shift in $\delta^{18}O$ (‰) from one phase to another as reported in the Awash basin (Wagari, 2010) and Afar rift (Kebede, 2008). The isotopic exchange between water and rock minerals becomes higher enhancing the isotopic fractionation and hydrochemical evolution of the groundwaters is also higher along the higher isotopic fractionation as described in chapter 6 and 7.

8.3.4. Group IV (highly depleted and less concentrated rift floor groundwaters

Rift floor highly depleted deeper hydrogeological systems in the Abaya Chamo Lakes basin are characterized using deep wells and hot springs (RW1, RW5, RW6, RW8, RW12, HSP8, and HSP10) (Fig.75). The waters are located at altitude range 1157masl (south of Lake Chamo) to 1869masl (northern rift floor top of the basin). These depleted aquifers are distinct hydrogeological systems

below the aquifers of rift wells and thermal springs of meteoric origin surrounding the Lakes ($\dot{o}^{18}O$=7.25‰) (Fig.78). This system has an isotopic composition of $\dot{o}^{18}O$‰ (-6.82 to -5.07), $\dot{o}^{2}$ H‰ (-42.2 to -2.44), d-excess‰ (6.68 to 52.2), under a temperature of (24.3^{0}c to 71^{0}c). These waters occur in sand with gravel and volcaniclastic rock aquifers in well depth range of 151 to 400mbgl.

The isotopic signatures of the waters are highly depleted compared to the rainfall isotopic composition of the basin implying that the source of recharge is not recent rainfall. This assists in understanding the origin, controls recharge and flow dynamics. These waters have two major sources and mechanisms of recharge. The first water samples RW1, HSP8 and HSP9 (Fig.75) are relatively highly depleted waters with EC above (733 -1180) µS/cm plot at the depleted end below the LMWLs representing the old waters (higher residence time) recharged under wet climate from evaporated source (lower d-excess ‰ of 6.68 to 16.8). The other highly depleted waters are represented by rift floor deeper wells RW5, RW6, RW8 and RW12 plot above LMWL at depleted side indicating relatively less concentrated EC µS/cm (341-873) and higher d-excess‰ (19.5-52) most likely indicating waters which had been recharged by high intensity local rainfall during wet climate periods through faults and fractures. The stable isotopes and the d-excess of waters indicate that there is no hydraulic connection in between Lake Waters with sand and gravel aquifers in the wells.

8.3.5. Group V (evaporated waters)

Evaporated waters are highly enriched in heavy isotopes of $\dot{o}^{18}O$ and $\dot{o}^{2}H$. These waters are plotted along with Lakes waters are identified in two localities namely: RW39 at southern boundary and HSP10 along the rift fault Zone of Bilate River (Fig.75). The groundwaters have $\dot{o}^{18}O$ ‰ (5.04 to 6.54), $\dot{o}^{2}$ H‰ (29.2 to 44.4), d-excess‰ (-11 to -7.92). The hot spring has a temperature of 59^{0}c and the well water is cold (23^{0}c) but both are slightly concentrated EC µS/cm (1249 to 1592). The enriched water of the hot spring (HSP10) is the Na-HCO3 type and is close to permanent flowing river water of Bilate. The isotopic composition of the thermal spring ($\dot{o}^{18}O$=6.54‰ and d-excess (-7.9) indicate that the hot spring (T=59^{o}c) is recharged from evaporated source, either prior to recharge or the spring has a direct connection with the Abaya Lake ($\dot{o}^{18}O$= 7.25‰ and d-excess = -8.4) through open faults cutting Pleistocene basalt. The well

(RW39) water from the Gneissic aquifer at the southern margin of the basin is a Ca-Mg-HCO3-Cl type, but is highly enriched as well might be related to the connection of lake water to the aquifer system or recharge from evaporated rivers in the arid climates of the area.

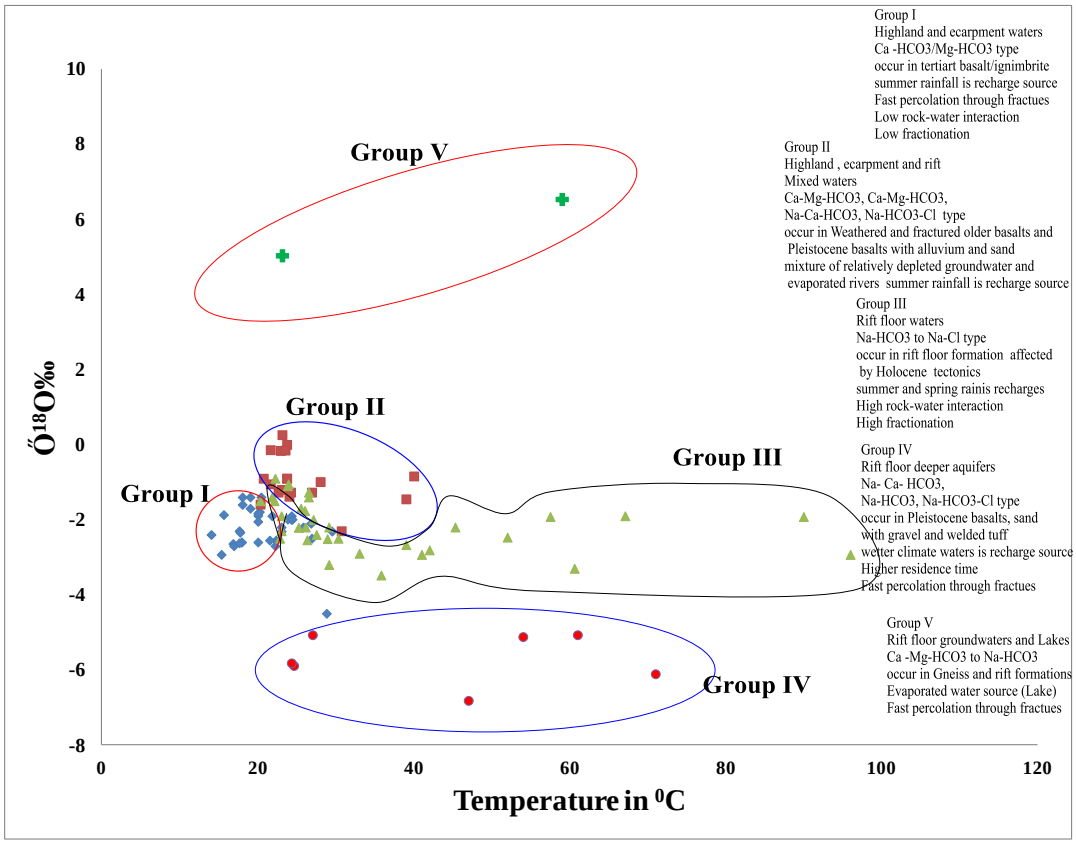

Fig 79 The plot of Temperature versus ȯ^{18}O‰ showing the different groups of waters

8.4. Interconnection of the different aquifers systems

The distribution of d-excess (Fig.80), LMWL (Fig.77, 78) and scatter plots of ȯ^{18}O‰ versus temperature (Fig.79) show that most of the highland, escarpments and rift floor aquifers are connected. The d-excess of highland and rift groundwaters in most parts of the River basins is almost similar except along the River courses in the highlands, towards the rift floor and the rift deeper aquifers. This is related to the interaction of the relatively evaporated River's waters with the nearby groundwaters making the d-excess lower. The rift floor deeper sand and volcaniclastic aquifer with very high d-excess (52‰) to the north of Lake Abaya is distinct and has no connection with the other top aquifers. Deeper wells of the rift floor having an extremely low d-

excess (-7.92‰ and -11.1‰) are related to the evaporated water reservoir. The waters plotted on the LMWL and a scatter plot of ȯ^{18}O‰ versus temperature indicating that both Group I, II, and III highland, mixed and rift floor waters plot along the alignment of meteoric origin. This alignment along almost depleted part of ȯ^{18}O‰ regardless of the elevated temperature represent the same source of recharge and connected aquifers governing the flow and evolution direction as also confirmed by the evidence of hydrochemical evolution.

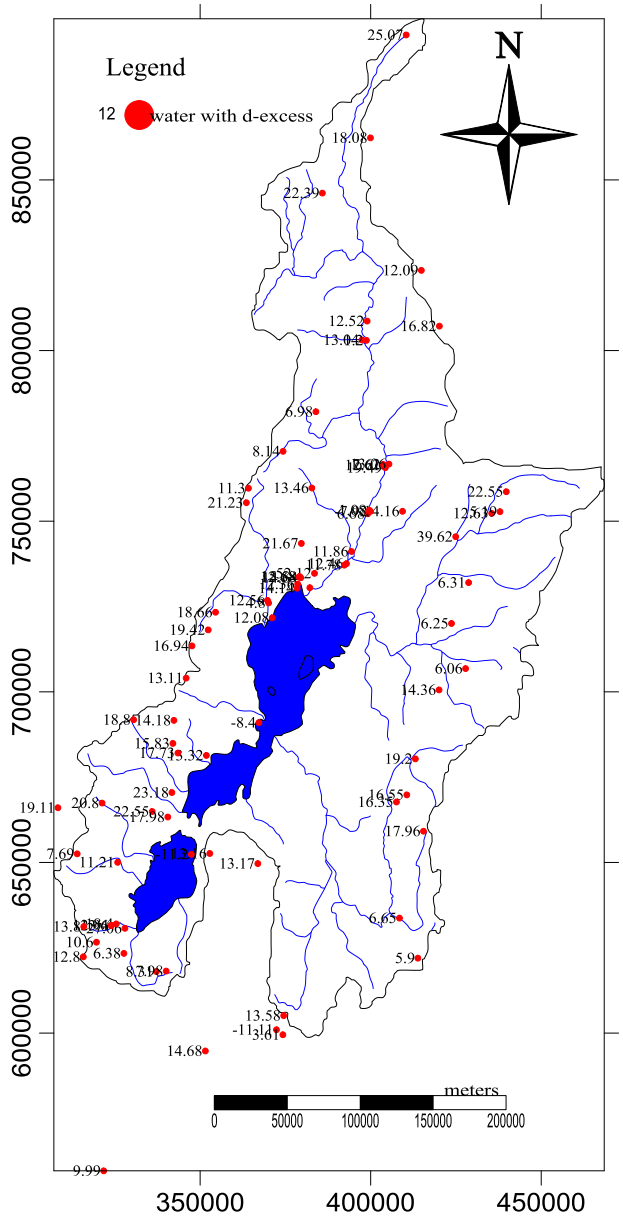

Fig 80 the spatial distribution of d-excess in Abaya Chamo Lakes basin.

As far as the interaction of groundwater in aquifers between Awasa and Abaya Chamo Lakes basin is concerned, the maps of d-excess (Fig.80) and water type (Fig.58) show clear evidence of the groundwater exchange. The d-excess values of the deep wells and large springs samples from the southern Awassa Lake basin is in the range of 13.4 to 19.8‰ which is similar value for the groundwater in the northern Gidabo river basin aligned along a NNE-SSW parallel to the fault. The similarity in the distribution of d-excess in these two corridors indicates that the source of recharge and the aquifer materials are almost similar though the areas are affected by different microclimatic conditions. The influence of big inland fault affected Gidabo river basin identified on where more evolved groundwater extend from the southern highlands of Awassa towards North of Dilla hot springs (Na-Ca-HCO3) through Yigalem (Mg-Na-HCO3) (Fig.37). Therefore, the fault is the conduit for the exchange of the groundwater.

9. SYNTHESIS OF THE HYDROGEOLOGY OF THE BASIN

Hydrogeological system analysis of the Abaya Chamo Lakes basin is the first study of its kind with the objective of understanding the basin hydrogeology using hydrochemistry and stable isotopes. The study started with the characterization of the stable isotopic composition of Rainfall waters in the basin to trace the groundwater recharge. With this, other source and its mechanism of recharge is understood. The aquifer system configuration and its relation to tectonic structures controlling the groundwater occurrence, composition and flow are described. Finally, the evidences of results are used to conceptualize the different hydrogeological systems and its groundwater dynamics in the basin. The existing and some newly collected data are integrated and correlated to represent actual field condition and the reliability of the hydrogeological systems.

9.1. Geologic and tectonic variations controlling the hydrogeology of the basin as evidence

Four major classes of the sixteen stratigraphic units and tectonic elements (chapter 3 and Fig.4) stratified up from the older (Precambrian) to the recent (volcanic and alluvial sediments) controlled the hydrogeology of the basin. The northern mouth of Lake Abaya possesses high geologic and tectonic heterogeneity whereas the southern half of the basin is relatively less affected (Fig.31). Basically, four major categories of tectonic features affected the area. The NNE-SSW Tertiary boundary faults affected the highlands. Whereas the escarpments are dominantly cut by the NNE-SSW parallel faults, fractures and Pleistocene sub-circular caldera collapse walls. The N-S and /or NNE-SSW Wonji fault belt series smaller “rift in rift” structures are active rift floor tectonics. The geology and tectonics control the hydrogeological characteristics of the basin as aquifers and flow media. It determined the spring and well discharges, interaction of surface - ground water systems, and mixing the deep magmatic source with upper shallow aquifers.

Older Tertiary units of the basin (Pgl, Pgs, Ngm, NQs, Qdi, N1-2n) are affected by boundary faults, weathering, and fracturing (Fig.31).The weathered portion of these rocks, and the intercalation of pumice and Tuff form prevalence of alternating pervious and impervious layers determine the local flow and variable hydraulic parameters of shallow hydrogeological systems.

Deeper and highly productive aquifers of highlands are due to hidden faults collecting recharge to the system. Emanation of higher discharging springs in lower reliefs is recharged at highlands through open faults.

Escarpments of the basin are covered by Tertiary formations (Ngm, Pgl, NQs) and Pleistocene and Nazareth series (Qdi, Qdp, QWbp). The rocks are cut by NNE-SSW and caldera collapses wall controlling the hydrogeological systems of the area by emanation of large cold springs (Fig.37). Along the deep penetrating faults of the escarpment dipping eastward, hot springs occur in localities like Alaba Arto and Yirgalem (Aposto) (Fig.81). The NNE-SSW escarpment faults across Gidabo basin connects Lake Awasa Basin to the north of Dilla controls the occurrence and composition of escarpment hot groundwaters (Fig. 31, 37, 58, 83). Rift floor Holocene volcanic rocks (Qws, QWbp, Qdp, QWpu) are highly affected by recent Wonji fault belt series and in places overlain by recent formations (QVs, Ql, Qa). Deeper faults of the rift floor having dip direction facing to east and "rift-in-rift" faults are responsible for discharge of hot springs. But, along the faults where there is infilling of fault and fracture spaces by recent formations and pyroclasts, hot springs discharge less. high discharge hot springs as in the north of Lake Abaya flank (Fig. 37) forming regional groundwater flow systems through convergence of all the local and intermediate flows.

In general, geological formations and geological structures of Abaya Chamo Lakes basin mainly controlled the spatial and vertical variations in groundwater recharge mechanism, the interaction of surface and groundwater systems, groundwater compositions, isotopic fractionations, aquifer continuity and the hydrogeochemical processes in the hydrogeological systems (section 6,7,8) (Fig.81, 82,83,84).

9.2. Source and mechanism of groundwater recharge as evidence

Characterization of the stable isotopic composition of rainfall in relation to the groundwaters helped to understand the source of rainfall, the mechanism of the recharge, and the approximate depth of the recharge to the hydrogeological systems in the basin. The migration of the ITCZ in North-South direction controls the Seasonal shifting of the moisture sources, mainly between the Indian Ocean (spring season) and the Atlantic Ocean (summer season) in the basin. The spatial

variation of the rainfall amount indicated that summer rainfall is stronger (about half of annual) along western highlands and the northern portion of the basin. Whereas, the spring season rainfall is strong (about 35% of annual) around eastern and western highlands of the southern part of the basin (Fig.9). The variation in the sources and distances of moisture, and micro-climate effects along the windward and leeward of summer and spring moisture determined the isotopic composition of the rainfall (Fig.24, 25) in section 4.7.

When the summer rainfall bearing moisture enters into Abaya Chamo Lakes basin through southwestern highlands, it condenses at altitude (>2500masl) (Fig.24). At this altitude, the equilibrium isotopic fractionation makes the remaining vapor and the latter precipitation become more and more depleted ($\delta^{18}O$=-4.2‰ and $\delta^{2}H$=-13‰) (Fig.22).The windward altitude effect of the summer moisture is -0.2‰ per 100m (depleted) but the leeward enriched moisture towards the rift floor has pseudo-altitude effect of 0.12‰ per 100m for the rise of 0.23‰ per 1°C. Summer moisture extends to the eastern highlands and the residual moisture climbs with the residual altitude effect of -0.05‰ per 100 and condenses with relative enrichment ($\delta^{18}O$=-2.14‰). This could be related to a hotter temperature favoring evaporation beneath the cloud base and the smaller size of the precipitation drop.

The spring season rainfall is entered into the basin from hot, humid winds of the northern Indian Ocean in March. The rainfall showed progressive enrichment from Neghele Borena GNIP station ($\delta^{18}O$ =-3.18‰ and d-excess = 17‰) towards Hagereselam (($\delta^{18}O$ =-1.82‰ and d-excess =13.96‰) with the altitude effect of 0.1‰ per 100m (Fig.25). The moisture further enriches with the pseudo-altitude effect of 0.15‰ per 100m towards the rift floor (north of Lake Abaya) having temperature factor of 0.24‰ per 1^{0}c. The spring moisture source ascends and condenses with the with residual depletion altitude effect of – 0.02‰ per 100m towards Wolaita sodo. The enrichment of spring season rain waters and proxies could be related to the amount effect and a hotter season that eases evaporation of rainfall beneath the cloud base towards the Northwest

The variation in the (slope and D-excess) of the LMWLs of Wolaita sodo (6.9, 10.93), Hagereselam (8.7, 17.4) and Hawassa (7.2, 10.95) compared to the GMWL (8, 10) indicated the sign of evaporation and condensation that modify the recharging rainfall. The plot of ($\H{O}^{18}O$ and

δ^2H) of the different waters over the LMWLs and GMWL (Fig.26) indicated the difference in the source and mechanism of the recharge to the hydrogeological system. The isotopic composition of summer rainfall ($\delta^{18}O$‰=-4.2 to -0.39 and D-excess‰ =9.3 to 25) and spring rainfall ($\delta^{18}O$‰=-2.6 to -0.01 and D-excess‰ =7.28 to 17) indicated relative enrichment of spring rainfall. But, the $\delta^{18}O$‰ and D-excess composition of groundwaters in Abaya Chamo Lakes basin range in between -6.82 to 6.54 and -11 to 52 respectively. This indicated that most of the groundwaters circulating within the basin depth range of 0 to 180mbgl are recharged from modern rainfall. The dominant portion of the recharge is from summer rainfall by percolation through fractures and fault blocks as local and regional flow systems.

Evaluation of the groundwaters isotopic composition over the LMWLs indicated different mechanisms of the recharges (Fig.26). 1) Highland groundwaters plot close to or above the LMWLs indicating summer rainfall waters of high D-excess joined the hydrogeological system when evaporation prior recharge is less. 2) Groundwaters plotted below LMWLs at the range of modern rainfall indicate evaporative fractionation before recharge more from spring rains during hotter months (March to May). 3) Groundwaters plotted to the right side of LMWLs at the initial stage of evaporation are recharged by highland rainfall, but evaporated from upper water table or Rivers feeding through vertical leakage and side flows. The interaction of River –groundwater is indicated from the spatial similarity of the D-excess (4.8‰ to 9.9‰) of the groundwaters along the River route (Fig 27). 4) Groundwaters aligned along an evaporation line (D-excess‰ up to -11) are recharged either from the Lakes. Direct recharge from the recent rainfall is the most important source supplying water to the hydrogeological systems of the basin. But, the trend of groundwaters aligned along the LMWLs is getting enriched in the direction of SSW to NNE of Abaya Chamo Lakes basin (Fig. 11, 28). 5) Groundwaters plotted at the depleted end ($\delta^{18}O$‰ below -4.2) below the LMWLs with lower D-excess ‰ (6.68 to16) are old waters recharged from relatively evaporated waters. 6) Highly depleted waters plotted above LMWLs with D-excess ‰ (19.5 to 52) indicated waters which had been recharged by high-intensity local rainfall during past wet climate times from south Indian Ocean. The old groundwaters occur in deeper rift floor aquifers (sand and gravel) in the depth range of aquifers (150 to 400) (Fig 26).

The higher D-excess, clustering along the LMWLs towards summer rainfall isotopic composition range and the discharge variability of cold and hot springs in the Abaya Chamo Lakes basin makes the groundwaters meteoric in origin. However, the basin scale isotopic analysis of tracing the recharge sources indicated that direct infiltration of precipitation is direct recharge to the system. The indirect recharges include seepage from Rivers and Lakes sides, Indirect recharge of highlands and escarpment interconnected aquifers, and the contribution from paleowaters are major sources of recharge to the hydrogeological systems of the basin (Fig.77,84).

9.3. Aquifer configuration and hydraulic parameters of volcanic rocks as evidence

The variability in the source and amount of recharge, the configuration of lithostrata and tectonic features (part 9.1) controlled the difference in the occurrence, distribution and composition of groundwaters in the different terrains of the Abaya Chamo Lakes basin. Aquifer systems of the highlands and escarpments of the basin are older acidic and basic Tertiary formations affected by Tertiary and pleistocene tectonics with deep weathering (Fig.31, 39, 81 and 82). These aquifers are unconfined to semi-confined and confined with depth. The Southern half eastern and western highlands and escarpments of the basin are mainly framed by Tertiary basalts aquifers. Whereas, the northern half of the same sides of the basin are composed of mainly upper Tertiary to lower Pleistocene acidic volcanic aquifers.

Deep wells drilled to the depth of up to 120mbgl in Tertiary basalts discharge 0.2 to 16lit/sec. In places, open faults cut the highland older rocks facilitate the occurrence of high discharging cold springs (35 to 260l/s) towards the escarpments and rift floor (Fig.37). Wells drilled in older ignimbrites and acidic volcanic aquifers discharge 1.4 to 20lit/sec for a depth range of 60 to 253mbgl and are represented by lower ranges of hydraulic properties (T=50 to 350m^2/d) and (K=1 to 13m/day). Higher hydraulic properties of highlands are related to the location of wells along major boundary faults and fractures, whereas lesser values are linked with the intercalation of younger flows/fall filling the faults/fractures. Cold sprigs from the same units in localities cut by big faults dipping to west discharge up to 120lit/sec. The depth to yield relation (Fig.29, 30) along highlands and escarpment aquifer units showed a decrease of the yield with increasing

depth in both basaltic and ignimbrite formations. This indicated the extent of fracturing and weathering is lesser with depth, but fault affected areas give exceptional yields.

.

Pleistocene basalts and associated formations of the Rift floor aquifers are unconfined in overlying recent sediments and faulted areas with high discharging hot springs (>50lit/sec). But, the aquifers are confined in wells depth range of 60 to 160mbgl discharging 3.5 to 12l/s. The sand and gravel units form deeper confined aquifers (150 to 400mbgl) below Pleistocene basalts where wells discharge 12 to 26lit/sec (section 5.6). Hydraulic properties of the rift aquifers is relatively higher (T=50 to more than 800m^2/d) and (K=3 to 15m/day) which is linked to higher fracture permeability and deeper sand and gravel aquifers (section 5.5) (Fig. 33, 34, 35, 39). Recent sediments such as Lacustrine, alluvial, and volcano-sedimentary units form unconfined porous aquifers having well discharge of 0.2 to 6l/s (Fig.31).

The composite groundwater level map helped to identify the groundwater divide among the surrounding basins. The surface water divide as in places differ from the groundwater divide. The composite (shallow and deep) groundwater heads in the highland and escarpment aquifers of the basin follow more or less the topography of the areas. The perpendicular flow direction of the highland and escarpment aquifers is towards the rift, except in places laterally connected by faults and fractures allowing outflow from the basin or connect inter-basins. These tectonic structures and thick permeable pumice layer (>340m) made the regional groundwater flow pattern of the escarpments complicated (Fig.32) in aquifers of Bilate and Gidabo River basins. The groundwater level map showed that in the rift floor the flows are converging across the rift from eastern (E-W), western (W-E) sides and parallel to the rift (N–S). “Rift in rift” structure control swamps and hot grounds on the rift floor of the area (section 5.4 to 5.5). The groundwater level is deeper towards highlands and gets shallower when coming to the rift floor of the basin

9.4. Water chemistry and hydrochemical facies in aquifers as evidence

The composition of summer recharging rainfall water samples from some stations (Wolaita sodo, Arbaminch and Dilla) in the basin is a Ca-HCO_3 type. The River water sample data of 15 points (Fig.42) of the basin are Ca-Mg-HCO_3 to Na-HCO_3-SO_4 types and determined the composition of indirectly recharging components of the groundwater. Ca-Mg-HCO_3 dominating water types

are related to the flow of River over basaltic formations whereby weathering and dissociation of basic minerals from catchment soils and rocks in the Rivers routes of the southern half of the basin. Na-HCO_3 dominating River waters along the Bilate River flow is attributed to the weathering of acidic volcanic rocks/soils and mixing of thermal springs along the Rivers. The input of precipitation in the catchment hydrology, land use, geology and interaction of ground-surface water along the Rivers routes determined the composition of River waters. The Lakes water chemistry of Abaya and Chamo mainly showed that Na^+, HCO_3^- and Cl^- are dominant ions of Lakes waters forming Na-HCO_3 and Na-HCO_3-Cl water types (Fig.45).

The hydrochemical signature of 608 groundwater samples identified the groundwater types, its evolution along the flow path, and the hydrogeochemical processes based on the variability in geological and tectonic factors. The distinction of groundwater types in the study area is due to the difference in the degree of variation in EC, TDS, PH, T^0, Na^+, Ca^{+2}, Mg^{2+}, Cl^-, $SO4^{2-}$, HCO_3^- and F^-. Physical parameters such as EC, PH and temperature increase from highlands towards rift floor. Highland groundwaters are less mineralized (EC=2.7 to 1592µS/cm and an average of 324 µS/cm) but rift floor and thermal waters are highly mineralized (EC=5450 µS/cm) (Table 5). This rift ward groundwater evolution is due to increased groundwater temperature from 15^0c in highlands to 96^0c in rift floor aquifers. The elevated temperature of the rift floor enhances the water-rock interaction in aquifers thereby raising the alkalinity from 4.2mg/l to 1440mg/l (Fig.50). Bicarbonate alkalinity is dominant in the basin and increases with depth (Fig.53).

Based on this, four groups of and eleven sub-groups of groundwaters are identified in three physiographic regimes (highland, escarpment with piedmont plains and lowland). These include: Ca-HCO3, Ca-Mg-HCO3, Ca-Na-HCO3, Mg-Ca-HCO3, Mg-Na-HCO3, Na-Ca-HCO3, Na-Ca-HCO3-Cl, Na-HCO3, Na-HCO3-SO4, Na-HCO3-Cl and Na-Cl (Fig.54, 55, 56, 57,58,59,60 and Table 7, 8). Ca-HCO3 water type is dominant in basic volcanic aquifers and Na-HCO3 in acidic volcanics.

Group I (G1) Ca^{2+} and HCO_3^- rich waters are dominant in highland and towards escarpment recharge areas of the basin. Ca and Mg are derived from basic volcanic rocks (basalt and volcanic sediments of basaltic origin. The dominance of HCO_3^- in the highland waters is related to its derivation from the upper soil zone and unequal dissolution of silicate minerals in places

covered by volcanic rocks. Group I (G1) waters have three sub-groups: S11 (Ca-HCO3), S12 (Ca-Mg-HCO3) and S13 (Ca-Na-HCO3). It indicated that Ca, Mg, Na and HCO3 vary from S11 towards S13 where Ca and Mg decreased, but Na and HCO3 increased (Table 8). This indicated that groundwaters evolve from both eastern and western highlands towards Escarpments (Fig.58), and Ca^{2+} rich waters towards the Lakes are related to sediments of basic rocks origin. The average proportion of ions of the G1 waters is Ca (52%)>Mg (22.8%)>Na (18.9%) and HCO3 (85.39%). G1 waters are dilute (EC =2.7 to 1592, and average 324) µS/cm and circulate in shallow depth with short groundwater flow paths in weathered and fractured media of the basement and highland Tertiary formations under an average temperature of 23.4^0c (Table 5). Higher variability of EC among samples in G1 is related to the occurrence of the waters in gneissic rocks (BH98), waterlogged marshy areas (SW77, SW120, SW200, SW221, and SW224) (annex 4). Fast fracture flow from highland recharge areas towards rift floor is responsible for the formation of diluted large springs of lowlands (SP79) of Arbaminch spring. Along the fault-controlled Gidabo and Gelana River channels, the Ca and HCO3 rich waters is related to River bed recharge (Fig.58). Though highland waters have lower ions concentration, averaged physical and some chemical (Na, HCO3, F, Cl) parameters of waters increase from shallow (Ca-HCO3) to deeper depth (Ca-Mg-HCO3).

Group II (G2) waters are Mg^{2+} and HCO_3^- dominant groundwaters with three subgroups S21 (Mg-Ca-HCO3), S22 (Mg-Na-HCO3) and S23 (Na-Ca-HCO3) in the aquifers of escarpment, inter-mountains, and along Rivers channels (Fig.59, 60). Group II waters have ionic proportion of Ca (23.7%), Mg (48.3%), Na (20%) and HCO3 (86%) mainly in Tertiary basalt, Pleistocene basalts, and mixed volcano-sedimentary aquifers (Fig.39, Table 7). These waters are less mineralized with lower EC (32 to 940 and average 237) µS/cm in shallow depth (Fig.55, 56). The less average EC of the Group II waters indicate the mixing of fast flowing highland waters and the escarpment recharged groundwaters. Silicate weathering of Anorthite and Forsterite in the highlands and escarpment Tertiary aquifers form Group I and Group II.

Group III (G3) waters are rich in Na^+ and HCO_3^- ions in localities of west and north of Dilla and north of Lake Abaya where NNE-SSW or N-S trending deep rift faults cut recent basic/acidic rocks and recent volcano-sedimentary rocks (Fig. 58). This group of water represents a rift floor

cold and thermal waters having four sub-groups S31 (Na-Ca-HCO_3-Cl), S32 (Na-HCO_3), S33 (Na-HCO_3-SO_4) and S34 (Na-HCO_3-Cl) (Table 8, Fig.59, 60). The subgroups of water are mineralized representing thermal springs and wells with EC (147 to 4220µS/cm and have average EC=467 µS/cm) and water temperature ranges of 17^0c to 94.3^0c. Faulted escarpments in places, discharge high-temperature hot springs as in Yirgalem, Dila and Halaba Arto are characterized by high Na^+ and dominated by a HCO_3^-.

The fourth group (G4) water is highly evolved Na-Cl/HCO_3^- type volcanic water represented by one thermal spring with EC (5450µS/cm) and a temperature of 96^0c. SP49 thermal spring occurs along NNW-SSE and N-S trending recent faults cutting stratoid silicics and rift basalts (Fig. 31). SP49 and SP57 (annex 4) have high variability in the concentration of Cl^-(762,126), HCO_3^- (1450, 2830) mg/l and PH (9.6, 8.2) respectively. This indicated that SP49 is discharged from a highly evolved deep high-temperature reservoir (250^0C) (Fig.59). This group of water is highly evolved where Ca and Mg is almost totally precipitated and replaced by Na in the aquifers under high temperature and higher dissolution of silicate minerals. Silicate weathering of the rift acidic volcanic rocks and ion exchange hydrogeochemical processes are responsible for the formation of Group III and IV groundwaters of the rift floor (Table 11, Fig.61).

The groups /subgroups of major water types across the rift valley suggests that there is a distinct pattern of hydrochemical evolution. The most important trends are increasing in Na^+, HCO_3^-, T, Cl, and EC towards the rift from S11 (Ca-HCO_3) to S41 (Na-Cl) (Fig.58 and Table 8). The good coherence among mean values of the subgroups can be clearly explained in terms of the hydrochemical characterization of groundwater circulations. However, the extent of groundwater evolution is not consistent in the southern half of the basin and across Gidabo River basin. The NNE-SSW alignment of $NaHCO_3$ waters across Gidabo River basin reflects the inland connection of the groundwater system by recent rift faults deflecting at the north of Dilla.

Hydrochemical strata of aquifers (0 to 400mbgl) of the Abaya Chamo Lakes basin have showed variation in the composition of groundwaters with depth both in the highlands, escarpments and the rift floor. Highland Shallow groundwaters are Ca-HCO_3 typed, but with depth (>60mbgl), it becomes a Na-Ca-HCO_3 type where parameters such as EC increases from 185µS/cm to 349

µS/cm, Na^+ raises from 19% to 60% and Ca^{2+} lowers from 59% to 32%. In escarpment aquifers, shallow groundwaters are Mg-HCO_3, but evolved to Na-HCO_3 in deep wells. However, in localities affected by differently dipping faults, the water types vary as a result of penetration depth and migration of hot groundwater in nearby aquifers through fractures and the interstices. (Fig.37). Rift shallow aquifers recharged by recent rainfall are Na-HCO3 type, but in places deeper faults reach thermal sources, it is Na-Cl type. Deeper rift aquifers recharged by Holocene old waters Na-HCO_3 type in distinct sand and gravel aquifers. The difference in the composition of the groundwaters with depth in the basin could be linked to the difference in hydrogeochemical processes occurring in different hydrogeological systems as discussed in section 9.5.

9.5. Ionic relations and hydrogeochemical processes in aquifers as evidence

The spatial variation of water types in the Abaya Chamo Lakes basin is related to the variation of major water forming rock–water interactions and ionic relations. This assisted in the understanding and identification of the hydrogeochemical processes occurring in different hydrogeological systems. Silicate weathering, ion exchange, and evaporation are three dominant hydrogeochemical processes occurring in the hydrogeological systems in the basin.

Dissolution of the silicate minerals in groundwater is identified using Ca^{2+}/Mg^{2+} ratio greater than 2 (Fig.64,65) where calcium and magnesium join the groundwater. This is due to the dissolution of silicate minerals such as Anorthite ($CaAl_2Si_2O_8$) and Forestrite (Mg_2SiO_4) in aquifers of older and younger basalts of highlands (Group I) and escarpments (Group II) respectively. Groundwaters of Na^+/Cl^- ratio greater than or equal to 1 indicates that the dominant process for the formation of Na^+ ion is silicate weathering. It showed that (Na/Cl) <1 in highland and escarpment groundwaters, 1<(Na/Cl)<100 in all the basin sectors , and (Na/Cl)>1 in rift floor tectonic areas. The ratio showed that , silicate weathering responsible for the formation of Na^+ is less in highlands and high in rift floor. This is related to higher rock-water interaction at elevated temperature (Fig.66) responsible for the formation of Group III and Group IV groundwaters

Ion exchange process between the groundwater and its host rock in the hydrogeological systems is understood from the Chloro-alkaline index (CAI) (Fig.68, 69). When the result of CAI1 and CAI2 indices are negative, there is an exchange between Ca and Mg in the groundwater with Na and/or K in the aquifer material. When CAI1 and CAI2 indices are positive, there is the reverse ion exchange (an exchange between Na and K in the groundwater with Ca and Mg in the aquifer material). The spatial distribution of the CAI1 and CAI2 in the Abaya Chamo Lakes basin indicated that in most parts of the basin, ion exchange is the dominant hydrogeochemical process. Ion exchange is lesser along highlands and southern half of the basin, but its extent is higher in localities north and northeast of Lake Abaya. In these areas, higher degree of rock-water interaction is facilitated by elevated temperature of rift floor thermal aquifers, where almost all Ca and Mg are exchanged by Na and K. Reverse ion exchange is identified in some localities where the water types are Ca-HCO_3 (Fig.58).

Evaporation altered the groundwater composition in the localities of the Abaya Chamo Lakes basin experiencing dry and semi-arid climates. A simple plot of TDS versus the weight ratio of $Na^+/(Na^+ + Ca^{2+})$ and Cl/ (Cl + HCO3) helped in differentiating the influences of rock-water interaction, evaporation, and precipitation as dominant processes on water chemistry (Fig.70, 71,72). Groundwaters of low TDS (<100mg/l) in unconfined aquifers are plotted in the region of the major hydrogeochemical process of rainfall dominance fields. These shallow circulating waters occur in the eastern and western highlands of the basin. Most of the groundwaters (TDS > 100mg/l) occur in the field of rock dominance, where along the groundwater flow direction rock-water interactions increases with increasing TDS. High TDS (>1000mg/l) showed the process of evaporation in places like the thermal springs around Dilla area and north of Lake Abaya plotted on the evaporation dominating field. This could be related to either evaporation prior recharge or evaporation from groundwater under a high temperature gradient of the rift floor.

The map of Cl^-/HCO_3^- ratio (Fig.72) shows localities of increasing salinity as a result of saline water mixing to the groundwater systems. The ratio ranges between 0.5 – 1.9 in aquifers surrounding the Lakes and the basement terrain SSW of the Lake Abaya showing that the water is slightly or moderately affected by salinization. The ratio is less than 0.5 in most parts of the basin indicating that groundwaters are fresh or unaffected by the salinity. Generally,

groundwaters in most parts of the aquifers in the Abaya Chamo Lakes basin are formed due to combined hydrogeochemical processes of dissolution hydrolysis and cation exchange, but evaporation process is limited to the arid climates of the basin.

9.6. Stable isotopic (ȯ^{18}O and ȯ^{2}H) signatures of waters as evidence

The investigation of hydrogeological systems of the Abaya Chamo Lakes basin using stable isotopes (δ^2H and δ^{18}O) followed five basic principles discussed in detail in chapter 8. The monthly average values of (δ^{18}O, δ^2H) of one-year rainfall stations of Hagereselam (-1.97‰, 0.27‰), Awassa (-0.72‰, 5.83‰) and sodo (-1.44‰,-0.96‰) respectively showed deviation from GMWL average (-4‰, -22‰). This indicates the difference in the slope and d-excess of the LMWLs (Fig.73), the change in the isotope value of the source, the rate of evaporation of source, the isotopic evolution of the air mass, relative humidity during precipitation. The regression lines of sodo and Awasa are plotted to the right of the GMWL because of substantial evaporative enrichment except for Hagereselam which is at an elevation of about 2600masl. Using the rainfall isotope compositions and the proxies, the altitudinal variation of summer rainfall on the Abaya chamo Lakes basin along the eastern and western highlands is -0.33‰/100m and -0.36‰/100m respectively. Southern highlands and rift floor get more depleted rainfall than the central rift valley and highlands showing the northward enrichment.

The intersection of the averaged LMWL of the three GNIP rainfall stations (ȯ^{2}H‰=7.14ȯ^{18}O ‰+12. 4) and the ȯ^{18}O-ȯ^{2}H regression line for highland groundwaters of the basin (ȯ^{2}H‰= 5.2 ȯ ^{18}O‰ +9.74) is at (-1.32, 2.84) for (ȯ^{18}O, ȯ^{2}H). This shows the basin scale average stable isotopic composition of the surface water before recharge. But, the average isotopic composition of waters (ȯ^{18}O, ȯ^{2}H, d-excess) before recharge is (-3.8,-12, 18.4) at southwestern highlands, (-0.82, 10.3, 16.9) at eastern highlands and (-1.6,-0.54, 12.3) at rift floor respectively. The composition represents the isotopic composition of waters before recharge is variable in different parts of the basin related to the variability in the humidity of the vapor forming the rainfall and the re-evaporation during rainfall.

Groundwater samples plotted on the LMWL indicated that the hydrogeological systems in the Abaya Chamo Lakes basin are grouped into five based on the isotopic signatures of the groundwaters (Fig.78, 79).

The group I represent highland and escarpment groundwater systems having the isotopic signature of ó^{18}O‰ (-4.5 to -1.4), ó^{2}H‰ (-21 to 10.1) and d-excess ‰ (10.6 to 25.1). Water samples of Group I are plotted towards depleted side along the LMWLs. This indicated that highland and associated hydrogeological systems are recharged directly by depleted highlands and escarpments summer rainfall (ó^{18}O ‰= -4.2 to -0 3) under cold air condition. In places, where big faults and wide fractures connect highland aquifers with lowland discharging areas, the groundwater (RCSP 8) is depleted with respect to heavy isotopes (ó^{18}O‰= -3, ó^{2}H‰= -8 and d-excess ‰ = 16). This indicated that Arbaminch spring (1189masl) is recharged in cooler climate condition at recharge altitude greater than 2000masl. The turbulent and fast flow of the spring through big fault scarps reveal less residence time from point of recharge altitude.

Group II represents mixed ground and surface waters from the highlands, escarpments, and a rift floor that plot below LMWLs towards the Line of evaporation (Fig.77, 78). The waters have ó^{18}O‰= (-2.47 to 0.27), ó^{2}H‰ = (-8.3 to 8.8), d-excess ‰ (1.08 to 10) and T^{0}c of (20.3 to 40) and EC in the µS / cm of (143 to 847). Shallow groundwater circulation along highlands in water table aquifers is susceptible to evaporation and cause relative enrichment of the heavy isotopes of small springs (WHCS18, WHCS19, EHCS7, EHCS9, and EHCS10) (Fig.75). Other groundwaters (WHW3, EHW17, RW2, RW4, RW9, RW10, RW11, RW17, RW21, RW29, RW32, RW35, RW40, RCS2, HSP6, R3, and R4) located closer to Rivers are enriched due to River-groundwater interaction (Fig.80). This is true as groundwater types along the River courses (Fig.58) are more evolved Na-HCO3 type compared to other waters indicating vertical leakage and side flow of the evaporated River to the groundwater systems.

Group III represents rift groundwaters of the basin (Fig.75, 78, 79). The waters have a high range of variability in ECµS/cm (117 to 5450), T^{0}c (20 to 96), ó^{18}O‰ (-3.48 to -0.9), ó^{2}H‰ (-15.2 to 6.5), d-excess ‰ (11.2 to 21.6). Indirect recharge of highland and escarpment groundwaters, and direct recharge summer and spring rains feed the aquifers of this group. These water samples are clustered along the LMWLs towards the enriched side and differ from Group I

depleted highland and escarpment waters in its higher temperature, and relative enrichment in heavy isotopes. Thermal spring Wache1 (HSP4) under boiling point (96^0c) (annex 5) at the NNW flank of Lake Abaya is characterized by a higher positive oxygen shift (^{18}O-shift) in order of 1.5‰. This indicates an exchange of ^{18}O with rock having the $^{18}O/^{16}O$ ratio with respect to an original water source (high circulation period).

Group IV includes highly depleted rift floor deeper groundwaters represented by the deep wells and hot springs (RW1, RW5, RW6, RW8, RW12, HSP8, and HSP10) (Fig.75, 78, 79). These deeper aquifers are distinct having ȯ^{18}O‰ (-6.82 to -5.07), ȯ^2 H‰ (-42.2 to -2.44), d-excess‰ (6.68 to 52.2) around the enriched Lakes and thermal springs of meteoric origin. These highly depleted waters in the sand and gravel aquifers in the depth range of 151 to 400mbgl, plot at the depleted end of the LMWLs. These waters are recharged by two mechanisms during humid Holocene time older than recent rain recharged waters. Older groundwaters plotted at depleted end below the LMWLs had been recharged by high intensity local rainfall during Holocene period through faults and fractures. These waters are less concentrated EC µS/cm (341-873) and have higher d-excess‰ (19.5-52) most likely indicating wet climate and dilute sources. The other older water recharged under wet climate from evaporated source (lower d-excess ‰ of 6.68 to 16.8) plot above LMWL at depleted side. The slight higher EC (733 -1180) µS/cm indicate relatively evaporated source of Holocene times. The stable isotopes and the d-excess of waters indicate that there is no hydraulic connection in between Lake Waters with sand and gravel aquifers in the wells.

Group V Evaporated waters are highly enriched in heavy isotopes of ȯ^{18}O and ȯ^{2}H plotted along with the Lakes waters and are identified in two localities including RW39 at southern boundary and HSP10 along the rift fault Zone of Bilate River (Fig.75, 78, 79). The groundwaters have ȯ^{18}O ‰ (5.04 to 6.54), ȯ^2 H‰ (29.2 to 44.4), d-excess‰ (-11 to -7.92). The hot spring is Na-HCO3 type, enriched (ȯ^{18}O=6.54‰ and d-excess =-7.9) under a temperature of 59^0c. The isotopic composition of HSP10 indicate that it is recharged from evaporated source, either prior to recharge or the spring has a direct connection with the Abaya Lake (ȯ^{18}O= 7.25‰ and d-excess = -8.4) through open faults. The well (RW39) water is a cold (23^0c) and Ca-Mg-HCO3-Cl type, but is slightly concentrated EC=1592 µS/cm. It implied that the well water in Gneiss aquifer is basic in composition at the southern margin of the basin, but its enrichment could be related to

the connection of Lake water to the aquifer system or recharge from evaporated rivers in the arid climates of the area.

Interconnection of the different aquifer systems (highland, escarpments and rift floor) of the basin is identified from the distribution of d-excess (Fig. 77, 78, 79, 80). The maps and plot reveal that highland and rift groundwaters in most parts of the river basins have almost similar ranges of stable isotopic values. This showed that the connected aquifers have similar source of recharge except in aquifers of highly evaporated waters, deeper rift systems, and beneath the River courses. The waters plotted on the LMWL and a scatter plot ($\delta^{18}O$‰ versus temperature) indicated that Groups I, II and III (highland, mixed and rift floor respectively) are connected groundwater systems align along the LMWLs. The spatial similarity of lower d-excess of groundwaters along the along the River routes of escarpments and rift floor indicate the interaction of evaporated River water with the groundwater aquifers. The d-excess values of the deep wells and large springs samples from the southern Awassa Lake basin is in the range of 13.4 to 19.8‰ which is similar to the ground waters in the northern Gidabo River basin. This could be due to the similarity in the source of recharge, the aquifer materials and alignment of a NNE-SSW parallel to the fault connecting the basins.

The isotopic composition of most of Rivers samples of the basin is relatively depleted and plot on the LMWL towards the depleted side. It is the effect of immediate runoff after rainfall, base flow and mixing of tributaries. Enriched Rivers of Bilate at Halaba and Bilate at Dimtu are plotted on evaporation line due to the mixing of evaporated and alkaline hot springs. The Lake waters from Abaya and Chamo are highly enriched as it is exposed to evaporation, but Abaya Lake sampled at the inflow of Amesa River to the Lake is depleted due to the depleted River source.

9.7. Conceptualization of the hydrogeological systems of Abaya Chamo Lakes basin

The variability in rock age and distribution of geologic materials, role of geologic structures, rainfall sources and amount to the basin, productivity of various aquifers, chemical composition of the groundwaters, the role of hydrogeochemical processes, and the spatial variation in the isotopic composition of waters ($\delta^{18}O$ and $\delta^{2}H$)‰ provide viewpoints to understand the

hydrogeological systems in the complex rift systems through the evaluation of sources and mechanism of recharge to different aquifer systems, configuration of the aquifer system and its relation to tectonic structures controlling the occurrence and distribution of different water types, its hydrochemical facies and the groundwater flow. Based on the findings from hydrochemical and environmental isotopes data of rainfall, groundwaters and surface waters in combination with geologic units and tectonics, four hydrogeological systems could be conceptualized (Fig. 39, 40, 81, 82, 83, 84).

1. ***Highland hydrogeological systems*** mainly occur in eastern and western mountainous areas (above 2000masl) with steep and inter-mountainous topography covered by older Tertiary units (Pgl, Pgs, Ngm, NQs, Qdi, and N1-2n) and streams filled with sediments of parent rocks. Older rock units are affected by boundary faults, weathering, and fracturing. Tertiary basalt aquifers are dominant in the southern half and tertiary to late Tertiary acidic volcanics are in northern half highlands of the basin (Fig. 4, 31.39). In places, Tertiary basalts are underlain by Precambrian formations and overlain by acidic volcanic of late Tertiary and upper Pleistocene. The western highland gets strong summer rain with altitudinal variation in $\dot{o}^{18}O‰$ of -0.36‰/100m but eastern and southwestern highlands get strong spring and weak summer rainfall with altitudinal variation in $\dot{o}^{18}O‰$ of -0.33‰/100m (Fig. 23).

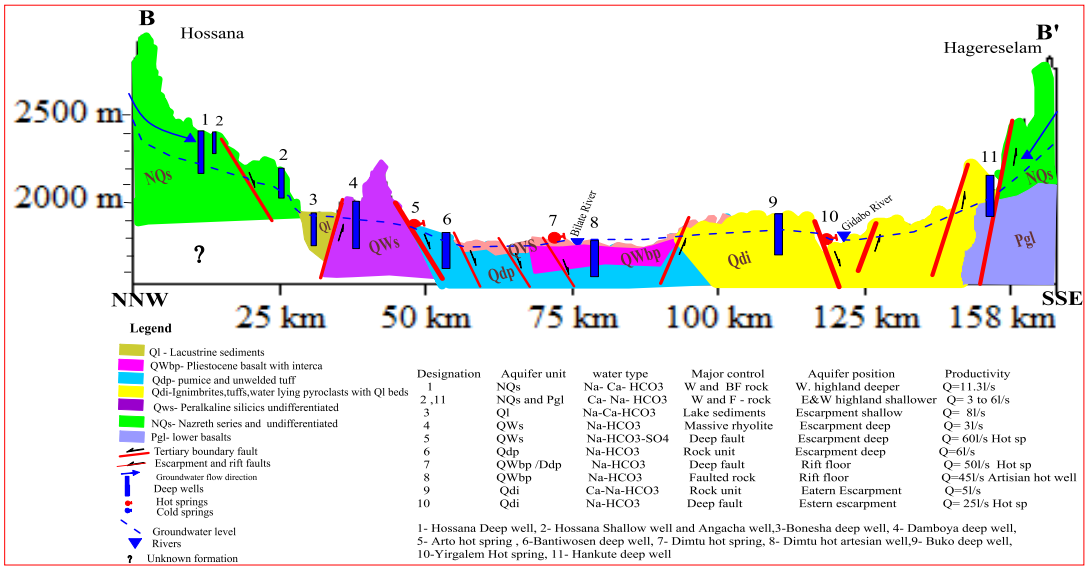

Fig 81 conceptual model of aquifers systems across B-B'

Due to microclimatic factors such as rain forming vapor humidity and the re-evaporation during rainfall, the isotopic composition of rainwater before a recharge is depleted along southwestern

(ȯ^{18}O= -3.8‰, d-excess=18.4‰) but relatively enriched at eastern highlands (ȯ^{18}O = -0.82‰, d-excess = 16.9‰). Direct recharge of depleted highland rain (ȯ^{18}O ‰= -4.2 to -0 3) under cold air (Fig.78) and indirect recharge from streamlines seepage and base flow by means of percolation through fractures and fault blocks contribute to the groundwater system of the area. It is indicated from the alignment of highland groundwaters (WHW, EHW, WHCs, EHCs) and highland Rivers on LMWLs of highland stations (sodo and Hagereselam).

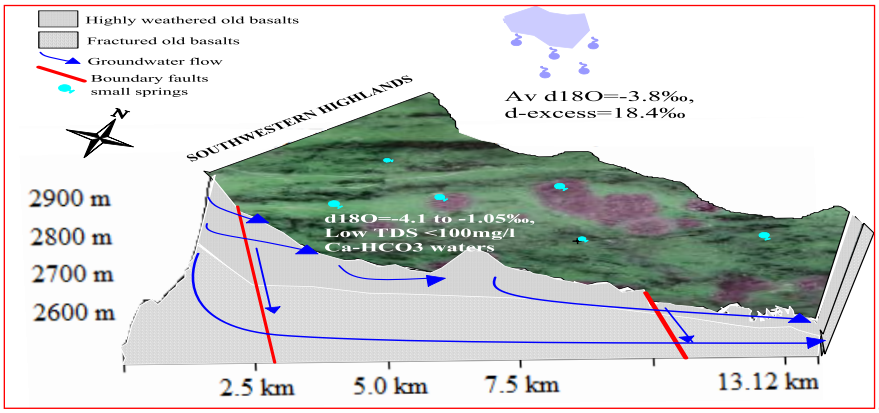

Fig 82 conceptualization of highlands hydrogeological system in SW highlands

Highland aquifers are unconfined to semi-confined and confined in the plains. These aquifers in Tertiary basalts discharge 0.2 to 16l/s in the depth range up to 120mbgl. High discharging cold springs of highlands (up to 100lit/Sec) and wells discharge from 1.4 to 20l/s occurred in Tertiary ignimbrites of highly faulted and fractured zones. The highland hydrogeological system is characterized by Shallow and local to intermediate and sometimes regional groundwater flow system in moderately productive fissured and locally highly productive mixed aquifers with hydraulic properties (T=50 to 350m^2/d and K=1 to 13m/day) in well depth range of surface to 253mbgl. Aquifers position away from major faults/fractures, the intercalation of thick layers of tuff /pumice, younger flows filling the faults, determine the variation in the hydraulic properties and discharges of the aquifers (Fig.31, 35).

Shallow circulating Ca^{2+} and HCO_3 rich dilute (average EC=324µS/cm) recharge area cold (T≤23^{0}c) groundwaters have three sub-groups, including S11 (Ca-HCO3), S12 (Ca-Mg-HCO3) and S13 (Ca-Na-HCO3) based on the variability of major ion concentration evolving from S11 towards S13 in eastern and western sides of the basin (Fig. 54-60, Table 8). Ca^{2+} rich waters of highlands are derived from basaltic mineral (Anorthite-$CaAl_2Si_2O_8$) through

the process of silicate dissolution and ion exchange identified using ion ratio Ca^{2+}/Mg^{2+} of (Fig.65). HCO_3^- in highland waters is from upper soil zone/silicate dissolution. This indicated that highland groundwaters of low TDS (<100mg/l) in unconfined to confined aquifers circulating in shallow depth are in rock dominance and rain dominance fields (Fig.70). The chemical modification of highlands groundwater with depth is identified from Shallow wells and small cold springs which are Ca-HCO_3 typed, but deep wells (>60mbgl) and larger cold springs are Na-Ca-HCO_3 type (Fig.55, 63). Highland water is relatively depleted in stable isotopes ($\acute{o}^{18}O‰$ = -4.2 to -1.4, $\acute{o}^{2}H‰$ = -21 to 10.1 and d-excess ‰= 10.6 to 25.1) and plotted towards the depleted side of the LMWLs of the basin as Group I (Fig 74). The variability in ionic concentration and stable isotopic composition among samples in highlands groundwater systems is related to the difference in rock units, evaporation from shallow unconfined aquifers, waterlogged marshy plains, River bed recharge and fast fault/fracture flow of relatively depleted cold spring (RCSP 8 ($\acute{o}^{18}O‰$= -3, $\acute{o}^{2}H‰$= -8 and d-excess ‰ = 16) (Fig.75).

2. ***Escarpment hydrogeological systems*** occur in eastern and western steep escarps and sloppy plains of the basin in between 1500mbgl to 2000masl covered by Tertiary formations (Ngm, Pgl, NQs) and Pleistocene and Nazareth series (Qdi, Qdp, QWbp) and cut by NNE-SSW faults and caldera collapses in places down throwing to the rift center (Fig.4, 31). Deep penetrating faults and caldera walls of escarpments dipping eastward are responsible for the discharge of hot springs at localities like Alaba Arto and Yirgalem (Aposto) (Fig.81). The NNE-SSW escarpment fault connects the hydrogeological system in the north of Dilla to the Lake Awasa basin across the Gidabo River (Fig.58). Escarpments are leeward sides where the moisture descends over the face of western and eastern sides to the rift floor with pseudo-altitude effect enriching the rainfall by 0.12‰ per 100m and 0.15‰ per 100m respectively. The descending moisture gets warmer and enriched with $\delta^{18}O‰$ at eastern escarpment (0.24‰ per 1^0c) than that of western (0.23‰ per 1°C) (Fig. 23, 24, 25) supporting the eastern face enrichment of isotopic composition of the rainwater before recharging the system in the basin. Direct recharge from escarpment rain and indirect infiltration and percolation through fractures or escarpment faults from highlands aquifers from local or intermediated flow systems. The escarpment is the transition sector for the highlands and rift of the basin. Most

of the aquifers in escarpments are unconfined in places along River channels, spring discharge points and marshy lands whereas semi-confined to confined across sloppy and plains. Highland aquifers are extended towards escarpments both in southern and northern half of the basin, but the discharge of both wells and springs increase from highlands towards escarpment areas due to the increased catchment area and recharge amount (Fig.37). Shallow, composite and deep groundwater head in escarpment aquifers forms local, intermediate and regional flow systems respectively (Fig.32). Fissured and porous aquifers of the escarpments are moderately or locally highly productive with hydraulic properties greater (Fig.35) and increased cold spring discharge of up to 120l/s and in places hot springs discharge up to 50l/s. Increased well discharge with depth, spring discharges and hydraulic properties of the escarpments aquifers are related to increased fracturing and faulting rate. The regional groundwater flow pattern is complicated along eastern escarpments due to inland regional faults connecting Gidabo River basin to Lake Awassa where hot springs are aligned and in areas eastern face of Bilate River basin flowing out from the basin due to thick permeable pumice (Fig.31.32).

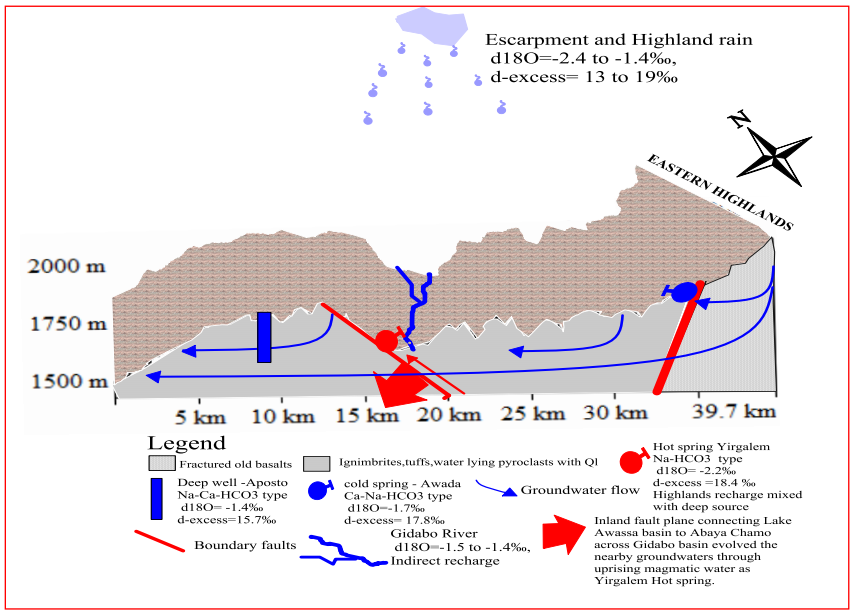

Fig 83 conceptualization of escarpment hydrogeological system in the eastern part

Escarpment groundwaters are mixed (Mg, Ca, Na) HCO3 water types, but rich in Mg^{2+} and HCO_3^- and have three sub-groups S21 (Mg-Ca-HCO3), S22 (Mg-Na-HCO3) and S23 (Na-Ca-HCO3). Subgroups have ionic proportion Ca (23.7%), Mg (48.3%), Na (20%) and HCO3 (86%) indicating the slight evolution of Ca to Mg in the escarpments and Na towards the rift

(Table 8). These waters are shallow circulating and less mineralized with lower (EC=32 to 940) µS/cm and average EC=237 µS/cm showing less resident highland waters with fast fracture flow of highland waters and percolation of escarpments recharges through fault scarps (Fig. 55,56,58,59,60 and Table 8). Escarpment waters are mixed waters of Group I and Group II; hence the stable isotopic composition is in the range of $\acute{o}^{18}O‰$ (-4 to 0.27), $\acute{o}^{2}H‰$ (-21 to 10.1) and d-excess ‰ (1.08 to 25.1) and $T^{0}c$ of (up to 40) (Fig. 77, 79). Mg-HCO_3 rich escarpment waters are formed due to the dissolution of silicate minerals (forsterite) of escarpment rock formations and ion exchange processes as discussed in highland systems (Fig. 64, 65).

3. ***Rift hydrogeological system*** of Abaya Chamo Lakes basin occurs in the active tectonic zone covered by Holocene volcanic formations (Qws, QWbp, Qdp, QWpu) overlain by recent formations (QVs, Ql, Qa) in altitude ranges of below 1500masl. Lower escarpment faults, deep cutting rift faults facing to the floor and "rift-in-rift" faults are responsible for the occurrence and distribution of groundwaters of the system (Fig.4, 31, 37). Pleistocene basalt (QWbp) is the dominant water-bearing formation in the rift floor associated with recent acidic volcanics and shallow unconfined lacustrine and fluvial sediments. The moisture that descends to the rift floor from southwestern and eastern highlands and escarpments of the basin is enriched due to increased evaporation of rainwater (Fig.24, 25). Higher evaporation is because of the lower amount and smaller sized rains (Fig.23). Rift groundwaters (RCS, RW, HSP) plotted along LMWL (Fig.77, 78) indicated that direct recharge of rift rainfall through recent faults and wide fractures to the hydrogeological system. But indirect recharge is from sources including: 1) highlands and escarpment shallow/deep groundwaters, 2) Lakes, wetlands, Rivers and small reservoirs as indicated in enriched groundwaters (Fig.80). Indirect recharge is facilitated by means of seepage and percolation through fractures and rift fault. Rift aquifers of the basin (QWbp, QWh, QWpu) are confined as depth increases in fissure /mixed aquifers in wells (60 to 160mbgl) discharging 3.5 to 12l/s. These aquifers are highly affected by rift tectonics controlling the unconfined discharge of hot springs 10 to 76l/s and small locally discharging cold springs. Large cold spring (260l/s) situated between Abaya and Chamo is discharging from escarpment fault to rift floor is indirectly recharged from southwestern highlands of the basin (Fig.37). But Holocene volcanic formations

associated with recent sediments (Ql, Qa, QVs) form unconfined shallow porous aquifers having well discharge of 0.2 to 6l/s. Swamps to the north of Lake Abaya and its surrounding are sources of small cold springs from recent sediments. Regional/intermediate groundwater flow from both sides of the basin converges towards the rift floor and makes the groundwater shallower. Increased fracturing and faulting rate towards the rift enhances the hydraulic properties of rift floor and is highly productive (T=50 to more than 400m^2/d) (Fig. 31, 35). Infilling of recent sediments and falls on the rift floor determine the spring discharge and hydraulic properties variability. Na^+ and HCO_3^- rift groundwaters include waters from highly mineralized deep wells and thermal springs EC (147 to 5450µS/cm and have average EC=467 µS/cm) with temperature ranges of 17^0c to 96^0c. However, some rift groundwaters, particularly in aquifers of southern half basalts and its weathered products, are Ca-HCO_3 to Mg-HCO_3. Subgroups of Group III and IV (Fig.58) of the rift floor Na and HCO_3 rich groundwaters are S31 (Na-Ca-HCO_3-Cl), S32 (Na-HCO_3), S33 (Na-HCO_3-SO_4) and S34 (Na-HCO_3-Cl) and S41 (Na-Cl/HCO_3^-) (Fig.58, Table 8). The occurrence of the Na–HCO3 type waters mainly in the Rift floor aquifers is attributed to the increase in Na^+ concentrations partly by the dissolution of Na-feldspars from acidic/rhyolitic rocks. Ion exchange and precipitation in rift floor significantly lower Ca^{2+} and Mg^{2+} and evolve the waters to Na-dominated as in the thermal groundwaters sampled from hot springs in fault zones and active volcanic centers especially in the north of Lake Abaya (Fig. 68,69). Such silicate hydrolysis is aided by the high CO_2 partial pressure controlling the higher concentration of HCO_3^-.

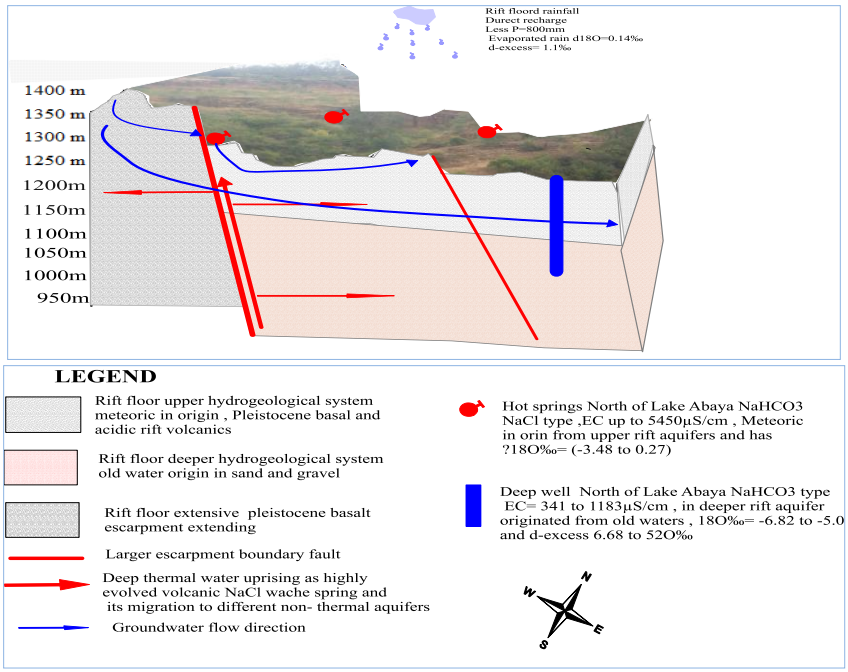

Fig 84 conceptualization of rift hydrogeological systems in the north of Lake Abaya

Though Na-Cl type is the most evolved magmatic spring, it is meteoric in origin. The mixing effects of thermal waters with the shallower, non-thermal sources elevate the temperature and enhance the dissolution of silicate minerals of the rift floor. The isotopic composition of rift groundwaters groups GII and GIII (Fig.78) vary greatly ȯ^{18}O‰= (-3.48 to 0.27), ȯ^{2}H‰ = (-15.2 to 8.8), d-excess ‰ (1.08 to 21.6) and T^{0}c of (20.3 to 96). The cluster of Na-Cl typed water on the LMWLs towards the enriched side and its higher temperature favoring higher rate of fractionation (positive oxygen shift). Rift deep wells and hot springs of higher TDS showed high rate silicate weathering (Fig.71). Hot springs of the basin with TDS (>1000mg/l) plotted on the evaporation dominating field could be related to either evaporation prior recharge or evaporation from groundwater under higher temperature (Fig.70). The similarity in the distribution of d-excess (Fig.80), the plot of different groups I, II and III of groundwaters along LMWLs and the scatter plot of ȯ^{18}O‰ versus temperature (Fig.79) indicated that different aquifers (mainly recharged from the meteoric origin) of highland, escarpments and the rift floor of the basin are interconnected.

4. ***Rift floor deeper highly depleted distinct hydrogeological system*** is below rift recent formations containing less concentrated groundwaters EC (≥733µS/cm) in sand and gravel

aquifers forming Na-HCO3 waters. It is represented by the deep wells and hot springs (RW1, RW5, RW6, RW8, RW12, HSP8 and HSP10) (Fig.75). Aquifers of wells drilled depth (151-400mbgl) in volcaniclastic sand has ($\dot{o}^{18}$O‰ = -6.82 to -5.07, $\dot{o}^{2}$ H‰= -42.2 to -2.44, d-excess‰=6.68 to 52.2), under a temperature of (24.3^{0}c to 71^{0}c). These depleted wells are in separate aquifers of the rift floor surrounding the Lakes ($\dot{o}^{18}$O=7.25‰) and thermal springs of meteoric origin aligned along a NNE-SSW rift tectonic region (Fig.57, 78). This system is most likely recharged under wetter and cooler climate below 340m thick pumice in the northern rift of the basin and below 140m thick formation in the southern rift of the basin. The variability in chemical and isotope signatures of the aquifer system are related to the difference in sources and mechanisms of recharge and flow dynamics. Highly depleted isotopic signatures of the waters imply that the source of recharge is not recent rainfall but old paleowaters. It had been recharged in two mechanisms. The first includes groundwater samples RW1, HSP8 and HSP9 that are relatively highly depleted waters with EC above (733 -1180) µS/cm plot at the depleted end below the LMWLs and lower d-excess ‰ (6.68 to 16.8). These waters are Na-HCO3-SO4 and Na-HCO3-Cl type under a high deeper temperature of more than 61^{0}c representing recharge from old evaporated moisture source under wet climate. Whereas the second highly depleted and relatively less concentrated EC µS/cm (341-873) mixed Na (Ca) HCO3 waters are represented by rift floor deeper wells RW5, RW6, RW8 and RW12 plot above LMWL at depleted side and higher d-excess‰ (19.5-52) most likely indicating waters which had been recharged by high intensity non-evaporated local rainfall during wet climate periods through faults and fractures. The stable isotopes and the d-excess of groundwaters indicate that there is no hydraulic connection between Lake Waters and upper rift aquifers with sand and gravel aquifers in the wells (Fig.78). Sand and gravel aquifers give higher well discharge (38l/s) with increased depth of 500mbgl as drilled in the northern rift floor of the basin towards the shallow Lake basin.

10.CONCLUSION AND RECOMMENDATION

10.1. Conclusion

Hydrogeological system analysis of the Abaya Chamo Lakes basin is the first study in its kind using hydrochemistry and stable isotopes. The Lakes basin covers the large area extent of about 18,100km^2 in complex southern Ethiopian volcanic terrain. To understand the actual field condition of the system in such big and complex basins, it needed proper spatial distribution and temporal monitoring of basic data stations and database. Though challenges were faced in getting the data in some parts of basins, efforts have been made to conceptualize the system by filling the gaps from primary sources. With the available data in the study area, the source and mechanism of recharge to the hydrogeological systems is understood. The aquifer system configuration and its relation to tectonic structures controlling the groundwater occurrence, composition and flow are described and conceptualized using hydrochemical and stable isotope signatures.

Abaya and Chamo Lakes drainage basin is located in the southern part of the Main Ethiopian Rift that has significant elevation differences between the rift floor and the adjacent highlands. The contrasting topography of the basin ranges from rift floor Lakes (1110masl) towards highlands (more than 3000masl) basin boundaries. Escarpments are steep fault margins following NE-SW trends. The lowland highly tectonic affected areas occupy the rift floor flat to gently sloping plains that is occupied by the two major Lakes. The Lakes are fed by a number of perennial Rivers that originated from the adjacent highlands.

Two dominant moisture sources bring rainfall to the area in summer and spring seasons, which are affected by the different climatic condition yielding variable amounts of rainfall with different isotopic and hydrochemical signature. The isotopic signature of rainfall changes along the moisture path and is addressed in detail.

The study mainly focused on the analysis of the hydrogeological systems of the Abaya Chamo Lakes basin using hydrochemical and stable isotope signatures through converging evidence from sources and mechanism of recharge, geologic and tectonic controls of groundwater

movement, and hydraulic properties of volcanic rocks, hydrochemistry, ionic ratio relations and stable isotope hydrology. It was found that the isotope and hydrochemistry signature played vital role in understanding the movement and occurrence of groundwater in this complex basin with volcano-tectonically distinct area along the rift, escarpment and highlands transect.

Sixteen geologic units of the basin are stratified up from Precambrian to the recent formations. Four major tectonic sets affected the area including: (1) the Tertiary highlands and escarpment boundary faults along the NNE-SSW cutting older Tertiary units (Pgl, Pgs, Ngm, NQs, Qdi, N1-2n, (2) escarpment normal faults along NNE-SSW affected escarpment Tertiary units (Ngm, Pgl, NQs) and some Pleistocene formations, (3) Pleistocene caldera collapse walls in places that cut Pleistocene and Nazareth series (Qdi, Qdp, QWbp) rocks, and (4) Recent tectonic/ wonji fault belt series intensively cut the rift volcanic formations and sediments. The geologic and tectonic background of the basin helped to understand the recharge mechanism, distribution of cold and hot groundwaters, hydraulic properties of the volcanic rocks, groundwater compositions, interaction of surface and groundwater, isotopic fractionations, aquifer continuity ,transfer of groundwater, mixing of different aquifers, and the hydrogeochemical processes in the aquifers of highlands, escarpments and the rift floor.

The migration of the ITCZ in North-South direction mainly controlled sources and distances of moisture, rainfall amount and distribution, and its isotopic composition. The basin microclimate, the altitude and pseudo-altitude effects of summer and spring moisture determined the isotopic composition of the rainfall. Summer rainfall from the Atlantic Ocean is stronger (50% of the annual) around the eastern and western highlands, and that of spring is strong (35% of the annual) at the southern part of the basin. Summer rainfall showed windward altitude effect of $\H{O}^{18}$O‰ per 100m to be -0.2‰ (depletion) towards southwestern highlands of the basin from the moisture source. The moisture descends towards Arbaminch area with pseudo altitude effects of δ^{18}O‰=0.12‰ per 100m (enriched) for the rate of δ18O‰= 0.23‰ per 1°C rise. The altitude effect of Spring rainfall from source towards Hagereselam area is about 0.1‰ per 100m (enriched) and the descending leeward towards North of Lake Abaya showed pseudo-altitude rate of 0.15‰ per 100m (enriched) with δ^{18}O ‰= 0.24‰ per 1^0c. Relative enrichment of spring rainfall and proxies regardless of increased altitude could be related to the decreased amount of

rainfall. In summer and spring seasons, the residual moisture sources after leeward direction showed slight depletion ($\delta^{18}O$ ‰= -0.02 to -0.05) per 100m while climbing in the highlands of their opposite sides.

The ŏ^{18}O‰ and D-excess composition of groundwaters in Abaya Chamo Lakes basin range in between -6.82 to 6.54 and -11 to 52 respectively. Compared to the isotopic composition of summer rainfall (ŏ^{18}O‰=-4.2 to -0.39 and D-excess‰ =9.3 to 25) and spring rainfall (ŏ^{18}O‰=-2.6 to -0.01 and D-excess‰ = 7.28 to 17), most of the groundwaters circulating in the basin is recharged directly from modern rainfall. Evaluation of the groundwaters isotopic composition over the LMWLs indicated different sources and mechanisms of the recharges. 1) Highland groundwaters plot close to or above the LMWLs indicating summer rainfall waters of high D-excess joined the groundwater when evaporation prior recharge is less. 2) Groundwaters plotted below LMWLs at the range of modern rainfall indicate evaporative fractionation before recharge more from spring rains during hotter months (March to May). 3) Groundwaters plotted to the right side of LMWLs at the initial stage of evaporation are recharged by highland rainfall, but evaporated from upper water table or Rivers feeding through vertical leakage and side flows. 4) Groundwaters aligned along an evaporation line (D-excess‰ up to -11) are recharged from the Lakes. 5) Groundwaters plotted at the depleted end (ŏ^{18}O‰ below -4.2) below the LMWLs with lower D-excess ‰ (6.68 to16) are old waters recharged from relatively evaporated waters. 6) Highly depleted waters plotted above LMWLs with D-excess ‰ (19.5 to 52) indicated waters which had been recharged by high-intensity local rainfall during past wet climate times from south Indian Ocean. The old groundwaters occur in deeper rift floor aquifers (sand and gravel) in the depth range of aquifers (150 to 400). Generally, the basin scale isotopic analysis of tracing the recharge sources indicated that direct infiltration of precipitation is the dominant. The indirect recharges include seepage from Rivers and Lakes sides, interconnected aquifers, and the contribution from paleowaters.

The highlands and escarpments aquifers of the basin are unconfined to semi-confined/confined with depth in the older acidic and basic Tertiary formations affected by weathering and Tertiary and Pleistocene tectonics. The Southern half eastern and western highlands and escarpments of the basin are mainly framed by Tertiary basalts aquifers (with well depth up to 120mbgl and

discharge 0.2 to 16lit/sec). The northern half of the basin is dominated by Tertiary to lower Pleistocene acidic volcanic aquifers (depth range of 60 to 253mbgl and discharge 1.4 to 20lit/sec). The hydraulic properties of older rocks ranges from T=50 to 350m^2/d and K=1 to 13m/day. In localities, open faults dipping to west cut the highland older rocks and facilitate the high discharge of cold springs (35 to 260l/s) occuring towards the escarpments and rift floor. The depth to yield relation along highlands and escarpment aquifer units showed a decrease of the yield with increasing depth in both basaltic and ignimbrite formations. The spatial and vertical variation in yield could be linked to the location of wells or springs along major boundary faults and fractures, the intercalation of younger flows/fall and fracturing and weathering. The rift floor aquifers are unconfined in overlying recent sediments and faulted areas with high discharging hot springs (>50lit/sec) and are confined in wells depth (60 to 160mbgl discharging 3.5 to 12l/s). The deeper aquifer (sand and gravel units) form confined aquifers (150 to 400mbgl discharging 12 to 26lit/sec) below Pleistocene basalts. Rift aquifers have Hydraulic properties of (T=50 to more than 800m^2/d) and (K=3 to 15m/day) which is linked to higher fracture permeability and deeper sand and gravel aquifers. The groundwater head follows more or less topography of the basin and the flow direction is highly affected by the hydrostratigraphic units and tectonic features. Deeper groundwater in the northeastern part of the basin is responsible for the outward flow of groundwater from Bilate basin towards Lake Awassa /shalla basins. The inland interconnecting faults of the Gidabo River basin to the southern part of Lake Awassa make the deeper flow of the area complex. The groundwater head is deeper in the highlands and escarpments, but shallower in the rift floor.

The water type map, piper plot and dendrogram clustering diagram of 608 groundwater samples indicated the existence of four main groups and eleven subgroups of groundwaters in the basin based on the geologic and tectonic variability. The water types include ***(1)*** Ca^{2+} and HCO_3^- rich Group I waters having three subgroups :S11 (Ca-HCO3), S12 (Ca-Mg-HCO3) and S13 (Ca-Na-HCO3), ***(2)*** Mg^{2+} and HCO_3^- rich Group II waters with three sub-groups S21 (Mg-Ca-HCO3), S22 (Mg-Na-HCO3) and S23 (Na-Ca-HCO3), ***(3)*** Na^+ and HCO_3 rich Group III waters with four subgroup waters S31 (Na-Ca-HCO_3-Cl), S32 (Na-HCO_3), S33 (Na-HCO_3-SO_4), S34 (Na-HCO_3-Cl) and ***(4)*** Na and Cl/HCO_3^- type evolved volcanic water represented by one thermal spring.

Dilute and shallow circulating G1 and G2 waters are dominant in highland and escarpment weathered and fractured media tertiary, Pleistocene basalts, mixed volcano-sedimentary aquifers of recharge areas. G1 waters are dilute (EC=324µS/cm) and shallow circulating in weathered and fractured medias but G2 waters form more dilute intermediate and fast fractured / fault flow. G3 are relatively mineralized waters (EC =147 to 4220µS/cm) occurred in aquifers of recent rift floor rocks affected by NNE-SSW or N-S trending rift faults. Highly evolved G4 (EC=5450µS/cm) waters are occur in deep thermal (at temperature of 96^0c) aquifers connected to the surface via deep faults.

In the connected aquifers, the groundwater evolution took place from G1→G2→G3→G4 along the groundwater flow direction where there is increasing trend of in Na^+, HCO_3^-, T, Cl, and EC towards the rift. This indicates clear geo-hydrological patterns along the groundwater flow path representing different degrees of rock-water interaction tending to evolve from recharge area to escarpment and finally rift floor. The consistent evolution of the groundwaters in the basin is locally blocked by the presence of escarpment fault that control thermal springs and a low EC fast flowing highland recharged groundwaters discharged in rift floor. It is evident that the groundwater evolution is significant with depth in highlands (Ca-HCO_3 to Na-Ca-HCO_3), escarpments (Mg-HCO_3 to Na-HCO_3) and rift floor (Na-HCO3 evolved to Na-Cl). The substantial positive loading (71.6%) of PC1 with respect to EC with Na^+, HCO_3^-, F^- supports the groundwater evolution towards rift. The groundwater evolution is facilitated by the extent of hydrogeochemical processes (silicate weathering and ion exchange) occurring in the basin which is higher in rift aquifers where rock-water interaction is higher due to elevated temperature.

Based on the stable isotopic signatures, there are five groups of groundwaters in the basin. Group I waters with $\dot{o}^{18}$O‰ (-4.2 to -1.4), $\dot{o}^2$H‰ (-21 to 10.1) and d-excess ‰ (10.6 to 25.1) are highland and escarpment unconfined to semi-confined/confined aquifers of Tertiary formations. Group II is mixed waters of the highlands, escarpments, and rift floor plot towards the line of evaporation. Group III rift floor hot springs are in aquifers of recent volcanics, Pleistocene basalt, and rift sediments which are recharged directly from rift rain and indirectly from highland and escarpment aquifers. Group IV Rift floor deeper sand and gravel aquifers below 150mbgl in the depth range of up to 400mbgl are recharged from Holocene humid sources. Their d-excess

indicate that there is no hydraulic connection with other waters. Group V enriched groundwaters with d-excess‰ (-11 to -7.92) are highly evaporated waters which could probably be connected to Lake Abaya via rift faults. The spatial similarity of d-excess together with plots of ȯ^{18}O‰ versus temperature, water type and groundwater flow lines indicated the aquifers interconnection of highlands, escarpments and rift. But in few places, where the inter-basin connection of Lake Awassa and northern corridor of Gidabo, the d-excess is smaller (evaporated) and water type is Na-HCO_3.

In the end, the conceptualization of hydrogeological systems is developed by converging evidences from various data sets of the hydrostratigraphic unit, geological structures, rainfall stable isotopic composition and distribution, hydrogeological characterization of volcanic aquifers, hydrochemistry and its ionic relations, and isotope hydrology. Spatial maps, cross sections and profiles prepared based on the evidence, provided worthy information on the major objective i.e significance of hydrochemistry and stable isotope signatures in the analysis of hydrogeological systems of Abaya Chamo Lakes basin.

Based on the converged evidences, the hydrogeological systems in the Abaya Chamo Lakes basin are finally conceptualized into highland systems, escarpments systems, rift floor systems and deeper rift systems. The hydrogeological systems and groundwater dynamics in the Abaya Chamo Lakes basin is in the agreement with the other studies in different parts of Ethiopian volcanics. The study as it is the first of its kind in the southern Ethiopian rift valley; it will be used as a benchmark in a large scale hydrogeological system analysis of the Abaya Chamo Lakes basin using hydrochemistry and isotope hydrology. Based on the findings some of the recommendations are forwarded.

10.2. Recommendation

Though the objectives of the study are met, there are some recommendations which could be important instrument to upgrade the work in future. These include:

1. The precipitation stable isotopic data used in the study are not of recent years. Therefore future sampling of the rainfall from different stations in combination with proxies is required to understand the recent dynamics of the rainfall and its recharge condition in

the basin and surroundings. In addition, temporal sampling of the rainfall should be made for several stations in the basin which could help to understand the different sources and events of the rainfall, circulation of the moisture and its environmental conditions.

2. The hydrogeological knowledge of the complex volcanic terrain of Abaya Chamo Lakes basin needs detail and magnified geological and tectonic maps to analyze the system in detail using the current work as a benchmark. Therefore, detail hydrogeological map should be made to exploit the quality and usable amount of the groundwater in the basin.

3. The wells data used in the study of hydrogeological and groundwater flow dynamics were constructed for the purpose of water supply. In these wells, the chance to get appropriate data is based on full penetration of aquifer depth, careful data collection and evaluation of hydraulic properties. Unfortunately, the chance is less in many parts of the basin and hence the need of monitoring wells in different physiographic sectors of the basin is crucial to validate the data so that the actual field condition will be known.

4. The spatial distribution of the groundwater stable isotope data is scarse in some parts of the basin. Therefore more groundwater, River and Lakes samples is needed to have more knowledge in the source and mechanism of the recharge. Moreover , the knowledge of the groundwater residence time is scant in the basin, and hence analysis of tritium and carbon isotopes should be made.

5. Multi-approach conceptualization of the basin could bring the hydrogeological system scenario to actual field condition and hence further integration of the research with numerical, chemical and isotope models should be done.

REFERENCES

Alley, W.M., 1993. Regional groundwater water quality. John Willey & Sons Inc., 634p.
Ababu T., 2005. Water quality monitoring in Lake Abaya and Lake Chamo region, Ph.D. thesis, University of Siegen Germany, 368p.

Abiy G. et al., 2014. Analysis of Seasonal Rainfall Variability for Agricultural Water Resource Management in Southern Region, Ethiopia

Abrham Asha 2006. An integrated hydrogeological study in Amesa river catchment, unpublished master thesis, Addis Ababa, Ethiopia. 111p.

Abraham M. et al., 2016. Groundwater flow dynamics in the complex aquifer system of Gidabo River Basin (Ethiopian Rift): a multi-proxy approach

Alemayehu T, 2006. Groundwater occurrence in Ethiopia. Addis Ababa University Press, 99pp, Addis Ababa, Ethiopia

Appello, C.A.J., Postma, D., 1993. Geochemistry, Groundwater, and Pollution. A.A. Balkema, Rotterdam, p. 536.

Ayenew, 2005. Major ion composition of the groundwater and surface water systems and their Geological and geochemical controls in the Ethiopian volcanic terrain. SINET: Ethiopian Journal of Science 28 (2), 171–188.

Ayenew T.,1998.The hydrogeological system of the Lake District basin, Central Main Ethiopian Rift.Ph.D. Thesis, ITC Publication 64

Berhanu Gizaw 1996. The origin of high bicarbonate and fluoride concentrations in waters of the Main Ethiopian Rift Valley, East African Rift system. *Journal of African Earth Sciences.* **22(4):**391-402.

Beck, W. 1966. Hydrochemical facies and groundwater flow pattern in northern part of Atlantic Coastal Plain. US Geological Survey Professional Paper 498A.

B. B. S. Singhal and R. P. Gupta, 2010. Applied Hydrogeology of Fractured Rocks, 429_{PP}
B.J. Cosby et al, 2001. Long-term and seasonal variations in CO2: linkages to catchment alkalinity generation

Boccaletti M., Mazzuoli R., Bonini M., Trua T., Abebe B.,1999. Plio-Quaternary volcano-tectonic activity in the northern sector of the Main Ethiopian Rift: relationships with oblique rifting. Journal of African Earth Sciences 29 (4): 679- 698

BoWI, 2014. Final report on the inventory of drinking water supply schemes in southern Ethiopia, unpublished report.

Chamberlin, P., 1997. Rainfall anomalies in the source region of the Nile and their connection with the Indian summer monsoon. J. Climate, 10, 1380-1392.

Chamberlin, P., and Okoola, R.E., 2003. The onset and cessation of the ‘‘long rains’’ in eastern Africa and their inter-annual variability. Theor. Appl. Climatol. 75, 43–54.

Clark I.D., Fritz P., 1997. Environmental isotopes in Hydrology. Lewis Pub. 328pp, NY, USA

Chernet T., Travi Y., Valles V., 2001. Mechanism of degradation of the quality of natural water in the lakes region of the Ethiopian Rift valley. Water Resources 35:2819-2832

Chorowicz J., 2005.The East African rift system. Jour. of African Earth Sciences 43:379–410

Coplen, T.B. 1993. Uses of environmental isotopes in regional groundwater quality.Van Nostr and Reinhold, New York.

Corti G., 2009. Continental rift evolution: from rift initiation to incipient break-up in the Main Ethiopian Rift, East Africa. Earth Science Reviews, 96, 1–53.

Coulie E., Quidelleur X., Gillot P., Courtillot V., Lefevre J., Chiesa S.,2003. Comparative K/Ar and Ar/Ar dating of Ethiopian and Yemenite Oligocene volcanism: implications for the timing and duration of the Ethiopian traps. Earth and Planetary Science Letters 206:477-492

Craig, H., 1961. Standards for reporting the concentration of deuterium and oxygen-18 in natural waters. Science 1333, 1833–1834.

Craig, H.,Lupton J.E. & Horowiff, R.M. 1977. Isotope geochemistry and hydrology of geothermal waters in the Ethiopian Rift Valley. Scripps Inst. of Oceanography. ept. 77-14, 160p

Daniel Gemechu, 1977. Aspects of Climate and Water Budget in Ethiopia, A Technical Monograph Published For Addis Ababa University.

Dansgaard, W. 1964. Stable isotopes in precipitation. Tellus 16, 436–468.

Darling, W.G., Gizaw, B. & Arusei, M.K. 1996. Lake-groundwater relationships and fluid-rock interaction in the African rift valley: Isotopic evidence. *Journal of African Earth Sciences*. **22**: 423-431.

Davis N. and DeWiest M., 1966. Hydrogeology. USA

Degalo, 2007. Analysis of biomass degradation as an indicator of the environmental challenge of Bilate watershed using GIS techniques, Addis Ababa University, unpublished MSc thesis 93pp

Drever, JI. (1997): The geochemistry of natural waters, Surface and groundwater environments. Prentice Hall, Upper Saddle River, NJ.

Di Paola, G.M. 1972. The Ethiopian Rift Valley (between 7^0 00' and 8^0 40' Lat. North). Bull. Volcanology. 36: 517-560.

Edmunds W.M, Smedley P.L, 1996. Groundwater geochemistry and health: an overview. Geological Society of America Special Publication 113: 91–105.

Edmunds, W.M., Smedley, P., 2000. Residence time indicators in groundwater: the East Midlands Triassic sandstone aquifer. Journal of Applied Geochemistry 15, 737–752.

FAO, 1995. <http://www.fao.org/waicent/faoinfo/agricult/agl/aglw/aquastat/ ethiopi.htm>
Fetter C. W., 1994. Applied Hydrogeology. Prentice Hall, Upper Saddle River, New Jersey

Fritz, P. & J.C. Fontes 1988. Handbook of environmental isotope geochemistry (volume 1). Elsevier, New York. 545 pp.

Fritz P., Fontes J.,1980.Handbook of Environmental Isotope Geochemistry. Elsevier Pub.Co., NY.

Fontes, J.C., and Edmunds, J.N. 1989. The use of environmental isotope techniques in arid zone hydrology. IHP-III project 5.2 UNESCO, Paris.

Freeze R. and Cherry A., 1979. Groundwater, a Simon and Schuster Company Englewood Cliffs. New Jersey the USA

Gat, J. R. 1996. Oxygen and hydrogen isotopes in the hydrologic cycle. Annual Review of Earth and Planetary Sciences, Vol. 24: 225-262.

Gat J., Bowser C., Kendall C., 1994.The contribution of evaporation from the Great Lakes to the continental atmosphere: estimate based on stable isotope data Geophys.Res. Letters 21:557-560.
Gat J., 1970. Evolution of the isotopic composition of atmospheric waters in the Mediterran Sea area. Jour. Geophys., 75:3039-3048.

Gat J., Gonfiantini R.,1981 Stable Isotope Hydrology: Deuterium and Oxygen-18 in the Water Cycle. IAEA Technical Report Series 210, Vienna, 337pp.

Gezahegn Yirgu, 1980. A geothermal study in northwest Lake Abaya area (southern Ethiopian Rift). M.Sc. thesis, AAU. Addis Ababa, Ethiopia.

Gibbs, 1970. Mechanisms Controlling World Water Chemistry, Journal of science American Asso, New Series, Vol. 170, No. 3962, pp. 1088-1090

GSE 1993. Geothermal Exploration Project data file. Geological Survey of Ethiopia, Addis Ababa, Ethiopia.

GSE,2007. Geochemical and Isotopic Study of North Lake Abaya geothermal Prospect, unpublished report, Addis Ababa.

Gonfiantini, R., Roche, M-A.,Olivry, J-C., Fontes, J-Ch., Zuppi, G.M., 2001. The altitude effect on the isotopic composition of tropical rains Chemical Geology 181:147–167.

Grunsky et al., 2014.Compositional data analysis in geochemistry, Journal of geochemical exploration.

Griffiths, J.F., 1972. Climates of Africa. In: Griffiths, J.F.(ed), World Survey of Climatology. Elsevier, Amsterdam.

Gu¨ler, C., Thyne, D.G., McCray, E.J., Turner, A.K., 2002. Evaluation of graphical and multivariate statistical methods for classification of water chemistry data. Hydrogeology Journal 10, 455– 474.

HALCROW 2008. Rift valley lakes integrated natural resources development master plan. Ethiopian Valleys Development Studies Authorities, Unpub. Report.

Hem, J.D., 1985. Study and interpretation of the chemical characteristics of natural waters.US Geological Surveys water supply paper 2254.

Hem, D. J. 1992. Study and interpretation of the chemical characteristics of natural water. Third edition, US geological survey water supply paper 2254, United States government printing office, Washington, 264pp.

http://people.cas.sc.edu/carbone/modules/mods4car/africa-itcz

Huntley, D., Nommensen, R. and Steffey, D. 1992. The use of specific capacity to assess transmissivity in fractured-rock aquifers. Ground Water 30:396–402.

Hussien, B.M. and Fayyad, A.S. 2016. Modeling the Hydrogeochemical Processes and Source of Ions in the Groundwater of Aquifers within Kasra - Nukhaib Region (West Iraq). International Journal of Geosciences, 7, 1156-1181

H. O Nwankwoala and G.J Udom,2011. Hydrogeochemistry of groundwater in Port Harcourt City, Southern Nigeria. Greener Journal of Physical Sciences, ISSN: 2276-7851 Vol. 3 (4), pp. 115-130.

Huaming Guo and Yanxin Wang, 2005. Geochemical characteristics of shallow groundwater in Datong basin, northwestern China, Journal of geochemical exploration, ISSN: 0375-6742.

Herczeg and Edmunds, 2000. Environmental Geochemistry, 242pp

IAEA/WMO, 2004. Global Network of Isotopes in Precipitation. The GNIP database. http://Isohis.iaea.org [accessed 2016].

Jalludin, M. and Razack, M. 2004.Assessment of hydraulic properties of sedimentary and volcanic aquifer systems under arid conditions in the Republic of Djibouti (Horn of Africa). Hydrogeol. J. 12, 159–170.

Jeff B LANGMAN, 2015.Spatial distribution of δ2H and δ18O values in the hydrologic cycle of the Nile Basin, Journal of Arid land.

Jica, 2012. The study of groundwater resources assessment in rift valley lakes basin, unpublished report

Jiri, 2015. Hydrogeology of Dilla sheet, unpublished report

Jiri, 2014. Hydrogeology of Hossana sheet, unpublished report

Kazmin, V., 1979. Stratigraphy and correlation of volcanic rocks of Ethiopia. Ethiopian Institute of Geological Surveys. Note number 106, pp. 1– 26

Kazmin, V., Berhe, S.M., Nicoletti, M., and Pertucciani, C., 1980. Evolution of the northern part of the Ethiopian rift: Sheet NC37-15, Memoir No.3, 26pp

Kebede S., 2004. Approaches isotopique et geochimique pour l'etude des eaux souterraines et des lacs:exemples du haut basin du Nil Bleu et du rift Ethiopien [Environmental isotopes and geochemistry in groundwater and lake hydrology: cases from the Blue Nile basin, main Ethiopian rift and Afar, Ethiopia]. Ph.D. Thesis, University of Avignon, France

Kebede S.,2013. Groundwater in Ethiopia: features, numbers and opportunities. Springer, Heidelberg, Germany

Kebede S, Travi Y.,2011. Origin of the δ18O andδ2H composition of meteoric waters in Ethiopia. Quat Int 257:4–12. doi:10.1016/j. quaint.2011.09.032

Kebede S, Travi Y, Asrat A, Alemayehu T, Ayenew T, Tessema Z .2008. Groundwater origin and flow along selected transects in Ethiopian rift volcanic aquifers. Hydrogeol J 16(1):55–73. doi:10.1007/s10040-007-0210-0

Kebede, S., Travi, Y., Alemayehu, T., Ayenew, T., 2005. Groundwater recharge, circulation, and geochemical evolution in the source region of the Blue Nile river, Ethiopia. Journal of Applied Geochemistry 20 (9), 1658–1676.

Kebede, S., Lamb, H., Telford, R.,Leng, M. and Umer, M.,2002b.Lake-Groundwater relationships, oxygen isotope balance and climate sensitivity of the Bishoftu Crater Lakes, Ethiopia. Advances in Global Change Research, 12: 261-275.

Kozłowski M., Komisarek J. 2017 Groundwater chemistry, and hydrogeochemical processes in a soil catena of the Poznań Lakeland, central Poland, J. Elem., 22(2): 681-695. DOI: 10.5601.

Kumari Rina et al., 2013. Determining the genetic origin of nitrate contamination in aquifers of Northern Gujarat, India, Journal of Ear and Env, sci.DOI: 10.1007.

Kendall and Coplan, 2001.Distribution of oxygen-18 and deuterium in river waters across the United States, journal of hydrological processes 15, 1363 – 1393 (2001)DOI: 10.1002/hyp.217

Kruseman, G.P. and De Ridder, N.A. 1990. Analysis and evaluation of pump test data. Ilri pub Ser: No 47, 377p.

Lambrakis N., Antonakos A., Panagopoulos G.,2004.The use of multi-component statistical analysis in hydrogeological environmental research. Water Research 38: 1862–1872.

Levin NE, Zipser EJ, Cerling TE .2009. Isotopic composition of waters from Ethiopia and Kenya: insights into moisture sources for eastern Africa. J Geophys Res 114: D23306. doi:10.1029/2009JD012166

Morbedelli *et al*. 1981. Basaltic volcanism in the northern sector of the main Ethiopian rift, a journal of volc. And Geothermal reas, 365-382pp

Michael Manga, 2001; using springs to study groundwater flow and active geologic processes, Department of Earth and Planetary Sciences, University of California, Berkeley, California 94720

Mazor, E. 1991. Applied Chemical and isotope groundwater hydrology. John Wiley and sons, New York: 274pp.

McKenzie, J., Siegel, D., Patterson, W., McKenzie, J., 2001. A geochemical survey of spring water from the main Ethiopian Rift Valley, southern Ethiopia: implications for wellhead protection. Hydrogeology Journal 9, 265– 272.

Meinzer OE. 1927. Large springs in the United States. US Geol. Surv.Water Supp. P. 557. 94 pp.

Meybeck 1987. Global chemical weathering of surface rocks estimated from river dissolved loads, American journal of science, vol.286, pp 401-428

Mohr P., Wood C.A., 1976. Volcano spacing and lithospheric attenuation in the eastern rift of Africa. Earth and Planetary Science Letters 33:173-189.

Molla D., Stefan W., Tenalem A. 2008. Major ion hydrochemistry and environmental isotope signatures as a tool in assessing groundwater occurrence and its dynamics in a fractured volcanic aquifer system located within a heavily urbanized catchment, central Ethiopia

Ministry of Water Resources, 1980. Twelve town water supply Project, Wolaita sodo , well report (unpublished). Addis Ababa.

Mulugeta M.,2007. Groundwater circulation and hydrochemistry of the corridor (Upper Gidabo River and Lake Awassa catchments, SNNPR, unpublished Master thesis,129pp.

Neven Kresic, 2009. Groundwater resources: Sustainability, management, and restoration, ISBN: 978-0-07-164091-6, 865PP.

Nicholson, S.E., 1996. A review of climate dynamics and climate variability in eastern Africa. In: The Limnology, Climatology and paleoclimatology of the East African Lakes (T.C. Johnson and E. Odada, eds), 2556, Gordon and Breach, Amsterdam, The Netherlands.

Peccerillo A., Yirgu G., 1996. Geochemical behavior of fluorine in the volcanic systems of the Ethiopian Rift valley: Implications for the problem of high fluorine waters. In: Program and abstracts of the third Ethiopian Geosciences and mineral Engineering Congress, Addis Ababa, Ethiopia

Piper A.M., 1944. A graphic procedure in the geochemical interpretation of water analysis. Trans.Am. Geophys.Union 25:914-923
Plummer L.N., GlynnP.D.,2005.Geochemistry and understanding of groundwater systems. Hydrogeology Journal 13:263-287.

Rango T, Bianchini G, Beccaluva L, Ayenew T, Colombani N., 2008. A hydrogeochemical study in the Main Ethiopian Rift: new insights into the source and enrichment mechanism of fluoride. Environ Geol 58:109–118

Raphae¨l Pik et al. 1997. The northwestern Ethiopian Plateau flood basalts: Classification and spatial distribution of magma types, Journal of Volcano and Geothe Resea 81 1998, pp 91–11.

Razack M., Huntley D., 1991. Assessing transmissivity from specific capacity data: Water Resources Bulletin 27 (1):47-58

Raunet, M., 1978. The geographical and morpho-pedological survey, Lake Abaya and Chamo western catchment, southern rift valley, Ethiopia.

Rozanski, K., Araguas-Araguas, L., Gonfiantini, R., 1996. Isotope patterns of precipitation in the East African Region. In: Johnson, T.C., Odada, E. (Eds). The Climatology, Palaeoclimatoloy, Paleoecology of the East African Lakes, Gordon and Breach, Toronto, pp. 79-93.

Stallard and Edmond, 1983. Geochemistry of the Amazon: 2. the influence of geology and weathering environment on the dissolved load, Journal of Geophysical research,

Schoell, M., Faber, E., 1976. Survey on the isotopic composition of waters from NE Africa. Geologisches Jahrbuch. 17, 197-213.

Sintayehu L., 2009. Integrated hydrogeological investigation of Upper Bilate River basin, unpublished MSc thesis, AAU,126PP

Sileshi Bekele, 2000. Investigation of water resources aimed at multi-objective development with respect to limited data situation: the case of Abaya-Chamo basin, Ethiopia. Ph.D. Thesis. Institute fur Waserbau und Technische Hydromechanik. Germany.

SWIRDB, 2012. Inventory of water supply schemes in all villages of southern Ethiopia, Awassa. Unpublished report.

Tamiru Alemayehu, 2003. Controls on the occurrence of cold and thermal springs in central Ethiopia. African geosciences review. Vol. 10, No. 3, pp. 245-251.

Theis, CV., 1963. Estimating the transmissivity of a water table aquifer from the specific capacity of a well. US Geological Survey Water supply Paper 1536-I. pp 332-336.

Teclu, A. 2007: A preliminary isotopic and geothermal study for the recharge identification of Abaya geothermal field, Ethiopian Institute of Geological Surveys. Unpublished report. Addis Ababa.

Telford, R.J., 1998. The palaeo-environmental record of Holocene environmental change in the Ethiopian Rift Valley. Unpublished Ph.D. Thesis, University of Wales.

Tahoora Sheikhy Narany, Mohammad Firuz Ramli, Ahmad Zaharin Aris, Wan Nor Azmin Sulaiman, Hafizan Juahir, and Kazem Fakharian , 2014. Identification of the Hydrogeochemical Processes in Groundwater Using Classic Integrated Geochemical Methods and Geostatistical Techniques, in Amol-Babol Plain, Iran. The Scientific World JournalVolume 2014, Article ID 419058, 15 pages

Tenalem A 1998. The hydrogeological system of the lakes district basin, Central Main Ethiopian Rift. Ph.D. thesis. The Free University of Amsterdam. 259 pp.

Tenalem A., 2003. Environmental isotope-based integrated hydrogeological study of some Ethiopian rift lakes. Journal of Radioanalytical and Nuclear Chemistry 257 (1), 11–16.

Tenalem A, 2005. Major ion composition of the groundwater and surface water systems and their geological and geochemical controls in the Ethiopian volcanic terrain. SINET: Ethiopian Journal of Science 28 (2), 171–188.

Tenalem A, Shimeles F, Frank Wisotzky, Molla D, and Stefan W, 2009. Hierarchical cluster analysis of hydrochemical data as a tool for assessing the evolution and dynamics of groundwater across the Ethiopian Rift

Tenalem A., Molla D, Stefan W,2008. Hydrogeological framework and occurrence of groundwater in the Ethiopian aquifers

Tesfaye T., 2010. Groundwater potential evaluation based on integrated GIS na dremote sensing techiniques, Bilate basin, Unpublished MSc thesis,94pp.

Toth, J., 1963. A theoretical analysis of groundwater flow in small drainage basins Journal of Geophysical Research, 68(16):4795-4812

Todd D. 1980. Groundwater Hydrogeology. Second Edition. USA

Seid G. 2011. Assessment of hydraulic properties of Ethiopian Ashange basalts, Unpublished MSc thesis, Addis Ababa University,124pp.

UNDP., 1973. Geology, geochemistry, and hydrology of hot springs of the East African Rift system within Ethiopia. UNDP report DD/SF/ON11, UNDP, New York, 300 pp

Wagari,, 2010. Hydrogeological characterization of the complex volcanic systems of Middle Awash basin. University of Poitiers, France, 301pp, unpublished thesis.

Waterloo Hydrogeologic, Inc. (2006): Aquachem version 4.0 for water quality analysis. Plotting and modeling.

Williams F., Williams M., Aumento F., 2004. Tensional fissures and crustal extension rates in the northern part of the main Ethiopian Rift. J.Afr.Eart Sci 38.

Woldegebriel, G., Aronson, J.L. & Walter, R.C. 1990. Geology, geochronology, and rift basin development in the central sector of the Main Ethiopian Rift. *Geological Society of America Bulletin*, 102 (1990):439-458. [B34. 022].

Yitbarek A.,2009.. Hydrogeological and hydrochemical framework of the complex volcanic system in Upper Awash River basin, Central Ethiopia: with special emphasis on inter-basins groundwater transfer between the Blue Nile and Awash rivers, Ph.D. Dissertation, Univ. of Poitiers, France

Yousef Nazzal et al., 2015_identification of potential artificial groundwater recharge zones in Northwestern Saudi Arabia using GIS and Boolean logic, Journal of African Earth science, VOL.111, 156-169pp.

Zinabu G. and E. Kebede, 2002. Long-term changes in chemical features of waters of seven Ethiopian rift-valley lakes, a journal of Hydrobiologia, Vol.477, 81-91pp.

Journals submitted for publication

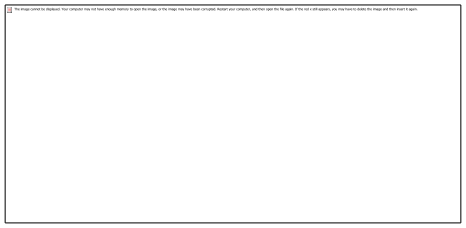

	Submitted to – Journal of spatial hydrology
Authors	Abrham Asha Tolke, Prof. Tenalem Ayenew
Title	The Use of Hydrochemical and Environmental Isotopes in Analysis of Hydrogeological Systems of Abaya - Chamo Lakes Basin
Original file	267-591-1-SM.DOCX 2017-04-06
Supp. files	None ADD A SUPPLEMENTARY FILE
Submitter	Mr Abrham Asha Tolke
Date submitted	April 6, 2017 - 09:04 AM
Section	Articles
Editor	None assigned
Author comments	Thank you editors for your contribution

Status

Status	Awaiting assignment
Initiated	2017-04-06
Last modified	2017-04-06

2. The second journal is sent to the journal of hydrogeology